Charles University in Prague
Faculty of Mathematics and Physics

DOCTORAL THESIS

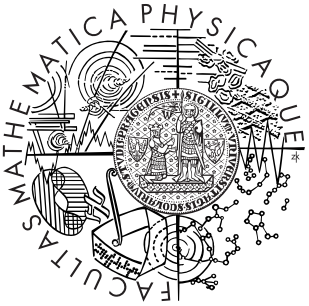

Norman Gürlebeck

Matter Models in General Relativity with a Decreasing Number of Symmetries

Institute of Theoretical Physics

Supervisor of the doctoral thesis:	Prof. RNDr. Jiří Bičák, DrSc., dr.h.c.
Study program:	Physics
Specialization:	Theoretical physics, astronomy and astrophysics

Prague, 2011

Acknowledgements
First, I am much obliged to my supervisor Jiří Bičák. With his deep understanding of physics, he was a constant help. Additionally, I always enjoyed and benefited from his crash courses in Czech arts and culture.

I am greatly indebted to David Petroff. He is a splendid colleague and friend. With his deliberate and candid manner, discussions could take surprising turns providing insights beyond physics. I also thank his family, which received me several times so warmly in their home.

I thank Jörg Frauendiener and Tomáš Ledvinka for agreeing to be the reviewers of my thesis. Furthermore, I thank the colleagues at the institute for creating a nice working atmosphere. All of them and especially Tomáš Ledvinka, Otakar Svítek and Martin Žofka had always an open ear for my question and were never short of helpful remarks. I sincerely appreciate the constant work of Jiří Horáček and Oldřich Semerak that kept my funding going like the Grant No. GAUK 22708. I was also financially supported by the Grant No. GAČR 205/09/H033.

The friendship of Ivan Pshenichnyuk, Martin Scholtz and of the spaceship crew Otakar Svítek and Martin Žofka was a big support in the last years (even though we did not meet with success in all space missions). I owe gratitude to Martin Scholtz and Martin Žofka, in particular, for all the translations they did for me and all the help with public affairs.

Let me also thank several institutes that invited me during the last years. These are the Albert Einstein Institute in Golm, the Institute of Theoretical Physics of the Friedrich Schiller University in Jena and the University of Wisconsin in Milwaukee. Among those who made these stays a memorable experience are Marcus Ansorg, John Friedman and Reinhard Meinel. I much appreciated the discussions with them on Dedekind ellipsoids.

I am obliged to my family not just for their support in the last years. My father showed me the love for mathematics and my mother that there is also something apart and beyond. My sister was always a role model for me and is greatly responsible for me turning out the way I did. At last, let me thank Julia Häuberer. She helped me a lot in the vicissitudes of my PhD student's life. She is the best reason imaginable to leave the Dedekind ellipsoids and dipole shells to their own fate for another night and go home.

I declare that I carried out this doctoral thesis independently, and only with the cited sources, literature and other professional sources.

I understand that my work relates to the rights and obligations under the Act No. 121/2000 Coll., the Copyright Act, as amended, in particular the fact that the Charles University in Prague has the right to conclude a license agreement on the use of this work as a school work pursuant to Section 60 paragraph 1 of the Copyright Act.

In Prague, July 15, 2011 Norman Gürlebeck

Title: Matter Models in General Relativity with a Decreasing Number of Symmetries
Author: Norman Gürlebeck
Institute: Institute of theoretical physics
Supervisor: Prof. RNDr. Jiří Bičák, DrSc., dr.h.c.
Abstract:

We investigate matter models with different symmetries in general relativity. Among these are thin (massive and massless) shells endowed with charge or dipole densities, dust distributions and rotating perfect fluid solutions. The electromagnetic sources we study are gravitating spherical symmetric condensers (including the implications of the energy conditions) and arbitrary gravitating shells endowed with a general test dipole distribution. For the latter the Israel formalism is extended to cover also general discontinuous tangential components of the electromagnetic test field, i.e., surface dipole densities. The formalism is applied to two examples and used to prove some general properties of dipole distributions. This is followed by a discussion of axially symmetric, stationary rigidly rotating dust with non-vanishing proper volume. The metric in the interior of such a configuration can be determined completely in terms of the mass density along the axis of rotation. The last matter models we consider are non-axially symmetric, stationary and rotating perfect fluid solutions. This is done with a first order post-Newtonian (PN) approximation to the Dedekind ellipsoids. We investigate thoroughly two limits of this 1-PN sequence, where the 1-PN Dedekind ellipsoids become axially symmetric 1-PN Maclaurin spheroids or degenerate to a rod-like singularity.
Keywords: Dipole layers in curved backgrounds, rigidly rotating dust, Dedekind ellipsoids, post-Newtonian approximation

Název práce: Modely hmoty v obecně relativitě s klesajícím počtem symetrií
Autor: Norman Gürlebeck
Ústav: Ústav teoretické fyziky
Školitel: Prof. RNDr. Jiří Bičák, DrSc., dr.h.c.
Abstrakt: V práci zkoumáme modely hmoty s různými symetriemi v obecné relativitě. Mezi nimi jsou tenké (hmotné a nehmotné) slupky s nábojovou či dipólovou hustotou, řešení s prachem či rotující ideální tekutinou. Elektromagnetické zdroje, které studujeme, jsou gravitující sféricky symetrické kondenzátory (zohledňující důsledky energetických podmínek) a libovolné gravitující slupky s obecným testovacím rozložením dipólů. Pro ty jsme zobecnili Israelův formalizmus na případ obecných nespojitých tečných složek testovacího elektromagnetického pole, tj. plošné hustoty dipólů. Formalizmus je aplikován na dva příklady a použít k dokázání některých obecných vlastností rozložení dipólů. Potom následuje diskuze axiálně symetrického, stacionárního rozložení prachu, který rotuje jako tuhé těleso a má nenulový vlastní objem. Metriku uvnitř takovéto konfigurace lze plně určit pomocí hustoty hmoty podél osy rotace. Posledními studovaími modely hmoty jsou stacionární, rotující řešení s ideální tekutinou, která nejsou axiálně symetrická. Používáme zde postnewtonovskou aproximaci (PN) Dedekindových elipsoidů do prvního řádu. Důkladně zkoumáme dvě limity této 1-PN posloupnosti, kdy se z 1-PN Dedekindových elipsoidů stávají axiálně symetrické 1-PN Maclaurinovy sféroidy nebo kdy degenerují na tyčovou singularitu.
Keywords: Dipólové vrstvy na zakřiveném pozadí, prach rotující jako tuhé těleso, Dedekindovy elipsoidy, postnewtonovská aproximace

CONTENTS

LIST OF FIGURES

LIST OF TABLES

CHAPTER

1

INTRODUCTION

General relativity plays an important role in current astrophysics and cosmology. It is indispensable for the description of compact objects like black holes and neutron stars. In particular, it is crucial for physical processes in their neighborhood like accretion, gamma ray bursts, gravitational wave emission and electromagnetic counterparts.

To describe such situations, Einstein's equations, a system of non-linear and coupled partial differential equations, have to be solved. A direct approach consisting of giving the matter distribution and solving the field equations is an extremely difficult task. Exact solutions describing a physically reasonable matter region and a vacuum exterior are scarce. Though, there are notable exceptions, e.g., the Schwarzschild interior and exterior solution, the Oppenheimer-Snyder spherical dust collapse matched to the Schwarzschild vacuum, see [53], and the Neugebauer-Meinel thin disk of rigidly rotating dust, see [54]. Besides obvious mathematical difficulties, there is also an uncertainty in the description of the matter. To name only two questions arising in modeling the matter: Which equations of state do we have to use? What are the magnetic fields inside a pulsar? Thus, idealized situations are considered and indirect methods or approximation techniques are applied in order to solve Einstein's equations. In the former case, a high degree of symmetry is often presumed like spherical symmetry, axially symmetry or stationarity. We discuss matter models of all of these three types. If the matter distribution is in one spatial dimension typically much smaller than in the others, the source is often idealized as a thin disk or shell. Hence, solving the interior equations reduces to a boundary value problem. Additionally, the type of matter present in the space-time is usually assumed to be "simple" like pure radiation, dust or perfect fluids.

Indirect methods proved powerful and led to physically reasonable sources. The principle idea of such methods is to prescribe the solutions of Einstein's field equations and calculate the matter content afterwards. In general, the energy momentum tensor obtained in such a way cannot be interpreted physically. However, in the case of shells, the matter is described by the jump of the extrinsic curvature across this shell. An interpretation as a (several component) perfect fluid is often found (for a description of the Israel formalism see, e.g., [3, 43]). Such an approach was used to generate, e.g., disk sources to the Weyl vacuum metrics and the Kerr(-Newman) metric in [4, 9, 48]. The merit of this method is that singularities of different kinds can be replaced by physically well-understood sources. In case of the Weyl solutions several relativistic generalizations of well-known Newtonian disks used in astrophysics were found, see [5]. This method was extended to electro-vacuum in [46] to include charged disks. This exact technique is used in Chapters 2 and 3 of this thesis.

Up to now only shells with monopole surface charges were included in the formalism of matching electro-vacua, e.g., in [46]. This is remedied in Chapter 3. One reason why dipole shells were not included might be the infinite electric field "between the two charged layers". The energy momentum tensor for such a field is not well-defined. Nonetheless, in the weak field approximation, this problem does not arise and dipole test fields can be considered. This is often justified, because the average energy density of the electromagnetic field is negligible compared to the gravitational field in many astrophysical situations. The general formalism, which is developed for any background in Chapter 3, is applied to a Schwarzschild disk background found in [9]. We use two different test field solutions known in the Schwarzschild space-time, see [7, 50]. The formalism might prove useful in situations like electromagnetic fields around relativistic stars or electromagnetic counterpart models of a merger of two neutron stars, see, e.g., [58, 60]. In such examples, an electromagnetic field has to be modeled in two different space-time regions. The tangential components of the electromagnetic fields are not necessarily continuous across the hypersurface separating those two regions. With the results of Chapter 3, the discontinuity is expressed in terms of a dipole density and an astrophysical interpretation can be sought after.

Another approach to solve Einstein's equations is the post-Newtonian (PN) approximation, where the field equations are expanded in a relativistic parameter (usually involving the inverse power of the velocity of light). Originally, Chandrasekhar and Fock, see [15, 30], developed the PN approximation as a limit of general relativity for weak gravitational fields and systems with small velocities (small compared to the velocity of light). Nevertheless, this method proved surprisingly effective also for highly relativistic regimes like binary black hole or neutron star mergers (for a recent review see [65]). The PN approximations as well as numerical results show that these binary systems emit gravitational waves. In the former approach, the energy loss due to gravitational radiation was derived to leading order in the aforementioned relativistic parameter. It was expressed in terms of the third time derivatives of the mass quadrupole moment of the related *Newtonian* configuration, see [24] for an account of the quadrupole formula. Thus, stars with a time dependent quadrupole moment are not stationary. But what is the end state of their evolution? An answer for a concrete example is given in [18] where the evolution of the PN Jacobi ellipsoids towards the Maclaurin ellipsoids is discussed.

The quadrupole formula gives also a necessary condition for the existence of stationary stars in a PN approximation: The third time derivative of the quadrupole moment of the Newtonian configuration must vanish. However, it does not imply that the lack of axially symmetry together with the rotation is a sufficient condition for the emission of gravitational waves. Still, the existence of non-axially symmetric, stationary and rotating solutions is disputed (often erroneously on the grounds of the quadrupole formula). If a non-axially symmetric, stationary and rotating solution with a constant mass quadrupole moment exists in Newtonian theory, then there is no contribution to the gravitational wave emission in leading order. The PN approximation of such a Newtonian solution is stationary at least up to 2.5-PN order. Even though, determining such solutions in Newtonian physics is difficult, a sequence of exact solution was found, namely the Dedekind ellipsoids. They preserve their shape in an inertial frame due to internal motion. Hence, the Dedekind ellipsoids, which are investigated in Chapter 5, are a natural starting point to try to answer the question whether non-axially symmetric, rotating and stationary solutions exist in general relativity (at least in a PN approximation). The 1-PN Dedekind ellipsoids are described in Chapter 6. Lindblom raised another question in conjunction with the existence in [49]: "Do such non-axisymmetric models have any other symmetries? For example, do such models always possess discrete symmetries such as reflections about an equatorial plane, or perhaps discrete rotations?" At least the Dedekind ellipsoids admit such discrete isometries. Moreover, the existence of non-axially symmetric solutions entails that they are possible end states of the evolution of stars. Nonetheless, stability is not ensued by the mere existence and has to be considered independently

(for a recent account on the stability of relativistic stars see, e.g., [31]).

The techniques and solutions mentioned above are global, i.e., the solutions describe an interior and an exterior region. However, it is not always necessary or desirable to find a global solution. If Einstein's equations are solved in a space-time region without any reference to its exterior, it has the following advantage: All conclusions, which are drawn for this solution, hold for all possible boundary data at the surface of the matter distribution. On the other hand, the properties of the exterior solution like asymptotic flatness or the matter content cannot be inferred. In Chapter 4 we study axially symmetric, stationary and rigidly rotating dust. We show that the interior solution of such dust configurations can be determined completely without reference to the exterior.

Results

Spherical condensers
In Chapter 2 we employ spherical symmetry to find a general relativistic formulation of a gravitating spherical condenser. This is a system of two concentric charged shells where the electromagnetic field is non-vanishing only between the shells. Nevertheless, we discuss the system of arbitrary numbers of shells first. The shells are constructed using the Israel formalism and are made of a charged perfect fluid. We derive the implications of the energy conditions depending on the total charge and position of the shells. For example, we show that a drop of the mass parameter in the space-time after crossing a shell does not necessarily entail a violation of the energy conditions. But the presence of horizons implies the violation of at least one energy condition. We prove that the inner shell can be made of dust, if the space-time between the shells is a piece of an extreme Reissner-Nordström space-time. In this case, an exterior shell satisfying the energy conditions can be found. However, it cannot be made of dust. Additionally, more exotic but interesting situations are studied, for instance, a gravitational field localized only between the shells.

Monopole and dipole shells
We construct in Chapter 3 the 4-current of a magnetic or electric test dipole density confined to a shell for a general background metric. We deduce the jump conditions of the Maxwell tensor and the 4-potential across the shell. We use them to prove the equivalence of the electromagnetic field of magnetic dipoles and electric charge currents outside of the shell. Our generalized Israel formalism is illustrated using the Schwarzschild disks as a background and two electromagnetic test fields. These are the asymptotically homogeneous electric/magnetic field and the field generated by a test charge at an arbitrary position. In this way, Schwarzschild disks endowed with different electric/magnetic dipole densities or charge densities are constructed. We interpret the resulting densities with the aid of the membrane paradigm. Afterwards a direct approach is taken. We prescribe a surface density, calculate the field and show the validity of the jump conditions. This is done for arbitrary dipole densities distributed on spherical shells in a Schwarzschild space-time.

The interior solution of dust configurations
The interior solution of axially symmetric, stationary and rigidly rotating dust is determined explicitly in Chapter 4. The metric is expressed in terms of the mass density along the axis of rotation. The results are used to prove the non-existence of homogeneous dust distributions. Additionally, we show that the mass density is always increasing perpendicular to the axis. Furthermore, we prove the non-existence of dust "stars" with a vanishing mass density at their surface.

PN Dedekind ellipsoids
After a short summary of the Newtonian ellipsoidal solutions in Chapter 5, we construct a family

of Dedekind ellipsoids in a 1-PN approximation in Chapter 6. This was done already by Chandrasekhar & Elbert in [22, 23]. However, we suggest a generalized version, which remedies several problems of the original solutions. Our family of solutions, contrary to the one proposed before, admits an axially symmetric, rigidly rotating limit as in Newtonian theory. The 1-PN Dedekind ellipsoids coincide with the 1-PN Maclaurin spheroids. The absence of such a limit in the Chandrasekhar & Elbert sequence raises the question whether the solutions in this sequence should actually be called 1-PN Dedekind ellipsoids. Moreover, the singularity present in the previous work can be removed or placed at different points along the sequence. This corroborates results regarding singularities in the parameter space for Jacobi and Maclaurin ellipsoids. Furthermore, a "Weyl-limit", i.e., an axially symmetric and static limit, can be found where the matter region is concentrated at the axis and a rod like-singularity is formed. We discuss the physical properties of the 1-PN Dedekind sequence like mass, angular momentum, the velocity field and the shape of the 1-PN ellipsoids in detail. For the latter two, we use the gravitomagnetic effects to explain the results, at least qualitatively. Additionally, we calculate the exterior solution for the metric.

Organization of the thesis

The thesis is organized as follows. In Chapters 2 and 3 electrodynamics in curved space-time is discussed. This consists of the three Papers [8], [39] and [38], which are denoted by the Roman numerals I, II III, respectively. In Chapter 4, the interior solution of certain dust configurations is studied. This incorporates the results presented in [37], subsequently denoted by Paper IV. After a brief introduction of ellipsoidal figures of equilibrium in Newtonian physics in Chapter 5, their 1-PN approximation is given in Chapter 6. The properties discussed in this chapter include the results on the axially symmetric and rigidly rotating limit published in [40], hereafter Paper V. Several formulas in this chapter exceed the length required for a comfortable reading (certainly a subjective quantity). Therefore, they are attached in the appendix. Additionally, we give in the appendix several "basic" formulas like the definition of the Lamé functions. At the same time, this fixes the convention used in this thesis.

We quote formulas and sections from Papers I to V as in the following examples: Equation (I.2) refers to Equation (2) in Paper I and Section I.II.2 refers to Section II.2 in Paper I. The table of content of the present thesis lists also the content of Papers I to V preserving the convention used therein.

The notation used in this thesis is defined in the beginning of the Papers or in the respective chapters.

CHAPTER

2

SPHERICAL CONDENSERS

Spherical Condensers are a standard example in classical Maxwell's theory. They consist of two concentric, charged spherical shells. An electromagnetic field is present only between the shells. Notwithstanding its simplicity and fundamental role in classical physics, a general relativistic spherical condenser was not yet discussed. Since the whole system is spherical symmetric, the vacuum regions are pieces of the Reissner-Nordström space-time. In order to study a "pure" condenser not affected by other gravitational sources, we focus on the case in which the central region is a part of the Minkowski space-time. Nevertheless, a central singularity is considered in some situations as well. The shells are modeled by a perfect fluid and are constructed employing the Israel formalism. We pay particular attention to the implications of the energy conditions. Thereby, we answer the questions where the shells can be situated, and how much charge can they carry in order to allow physically reasonable solutions. The results are given in our Paper I[1] which follows.

[1] A small correction regarding the strong energy condition was incorporated in Paper I. Thus, there are slight differences between the published article [8] and the text here.

Spherical Gravitating Condensers in General Relativity

J. Bičák and N. Gürlebeck
Institute of Theoretical Physics, Charles University, V Holešovičkách 2, 180 00 Praha 8 - Holešovice, Czech Republic and
Max Planck Institute for Gravitational Physics, Albert Einstein Institute, Am Mühlenberg 1, D-14476 Golm, Germany

By a spherical gravitating condenser we mean two concentric charged shells made of perfect fluids restricted by the condition that the electric field is nonvanishing only between the shells. Flat space is assumed inside the inner shell. By using Israel's formalism we first analyze the general system of N shells and then concentrate on the two-shell condensers. Energy conditions are taken into account; physically interesting cases are summarized in two tables, but also more exotic situations in which, for example, the inner shell may occur below the inner horizon of the corresponding Reissner-Nordström geometry or the spacetime is curved only inside the condenser are considered. Classical limits are mentioned.

PACS numbers: 04.20.-q;04.20.Jb;04.40.Nr
Keywords: charged shells, gravitating spherical condenser

I. INTRODUCTION

Modeling physical systems by 2-dimensional thin shells sweeping out 3-dimensional timelike hypersurfaces in spacetime found numerous applications in general relativity and cosmology, in particular after the work of Israel [1] and his collaborators (see [2] for a more recent account). The material properties are characterized in terms of geometrical quantities like the jumps of the external curvature of the hypersurfaces. In contrast to pointlike or 1-dimensional sources this idealization is mathematically well defined [3].

In the following we shall be interested in shells made of a (2-dimensional) perfect fluid with a surface charge density. Israel's method was generalized to thin charged shells without pressure by de la Cruz and Israel [4]. A comprehensive treatment of charged shells with pressure satisfying the polytropic equation of state was given by Kuchař [5]; Chase [6] placed no restriction on the equation of state and a spherically symmetric Reissner-Nordström field inside the shell was admitted.

Until now a number of papers employed charged thin shells to tackle various problems, mostly under the assumption of spherical symmetry. For illustration: Boulware [7] studied the time evolution of such shells and showed that their collapse can form a naked singularity if and only if the matter density is negative, in Ref. [8] the third law of black hole mechanics was investigated by a charged shell collapsing in a Reissner-Nordström field. Going over to most recent contributions (where many references to older literature can be found) , the shells are often renamed "membranes" or "bubbles;" the equations of state become more exotic but the formalism remains. In Ref. [9] the stabilizing effects of an electric field inside a neutral shell made of dust or from a "string gas" (equation of state $p = -\frac{1}{2}\sigma$) were studied using Israel's formalism, whereas in Ref. [10] the authors analyze charged spherical membranes by the direct integration of the Einstein field equations with δ-function sources (and show coincidences with the results of [1] and [6]). In particular, it is demonstrated in [10] that acceptable parameters can be chosen such that stable charged membranes producing the over-extreme Reissner-Nordström geometry with "repulsive gravity" effects exist. Gravity becomes repulsive also with uncharged "tension shells" if the tension is sufficiently high [11].

From our perspective we wish to mention yet the work of King and Pfister [12] in which electromagnetic dragging ("Thirring") effects are investigated by considering systems of two concentric spherical shells. Before (small) angular velocities are applied to the shells, the authors study the static two-shell model as we do in the present paper. However, in [12] for the purpose of dragging effects it was sufficient to assume a special system: the interior shell carries charge and tension but no rest mass, the exterior shell carries mass but no charge. No treatment of spherical condensers in the context of general relativity appears to have been given so far.

What, in fact, do we mean by such condensers? We consider two concentric spherical charged shells made from 2-dimensional perfect fluids with either pressure or tension, with arbitrary mass and charge densities. All parameters entering the problem are restricted by just one condition: the radial field may exist only in the region between the shells; of course, we take flat space inside the inner shell. We also regard energy conditions and allow the inner shell to occur below the inner horizon of the Reissner-Nordström geometry. The existence of the electric field between the shells is the basic feature of our definition of a condenser in general relativity. We shall see how our results corroborate various expressions for a quasilocal mass in Reissner-Nordström spacetime. For a specific example of a plane gravitational condenser with a positive cosmological constant, see [13].

The gravitating condensers are primarily of theoretical interest. Since, however, their total charge vanishes, they may be closer to astrophysical models than objects carrying a net charge. Indeed, some numerical calculations [14] indicate that the gravitational collapse to neutron stars can lead to a charge separation but the whole system of

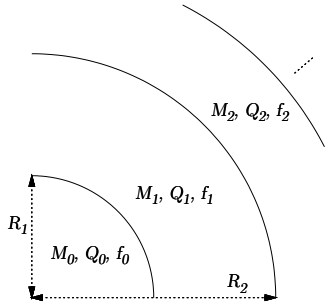

FIG. 1. A sketch of the sequence of shells: M_A, Q_A are the masses and charges in the respective spaces and R_A the radii of the shells. The metric function f_A will only play a role in Sec. III.

star and envelope is neutral. A charge separation can also arise in plasma accreting into a black hole [15] (see also [16]). Recently, detailed numerical investigations of the collapse of a stellar core with a net charge were performed [17, 18] with understanding, however, that the total charge of the star may be zero.

Throughout the text geometrical units with $G = c = 1$ are used.

II. THE CLASSICAL SYSTEM

In order to introduce the notation and gain an intuition we now first analyze briefly a spherically symmetric condenser in Newton's gravity and Maxwell's electromagnetism in flat space. Let us consider charged perfect fluid spherical thin shells Σ_A $(A = 1, 2, \ldots, N)$ at radii R_A $(R_A < R_{A+1})$ endowed with surface mass densities σ_A, surface charge densities η_A and (2-dimensional) homogeneous surface pressures p_A. M_A $(A = 0, \ldots, N)$ denotes the total mass enclosed by a sphere with a radius $r \in (R_A, R_{A+1})$ with $R_0 = 0$ and $R_{N+1} = \infty$. The charges Q_A are defined analogously, see Fig. 1. After the solution for a general system with an arbitrary number of shells is obtained we discuss the case of a condenser $(N = 2,\ M_0 = Q_0 = Q_2 = 0,\ Q_1 = Q)$ in full detail. The gravitational potentials U_A and the electrostatic potentials Φ_A $(A = 0, \ldots, N)$ in spherical coordinates read

$$\begin{aligned} U_A(r) &= -\frac{M_A}{r} + C_A, \\ \Phi_A(r) &= \frac{Q_A}{r} + D_A \quad \text{for } r \in [R_A, R_{A+1}). \end{aligned} \tag{1}$$

The constants C_A and D_A are determined by the choice $D_N = C_N = 0$ so that both U_N and Φ_N vanish in infinity and by the requirement of continuity of the potentials across the shells. The surface densities can be determined from the jumps of the normal derivatives of the potentials across the shells Σ_A. This yields $(A = 1, \ldots, N$ here and in the remainder of this section)

$$\sigma_A = \frac{M_A - M_{A-1}}{4\pi R_A^2}, \quad \eta_A = \frac{Q_A - Q_{A-1}}{4\pi R_A^2}. \tag{2}$$

In order to obtain a stationary system the sum of all forces acting on a small element of each Σ_A should vanish. The forces acting on a surface element $\mathrm{d}S_A = R_A^2 \mathrm{d}\Omega = R_A^2 \sin^2\theta \mathrm{d}\theta \mathrm{d}\varphi$ have only radial components because of the symmetry. The gravitational forces are given by $\mathrm{d}F_{(A)G} = -\frac{(M_A^2 - M_{A-1}^2)}{8\pi R_A^2}\mathrm{d}\Omega$. These are always pointing inward for positive surface mass densities σ_A. The electrostatic contributions are $\mathrm{d}F_{(A)E} = \frac{(Q_A^2 - Q_{A-1}^2)}{8\pi R_A^2}\mathrm{d}\Omega$. The pressure forces $\mathrm{d}F_{(A)p}$ on $\mathrm{d}S_A$ are given by $2p_A R_A \mathrm{d}\Omega$; these point always outwards for positive pressures p_A and inwards for negative pressures (tension).

The equilibrium is achieved if the total force on each $\mathrm{d}S_A$ vanishes:

$$16\pi R_A^3 p_A = M_A^2 - M_{A-1}^2 - Q_A^2 + Q_{A-1}^2. \tag{3}$$

Equations (2) and (3) give a complete solution with $3N+2$ free parameters; e.g., M_A, Q_A can be chosen for $A = 0, \ldots, N$ and R_A for $A = 1, \ldots, N$.

III. THE EINSTEIN-MAXWELL SYSTEM

Now we turn to spherical condensers in the Einstein-Maxwell theory. First we consider a more general system of N shells Σ_A as in the Newtonian case, then we analyze thoroughly just the condensers $(N = 2, M_0 = Q_0 = Q_2 = 0, Q_1 = Q)$. By Σ_A we now understand 3-dimensional timelike hypersurfaces representing the histories of the individual shells in the spacetime.

Since the system is spherically symmetric and between the thin spherical shells there is electrovacuum, the spacetime must consist of $N+1$ pieces, V_A, $A = 0, \ldots, N$, of Reissner-Nordström spacetimes with the following line elements:

$$\begin{aligned} \mathrm{d}s_A^2 =& -f_A(r_A)\mathrm{d}t_A^2 + \frac{1}{f_A(r_A)}\mathrm{d}r_A^2 \\ &+ r_A^2(\mathrm{d}\theta^2 + \sin^2\theta \mathrm{d}\varphi^2), \\ f_A(r_A) =& 1 - \frac{2M_A}{r_A} + \frac{Q_A^2}{r_A^2}, \end{aligned} \tag{4}$$

where coordinates $x^\mu_{(A)}$ have ranges $t_A \in (-\infty, \infty)$, $r_A \in [R_{A-}, R_{A+})$, $\theta \in [0, \pi]$, $\varphi \in [0, 2\pi)$ and the constants M_A and Q_A denote the mass and the charge parameters; we take $R_{1-} = 0$ and $R_{N+} = \infty$. In general the coordinates t_A jump across the shells (related to the jumps of the red shift factors due to the massive shells), but R_{A+} and $R_{(A+1)-}$ must coincide since they have an invariant geometrical meaning giving the proper areas of

the shells; so we set $R_{A+} = R_{(A+1)-} \equiv R_{A+1}$ and drop the index A for the radial coordinate r. The angles θ and φ change smoothly due to the symmetry.

In order to obtain timelike hypersurfaces Σ_A, it is assumed that $f_A(R_{A+1}) > 0$ and $f_{A+1}(R_{A+1}) > 0$, i.e., the shells are either situated in the exterior of the outer event horizon of the respective piece of the Reissner-Nordström spacetime or inside the inner event horizon.

On the hypersurfaces Σ_A "inner" coordinates $(\xi^c_{(A)}) = (\tau_A, \theta, \varphi)$ are chosen, τ_A is the proper time of an observer with fixed (R_A, θ, φ); $\mathrm{d}\tau_A = [f_A(R_A)]^{\frac{1}{2}}\mathrm{d}t_A = [f_{A+1}(R_A)]^{\frac{1}{2}}\mathrm{d}t_{A+1}$. The metric in V_A is denoted by $g_{(A)\mu\nu}$. Indices of tensor quantities on Σ_A are labeled by $a, b, \ldots$. The metrics $h_{(A)ab}$ induced by $g_{(A-1)\mu\nu}$ and $g_{(A)\mu\nu}$ on Σ_A from both sides read

$$h_{(A)ab}\mathrm{d}\xi^a_{(A)}\mathrm{d}\xi^b_{(A)} = -\mathrm{d}\tau_A^2 + R_A^2(\mathrm{d}\theta^2 + \sin^2\theta\mathrm{d}\varphi^2). \quad (5)$$

The electric field is given by

$$F^{\mu\nu}_{(A)} = \frac{Q_A}{r^2}(\delta^\mu_t\delta^\nu_r - \delta^\mu_r\delta^\nu_t) \text{ for } r \in [R_A, R_{A+1}). \quad (6)$$

The hypersurfaces Σ_A are endowed with surface mass densities σ_A, surface pressure densities p_A and surface charge currents $s^a_{(A)}$. The tangential electrical *net* current on Σ_A reads (see [5])

$$\begin{aligned} 4\pi s_{(A)c} =& \left(F_{(A)\alpha\beta}\frac{\partial x^\alpha_{(A)}}{\partial\xi^c_{(A)}}n^\beta_{(A)} \right. \\ & \left. -F_{(A-1)\alpha\beta}\frac{\partial x^\alpha_{(A-1)}}{\partial\xi^c_{(A-1)}}n^\beta_{(A-1)} \right)\Big|_{r=R_A} \\ =& \frac{Q_{A-1}-Q_A}{R_A^2}\delta^\tau_c, \end{aligned} \quad (7)$$

where $n^\alpha_{(A-1)}$ ($n^\alpha_{(A)}$) denotes the outwards pointing normal of Σ_A as seen from V_{A-1} (V_A). There can be more currents representing counter-rotating charges whose net contribution to the motion cancels out so that the spherical symmetry is preserved.

The extrinsic curvature of Σ_A defined respectively by $x^\mu_{(A-1)}$, $g_{(A-1)\mu\nu}$ and $x^\mu_{(A)}$, $g_{(A)\mu\nu}$ is denoted by $K_{(A-1)cd}$ and $K_{(A)cd}$, its jump $K_{(A)cd} - K_{(A-1)cd}$ across Σ_A by $[K_{(A)cd}]$, analogously for its trace $K_A = K_{(A)cd}h^{cd}_{(A)}$. The surface stress-energy tensor $t_{(A)ab}$ on Σ_A is now determined by [1, 2, 5]

$$t_{(A)cd} = \frac{1}{8\pi}([K_{(A)cd}] - h_{(A)cd}[K_A]). \quad (8)$$

In our case of spherical shells the jumps are given by

$$\begin{aligned} [K_{(A)cd}] &= L_A(R_A)\mathrm{diag}\Big(\frac{L'_A(R_A)}{L_A(R_A)}, -R_A, -R_A\sin^2\theta\Big), \\ [K_A] &= -L'_A(R_A) - \frac{2}{R_A}L_A(R_A), \\ L_A(r) &= f_A^{\frac{1}{2}}(r) - f_{A-1}^{\frac{1}{2}}(r); \end{aligned} \quad (9)$$

here a prime denotes a derivative with respect to r. In the case of a perfect fluid at rest its 4-velocity is simply $u^c_{(A)} = \delta^c_\tau$ and the stress-energy tensor reads

$$t_{(A)cd} = (\sigma_A + p_A)u_{(A)c}u_{(A)d} + p_A h_{(A)cd}. \quad (10)$$

The surface mass density and the surface pressure density can be read off Eqs. (8)-(10):

$$\sigma_A = -\frac{1}{4\pi R_A}L_A(R_A), \quad p_A = \frac{1}{8\pi}L'_A(R_A) - \frac{\sigma_A}{2}. \quad (11)$$

We shall use extensively the last two relations. To get a physical insight, consider just one charged shell of radius R with the Minkowski space inside and Reissner-Nordström field with parameters M, Q outside. Equation (11) then implies

$$\sigma = \frac{1}{4\pi R}\left(1 - \sqrt{1 - \frac{2M}{R} + \frac{Q^2}{R^2}}\right), \quad (12a)$$

$$p = \frac{\overline{M}^2 - Q^2}{16\pi R^2(R - \overline{M})}, \quad (12b)$$

where $\overline{M} = 4\pi R^2\sigma$ is the rest mass of the shell. The total energy of the shell at rest with a fixed charge Q and a fixed pressure p is given by M and can be interpreted as function of R. The result (12b) coincides precisely with Eq. (51) in [5]; this follows from the "second" equilibrium condition $M'(R) = 0$, the total energy is extremal in equilibrium. The expression for σ (12a) follows directly from the "first" equilibrium condition, Eq. (50) in [5] (in which a typographical error must be corrected in the last term on the right-hand side), which represents conservation of the total energy of the shell at rest given by

$$M(R) = \overline{M} + \frac{Q^2}{2R} - \frac{\overline{M}^2}{2R}. \quad (13)$$

The first term is the rest energy of the shell, the second describes the electromagnetic interaction energy of the particles of the shell, the last can be interpreted as the gravitational interaction energy — see [5] for more details on the subtleties of such an interpretation.

IV. CONDENSERS

A. Classical condensers

In the case of a condenser ($N = 2, M_0 = Q_0 = Q_2 = 0, Q_1 = Q$) the Eqs. (2) and (3) simplify to

$$\sigma_1 = \frac{M_1}{4\pi R_1^2}, \qquad \sigma_2 = \frac{(M_2 - M_1)}{4\pi R_2^2}, \quad (14a)$$

$$\eta_1 = \frac{Q}{4\pi R_1^2}, \qquad \eta_2 = -\frac{Q}{4\pi R_2^2}, \quad (14b)$$

$$16\pi R_1^3 p_1 = M_1^2 - Q^2,$$
$$16\pi R_2^3 p_2 = (M_2^2 - M_1^2) + Q^2. \tag{14c}$$

In this case the inner shell is not influenced by the field of the outer shell and must be in equilibrium in its own gravitational and electrical field. This can be achieved even with vanishing pressure if $M_1^2 = Q^2$. However, the outer shell is always attracted by gravity and Coulomb force due to the inner shell. Therefore, the outer shell cannot consist of dust and p_2 must be positive to prevent the collapse. Let us also remark that the limit to an electrostatic dipole shell ($R_1 \to R_2$, $Q \to \infty$) implies that either the surface pressure density or the surface mass density is also unbound. In this case the net force acting on a volume element containing both shells Σ_A has to be carefully treated to obtain physically meaningful results.

B. Einstein-Maxwell condensers

Let us now restrict to the case of a relativistic condenser. Primarily we wish to investigate whether the shells can be made of dust and whether the inner shell can be hidden below the horizon. Since the spacetime outside of the exterior shell is part of a Schwarzschild spacetime the radius of the outer shell must satisfy $R_2 > 2M_2$, so no horizon can exist there. In the following we will measure all quantities in units of M_1 and denote them by small Latin letters or by a hat in the case of the pressure and the mass density, e.g., $R_A = M_1 r_A$ and $\sigma_A = \frac{\hat{\sigma}_A}{M_1}$. In the case of positive M_1 this notation does not bear the risk of any confusion; however, if $M_1 \leq 0$ and $Q^2 > 0$, then $\sigma_1 < 0$. We assume $M_1 > 0$ in the remainder. The stability of such shells was discussed in [5, 6]. The stability considerations apply for each shell entirely analogously in our case and so we do not repeat them here.

We obtain the densities and pressures from Eq. (11):

$$\begin{aligned}
\hat{\sigma}_1 =& \frac{1}{4\pi r_1^2}\left(r_1 - \sqrt{r_1^2 - 2r_1 + q^2}\right),\\
\hat{s}^c_{(1)} =& \frac{q}{4\pi r_1^2}\delta^c_\tau,\\
\hat{p}_1 =& \frac{1}{8\pi r_1}\left((r_1-1)(r_1^2 - 2r_1 + q^2)^{-\frac{1}{2}} - 1\right),
\end{aligned} \tag{15a}$$

$$\begin{aligned}
\hat{\sigma}_2 =& \frac{1}{4\pi r_2^2}\left(\sqrt{r_2^2 - 2r_2 + q^2} - \sqrt{r_2^2 - 2m_1 r_2}\right),\\
\hat{s}^c_{(2)} =& -\frac{q}{4\pi r_1^2}\delta^c_\tau,\\
\hat{p}_2 =& \frac{1}{8\pi r_2}\Big((r_2 - m_2)\left(r_2^2 - 2m_2 r_2\right)^{-\frac{1}{2}}\\
&- (r_2 - 1)\left(r_2^2 - 2r_2 + q^2\right)^{-\frac{1}{2}}\Big).
\end{aligned} \tag{15b}$$

In the case of an under-extreme Reissner-Nordström spacetime, $q^2 < 1$, the additional conditions $r_1 < r_- = 1 - \sqrt{1-q^2}$ or $r_1 > r_+ = 1 + \sqrt{1-q^2}$ must be considered; the same must hold for r_2 because the shells can be at rest only in the regions where the Killing vector $\frac{\partial}{\partial t}$ is timelike. Furthermore, $r_2 > 2m_2$ must always be satisfied.

1. The inner shell

The energy conditions (dominant, weak, null, strong) and their implications are investigated below. Even though the calculations are in principle basic, they are tedious, so they are not shown here. Instead, the results are summarized in Table I in full detail. Looking solely at the inner shell yields the generic case of one charged, spherical thin shell and thus it is of interest of its own.

The null and the weak energy conditions are equivalent in this setting as shown in Table I. Therefore, we refer to the null energy condition only. From Table I it becomes clear that positive mass shells exist for all radii (though for a given charge of the shell there exists a minimal radius of $\frac{q^2}{2}$). In particular, $r_1 < 1$, $q^2 < 1$ can always be chosen; the shell then lies below the inner horizon. If, additionally, the second shell is chosen to be situated outside the outer horizon, which can always be achieved, the two shells of the condenser will be separated by two horizons. A massless shell is obtained for $q^2 = 2r_1$; this lies always below the inner horizon if there is one.

If the energy conditions are to be satisfied, then the radius r_1 has to have a lower bound of $\frac{8}{9}$. However, as long as $r_1 < 1$ we have $q^2 > 1$. Thus, the spacetime between the two shells is a piece of an over-extreme Reissner-Nordström spacetime and no horizons are present. If $r_1 > 1$, then $q^2 < 1$ is possible, but no horizon is present here either, since the inner shell lies outside of the outer horizon. Therefore, *horizons can only be present if some energy condition is violated*. In particular the tension (negative pressure) has to be high if the inner shell is situated below the inner horizon. This resembles the problem considered by Novikov: the matter of a static charged sphere below the inner horizon of the Reissner-Nordström geometry must have a high tension [19]. If additionally the charge q is chosen arbitrarily close to zero, a lower bound for r_1 of 2 for the null and stromg energy condition and of $\frac{25}{12}$ for the dominant energy condition is implied.

The pressure $\hat{p}_1$ is always non-negative if the spacetime between the shells is a piece of an under-extreme Reissner-Nordström spacetime and the inner shell is situated outside the outer horizon. In all other cases it is negative. Hence, a shell producing an over-extreme Reissner-Nordström spacetime or a shell situated below the inner horizon can only be supported by tension. In the first case contrary to the second all energy conditions can be satisfied.

If the inner shell is made of dust then – similarly to the Newtonian case – the spacetime between the two shells corresponds to a piece of an extremely charged Reissner-

Energy condition		Range of r_1	Range of q^2
Positive mass density	$\hat{\sigma}_1 \geq 0$	$r_1 \in (0, 2]$	$q^2 \in (2r_1 - r_1^2, 2r_1]$
		$r_1 \in (2, \infty)$	$q^2 \in [0, 2r_1]$
Null	$\hat{\sigma}_1 + \hat{p}_1 \geq 0$	$r_1 \in [\frac{8}{9}, 1)$	$q^2 \in [q_{2-}^2, q_{2+}^2]$[a]
		$r_1 \in [1, 2]$	$q^2 \in (2r_1 - r_1^2, q_{2+}^2]$
		$r_1 \in (2, \infty)$	$q^2 \in [0, q_{2+}^2]$
Weak	$\hat{\sigma}_1 \geq 0$, $\hat{\sigma}_1 + \hat{p}_1 \geq 0$		the same as null
Dominant	$\hat{\sigma}_1 \geq \lvert\hat{p}_1\rvert$	$r_1 \in [\frac{8}{9}, 1)$	$q^2 \in [q_{2-}^2, q_{2+}^2]$
		$r_1 = 1$	$q^2 \in (1, \frac{5}{4}]$
		$r_1 \in (1, \frac{25}{12}]$	$q^2 \in \left[\frac{r_1}{8}\left(20 - 3r_1 - 3\sqrt{8r_1 + r_1^2}\right), q_{2+}^2\right]$
		$r_1 \in (\frac{25}{12}, \infty]$	$q^2 \in [0, q_{2+}^2]$
Strong	$\hat{\sigma}_1 + 2\hat{p}_1 \geq 0$, $\hat{\sigma}_1 + \hat{p}_1 \geq 0$	$r_1 \in (1, 2]$	$q^2 \in (2r_1 - r_1^2, r_1]$
		$r_1 \in (2, \infty)$	$q^2 \in [0, r_1]$

[a] $q_{2\pm} = \frac{r_1}{8}\left(12 - 3r_1 \pm \sqrt{9r_1^2 - 8r_1}\right)$

TABLE I. Energy conditions for the inner shell. The table is to be read as follows: For example, the first two lines mean that the mass density σ_1 is positive if either $0 < R_1 \leq 2M_1$ and $2M_1R_1 - R_1^2 < Q^2 \leq 2M_1R_1$ or if $R_1 > 2M_1$ and $0 \leq Q^2 \leq 2M_1R_1$.

Nordström spacetime, i.e., $|q| = 1$ and the shell must be situated outside the horizon, $r_1 > 1$. The mass density evaluates in the extremely charged case to $\hat{\sigma}_1 = \frac{1}{4\pi r_1^2} > 0$. Since $\hat{p}_1 = 0$, all energy conditions (null, dominant and strong) are satisfied by such a shell.

2. The outer shell

The situation for the exterior shell is more involved since more parameters have to be taken into account. Therefore, we treat in detail only the case when the inner shell is made of charged dust, i.e., $\hat{p}_1 = 0$ – this is sufficient to exhibit some generic features of the condensers. As one easily checks the pressure $\hat{p}_2$ is always positive if $r_1 > 1$ in order to prevent the collapse. Thus, a positive mass density ensures the weak energy condition and vice versa; similarly, the null energy condition is equivalent to the strong energy condition. Consequences of all energy conditions are summarized in Table II. It is seen that, *a condenser can consist of an inner shell made of charged dust and an exterior shell* ($r_2 > r_1$), *both shells satisfying all the energy conditions.*

It is worth noting, that, in all discussed cases included in Table II a mass parameter M_2 can be chosen smaller than M_1 for any radius r_2. This is because the electromagnetic field decreases the value of a (quasi) local mass energy at given r. Indeed, various results for quasilocal masses like those of Hawking, Penrose, Brown and York, and others (though not Komar) lead to the same result for the mass energy inside a sphere of radius r in Reissner-Nordström spacetime

$$E(r) = M - \frac{Q^2}{2r}, \tag{16}$$

(see, e.g., [20–22]). This corresponds to the fact that the charge weakens the strength of the gravitational field (recall, for example, that the surface gravity of an extreme Reissner-Nordström black hole vanishes). Let us also note that the formula (16) does not contradict the conservation law (13) since there $M(R)$ represents the total Schwarzschild mass outside the shell with radius R and flat spacetime inside, whereas (16) is the expression for the energy of the Reissner-Nordström field inside the radius r (cf. also [22]).

If both shells are made of dust, one obtains $m_2 = 0$ and $\hat{\sigma}_2 = -\frac{1}{4\pi r_2^2}$. That surely violates all energy conditions but is interesting in the sense that the curvature is localized just between the two shells and has no effect on the outside world — similarly to the case of a sandwich plane gravitational wave. However, the exterior shell can easily be made of dust without admitting a negative mass density if a non vanishing field outside ($Q_2 \neq 0$) is allowed.

Next, we discuss some properties of the outer shell without any assumption about the inner shell. If the exterior shell is made of dust, though not necessarily the inner shell, then an equation for q^2 is implied. The positivity of q^2 requires $m_2 \leq 1$. The case $m_2 = 1$ leads to $q = 0$ and $\hat{\sigma}_2 = 0$, which contradicts our definition of a condenser. However, for $m_2 < 1$ the mass density $\hat{\sigma}_2$ is negative and all energy conditions are violated. Thus, *the exterior shell cannot be made of dust if any energy condition is to be satisfied.*

Finally we also allow a non vanishing pressure $\hat{p}_2$. The mass density $\hat{\sigma}_2$ is positive if either $m_2 > 1$ or $m_2 \leq 1, q^2 \geq 2r_2(1 - m_2)$. Even though the mass density is positive the Schwarzschild mass outside can again be smaller than between the shells, if the charge is sufficiently large, cf. (16). The Schwarzschild mass outside can, in fact, be negative but then the inner shell must have $\hat{\sigma}_1 < 0$. Furthermore, for $m_2 > 0$ all energy con-

Energy condition		Range of r_2	Range of m_2
Positive mass density	$\hat{\sigma}_2 \geq 0$	$r_2 \in (1, \infty)$	$m_2 \in [1 - \frac{1}{2r_2}, \frac{r_2}{2})$
Null	$\hat{\sigma}_2 + \hat{p}_2 \geq 0$	$r_2 \in (1, 2]$	$m_2 \in [m_{2,1+}, \frac{r_2}{2})$[a]
		$r_2 \in (2, \infty)$	$m_2 \in [m_{2,1-}, \frac{r_2}{2})$
Weak	$\hat{\sigma}_2 \geq 0$, $\hat{\sigma}_2 + \hat{p}_2 \geq 0$	the same as positive mass density	
Dominant	$\hat{\sigma}_2 \geq \lvert\hat{p}_2\rvert$	$r_2 \in [\frac{3+\sqrt{5}}{2}, \infty)$	$m_2 \in [m_{2,2-}, m_{2,2+}]$[b]
Strong	$\hat{\sigma}_2 + 2\hat{p}_2 \geq 0$, $\hat{\sigma}_2 + \hat{p}_2 \geq 0$	the same as null	

[a] $m_{2,1\pm} = \frac{2}{9r_2}(-2 + 2r_2 + r_2^2 \pm \sqrt{4 - 8r_2 + 9r_2^2 - 5r_2^3 + r_2^4})$

[b] $m_{2,2\pm} = \frac{2}{25r_2}(-2 + 6r_2 + 3r_2^2 \pm \sqrt{4 - 24r_2 + 49r_2^2 - 39r_2^3 + 9r_2^4})$

TABLE II. Energy conditions for the exterior shell and ranges of r_2 and m_2.

ditions can be satisfied for the outer shell with $q^2 < 1$ (under-extreme case) even if its radius $r_2 < r_-$ (i.e., r_2 is below r_- which would be the location of the inner horizon corresponding to the inner shell if the outer shell were not there). However, the inner shell violates then at least some energy conditions as discussed above. To avoid this we may consider just the under-extreme Reissner-Nordström field instead of the inner shell. Then the "outer" shell can satisfy all energy conditions. Interestingly, in this way we construct a spacetime which is Schwarzschild outside the outer (physical) shell inside of which then is just a naked singularity with $M_1^2 > Q^2$. Nevertheless, such a configuration cannot be formed by a dynamical process from Cauchy data without a naked singularity.

In the classical regime $r_1, r_2 \gg \max[1, m_2]$ the standard classical results (14) are retrieved.

ACKNOWLEDGMENTS

We thank Tomáš Ledvinka for discussions and the Albert Einstein Institute for kind hospitality. JB acknowledges the partial support from Grant No. GACR 202/09/00772 of the Czech Republic, of Grants No. LC06014 and No. MSM0021620860 of the Ministry of Education. NG was financially supported by the Grants No. GAUK 116-10/258025 and No. GACR 205/09/H033.

[1] W. Israel, Nuov, Cim. B**44**, 1 (1966); Errata: B**48**, 463 (1967)
[2] C. Barrabés and W. Israel, Phys. Rev. D **43**, 1129 (1991)
[3] R. Geroch and J. Traschen, Phys. Rev. D **36**, 1017 (1987)
[4] V. de la Cruz and W. Israel Nuov. Cim. A**51**, 744 (1967)
[5] K. Kuchař, Czech. J. Phys. B**18**, 435 (1968)
[6] J.E. Chase, Nuov. Cim. B**67**, 136 (1970)
[7] D.G. Boulware, Phys. Rev. D **8**, 2363 (1973)
[8] Ch.J. Farrugia and P. Hájíček, Commun. math. Phys. **68**, 291 (1979)
[9] E.I. Guendelman and I. Shilon, Class. Quantum Grav. **26**, 045007 (2009)
[10] V.A. Belinski, M. Pizzi, and A. Paolino, Int. J. Mod. Phys. D **18**, 513 (2009)
[11] J. Katz and D. Lynden-Bell, Class. Quantum Grav. **8**, 2231 (1991)
[12] M. King and H. Pfister, Phys. Rev. D **63**, 104004 (2001)
[13] J. Novotný and J. Horský, Czech. J. Phys.**24**, 718 (1974)
[14] J.R. Wilson, in Seventh Texas Symposium on Relativistic Astrophysics, eds. P.G. Bergmann, E.J. Fenyves and L. Motz, Annals of the New York Academy of Sciences Vol. 262, (New York Academy of Science, New York, 1975)
[15] R. Ruffini and J.R. Wilson, Phys. Rev. D**12**, 2959 (1975)
[16] R. Ruffini, J.D. Salomon, J.R. Wilson, and S.-S. Xue, Astron. Astrophys. **359**, 855 (2000)
[17] C.R. Ghezzi, Phys. Rev. D**72**, 104017 (2005)
[18] C.R. Ghezzi and P.S. Letelier, Phys. Rev. D**75**,024020 (2007)
[19] I.D. Novikov, JETP **59**, 262 (1970)
[20] K.P. Tod, Proc. R. Soc. London A **388**, 457 (1983)
[21] G. Bergqvist, Class. Quantum Grav. **9**, 1752 (1992)
[22] S. Bose and N. Dadhich, Phys. Rev. D **60**, 064010 (1999). See also N. Dadhich, Curr. Sci. **76**, 831 (1999), arXiv: gr-qc/9705037v1

CHAPTER

3

MONOPOLE AND DIPOLE LAYERS

In classical Maxwell theory, particularly in electrostatics, the introduction of monopole (charge) and dipole layers proves very useful. A mathematical reason is that all Dirichlet or Neumann boundary value problems for the Laplace equation can be solved using those two types of layers, see, e.g., [35]. They also play an important role in physics, especially in surface and charge separation phenomena. Because of this, charged shells are discussed widely in the literature including general relativity. So far, however, dipole shells in curved space-times have been neglected which is remedied in this chapter. To this end a generalization of the Israel formalism, see, e.g., [43, 46], is developed in Paper II, i.e., the article [39] below. In this formalism, the matter content, namely the dipole distribution on a shell, ensues from the jumps of the field and the potential across a hypersurface similarly to Maxwell's theory. The formalism is described for general backgrounds and test fields. It can be used to construct disk sources for vacuum space-times endowed with electric or magnetic test dipoles.

Subsequently, we use in Paper III (see our Paper [38]) a direct approach for spherical shells in a spherically symmetric space-time. The charge and dipole densities do not share this symmetry and can be arbitrary.

Monopole and dipole layers in curved spacetimes: formalism and examples

Norman Gürlebeck* and Jiří Bičák†
Institute of Theoretical Physics, Charles University, Prague, Czech Republic

Antonio C. Gutiérrez-Piñeres‡
Facultad de Ciencias Básicas, Universidad Tecnológica de Bolívar, Cartagena de Indias, Colombia
(Dated: May 5, 2011)

The discontinuities of electromagnetic test fields generated by general layers of electric and magnetic monopoles and dipoles are investigated in general curved spacetimes. The equivalence of electric currents and magnetic dipoles is discussed. The results are used to describe exact "Schwarzschild disk" solutions endowed with such sources. The resulting distributions of charge and dipole densities on the disks are corroborated using the membrane paradigm.

PACS numbers: 04.20.-q;04.20.Jb;04.40.Nr
Keywords: monopole and dipole layers, electrodynamics in curved background, thin massive disks

I. INTRODUCTION

The investigation of electromagnetic fields coupled to strong gravitational fields have an interest from both theoretical perspectives and from a variety of applications in astrophysics. Examples on the theory side include studies of gravitational collapse of charged configfigurations (see, e.g., [1, 2]), of the validity of the cosmic censorship conjecture [3], of the existence and properties of quasi black holes and wormholes (for recent accounts, see, e.g., [4, 5] and references therein), membranes producing repulsive gravity [6], and of many other issues. Very often analytical works employ, as tractable physical models, 2-dimensional thin shells sweeping out 3-dimensional timelike hypersurfaces. Recently, we used this idealization to construct "spherical gravitating condensers" – two concentric charged shells made of perfect fluids (satisfying energy conditions) under the condition that the electric field is non-vanishing only between the shells (see [7] and further references on charged shells therein).

The literature on electromagnetic fields in relativistic astrophysics[1] is vast. Here we restrict ourselves to referring to several monographs dealing in detail with black-hole electrodynamics, e.g., [10–12], and we mention the relatively recent work [13, 14] on electromagnetic fields around compact objects in which various papers are also summarized. In [13, 14] solutions to the Maxwell equations are presented both in the interior and outside a rotating neutron star and the matching conditions of the electromagnetic field at the stellar surface are analyzed in detail. The fields are not continuous across the stellar surface which gives rise to charges and currents.

In the present paper we study electromagnetic sources distributed on shells in curved spacetimes in general, considering in particular possible discontinuities of the electromagnetic field across the shells. The sources discussed are layers with monopole or dipole currents. As far as we are aware electric or magnetic dipole layers and the matching conditions for their fields were not studied before in the context of general relativity.

In general, in case of dipoles the currents and the electromagnetic field tensor will be distribution valued. This implies products of distributions in the stress-energy tensor. In order to avoid this, one can treat the electromagnetic field as a test field and solve the Maxwell equations in a given background metric. In many astrophysical situations this approach is well justified since typically the averaged energy density of the electromagnetic field is much smaller than that of the gravitational field. This approach is followed here and thus only the standard theory of generalized functions is used[2].

In another work [17] we discuss spherical thin shells endowed with arbitrary, not necessarily spherical distributions of charge or dipole densities in a Schwarzschild spacetime. There it was possible to employ the results of [18] to calculate the fields directly and read off their discontinuities across the shell. In the present paper we generalize the jump conditions to general backgrounds and general hypersurfaces. As a by-product of those jump conditions the equivalence of the external fields of magnetic dipoles and certain electric charge currents is proven in general. For elementary dipoles this was already known in special backgrounds like the Kerr spacetime [19].

The jump conditions can be used to obtain massive disks endowed with charge and dipole densities using the Israel-Darboux formalism. In the examples studied here, we use the Schwarzschild disk spacetime as

* norman.guerlebeck@gmail.com
† jiri.bicak@mff.cuni.cz
‡ acgutierrez@unitecnologica.edu.co

[1] A very large number of papers is devoted to electromagnetic fields in cosmology – both to more mathematical aspects like the Bianchi models with magnetic fields [8], and to the more physical question of the origin of the fields [9].

[2] If the full Einstein-Maxwell equations are to be solved, then the complicated formalism of generalized distributions, i.e., Colombeau algebras, might be used – see, e.g., [15, 16].

a background, cf. [20]. Therefore, we generate massive thin disks (Schwarzschild disks) endowed with either electric/magnetic test charges or electric/magnetic test dipoles. The surface currents are depicted and explained using the membrane paradigm.

We use throughout the article the metric signature $(+1,-1,-1,-1)$ and units in which $c = G = 1$.

II. MONOPOLE AND DIPOLE LAYERS IN GENERAL

Although in the examples analyzed in section III we use the Schwarzschild disk spacetimes as backgrounds, the results in the next section, i.e., the source terms and the jump conditions hold in a more general backgrounds. Of course, it has to admit a hypersurface, where the sources are situated, and the derivation of a dipole current requires, that a family of "parallel" hypersurfaces as defined below exists. In [1] the case of charged massive shells were already discussed in full Einstein-Maxwell theory. Nonetheless, we consider test charges in our work, mainly to show in which cases the field generated by an arbitrary dipole distribution can be seen outside of the source as generated by moving charges.

A. The 4-currents for charges or dipoles distributed on a shell

Denoting by $F_{\alpha\beta}$ the Maxwell tensor and by ${}^*F_{\alpha\beta}$ its dual[3], the Maxwell equations in a complex form read as follows:

$$\mathcal{F}^{\alpha\beta}{}_{;\beta} = 4\pi\mathcal{J}^{\alpha}, \tag{1}$$

where $\mathcal{F}_{\alpha\beta} = F_{\alpha\beta} + \mathrm{i}\,{}^*F_{\alpha\beta}$ is a self-dual 2-form. The 4-current $\mathcal{J}^{\alpha} = j^{\alpha}_{(e)} + \mathrm{i}j^{\alpha}_{(m)}$ consists of an electric part $j^{\alpha}_{(e)}$ and a magnetic part $j^{\alpha}_{(m)}$. If $j^{\alpha}_{(m)}$ is vanishing the imaginary part of the Maxwell equations (1) allows us to introduce an electric 4-potential $A^{(e)}_{\mu}$ such that $F_{\mu\nu} = A^{(e)}_{\nu,\mu} - A^{(e)}_{\mu,\nu}$. In case there are no electric sources present, we can analogously introduce a magnetic 4-potential $A^{(m)}_{\mu}$ such that ${}^*F_{\mu\nu} = A^{(m)}_{\nu,\mu} - A^{(m)}_{\mu,\nu}$. In the vacuum region both 4-potentials can be defined and we denote the complex linear combination by $\mathcal{A} = A^{(e)} + \mathrm{i}A^{(m)}$.

Timelike hypersurfaces Σ representing the history of charged 2-surfaces (shells) are discussed widely in the literature, see, e.g., [1]. We recall their main properties, in particular the form of the 4-current which will help us in formulating the expressions for the dipole current. Suppose the hypersurface Σ is described by $\Phi_{\pm}(x^{\mu}_{\pm}) = 0$, where $x^{\mu}_{\pm}$ are coordinates in the two parts of the spacetime on the two sides of Σ and the index $\pm$ denotes from which side a quantity is seen. The unit normal of Σ is given by $n_{\pm\mu} = \kappa N_{\pm}^{-1}\Phi_{\pm,\mu}|_{\Phi_{\pm}=0}$, where $N_{\pm} = (-\Phi_{\pm,\mu}\Phi^{\mu}_{\pm}|_{\Phi_{\pm}=0})^{\frac{1}{2}}$ and $\kappa = \pm 1$ is chosen such that the normal points from $-$ to $+$. To shorten the notation we drop the index $\pm$ in the following wherever no confusion is to be expected. If the intrinsic coordinates of Σ are called ξ^a, where a runs from 0 to 2 and ξ^0 is a timelike coordinate, then the tangential vectors are $\mathrm{e}^{\mu}_{a} = \frac{\partial x^{\mu}}{\partial \xi^a}$. A tensor field $B_{\mu\ldots}$ can be projected onto these directions at Σ and we denote this by

$$B_{a\ldots} = B_{\mu\ldots}\mathrm{e}^{\mu}_{a}, \quad B_{\perp\ldots} = B_{\mu\ldots}n^{\mu}. \tag{2}$$

The 4-current of an electrically charged monopole layer is given by

$$j^{\mu}_{(e\mathcal{M}o)} = s^{a}_{(e\mathcal{M}o)}\mathrm{e}^{\mu}_{a}N\delta(\Phi), \quad s^{a}_{(e\mathcal{M}o)} = \sigma_e u^a, \tag{3}$$

where $s^{a}_{(e\mathcal{M}o)}$ is the surface current of the electrical charges, σ_e is the rest electric surface charge density and u^a the 4-velocity of the charged particles projected onto Σ.

Let us consider, at least locally, a Gaussian normal coordinate system generated by the geodesics χ_p orthogonal to Σ and going out from points $p \in \Sigma$. Then the metric is block diagonal

$$g_{\mu\nu} = -\left(\mathrm{d}x^3\right)^2 + \gamma^{(3)}_{ab}\mathrm{d}x^a\mathrm{d}x^b, \tag{4}$$

and $\Phi = x^3 - x^3_0$. The family of hypersurfaces $x^3 = x^3_0 + h$, i.e., $\Sigma(h)$, are still orthogonal to the family of geodesics χ_p and are at a proper distance h measured along χ_p from $\Sigma(0)$. The coordinates x^a can be used as intrinsic coordinates, thus $\mathrm{e}^{\mu}_{a} = \delta^{\mu}_{a}$ with the Kronecker delta δ^{μ}_{a}, and $\gamma^{(3)}_{ab}(x^a, x^3_0 + h)$ denote the intrinsic metrics of the hypersurfaces $\Sigma(h)$ and $\gamma^{(3)}(x^a, x^3_0 + h)$ their determinant. A slightly more general form of the metric arises when the coordinate x^3 along geodesics χ_p is not measuring anymore the proper distance, implying $g_{33} \neq 1$. These "generalized" Gaussian normal coordinates are used in the examples in section III. The 4-current of a charge distribution on the surface in the generalized Gaussian normal coordinates is given by

$$j^{\mu}_{(e\mathcal{M}o)} = s^{a}_{(e\mathcal{M}o)}\mathrm{e}^{\mu}_{a}\left(-g_{33}(x^a, x^3_0)\right)^{-\frac{1}{2}}\delta(x^3 - x^3_0). \tag{5}$$

To avoid confusion, we recall the definition of the 1-dimensional δ-distribution: For any sufficiently smooth test function f the following integral over a spacetime region Ω in the generalized Gaussian normal coordinates reduces to the integral over $\Sigma(0)$ as follows:

$$\int_{\Omega} f(x^a, x^3_0)\left(-g_{33}(x^a, x^3_0)\right)^{-\frac{1}{2}}\delta(x^3 - x^3_0)\mathrm{d}\Omega = \int_{\Sigma\cap\Omega} f(x^a, x^3_0)\mathrm{d}\Sigma, \tag{6}$$

[3] Note that we use the signature -2 of the metric and the orientation of the volume form as in [21], with the important difference that the indices of our Maxwell tensor $F_{\alpha\beta}$ are interchanged.

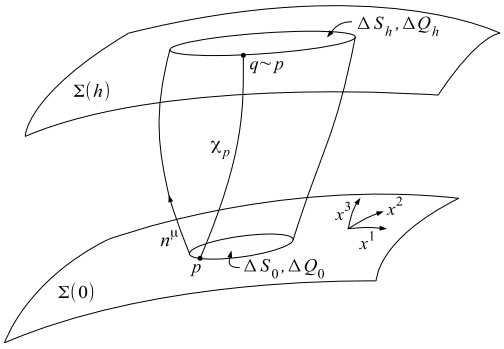

FIG. 1. Equivalent points and associated 3-volumes. The timelike coordinate x^0 is suppressed.

where $d\Omega$ is a spacetime volume element, $d\Sigma$ is a volume element of the hypersurface $\Sigma(0)$.

We construct dipole layers from two oppositely charged monopole layers which are separated by a proper distance h. For simplicity we derive the 4-current in the Gaussian normal coordinates (4) and make a coordinate transformation to the generalized Gaussian normal coordinates subsequently. Dipole layers arise in the limit of vanishing h with a simultaneous limit to infinite (and opposite) rest surface charge densities of the two shells. This means we consider two hypersurfaces $\Sigma(0)$ and $\Sigma(h)$ endowed with surface rest charge densities of opposite sign[4] $\sigma_h(x^a; x_0^3)$ and $\sigma_h(x^a; x_0^3 + h)$ and with velocity fields $u^\mu(x^a; x_0^3)$ and $u^\mu(x^a; x_0^3 + h)$, so giving rise to two 4-currents. Note that the change of the charge densities in the limit is such that it does not effect the velocity fields. Dipole layers result only in the limiting process $h \to 0$ if certain properties hold true in the limit which, for simplicity, we assume to hold throughout the entire limiting procedure. The family of geodesics χ_p gives locally rise to an equivalence relation of points similarly to [22], i.e., $p \sim q$ if there exist a point p_0 such that $p,\ q \in \chi_{p_0}$, cf. Fig. 1. Since the intrinsic coordinates are carried along the geodesics, equivalent points are characterized by the same intrinsic coordinates. Let us assume that two charge elements initially placed at two equivalent points (ξ^a, x_0^3) and $(\xi^a, x_0^3 + h)$ stay in course of there motion in equivalent points at every moment of time, e.g., the intrinsic time coordinate x^0, cf. Fig. 2. Then the coordinate velocities of the charge elements are the same, so we have

$$\frac{u^\mu(\xi^a; x_0^3)}{u^0(\xi^a; x_0^3)} = \frac{u^\mu(\xi^a; x_0^3 + h)}{u^0(\xi^a; x_0^3 + h)}. \tag{7}$$

[4] The second argument of the function $\sigma_h(\xi^a; x^3)$ denotes the layer $\Sigma_{x^3 - x_0^3}$ on which the current is given and the index h labels different currents during the limiting procedure – the increase/decrease of the charge densities while bringing both shells together.

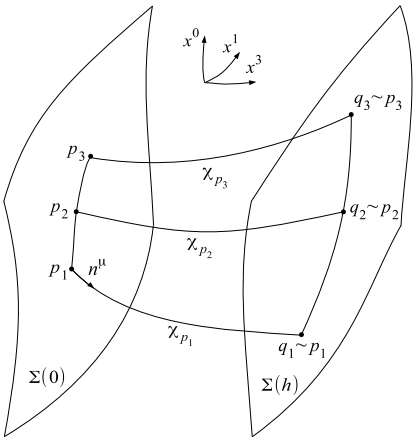

FIG. 2. The motion of two associated infinitesimal charges. The spacelike coordinate x^2 is suppressed.

Analogously to the the equivalence of points, we also can, with each area element ΔS_0 in $\Sigma(0)$, associate an area element ΔS_h in $\Sigma(h)$ which is cut out by the geodesics emanating from the boundary of ΔS_0, cf. Fig. 1. Since the total charge of the dipole shell has to vanish, we suppose that the charge ΔQ_0 enclosed in any area ΔS_0 (as seen by observers at rest with respect to the intrinsic coordinates) is the opposite of that enclosed in ΔS_h. This condition yields

$$\frac{\sigma_h(\xi^a; x_0^3) u^0(\xi^a; x_0^3)}{\sqrt{\gamma^{(3)}(x^a, x_0^3 + h)}} = -\frac{\sigma_h(\xi^a; x_0^3 + h) u^0(\xi^a; x_0^3 + h)}{\sqrt{\gamma^{(3)}(x^a, x_0^3)}}. \tag{8}$$

As in the classical case, the charge density $\sigma_h(x^a; x_0^3) \to \pm\infty$ as $h \to 0$. The electrical rest dipole moment surface density is then naturally defined as $d_e(x^a) = -\lim_{h \to 0} \sigma_h(x^a; x_0^3)\, h$.

Therefore, the limiting procedure based on (3), (7) and (8) yields the resulting dipole 4-current in the form

$$j^\mu_{(e\mathcal{D}i)} = -d_e(x^a) u^\mu(x^a) \frac{\sqrt{\gamma^{(3)}(x^a, x_0^3)}}{\sqrt{\gamma^{(3)}(x^a, x^3)}}\, \delta'(x^3 - x_0^3). \tag{9}$$

Of course, the total charge contained in any proper volume enclosing a part of the electric dipole layer is vanishing. Rewriting this in the generalized Gaussian normal coordinate system we find the 4-current to read

$$\begin{aligned} j^\mu_{(e\mathcal{D}i)} &= s^a_{(e\mathcal{D}i)} \mathrm{e}^\mu_a \left.\frac{\sqrt{\gamma^{(3)}}}{\sqrt{-g_{33}}}\right|_{x^3 = x_0^3} \frac{1}{\sqrt{-g}} \delta'(x^3 - x_0^3), \\ s^a_{(e\mathcal{D}i)} &= -d_e u^a, \end{aligned} \tag{10}$$

where $s^a_{(e\mathcal{D}i)}$ is the surface current of the electrical dipoles and u^a is the 4-velocity of the dipoles projected onto Σ.

Let us repeat the definition of the normal derivative of a δ-distribution in a curved background. For an arbitrary, sufficiently smooth test function f the following holds:

$$\int_\Omega f(x^a,x^3)\left.\frac{\sqrt{\gamma^{(3)}}}{\sqrt{-g_{33}}}\right|_{x^3=x_0^3}\frac{1}{\sqrt{-g}}\delta'(x^3-x_0^3)\mathrm{d}\Omega = -\int_{\Sigma\cap\Omega}(n^\mu f_{,\mu})(x^a,x_0^3)\mathrm{d}\Sigma. \tag{11}$$

Note that even though a derivative of the delta function appears, no metric functions have to be differentiated because of the integral definition of distributions where $\sqrt{-g}$ appears and cancels with the only metric term in the 4-current depending on x^3. Thus also metrics which are not C^1 as they arise in the Israel formalism are allowed. It is also clear by construction and a short calculation, that the continuity equation for j^μ implies that the surface currents $s^a_{(e\mathcal{M}o)}$ and $s^a_{(e\mathcal{D}i)}$ satisfy the continuity equation on Σ. The currents for shells endowed with a magnetic charge or a magnetic dipole density are analogously defined, i.e., we just have to replace the index e by the index m.

B. Discontinuities in the potential and the fields

As is well known from flat space, the jumps of various components of the fields or potentials across a surface are related to electromagnetic sources distributed on that surface. However, even in special relativity magnetic charges are usually not discussed. The jumps resulting from a dipole layer were, to the best of our knowledge, not discussed in curved spacetimes. We denote the jumps of a function f by $[f]=f_+-f_-$. We study the four cases of electric/magnetic charged shells and electric/magnetic dipole shells separately. All of them can be obtained using the equivalence principle and Maxwell theory.

In the case of an electrically charged surface Kuchař showed in [1] (see also [23–25]) that[5]

$$[F_{(e\mathcal{M}o)a\perp}]=-4\pi s_{(e\mathcal{M}o)a},\quad [F_{(e\mathcal{M}o)ab}]=0. \tag{12}$$

Note that these equations are covariant with respect to a change of intrinsic coordinates ξ^a and scalars with respect to the coordinates x^μ. For the electric 4-potential in an appropriate Lorenz gauge it follows

$$[A^{(e)}_{(e\mathcal{M}o)a}]=[A^{(e)}_{(e\mathcal{M}o)\perp}]=0. \tag{13}$$

The magnetic 4-potential $A^{(m)\mu}$ will in general not be continuous across Σ owing to the fact that it can only be introduced in the absence of electrical currents and, therefore, different potentials will occur in the lower and the upper half of the spacetime. Furthermore, introducing the potential $A^{(e)\mu}$ on both sides of Σ in different gauges will not change the external field, however, jumps in the potential are, as seen below, related to dipole densities and therefore describe a different physical system; in particular, the field *in* Σ is changed.

In case of a shell endowed with magnetic charges the same equations as (12) and (13) hold for the dual of the Maxwell tensor and for the magnetic 4-potential in a Lorenz gauge:

$$[{}^*F_{(m\mathcal{M}o)a\perp}]=-4\pi s_{(m\mathcal{M}o)a},\quad [{}^*F_{(m\mathcal{M}o)ab}]=0,\quad [A^{(m)}_{(m\mathcal{M}o)a}]=[A^{(m)}_{(m\mathcal{M}o)\perp}]=0. \tag{14}$$

For the Maxwell tensor it follows that the tangential components jump and the normal components are continuous:

$$[F_{(m\mathcal{M}o)a\perp}]=0,\quad [F_{(m\mathcal{M}o)ab}]=4\pi\epsilon^{(3)}_{abc}s^c_{(m\mathcal{M}o)}, \tag{15}$$

where $\epsilon^{(3)}_{abc}=\epsilon_{abc\perp}$ is the volume form of Σ related to the induced metric γ_{ab} of Σ whereas $\epsilon_{\alpha\beta\gamma\delta}$ is the volume form of the spacetime. Tangential indices are raised and lowered with the induced metric and its inverse.

Analogously, from the equivalence principle the discontinuities of the Maxwell tensor for electric and magnetic dipole densities follow:

$$[F_{(e\mathcal{D}i)a\perp}]=0,\quad [F_{(e\mathcal{D}i)ab}]=-8\pi s_{(e\mathcal{D}i)[a,b]},\quad [{}^*F_{(m\mathcal{D}i)a\perp}]=0,\quad [{}^*F_{(m\mathcal{D}i)ab}]=-8\pi s_{(m\mathcal{D}i)[a,b]}. \tag{16}$$

Here the antisymmetrization in the derivatives of s_a is defined as $B_{[ab]}=\frac{1}{2}(B_{ab}-B_{ba})$. Note that a layer with a curl-free $s_{(m\mathcal{D}i)a}$ will not produce a jump in the external field and thus the source can only be detected by observing the trajectories of particles crossing that layer, i.e., by measuring the internal field in Σ.

The 4-potentials satisfy in these cases the following jump conditions:

$$[A^{(e)}_{(e\mathcal{D}i)\perp}]=0,\qquad [A^{(e)}_{(e\mathcal{D}i)a}]=4\pi s_{(e\mathcal{D}i)a}, \tag{17}$$

$$[A^{(m)}_{(m\mathcal{D}i)\perp}]=0,\qquad [A^{(m)}_{(m\mathcal{D}i)a}]=4\pi s_{(m\mathcal{D}i)a}. \tag{18}$$

Additionally, the normal components of the Maxwell tensor have a δ-like contribution $V_a=[A_a]N\delta(\Phi)$, the field "between the two layers". In order to see this contribution, we insert the aforementioned jumps into the Maxwell equations and calculate the source. Using again Gaussian normal coordinates we start with an electric 4-potential which is discontinuous across Σ and calculate the sources. Hence, we write

$$A^{(e)}_\mu=A^{(e)+}_\mu\theta(x^3-x_0^3)+A^{(e)-}_\mu\theta(-x^3+x_0^3), \tag{19}$$

with $[A^{(e)}_z]=0$, which implies the Maxwell tensor to be

$$F_{a\mu}=F^+_{a\mu}\theta(x^3-x_0^3)+F^-_{a\mu}\theta(-x^3+x_0^3)-\delta^z_\mu[A^{(e)}_a]\delta(x^3-x_0^3). \tag{20}$$

[5] The differences in the sign have their origin in a different signature of the metric.

Inserting this into the Maxwell equations and using the jump conditions above yields

$$\begin{aligned} F^{\mu\nu}{}_{;\nu} =& 4\pi s^a_{(e\mathcal{M}o)} \mathrm{e}^\mu_a \delta(x^3 - x^3_0) + \\ & 4\pi s^a_{(e\mathcal{D}i)} \frac{\sqrt{\gamma^{(3)}(\xi^a, x^3_0)}}{\sqrt{\gamma^{(3)}(\xi^a, x^3)}} \mathrm{e}^\mu_a \delta'(x^3 - x^3_0) + \\ & 4\pi j^\mu_+ \theta(x^3 - x^3_0) + 4\pi j^\mu_- \theta(x^3_0 - x^3), \end{aligned} \tag{21}$$

where the first two terms are the source terms for a charged layer and for a dipole layer. The last two terms are sources outside of Σ, for instance a volume charge density. In the remainder we will assume that outside of the shell there are no magnetic or electric sources.

C. The equivalence of electric charges and magnetic dipoles

In flat spacetimes and also in certain cases of electromagnetism in curved backgrounds, e.g., in the Schwarzschild and the Kerr spacetimes [18, 19], the equivalence of the external field of a magnetic point dipole and of an infinitesimal electric charge current loop is known and often used. Naturally, it can also be easily shown that the external field of an electric point dipole is indistinguishable from that of an infinitesimal magnetic charge current loop. A similar result can be shown to hold in the case of layers of dipoles. In our Gaussian normal coordinates the dual of the Maxwell tensor for a shell endowed with magnetic dipoles reads as follows, cf. (17) and (20):

$$\begin{aligned} {}^*F^{(m\mathcal{D}i)}_{a\mu} =& {}^*F^{(m\mathcal{D}i)+}_{a\mu} \theta(x^3 - x^3_0) + {}^*F^{(m\mathcal{D}i)-}_{a\mu} \theta(x^3_0 - x^3) \\ & - 4\pi \delta^z_\mu s^{(m\mathcal{D}i)}_a \delta(x^3_0). \end{aligned} \tag{22}$$

Of course, the internal field must be changed to transform locally from sources in the form of magnetic dipoles to electric currents. However, if we remove the last term in (22) from the field the external field remains unchanged. An observer outside can detect the difference only by examining trajectories of charged test particles crossing the shell. Furthermore, the jumps of the Maxwell tensor remain the same:

$$[F_{(m\mathcal{D}i)a\perp}] = 4\pi \epsilon^{(3)}{}_a{}^{bc} s_{(m\mathcal{D}i)b,c}, \quad [F_{(m\mathcal{D}i)ab}] = 0. \tag{23}$$

Using equation (12), these jumps are produced by an electric current $s^a_{(e\mathcal{M}o)}$ if

$$s^a_{(e\mathcal{M}o)} = -\epsilon^{(3)abc} s_{(m\mathcal{D}i)b,c}. \tag{24}$$

The electric charge current defined in such a way can also be seen as a source. The continuity equation for $s^a_{(e\mathcal{M}o)}$ is satisfied trivially. However, since the charge density $s^0_{(e\mathcal{M}o)}$ does not need to vanish, electrical charges are introduced in general. The total charge is in principle detectable at infinity in the asymptotics of the field assuming it falls off sufficiently fast. Nonetheless, the total charge for a field generated by magnetic dipoles is vanishing. How is this to be resolved? The total electric charge Q of Σ as seen for observers at rest with respect to the intrinsic coordinates is given by

$$Q = \int\limits_{\Sigma \cap \{x^0 = x^0_0\}} s^0_{(e\mathcal{M}o)} \sqrt{\gamma^{(3)}(\xi^a, x^3_0)} \Big|_{\xi^0 = x^0_0} \mathrm{d}\xi^1 \mathrm{d}\xi^2. \tag{25}$$

Together with equation (24) and Stokes' theorem we obtain

$$Q = \int\limits_{\partial(\Sigma \cap \{x^0 = x^0_0\})} (s_{(m\mathcal{D}i)1} \mathrm{d}\xi^1 + s_{(m\mathcal{D}i)2} \mathrm{d}\xi^2). \tag{26}$$

The asymptotic behavior of the field implies a vanishing current at infinity[6]. Thus, no *total* electric charge Q will be present though "local" volumes can contain a net charge. This is also in correspondence with the known results for point dipoles. In a rest frame of a point dipole the external field can be seen as caused by an infinitesimal charge current loop with a vanishing time component. This is usually interpreted as two currents of positive and negative charges such that the charge densities in the rest frame of the dipole cancel each other and – for example the positive charges are at rest (ions of the conductor) and the negative charges (electrons) contribute to the current. However, in a general frame as used here the charge densities do not necessarily cancel anymore. To generalize this to layers these point dipoles have to be superposed and so the current loops. The net current can have a charge density because one is not in a comoving frame of the dipoles.

If the fields do not fall off sufficiently fast, then the total charge of the shell need not vanish or be definable. In such a case charges can also be "placed at infinity" which is reflected by a corresponding boundary condition. An example is given in section III A.

The argument given above can be reversed and used to show that the external field of every electric charge surface current can also be produced by a charge density at rest in a given frame of reference and a magnetic dipole surface current. The integrability condition of equation (24) for $s^a_{(m\mathcal{D}i)}$ is then equivalent to the continuity equation of the electric charge surface current. It is obvious that an analogous equivalence between electric dipoles and magnetic charges can be established. Except for this kind of non-uniqueness, the field and its sources are completely determined by the jump conditions (12)-(17).

[6] For closed shells this integral vanishes trivially.

III. SCHWARZSCHILD DISKS WITH ELECTRIC/MAGNETIC CHARGE AND DIPOLE DENSITY

The Schwarzschild metric in Schwarzschild coordinates $(x^\mu) = (t, r, \theta, \varphi)$ reads

$$\begin{aligned} \mathrm{d}s^2 = &\left(1 - \frac{2M}{r}\right)\mathrm{d}t^2 - \left(1 - \frac{2M}{r}\right)^{-1}\mathrm{d}r^2 \\ &- r^2\left(\mathrm{d}\theta^2 + \sin^2\theta\mathrm{d}\varphi^2\right). \end{aligned} \tag{27}$$

In [20] massive disks of counterrotating matter, the "Schwarzschild disks", were constructed from this spacetime using the Israel-Darboux formalism and Weyl coordinates $(x^\mu) = (t, \rho, z, \varphi)$

$$\rho = \sqrt{r^2 - 2Mr}\sin\theta, \quad z = (r - M)\cos\theta. \tag{28}$$

This was done by identifying the surfaces $z = z_0$ and $z = -z_0$. From the jumps of the extrinsic curvature of the resulting surface an energy-momentum density of the disk was obtained. The disks are infinite but their mass is finite and the mass density decreases rapidly at large radii. We show here how to endow such disks with an electric/magnetic charge densities or electric/magnetic dipole densities in a test field approach. We demonstrate this with two examples using the asymptotic homogeneous field and the field generated by a point charge. The same can be done to model more general distributions using the general solutions of the Maxwell equations for test fields on a Schwarzschild background given in [18].

In Σ defined by $z = z_{\pm 0}$, we introduce intrinsic coordinates $(\xi^0, \xi^1, \xi^2) = (T, R, \Phi)$ which coincide with the Schwarzschild coordinates (t, r, φ) in the disk but are capitalized to prevent confusion. The components of the normal vector in Schwarzschild coordinates are given by

$$\begin{aligned} (n_\mu) &= N(0, \cos\theta_\pm, -(R - M)\sin\theta_+, 0) \\ N &= -\left(1 - \frac{2M}{R} + \frac{M^2}{R^2}\sin^2\theta_+\right)^{-\frac{1}{2}}, \end{aligned} \tag{29}$$

where again "+" denotes the quantities as seen from $z > z_0$ and "−" as seen from $z < -z_0$. Note that $\cos\theta_\pm = \pm\frac{z_0}{R-M}$.

A. Asymptotically homogeneous electric and magnetic field

The first test field to be discussed is the asymptotically homogeneous electric and magnetic field, for which the complex 4-potential and Maxwell tensor in Schwarzschild coordinates read as follows (see, e.g., [18])

$$\begin{aligned} \mathcal{A}_t &= -\mathcal{F}_0(r - 2M)\cos\theta + \mathcal{A}_{t0}, \\ \mathcal{A}_\varphi &= -\frac{\mathrm{i}}{2}\mathcal{F}_0\sin^2\theta r^2 + \mathcal{A}_{\varphi 0}, \\ \mathcal{A}_r &= \mathcal{A}_\theta = 0, \\ \mathcal{F}_{tr} &= \mathcal{F}_0\cos\theta, \\ \mathcal{F}_{t\theta} &= -\mathcal{F}_0(r - 2M)\sin\theta, \\ \mathcal{F}_{\theta\varphi} &= -\mathrm{i}\mathcal{F}_0 r^2\cos\theta\sin\theta, \\ \mathcal{F}_{r\varphi} &= -\mathrm{i}\mathcal{F}_0 r\sin^2\theta, \\ \mathcal{F}_{t\varphi} &= \mathcal{F}_{r\theta} = 0, \\ \mathcal{F}_0 &= E_0 + \mathrm{i}H_0. \end{aligned} \tag{30}$$

The 4-potential is in fact not given in [18] but can be calculated easily. Assume the field in the upper/lower half is parametrized by $\mathcal{F}_{0\pm}$, $\mathcal{A}_{t0\pm}$ and $\mathcal{A}_{\varphi 0\pm}$. The jumps of the potential across Σ are given by

$$\begin{aligned} &[\mathcal{A}_T] = -(R - 2M)\cos\theta_+(\mathcal{F}_{0+} + \mathcal{F}_{0-}) + \mathcal{A}_{T0+} - \mathcal{A}_{T0-}, \\ &[\mathcal{A}_R] = [\mathcal{A}_\perp] = 0, \\ &[\mathcal{A}_\Phi] = -\frac{\mathrm{i}}{2}\sin^2\theta_+ R^2(\mathcal{F}_{0+} - \mathcal{F}_{0-}) + \mathcal{A}_{\Phi 0+} - \mathcal{A}_{\Phi 0-}. \end{aligned} \tag{31}$$

As it should be according to the equations (13), (14) and (17), the orthogonal component of the potential is continuous. Furthermore, the radial component is continuous as well, i.e., the dipole currents (electric or magnetic) in the radial direction are vanishing. The dipole density approaches a constant value, so does the current in the Φ direction, as one can expect from the analogous result obtained in Maxwell theory in flat space or after setting the mass M to zero in the equations above. The jumps in the fields read

$$\begin{aligned} &[\mathcal{F}_{T\perp}] = N\left(1 - \frac{2M}{R}\right)\left(1 - \frac{M}{R}\sin^2\theta_+\right)(\mathcal{F}_{0-} - \mathcal{F}_{0+}), \\ &[\mathcal{F}_{\Phi\perp}] = \mathrm{i}NM\cos\theta_+\sin^2\theta_+(\mathcal{F}_{0+} + \mathcal{F}_{0-}), \\ &[\mathcal{F}_{TR}] = \frac{M}{R - M}\cos\theta_+(\mathcal{F}_{0+} + \mathcal{F}_{0-}), \\ &[\mathcal{F}_{R\Phi}] = -\mathrm{i}\frac{R}{R - M}\left(R - M\sin\theta_+^2\right)(\mathcal{F}_{0+} - \mathcal{F}_{0-}), \\ &[\mathcal{F}_{R\perp}] = [\mathcal{F}_{T\Phi}] = 0. \end{aligned} \tag{32}$$

Using equations (12) and (14)–(16) we observe again that for electric/magnetic charges the radial current is vanishing and that the electric and magnetic charges do rotate around the axis. The current is vanishing for $R \to \infty$. The total electric or magnetic charge of such a system will be infinite. This will be different for the case of the field discussed in the next subsection.

We will now treat the case of electric monopoles and magnetic dipoles independently of the case of magnetic monopoles and electric dipoles. Afterwards the results can be superposed.

a. Electric monopoles or magnetic dipoles This case is obtained for $E_{0+} = -E_{0-} = E_0$ and $H_{0+} = H_{0-} = H_0$, together with $A^{(e)}_{t0+} = A^{(e)}_{t0-}$ and $A^{(e)}_{\varphi 0+} = A^{(e)}_{\varphi 0-}$. This leads to a surface current

$$\begin{aligned} s^T_{(e\mathcal{M}o)} &= -\frac{E_0}{2\pi} N \left(-1 + \frac{M}{R}\sin^2\theta_+\right), \\ s^R_{(e\mathcal{M}o)} &= 0, \\ s^\Phi_{(e\mathcal{M}o)} &= -\frac{H_0}{2\pi} N \frac{M}{R^2}\cos\theta_+. \end{aligned} \tag{33}$$

In the classical case $M = 0$ the charges are at rest with a charge density equal to the first factor in the first equation. The discontinuities in the magnetic potential and the tangential components of the dual of the Maxwell tensor are in this case understood as being caused by the discontinuities of the orthogonal components of the Maxwell tensor and the presence of the electric monopole layer and, hence, the impossibility to introduce a magnetic potential globally. Looking at the classical case $M = 0$, the principal problem mentioned after equation (26) becomes apparent when dealing with fields which are not falling off sufficiently fast at infinity. The axial current vanishes in this limit and thus cannot cause the magnetic field. The existing magnetic field can be explained by "magnetic charges or electric currents at infinity". Therefore, the disk is not the only source of the external field. This problem does not occur for fields which are falling off sufficiently fast. Such are discussed in the next example. However, for completeness we give here the 4-current provided that the discontinuities are interpreted as the result of a magnetic dipole layer according to equation (16):

$$\begin{aligned} s^T_{(m\mathcal{D}i)} &= \frac{H_0}{2\pi}\frac{MR}{R-2M}\cos\theta_+, \\ s^R_{(m\mathcal{D}i)} &= 0, \\ s^\Phi_{(m\mathcal{D}i)} &= \frac{E_0}{4\pi}. \end{aligned} \tag{34}$$

Here the constants $A^{(m)}_{T\pm}$ and $A^{(m)}_{\Phi 0\pm}$ are chosen such that the current is not singular at the axis and the dipole density vanishes at infinity.

Analogously, we can study disks endowed with a magnetic charge density or electric dipole density by setting $E_{0+} = E_{0-} = E_0$ and $H_{0+} = -H_{0-} = -H_0$. The results are very similar to (33) and (34); they can be obtained by a substitution $E_0 \to H_0$ and $E_0 \to -H_0$ into (33) and (34).

B. Disks generated by point charges

The question whether a field is generated solely by disks or also by sources at infinity is circumvented if a solution is chosen such that it falls off sufficiently fast at infinity. We now consider the electromagnetic field produced by a point charge e situated in an arbitrary position $(r_0, \theta_0, \varphi_0)$. The electric 4-potential for such a point charge was given in [18], and in closed form by Linet in [26]. It reads[7]:

$$\begin{aligned} A^{(e)}_t &= -\frac{Me}{rr_0} - \frac{e}{Drr_0}\left((r-M)(r_0-M) - M^2\lambda\right), \\ A^{(e)}_r &= A^{(e)}_\theta = A^{(e)}_\varphi = 0, \\ \lambda &= \cos\theta\cos\theta_0 + \sin\theta\sin\theta_0\cos(\varphi-\varphi_0), \\ D &= \big((r-M)^2 + (r_0-M^2) - M^2 \\ &\quad -2(r-M)(r_0-M)\lambda + M^2\lambda^2\big)^{\frac{1}{2}}. \end{aligned} \tag{35}$$

We consider two different test fields in the Schwarzschild spacetimes: the field produced by a point charge at $(r_+, \theta_+, \varphi_+)$ and the field produced by a point charge at $(r_-, \theta_-, \varphi_-)$. In the spacetime with the first test field we make a cut at such $z = z_0$ that the black hole and the point charge are *below* the cut. For the second test field the cut is made at $z = -z_0$ such that the charge and the black hole are *above* the cut. After identifying the two hypersurfaces $z = \pm z_0$ there is no black hole or point charge in the spacetime, rather a massive disk with electromagnetic sources. However, the electromagnetic field outside the disk and thus the sources can be understood using the field lines in the "original" spacetime for the "original" test field, i.e., the Schwarzschild black hole spacetime with a point charge. This point of view is employed several times in the following; e.g., the charge density of the disk is explained by referring to the "original" black hole and its polarization.

The fields of the two point charges can be obtained from the 4-potential (35) in a straightforward way and so also the jumps. In order to obtain a layer endowed with either only charges or dipoles we have to require that the point charges have to be located symmetrically in the original spacetime, i.e., $r_{0+} = r_{0-} = r_0$, $\varphi_{0+} = \varphi_{0-}$, $\theta_{0+} = \pi - \theta_{0-}$, as well as that the charges are either equal, $e_+ = e_-$, or opposite, $e_+ = -e_-$. Because of the axially symmetry of the spacetime we can set $\varphi_{0+} = 0$. The jumps evaluate to

$$\begin{aligned} [A^{(e)}_T] &= \frac{(e_2-e_1)}{r_0 RD}\left((R-M)(r_0-M) + MD - M^2\lambda\right), \\ [A^{(e)}_R] &= [A^{(e)}_\Phi] = [A^{(e)}_\perp] = [F_{R\perp}] = [F_{\Phi\perp}] = 0, \\ [F_{T\perp}] &= \frac{(e_1+e_2)(\xi_2-2M)}{r_1\sqrt{(M-\xi_2)^4 - z_0^2M^2\xi_2^2 D^3}}\times \\ &\quad \big[z_0\left((M-r_1)\left((M-\xi_2)^2\xi_2 - MD^2\right) - MD^3\right) \\ &\quad +z_0\left((\xi_2-M)\xi_2(M^2+(M-r_1)^2) + M^2D^2\right)\lambda \\ &\quad +z_0M^2(M-r_1)\xi_2\lambda^2 \\ &\quad +(2M-r_1)r_1\sin\theta_+(M-\xi_2)^2\xi_2\lambda_{,\theta}\big], \end{aligned} \tag{36}$$

[7] The different sign in the potential has its origin in the exchange of the indices of the Maxwell tensor, cf. footnote 3.

Note that functions D and λ have to be evaluated at the respective $\Sigma_\pm$ with the respective point charge. However, it holds that $\lambda(\theta_+, \theta_{0+}) = \lambda(\pi-\theta_+, \pi-\theta_{0+})$, so the same holds for D. Therefore, functions D, λ and $\lambda_{,\theta}$ should be read as functions with the argument $r = R,\ \theta = \theta_+ = \arccos\frac{z_0}{R-M},\ \varphi = \Phi,\ r_0 = r_{0+},\ \theta_0 = \theta_{0+},\ \varphi_{0+} = 0$. The jumps of the tangential components of the Maxwell tensor can be inferred from the jumps of the 4-potential. We can now discuss two cases – a monopole layer and a dipole layer.

b. Electric monopoles or magnetic dipoles In order to obtain continuous tangential components of the 4-potential we have to set $e_1 = e_2$. Then the surface 3-current can be read off (36) and (12). The only non-vanishing component is s_T. However, it is possible to consider two counterrotating streams with an equal charge, cf. with the underlying matter currents in the Schwarzschild disk [20]. This would of course change the charge density seen by a comoving observer. There are several parameters governing the behavior of the solution: the cut parameter z_0, the charge e_1 which acts as scaling, and the position of the two charges $\{r_0, \theta_{0\pm}, 0\}$. In general, there is one maximum associated with the position of the charge e_1 as in classical electrodynamics, and there is also the second maximum due to the influence of the black hole, as depicted in Fig. 3. Although for $\theta_{0+} = 0$ an axially symmetric distribution is obtained, so, only one maximum is present in this case. In the general case the first maximum lies at $\Phi = 0$ and

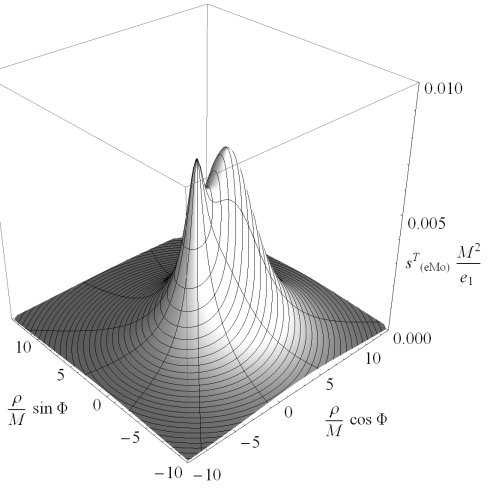

FIG. 3. The time component of the surface current $s^a_{(e\mathcal{M}o)}$ (i.e., the charge density) endowed with electric charges for the parameters $r_{0+} = 5.1M$, $\theta_{0+} = 0.7\pi$, $z_0 = 1.7M$.

the second at $\Phi = \pi$, i.e., on opposite the side of the black hole in the "original" spacetime. The second maximum can be understood using the membrane paradigm [10] (alternatively by discussing the boundary conditions at the horizon [11]). Interpreting the horizon as a conducting sphere, a polarization is to be expected due to the field of the test charge. This will lead to a fictitious charge density at the horizon, cf. [27], as follows:

$$\sigma_{H\pm} = e_1 \frac{M(1+\lambda_\pm^2) - 2(r_0 - M)\lambda_\pm}{8\pi r_0 (r_0 - M(1+\lambda_\pm))^2}, \qquad \lambda_\pm = \pm\cos\theta\cos\theta_{0+} + \sin\theta\sin\theta_{0+}\cos\varphi, \tag{37}$$

where the upper sign denotes the induced charge density for the charge e_1 at $\{r_0, \theta_{0+}, 0\}$ and the lower for the charge e_1 at $\{r_0, \pi - \theta_{0+}, 0\}$. In the following we discuss only the + case, the other one follows from the reflection symmetry. Assuming $e_1 > 0$, the area of the conducting sphere characterized by

$$r_0 - \left(r_0^2 - 2Mr_0\right)^{\frac{1}{2}} \le M(1+\lambda_+) \le r_0 + \left(r_0^2 - 2Mr_0\right)^{\frac{1}{2}} \tag{38}$$

is negatively charged. The opening angle α_{crit} as seen from the test charge e_1 for this area was described in [28]. There it was also discussed, that the field lines emanating from $\{r_0, \theta_{0\pm}, 0\}$ with an angle $\alpha \le \alpha_{crit}$ are bent towards the horizon and cross it eventually. Field lines starting at $\alpha > \alpha_{crit}$ are first bent towards the horizon due to the opposite sign of its charge density and then bent away because of the change of sign in the polarization density. This leads to an increase/decrease of the tangential/normal components of the electric field in the disk close to the axis of the black hole facing e_1. On the other side of the black hole the normal/tangential components of the electric field in the disk are increased/decreased. Thus in general, two maxima for the charge density are obtained on opposite sides of the axis. For the dipole density also two maxima are to be expected but both are lying on the side of the black hole facing e_1.

The surface charge current in Σ behaves for $R \to \infty$ like

$$s^T_{(e\mathcal{M}o)}(R, \Phi) \sim \frac{e_1(z_0 + (2M - r_{0+})\cos\theta_{0+})}{2\pi R^3}. \tag{39}$$

The fall off is sufficiently fast to permit the definition of the total charge which can of course be read off from the unchanged asymptotic behavior of the field and thus is still e_1. Having fixed r_{0+}, the parameter z_0 can be used to slow down the decrease of the charge density as can be seen from (39), but since the total charge must remain the same, the charge gets only "smeared out".

c. Dipole disk To obtain continuous normal components of the Maxwell tensor one has to choose $e_1 = -e_2$; the surface current is given by (17) and (36). Again, the surface current allows two interpretations: the distribution is static or it consists of two counterrotating streams. The same parameters arise here as in the last case and the generic behavior for some specific values is depicted in Fig. 4. The two maxima can again be understood

on the grounds of the membrane paradigm as described above. The asymptotic behavior of the dipole density is

$$s^T_{(e\mathcal{D}i)}(R,\Phi) \sim -\frac{e_1}{2\pi R}. \tag{40}$$

The relation between a monopole distribution and a dipole distribution is illustrated in the following[8]. Let us consider the electric 4-potential and the jumps in the tangential components of the Maxwell tensor as produced from the jumps in the normal components of the dual of the Maxwell tensor, i.e., of a magnetic charge density. If we remove the $\delta-$distribution terms of the field, we obtain a field which is generated by a magnetic current which satisfies

$$\begin{aligned} &s^T_{(m\mathcal{M}a)} = 0, \quad s^R_{(m\mathcal{M}a)} = -\epsilon^{(3)TR\Phi} s_{(e\mathcal{D}i)T,\Phi}, \\ &s^\Phi_{(m\mathcal{M}a)} = \epsilon^{(3)TR\Phi} s_{(e\mathcal{D}i)T,R}. \end{aligned} \tag{41}$$

As stated in section II B for the general case, it is obvious here that the continuity equation is also satisfied for the magnetic surface current. The magnetic charge density of this current is vanishing which can be interpreted as two currents with opposite charges, one of them at rest for example. Since the field falls off sufficiently fast and no total charge is present this is the sole source of the field.

It is again clear from the symmetry of the Maxwell equations that the calculations of this section can be repeated for a magnetic point charge in order to obtain a magnetic charge density or a magnetic dipole density.

From our analysis it follows that similarly we could endow disks with test charges and dipoles which produce Kerr spacetimes [29].

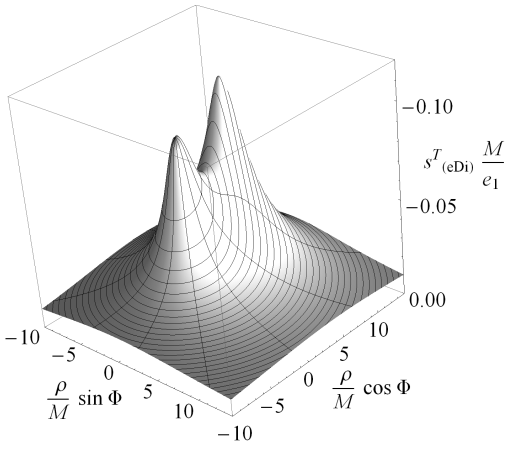

FIG. 4. The time component of the surface current $s^a_{(e\mathcal{D}i)}$ of the disk endowed with electric dipoles for the parameters $r_{0+} = 6.5M$, $\theta_{0+} = 0.48\pi$, $z_0 = 1.7M$.

ACKNOWLEDGMENTS

We thank Tomáš Ledvinka for helpful discussions. JB acknowledges the partial support from Grant No. GAČR 202/09/0772 of the Czech Republic, of Grants No. LC06014 and No. MSM0021620860 of the Ministry of Education. NG was financially supported by the Grants No. GAUK. 22708 and No. GAČR 205/09/H033. JB and NG are also grateful to the Albert Einstein Institute in Golm for the kind hospitality. AC G-P acknowledges the hospitality of the Institute of Theoretical Physics, Charles University (Prague) and the financial support from COLCIENCIAS, Colombia.

[1] K. Kuchař, Czech. J. Phys. **18**, 435 (1968).
[2] J. Bičák, Gen. Relat. Gravit. **3**, 331 (1972). J. Bičák, Gen. Relat. Gravit. **12**, 195 (1980).
[3] D. G. Boulware, Phys. Rev. D **8**, 2363 (1973).
[4] J. P. S. Lemos and O. B. Zaslavskii, Phys. Rev. D **82**, 024029 (2010).
[5] A. B. Balakin, J. P. S. Lemos, and A. E. Zayats, Phys. Rev. D **81**, 084015 (2010).
[6] V. A. Belinski, M. Pizzi, and A. Paolino, Int. J. Mod. Phys. D **18**, 513 (2009).
[7] J. Bičák and N. Gürlebeck, Phys. Rev. D **81**, 104022 (2010).

[8] A more common fact is that magnetic dipoles can be interpreted as generated by a current of electric charges. For brevity we consider here the analogous case of electric dipoles and magnetic charges.

[8] J. Wainwright and G. F. R. Ellis, editors, *Dynamical Systems in Cosmology* (Cambridge University Press, 1997).
[9] J. D. Barrow, R. Maartens, and C. G. Tsagas, Phys. Rept. **449**, 131 (2007).
[10] K. S. Thorne, R. H. Price, and D. A. Macdonald, *Black holes: the membrane paradigm* (Yale University Press, 1986).
[11] B. Punsly, *Black Hole Gravitohydrodynamics* (Springer Verlag, Berlin, 2008).
[12] V. Frolov and I. Novikov, *Black Hole Physics: Basic Concepts and New Developments* (Kluwer Academic Publishers, Dordrecht, 1998).
[13] L. Rezzolla, B. J. Ahmedov, and J. C. Miller, Mon. Not. R. Astron. Soc. **322**, 723 (2001).
[14] L. Rezzolla and B. J. Ahmedov, Mon. Not. R. Astron. Soc. **352**, 1161 (2004).
[15] M. Grosser, M. Kunzinger, M. Oberguggenberger, and R. Steinbauer, *Geometric theory of generalized functions*

with applications to general relativity. (Kluwer Academic Publishers, 2001).
[16] R. Steinbauer and J. A. Vickers, Classical Quant. Grav. **23**, R91 (2006).
[17] N. Gürlebeck, J. Bičák, and A. C. Gutiérrez-Piñeres, Submitted to Gen. Relat. Gravit.
[18] J. Bičák and L. Dvořák, Czech. J. Phys. **27**, 127 (1977).
[19] J. Bičák and L. Dvořák, Gen. Relat. Gravit. **7**, 959 (1976).
[20] J. Bičák, D. Lynden-Bell, and J. Katz, Phys. Rev. D **47**, 4334 (1993).
[21] J. D. Jackson, *Classical Electrodynamics, 3rd Edition* (John Wiley & Sons, New York, 1998).
[22] R. Geroch, Journal of Mathematical Physics **12**, 918 (1971).
[23] W. Israel, Nuovo Cimento B Serie **44**, 1 (1966).
[24] V. de la Cruz and W. Israel, Nuovo Cimento A **51**, 744 (1967).
[25] C. Barrabès and W. Israel, Phys. Rev. D **43**, 1129 (1991).
[26] B. Linet, J. Phys. A-Math. Gen. **9**, 1081 (1976).
[27] K. S. Thorne and D. MacDonald, Mon. Not. R. Astron. Soc. **198**, 339 (1982).
[28] R. S. Hanni and R. Ruffini, Phys. Rev. D **8**, 3259 (1973).
[29] J. Bičák and T. Ledvinka, Phys. Rev. Lett. **71**, 1669 (1993).

Electromagnetic sources distributed on shells in a Schwarzschild background

N. Gürlebeck · J. Bičák · A. C. Gutiérrez-Piñeres

Abstract In the Introduction we briefly recall our previous results on stationary electromagnetic fields on black-hole backgrounds and the use of spin-weighted spherical harmonics. We then discuss static electric and magnetic test fields in a Schwarzschild background using some of these results. As sources we do not consider point charges or current loops like in previous works, rather, we analyze spherical shells with smooth electric or magnetic charge distributions as well as electric or magnetic dipole distributions depending on both angular coordinates. Particular attention is paid to the discontinuities of the field, of the 4-potential, and their relation to the source.

Keywords Electrostatics in curved backgrounds · Monopole and dipole layers

1 Introduction

J. S. Bach's "Goldberg" variations represent the beginning of the theme of musical variations followed by works of Beethoven, Brahms, Reger, and many others, most recently by a "Bearbeitung" of Bach's original by D. Sitkovetsky for the string trio and for the string orchestra. J. N. Goldberg's own "Goldberg variations" on the themes of equations of motion, conservation laws and gravitational radiation were among the first in the 1950-1960's which started the revival of general relativity.

Here we deal with a much simpler problem – sources which are at rest. Still, we use the highly quoted work [1] by Goldberg and his colleagues in the

N. Gürlebeck · J. Bičák
Institute of Theoretical Physics, Charles University, Prague, Czech Republic
E-mail: norman.guerlebeck@gmail.com

A. C. Gutiérrez-Piñeres
Facultad de Ciencias Básicas, Universidad Tecnológica de Bolívar, Cartagena de Indias, Colombia
E-mail: acgutierrez@unitecnologica.edu.co

Syracuse University on the spin-weighted spherical harmonics. We are happy to dedicate this note to Professor Goldberg's 86th birthday. However, we would also like to recall another anniversary: in April 2011 it will be 100 years after Albert Einstein came to Prague to spend 16 months at the German part of the Charles University. In 1912 Einstein was followed by P. Frank whose student who "received much of his training with Philipp Frank in Prague before coming to the USA as Einstein's assistant" [2] was Peter Bergman. It was Frank who recommended him to Einstein. As is well-known, P.G. Bergman founded the relativity group in Syracuse and as E.T. Newman writes in [2] J.N. Goldberg became Bergman's first PhD student there. Is there not a clear connection between both anniversaries?

One of us used spin-weighted spherical harmonics extensively in several works. In [3] we applied the Newman-Penrose (NP) formalism to develop an approximation procedure suitable for treating radiation problems, including wave tails, in non-linear electrodynamics. We also found conserved quantities, analogous to those discovered by Newman and Penrose in Maxwell's and Einstein's theories (cf. e.g. [4]) and analyzed, among others, by Goldberg [5,6]. However, a deeper physical meaning of these quantities in, say, Born-Infeld non-linear electrodynamics remains to be seen.

The spin-weighted spherical harmonics and their generalization to spin-weighted spheroidal harmonics were crucial in the fundamental contribution by Teukolsky [7] in which the equations for perturbations of the Kerr black holes were decoupled and separated. Some time ago we systematically considered stationary electromagnetic perturbations of the Schwarzschild black holes [8] as well as of the Kerr black holes [9]. We also analyzed in detail coupled electromagnetic and gravitational perturbations of the Reissner-Nordström black holes [10,11]. In case of all these black holes we found general stationary vacuum solutions[1] and gave explicit solutions for fields of a number of special sources, like point charges and current loops in various positions outside the black holes. Stationary electromagnetic fields around black holes have later been used in various contexts in relativistic astrophysics, in particular in black-hole electrodynamics, [13,14], and in purely theoretical problems like discovering the Meissner effect for extremal objects in 3+1 and also in higher dimensions (see, e.g., [15,16]).

Recently, we were interested in the spherical gravitating condensers in general relativity [17] – two concentric shells made of perfect fluids restricted by the condition that the electric field is non-vanishing only between the shells. We used Israel's formalism and took energy conditions into account. When the shells approach each other while the total charge on a shell increases a sphere from spherical dipoles forms. However, in this process the energy condition cannot be satisfied, since the field between the shells becomes singular not even permitting to write down the energy-momentum tensor using classical

[1] In [12] we also considered scalar perturbations of the Kerr-Newman black holes and determined stationary solutions.

distributions. A possibility to circumvent these problems is to consider test dipoles as we do in the present paper.

In this context we realized that we are not aware of an example of a surface distribution of dipoles in a curved background, or even of a general surface distribution of (monopole) test charges which do not share the symmetry of the background. In this note we construct simple examples of charges and dipoles distributed on spherical surfaces (shells) in a Schwarzschild background. We use the general vacuum stationary electromagnetic fields on the Schwarzschild background given in [8] and formulate appropriate junction conditions. We are also interested in dipole distributions on the spheres, so we have to calculate 4-potentials of the vacuum fields, which was not done in the original work [8]. Since here we discuss distributions on spherical surfaces in the spherically symmetric background, the results are neat and simple, resembling the results in classical electrodynamics in flat spacetime. In a future paper [18], we turn to general dipole layers in general spacetimes.

2 Stationary fields in a Schwarzschild background

We discuss solutions of electromagnetic test fields in a Schwarzschild background with curvature coordinates $(x^\mu) = (t, r, \theta, \varphi)$:

$$\mathrm{d}s^2 = \left(1 - \frac{2M}{r}\right)\mathrm{d}t^2 - \left(1 - \frac{2M}{r}\right)^{-1}\mathrm{d}r^2 - r^2\left(\mathrm{d}\theta^2 + \sin^2\theta\mathrm{d}\varphi^2\right). \qquad (1)$$

We also allow magnetic sources in order to be able to describe magnetic dipole shells, so the Maxwell equations read[2]

$$F^{\alpha\beta}{}_{;\beta} = 4\pi j^\alpha_{(e)}, \quad {}^*F^{\alpha\beta}{}_{;\beta} = 4\pi j^\alpha_{(m)}, \qquad (2)$$

where the indices (e/m) distinguish the electric/magnetic quantities. We also include magnetic monopoles for mathematical purposes since this will allow us to describe charge distributions depending on φ in an easy way. In the absence of either magnetic or electric sources an electric 4-potential $F_{\alpha\beta} = A^{(e)}_{\beta,\alpha} - A^{(e)}_{\alpha,\beta}$ or a magnetic 4-potential ${}^*F_{\alpha\beta} = A^{(m)}_{\beta,\alpha} - A^{(m)}_{\alpha,\beta}$ can be introduced. However, we will solve the Maxwell equations for the field directly and only afterwards integrate the fields to obtain the 4-potentials in order to verify jump conditions. It is useful to introduce the complex 4-current J^α, 4-potential $\mathcal{A}_\alpha$, and Maxwell tensor $\mathcal{F}_{\alpha\beta}$

$$J^\alpha = j^\alpha_{(e)} + \mathrm{i}j^\alpha_{(m)}, \quad \mathcal{A}_\alpha = A^{(e)}_\alpha + \mathrm{i}A^{(m)}_\alpha, \quad \mathcal{F}_{\alpha\beta} = F_{\alpha\beta} + \mathrm{i}{}^*F_{\alpha\beta}. \qquad (3)$$

The equations for general electromagnetic test fields in a Kerr background were given within the NP formalism in the well-known paper by Teukolsky in [7].

[2] Note, that the signature of the metric and the orientation of the volume form are taken as in [19], with the important difference that our Maxwell tensor $F_{\alpha\beta}$ is the negative of the one defined there, i.e. the indices are exchanged.

Using a separation technique, relying heavily on the spin-weighted spherical harmonics introduced by Goldberg *et al.* in [1], general stationary solutions were given as series expansions for sources on the Schwarzschild background in [8]. Before we discuss our solutions we repeat briefly some of the formalism we are going to need and refer the reader for details to [8,9]. In the Schwarzschild spacetime the NP null tetrad used is given by

$$\begin{aligned} l^\alpha &= \left(\left(1-\frac{2M}{r}\right)^{-1},1,0,0\right), \quad n^\alpha = \frac{1}{2}\left(1,-\left(1-\frac{2M}{r}\right),0,0\right), \\ m^\alpha &= \frac{1}{\sqrt{2}r}\left(0,0,1,\frac{\mathrm{i}}{\sin\theta}\right), \quad \overline{m}^\alpha = \frac{1}{\sqrt{2}r}\left(0,0,1,\frac{-\mathrm{i}}{\sin\theta}\right), \end{aligned} \tag{4}$$

where a bar denotes complex conjugation. The Maxwell tensor $F_{\alpha\beta}$ expressed in terms of the three complex NP quantities $\phi_0,\ \phi_1,\ \phi_2$ reads[3]

$$F_{\alpha\beta} = 4\mathrm{Re}\left[\phi_0\overline{m}_{[\alpha}n_{\beta]} + \phi_1(n_{[\alpha}l_{\beta]} + m_{[\alpha}\overline{m}_{\beta]}) + \phi_2 l_{[\alpha}m_{\beta]}\right]. \tag{5}$$

Thus from the solutions for ϕ_i, given explicitly below in Eqs. (8), we can calculate the field $F_{\alpha\beta}$ and afterwards the four potential $A_\alpha^{(e/m)}$. Taking into account that the coefficients of the ϕ_i in (5) are self-dual, i.e., they satisfy ${}^*A_{\alpha\beta} = -\mathrm{i}A_{\alpha\beta}$, we rewrite (5) in the complex form

$$\mathcal{F}_{\alpha\beta} = 4\left(\phi_0\overline{m}_{[\alpha}n_{\beta]} + \phi_1(n_{[\alpha}l_{\beta]} + m_{[\alpha}\overline{m}_{\beta]}) + \phi_2 l_{[\alpha}m_{\beta]}\right). \tag{6}$$

Hence, to obtain the entire information about the field it is sufficient to study just the time-space components of the self-dual tensor $\mathcal{F}_{\alpha\beta}$ given by

$$\begin{aligned} \mathcal{F}_{tr} &= -2\phi_1, \\ \mathcal{F}_{t\theta} &= \frac{1}{\sqrt{2}}\left((r-2M)\,\phi_0 - 2r\phi_2\right), \\ \mathcal{F}_{t\varphi} &= -\frac{\mathrm{i}}{\sqrt{2}}\left((r-2M)\,\phi_0 + 2r\phi_2\right)\sin\theta. \end{aligned} \tag{7}$$

Let r_1 be the supremum and r_2 the infimum of the radii, such that points (t,r,θ,φ) lying in the support of J^α have $r \in (r_1,r_2)$. The electromagnetic field of a source with $2M < r_1 < r_2 < \infty$ is given in the region $2M \le r < r_1$ by

$$\begin{aligned} \phi_0 = &\sum_{l,m} a_{lm}\sqrt{\frac{8}{l(l+1)}}\,{}_2F_1\left(1-l,l+2;2;\frac{r}{2M}\right)\,{}_1Y_{lm}(\theta,\varphi), \\ \phi_1 = &\sum_{l,m} a_{lm}\,{}_2F_1\left(1-l,l+2;3;\frac{r}{2M}\right)\,{}_0Y_{lm}(\theta,\varphi), \\ \phi_2 = -&\sum_{l,m} a_{lm}\sqrt{\frac{8}{l(l+1)}}\frac{M}{r}\,{}_2F_1\left(-l,l+1;2;\frac{r}{2M}\right)\,{}_{-1}Y_{lm}(\theta,\varphi), \end{aligned} \tag{8a}$$

[3] In contrast to [8,9], we use here $A_{[\alpha\beta]} = \frac{1}{2}(A_{\alpha\beta} - A_{\beta\alpha})$.

whereas for $r > r_2$ it reads

$$\phi_0 = -\sum_{l,m} b_{lm}\sqrt{\frac{2l}{l+1}}\left(-\frac{2M}{r}\right)^{l+2}{}_2F_1\left(l+1,l+2;2l+2;\frac{2M}{r}\right){}_1Y_{lm}(\theta,\varphi),$$
$$\phi_1 = \sum_{l,m} b_{lm}\left(-\frac{2M}{r}\right)^{l+2}{}_2F_1\left(l,l+2;2l+2;\frac{2M}{r}\right){}_0Y_{lm}(\theta,\varphi)+\frac{Q}{2r^2},$$
$$\phi_2 = -\sum_{l,m} b_{lm}\sqrt{\frac{l}{2(l+1)}}\left(-\frac{2M}{r}\right)^{l+2}{}_2F_1\left(l+1,l;2l+2;\frac{2M}{r}\right){}_{-1}Y_{lm}(\theta,\varphi), \tag{8b}$$

where ${}_2F_1$ denotes a $(2,1)$-hypergeometric function, ${}_sY_{lm}$ is a spin-s-weighted spherical harmonic, cf. [1], and $\sum_{l,m}$ is an abbreviation for $\sum_{l=1}^{\infty}\sum_{m=-l}^{l}$ (see [8] for the detailed calculations). The constant $Q = Q^{(e)} + \mathrm{i}Q^{(m)}$ is the complex combination of the total electric charge $Q^{(e)}$ and magnetic charge $Q^{(m)}$. The constants a_{lm} and b_{lm} are also determined by the source via

$$a_{lm} = \int_{2M}^{\infty}\int_0^{2\pi}\int_0^{\pi} J_{lm}(r,\theta,\varphi)\,{}_2F_1\left(l,l+2;2l+2;\frac{2M}{r}\right)\left(-\frac{2M}{r}\right)^{l-2}\mathrm{d}\theta\mathrm{d}\varphi\mathrm{d}r,$$
$$b_{lm} = \int_{2M}^{\infty}\int_0^{2\pi}\int_0^{\pi} J_{lm}(r,\theta,\varphi)\,{}_2F_1\left(1-l,l+2;3;\frac{r}{2M}\right)\left(\frac{r}{2M}\right)^{4}\mathrm{d}\theta\mathrm{d}\varphi\mathrm{d}r, \tag{9}$$

where J_{lm} – vanishing for $r \notin (r_1, r_2)$ – is defined in terms of the complex 4-current J_α as follows, cf. (3):

$$J_{lm}(r,\theta,\varphi) = -\kappa_{lm}\sin\theta\overline{Y}_{lm}(\theta,\varphi)\left[\left(\sqrt{8}r\cot\frac{\theta}{2}\overline{m}^{\alpha}-\frac{2}{r}n^{\alpha}\right)J_\alpha + m^{\alpha}\left(\overline{m}^{\beta}J_\beta\right)_{,\,\alpha} - l^{\alpha}\left(n^{\beta}J_\beta\right)_{,\,\alpha}\right]. \tag{10}$$

The constants κ_{lm} are given by $\frac{4\pi M[(l+1)!]^2}{(2l+1)!}$.

In vacuum regions we can introduce a complex 4-potential $\mathcal{A}_\alpha$. For stationary sources we can integrate $\mathcal{F}_{\alpha\beta} = \mathcal{A}_{\beta,\alpha} - \mathcal{A}_{\beta,\alpha}$ for the time component $\mathcal{A}_t$. Using equations (7) and (8) we obtain

$$r < r_1:\ \mathcal{A}_t = -\sum_{l,m} a_{lm}\frac{8M}{l(l+1)}\,{}_2F_1\left(-l,l+1;2;\frac{r}{2M}\right)Y_{lm}(\theta,\varphi)+\mathcal{A}_{t0-},$$
$$r > r_2:\ \mathcal{A}_t = \sum_{l,m} b_{lm}\frac{4M}{l+1}\left(-\frac{2M}{r}\right)^{l+1}{}_2F_1\left(l,l+1;2l+2;\frac{2M}{r}\right)Y_{lm}(\theta,\varphi) + \frac{Q}{r}+\mathcal{A}_{t0+}. \tag{11}$$

The constants $\mathcal{A}_{t0\pm}$ represent the remaining gauge freedom of the potential. These potentials are new - they were not calculated in [8,9] since the field contains usually all needed information, however, for discussing dipole shells, it is important to know the potentials. For completeness we give also the remaining components of the 4-potential obtained by a separation ansatz. They read for $r < r_1$

$$\begin{aligned}
\mathcal{A}_r =& -\sum_{l,m} a_{lm} \frac{4Mr}{r-2M}\, {}_2F_1\left(-l, l+1; 2; \frac{r}{2M}\right) g_{lm}(\theta) \mathrm{e}^{\mathrm{i}m\varphi},\\
\mathcal{A}_\theta =& \sum_{l,m} R^{(i)}_{lm}(r) \left(g_{lm,\theta}(\theta)\mathrm{e}^{\mathrm{i}m\varphi} + \frac{{}_1Y_{lm}(\theta,\varphi) + {}_{-1}Y_{lm}(\theta,\varphi)}{\sqrt{l(l+1)}} \right),\\
\mathcal{A}_\varphi =& -\mathrm{i}\sum_{l,m} R^{(i)}_{lm}(r) \left(-m g_{lm}(\theta)\mathrm{e}^{\mathrm{i}m\varphi} + \frac{{}_1Y_{lm}(\theta,\varphi) - {}_{-1}Y_{lm}(\theta,\varphi)}{\sqrt{l(l+1)}} \right),\\
R^{(i)}_{lm}(r) =& a_{lm} r^2\, {}_2F_1\left(1-l, l+2; 3; \frac{r}{2M}\right),
\end{aligned} \tag{12}$$

and for $r > r_2$

$$\begin{aligned}
\mathcal{A}_r =& -\sum_{l,m} b_{lm} \frac{4M^2 l}{r-2M} \left(-\frac{2M}{r}\right)^l {}_2F_1\left(-l, l+1; 2; \frac{r}{2M}\right) h_{lm}(\theta) \mathrm{e}^{\mathrm{i}m\varphi},\\
\mathcal{A}_\theta =& \sum_{l,m} R^{(e)}_{lm}(r) \left(h_{lm,\theta}(\theta)\mathrm{e}^{\mathrm{i}m\varphi} + \frac{{}_1Y_{lm}(\theta,\varphi) + {}_{-1}Y_{lm}(\theta,\varphi)}{\sqrt{l(l+1)}} \right),\\
\mathcal{A}_\varphi =& -\mathrm{i}\sum_{l,m} R^{(e)}_{lm}(r) \left(-m h_{lm}(\theta)\mathrm{e}^{\mathrm{i}m\varphi} + \frac{{}_1Y_{lm}(\theta,\varphi) - {}_{-1}Y_{lm}(\theta,\varphi)}{\sqrt{l(l+1)}} \right) +\\
& \mathrm{i}Q\cos\theta,\\
R^{(e)}_{lm}(r) =& b_{lm} 4M^2 \left(-\frac{2M}{r}\right)^l {}_2F_1\left(l, l+2; 2l+2; \frac{2M}{r}\right).
\end{aligned} \tag{13}$$

The arbitrary functions $g_{lm}(\theta)$ and $h_{lm}(\theta)$ give some of the gauge freedom, e.g., the Lorenz gauge is achieved in the vacuum region with the choice $g_{lm}(\theta) = h_{lm}(\theta) = 0$. In general, we could have assumed a t-dependent and a general φ-dependent gauge function.

3 A direct approach for spherical shells

We now apply the solutions described above to the sources characterized by a 4-current

$$J^\alpha_{lm} = f_{lm}(r) Y_{lm}(\theta,\varphi)\xi^\alpha, \tag{14}$$

where indices l and m label the source, Y_{lm} denotes a spherical harmonic and ξ^α is the timelike Killing vector of the Schwarzschild metric. If $m = 0$ the 4-current is real, i.e., it consists just of an electric part. If it is complex one has

also magnetic parts. In order to obtain a 4-current which is proportional to ξ^α like in (14) we need a stationary source, i.e., at least the spatial components of the net current must vanish. Nevertheless, two components which, for example, counter-rotate would also be admissible but we restrict ourselves here to a source which is at rest with respect to the Schwarzschild coordinates. Such sources consist of electric and magnetic parts. For such sources the sums, like in (8), reduce to a single term and the calculations can be handled more easily. These sources form a complete set over the unit sphere which allows us to generalize the results to arbitrary sources.

If a purely electric (magnetic) stationary source is considered, only an electric (magnetic) field arises which amounts to taking the real (imaginary) part of the right-hand sides of equation (7). This means taking a combination of fields produced by currents J^α and $\overline{J}^\alpha$.

Although most of our results hold for a general $f_{lm}(r)$, we concentrate in particular on spherical thin shells with radius r_0 covered by generally distributed electric/magnetic charge densities or by electric/magnetic dipole densities. The sources of such shells are respectively given by

$$\begin{aligned} J^\alpha_{\mathcal{M}o} &= s^a_{\mathcal{M}o}\mathrm{e}^\alpha_a \left(1-\frac{2M}{r_0}\right)^{\frac{1}{2}} \delta(r-r_0), \\ J^\alpha_{\mathcal{D}i} &= s^a_{\mathcal{D}i}\mathrm{e}^\alpha_a \left(1-\frac{2M}{r_0}\right) \frac{r_0^2}{r^2}\delta'(r-r_0). \end{aligned} \tag{15}$$

We give a detailed derivation[4] of the exact form of $J^\alpha_{\mathcal{D}i}$ including general backgrounds and non-stationary sources in another paper [18]. The vectors $\mathrm{e}^\alpha_a = \frac{\partial x^\alpha}{\partial \zeta^a}$ denote the tangential vectors to the hypersurface Σ which represents the history of the shell. Using $(\zeta^a) = (t, \varphi, \theta)$ as intrinsic coordinates in Σ these vectors become the coordinate vectors associated with the Schwarzschild coordinates; in particular, e^α_t coincides with the Killing vector ξ^α. The monopole surface current $s^a_{\mathcal{M}o} = s^{(e)a}_{\mathcal{M}o} + \mathrm{i}s^{(m)a}_{\mathcal{M}o}$ as well as the dipole surface current $s^a_{\mathcal{D}i} = s^{(e)a}_{\mathcal{D}i} + \mathrm{i}s^{(m)a}_{\mathcal{D}i}$ consist of an electric and a magnetic part. The surface currents can be written as

$$s^a_{\mathcal{M}o} = \sigma u^a, \quad s^a_{\mathcal{D}i} = -du^a, \quad \sigma = \sigma^{(e)} + \mathrm{i}\sigma^{(m)}, \quad d = d^{(e)} + \mathrm{i}d^{(m)}, \tag{16}$$

where u^a is the velocity of the sources within the hypersurface Σ, $\sigma^{(e/m)}$ is the electric/magnetic rest surface charge density and $d^{(e/m)}$ the rest surface dipole density. For stationary sources we have $u^a\mathrm{e}^\alpha_a \propto \xi^\alpha$ and thus $u^a =$

[4] Note that the definition of δ-distribution is such that for any test function f the integral over a spacetime region Ω in the Schwarzschild coordinates yields $\int\limits_\Omega f(t,r,\theta,\varphi)\left(1-\frac{2M}{r_0}\right)^{\frac{1}{2}}\delta(r-r_0)\mathrm{d}\Omega = \int\limits_{\Sigma\cap\Omega} f(r_0,t,\theta,\varphi)\mathrm{d}\Sigma$, where $\mathrm{d}\Omega = \sqrt{-g}\mathrm{d}t\mathrm{d}r\mathrm{d}\theta\mathrm{d}\varphi$ is the volume element of the spacetime and $\mathrm{d}\Sigma$ is the volume element of the hypersurface Σ respectively. For the normal derivative of the δ-distribution we obtain $\int\limits_\Omega f(t,r,\theta,\varphi)\left(1-\frac{2M}{r_0}\right)\frac{r_0^2}{r^2}\delta'(r-r_0)\mathrm{d}\Omega = -\int\limits_{\Sigma\cap\Omega}(n^\mu f_{,\mu})(r_0,t,\theta,\varphi)\mathrm{d}\Sigma$ with the unit normal n^μ pointing outwards.

$((1-\frac{2M}{r_0})^{-\frac{1}{2}},0,0)$. Hence, functions f_{lm} in (14) are given in the case of charges distributed on the shell by

$$f_{lm}^{\mathcal{M}o}(r) = \hat{\sigma}_{lm}\delta(r-r_0), \tag{17}$$

where $\hat{\sigma}_{lm}$ are complex constants. Then the electric and magnetic charge densities become $\sigma_{lm}(\theta,\varphi) = \hat{\sigma}_{lm}Y_{lm}(\sigma,\varphi)$. Analogously, for shells covered by dipoles we obtain

$$f_{lm}^{\mathcal{D}i}(r) = \hat{d}_{lm}\left(1-\frac{2M}{r_0}\right)^{\frac{1}{2}}\frac{r_0^2}{r^2}\delta'(r-r_0), \quad d_{lm}(\theta,\varphi) = \hat{d}_{lm}Y_{lm}(\theta,\varphi). \tag{18}$$

Applying formulas (4)–(10) given in Section 2 to the sources (14) we get for the Maxwell tensor for $l=m=0$ [5]

$$\begin{aligned} r<r_1: &\quad \mathcal{F}_{t\theta}=\mathcal{F}_{t\varphi}=0, \quad \mathcal{F}_{tr}=0,\\ r>r_2: &\quad \mathcal{F}_{t\theta}=\mathcal{F}_{t\varphi}=0, \quad \mathcal{F}_{tr}=-\frac{Q}{r^2}, \end{aligned} \tag{19}$$

independently of $f_{00}(r)$. Of course, outside of a spherical symmetric distribution only the total charge is important, not its radial distribution. Note that this field coincides with the field obtained in electrostatics in flat space. Furthermore, if a spherical shell endowed with a constant dipole density is considered, i.e., $Q=0$ and (14) holds together with (18), there is no field present like in flat space. Therefore, the existence of such a dipole layer can be proven only by examining the trajectories of particles crossing it but not by measuring a distant field.

Given sources (14) with a fixed (l',m') with $l'>0$ and an arbitrary $f_{l'm'}$, the coefficients a_{lm} and b_{lm} vanish except for $(l,m)=(l',m')$. Assuming the radial distribution falls off sufficiently fast the coefficients read

$$\begin{aligned} a_{l'm'} &= -\frac{\kappa_{lm}}{8M^2}\int_{2M}^{\infty}\tilde{f}_{l'm'}\frac{\mathrm{d}}{\mathrm{d}r}\left(\left(-\frac{2M}{r}\right)^{l}{}_2F_1\left(l,l+2;2l+2;\frac{2M}{r}\right)\right)\mathrm{d}r,\\ b_{l'm'} &= -\frac{\kappa_{lm}}{8M^2}\int_{2M}^{\infty}\tilde{f}_{l'm'}\frac{\mathrm{d}}{\mathrm{d}r}\left(\left(\frac{r}{2M}\right)^{2}{}_2F_1\left(1-l,l+2;3;\frac{r}{2M}\right)\right)\mathrm{d}r,\\ \tilde{f}_{l'm'} &= (r^2-2Mr)f_{l'm'}(r). \end{aligned} \tag{20}$$

For example, the field of the source with $(l,m)=(1,0)$ can be simplified for $r<r_1$ to read

$$F_{tr} = (E_0+\mathrm{i}B_0)\cos\theta, \quad F_{t\theta} = -(E_0+\mathrm{i}B_0)(r-2M)\sin\theta, \tag{21}$$

where $E_0 = -a_{10}\sqrt{\frac{3}{\pi}}$. This solution coincides with the standard asymptotically homogeneous electric and magnetic field. In the limit $r_1\to\infty$, J_{10}^{α} provides a source of this field. In [18] we discuss a disc source generated by such a field.

[5] The indices l,m of the field $F_{\alpha\beta}$ and of the potential A_α are suppressed.

4 Discontinuities in the electric field and the potential

What are the jumps caused in the field and the potential by sources of the form (17) and (18)? Whereas the results regarding the first are known in general in the electric case, see [20], the jumps of the field of dipole layers were not analyzed before. After we obtain the jumps for these special sources we can superpose them to generalize the results to arbitrary charge and dipole distributions. The jump of a function g across a spherical shell with radius r_0 is defined as $[g] = \lim_{r\to r_0+} g(t,r,\theta,\varphi) - \lim_{r\to r_0-} g(t,r,\theta,\varphi)$.

Since we look at stationary sources the electric charges do not produce magnetic fields, the jump in these are solely caused by magnetic charges. Therefore, we can assume that both kind of charges are present at the same time. For such spherical shells we obtain from (17), (9), using some standard identities for hypergeometric functions, see e.g. [21], and Abel's identity, the following conditions:

$$[\mathcal{F}_{t\theta}] = [\mathcal{F}_{t\varphi}] = 0, \quad [F_{tr}] = -4\pi\hat{\sigma}_{lm}Y_{lm}(\theta,\varphi). \tag{22}$$

This resembles classical results – the normal component of the electric (or magnetic) field jumps across a layer of electric (or magnetic) charges, whereas the tangential components are continuous. The jump is given by the corresponding charge density. These jump conditions are in the form[6] found in [20] if the coordinates $(\zeta^a) = (t,\theta,\varphi)$ are used as intrinsic coordinates and $n^\mu = \left(1-\frac{2M}{r_0}\right)^{\frac{1}{2}}\delta^\mu_r$ as the unit normal pointing outwards:

$$\begin{aligned}
&[\mathcal{F}_{t\perp}] = [\mathcal{F}_{\mu\nu}\mathrm{e}^\mu_t n^\nu] = -4\pi\hat{\sigma}_{lm}Y_{lm}(\theta,\varphi)\left(1-\frac{2M}{r_0}\right)^{\frac{1}{2}} = -4\pi s^{\mathcal{M}o}_t,\\
&[\mathcal{F}_{\theta\perp}] = [\mathcal{F}_{\varphi\perp}] = 0.
\end{aligned} \tag{23}$$

These results can now be superposed to obtain an arbitrary charge density $\sigma(\theta,\varphi) = \sum_{l=0}^{\infty}\sum_{m=-l}^{l}\hat{\sigma}_{lm}Y_{lm}(\theta,\varphi)$ at the shell which results in the general jump conditions

$$[\mathcal{F}_{t\theta}] = [\mathcal{F}_{t\varphi}] = 0, \quad [F_{tr}] = -4\pi\sigma(\theta,\varphi). \tag{24}$$

In order to discuss the jumps in the 4-potential it is sufficient to consider only the scalar potential $\mathcal{A}_t = \mathcal{A}_\mu\xi^\mu$ and, of course, this is continuous across the shell.

[6] The difference in sign is due to a different conventions explained in footnote 2.

In the more interesting case of spherical shells endowed with a dipole density $\hat{p}_{lm}Y_{lm}(\theta,\varphi)$, analogous calculations lead to the relations

$$\begin{aligned}
[\mathcal{A}_t] &= 4\pi\hat{d}_{lm}\left(1-\frac{2M}{r_0}\right)^{\frac{1}{2}}Y_{lm}(\theta,\varphi),\\
[\mathcal{F}_{t\theta}] &= -4\pi\left(1-\frac{2M}{r_0}\right)^{\frac{1}{2}}\hat{d}_{lm}\frac{\partial}{\partial\theta}Y_{lm}(\theta,\varphi),\\
[\mathcal{F}_{t\varphi}] &= -4\pi\left(1-\frac{2M}{r_0}\right)^{\frac{1}{2}}\hat{d}_{lm}\frac{\partial}{\partial\varphi}Y_{lm}(\theta,\varphi),\\
[\mathcal{F}_{tr}] &= 0
\end{aligned} \tag{25}$$

where we used the gauge $A_{t0+}-A_{t0-}=4\pi d_{r0}Y_{00}\delta^0_l$, cf. (11) and the discussion after (19). They are again analogous to the conditions for a dipole layer in flat space. These relations can also be generalized for an arbitrary dipole density on the sphere using the completeness of spherical harmonics:

$$\begin{aligned}
[\mathcal{A}_t] &= 4\pi d(\theta,\varphi)\left(1-\frac{2M}{r_0}\right)^{\frac{1}{2}} = 4\pi s_t^{\mathcal{D}i},\\
[\mathcal{F}_{t\theta}] &= -4\pi\left(1-\frac{2M}{r_0}\right)^{\frac{1}{2}}\frac{\partial}{\partial\theta}d(\theta,\varphi) = -4\pi s^{\mathcal{D}i}_{t,\theta},\\
[\mathcal{F}_{t\varphi}] &= -4\pi\left(1-\frac{2M}{r_0}\right)^{\frac{1}{2}}\frac{\partial}{\partial\varphi}d(\theta,\varphi) = -4\pi s^{\mathcal{D}i}_{t,\varphi},\\
[\mathcal{F}_{tr}] &= 0.
\end{aligned} \tag{26}$$

The jumps of the tangential components are trivially obtained from the jump of the potential. Again, we have a situation like in the classical theory that the normal component of the field does not jump and the tangential components do jump, where the amount is given by the derivative of the surface current in the respective tangential direction, cf. (26). The jump of the potential is directly given by the surface current.

In this paper the behavior of the discontinuities for spherical, static dipole shells was directly proven in the Schwarzschild spacetime. This was possible since the general solution to the Maxwell equation in this background is known. Since in this note we wished to analyze both electrostatics and magnetostatics in a unified framework using complex quantities (3), we did not, for example, treat the case of electric currents moving along the shells and producing magnetic fields so that jump conditions like

$$[A^{(e)}_a] = 4\pi s^{\mathcal{D}i}_a \tag{27}$$

arise for moving electric dipoles. In a later paper [18], general sources, arbitrary hypersurfaces and arbitrary spacetimes will be considered.

In principle, it would also be possible to assume different mass parameters in the different portions of space, thereby generating a massive shell; in particular, introducing flat space inside the shell is of interest. The same analysis

can be done in such a case but the time coordinate will not go continuously through the shell anymore. Other intrinsic coordinates, e.g. the proper time of an observer at rest in the shell, are necessary in such a case (cf., e.g., [17]).

Knowing the junction conditions we can now use them in the following "indirect" approach: start out from some known metrics and fields, assume they are glued together and from the jumps deduce whether this procedure yields physically plausible sources on the junction. This procedure will be employed in our future work [18].

Acknowledgements We thank Tomáš Ledvinka for discussions. JB acknowledges the partial support from Grant No. GAČR 202/09/00772 of the Czech Republic, of Grants No. LC06014 and No. MSM0021620860 of the Ministry of Education. NG was financially supported by the PhD-student Grant No. GAUK. 22708 and No. GAČR 205/09/H033. JB and NG are also grateful to the Albert Einstein Institute in Golm for the kind hospitality. A. C. G-P. acknowledges the hospitality of the Institute of Theoretical Physics, Charles University (Prague) and the financial support from COLCIENCIAS, Colombia.

References

1. J.N. Goldberg, A.J. Macfarlane, E.T. Newman, F. Rohrlich, E.C.G. Sudarshan: Spin-s Spherical Harmonics and ð. J. Math. Phys. **8**, 2155 (1967)
2. Newman, E.T. A Biased and Personal Description of GR at Syracuse University, 1951-61 (2002). URL http://www.phy.syr.edu/faculty/Goldberg/GRHistory3Ted.dvi.pdf
3. J. Bičák, J. Slavik: Non-linear electrodynamics in the Newman-Penrose formalism. Acta Phys. Pol. **B6**, 489 (1975)
4. E.T. Newman, R. Penrose: 10 exact gravitationally-conserved quantities. Phys. Rev. Lett. **15**(6), 231 (1965)
5. E.N. Glass, J.N. Goldberg: Newman-Penrose constants and their invariant transformations. J. Math. Phys. **11**, 3400 (1970)
6. J.N. Goldberg: Conservation of the Newman-Penrose conserved quantities. Phys. Rev. Lett. **28**(21), 1400 (1972)
7. S.A. Teukolsky: Perturbations of a rotating black hole. I. fundamental equations for gravitational, electromagnetic, and neutrino-field perturbations. Astrophys. J. **185**, 635 (1973)
8. J. Bičák, L. Dvořák: Stationary electromagnetic fields around black holes. I. General solutions and the fields of some special sources near a Schwarzschild black hole. Czech. J. Phys. **27**, 127 (1977)
9. J. Bičák, L. Dvořák: Stationary electromagnetic fields around black holes. II. General solutions and the fields of some special sources near a Kerr black hole. Gen. Relat. Gravit. **7**, 959 (1976)
10. J. Bičák: On the theories of the interacting perturbations of the Reissner-Nordström black hole. Czech. J. Phys. **29**, 945 (1979)
11. J. Bičák., L. Dvořák: Stationary electromagnetic fields around black holes. III. General solutions and the fields of current loops near the Reissner-Nordström black hole. Phys. Rev. D **22**, 2933 (1980)
12. J. Bičák, Z. Stuchlík, M. Šob: Scalar fields around a charged, rotating black hole. Czech. J. Phys. **28**, 121 (1978)
13. K.S. Thorne, R.H. Price, D.A. Macdonald, *Black holes: the membrane paradigm* (Yale University Press, 1986). URL http://www.worldcat.org/oclc/13759977
14. B. Punsly, *Black Hole Gravitohydrodynamics* (Springer Verlag, Berlin, 2008)
15. J. Bičák, T. Ledvinka: Electromagnetic fields around black holes and Meissner effect. Nuov. Cim. B Serie **115**, 739 (2000)
16. A. Chamblin, R. Emparan, G.W. Gibbons: Superconducting p-branes and extremal black holes. Phys. Rev. D **58**(8), 084009 (1998)

17. J. Bičák, N. Gürlebeck: Spherical gravitating condensers in general relativity. Phys. Rev. D **81**(10), 104022 (2010)
18. N. Gürlebeck, J. Bičák, A.C. Gutiérrez-Piñeres: Electromagnetic sources distributed on shells in a Schwarzschild background Submitted to Gen. Relat. Gravit.
19. J.D. Jackson, *Classical Electrodynamics, 3rd Edition* (John Wiley & Sons, New York, 1998)
20. K. Kuchař: Charged shells in general relativity and their gravitational collapse. Czech. J. Phys. **18**, 435 (1968)
21. A. Erdélyi, W. Magnus, F. Oberhettinger, F.G. Tricomi, *Higher transcendental functions. Vol. I* (McGraw-Hill Book Company, New York, 1953)

CHAPTER

4

AXIALLY SYMMETRIC, STATIONARY AND RIGIDLY ROTATING DUST

The matter distributions studied so far were in one spatial direction much smaller than in the others, i.e., we considered thin disks and shells. This is a useful approximation even in astrophysical situations. However, it is also obvious that many objects like stars and certain galaxies cannot be described in this way. Therefore, a description of matter distributions with a non-vanishing proper volume is expedient. Here, we discuss such a matter model, namely dust.

For isolated dust configurations it is generally believed that they do not exist, see Section IV.1[1], although a rigorous proof is still lacking in general relativity. A new step towards a proof, not mentioned in Section IV.1, was taken in [57]. There it is shown that certain properties of the Ernst potential imply the non-existence of isolated, axially symmetric, stationary and differentially rotating dust configurations. But it is not proved yet that the Ernst potential always has to satisfy this property. On the other hand, the existence of dust configurations in the presence of other matter distribution is very likely; the other matter distributions may even be placed far away, cf. with an example in Newtonian physics [59]. Thus, it is useful to investigate the interior solution representing axially symmetric, stationary and rigidly rotating dust without knowledge of an exterior. We obtained the interior solution for these dust configurations in Paper IV. The metric is expressed as a series expansion in terms of the mass density along the axis of rotation.

The simplest example in this class is the dust cylinder of Lanczos and van Stockum, see [47, 63]. This solution is interesting in analytical investigations because of its simplicity. Nevertheless, the astrophysical importance is limited. On the one hand, the solution is cylindrically symmetric. We show that the assumption of cylindrical symmetry is not necessary for the interior solution to be of the van Stockum form. The only requirement is that the mass density is constant along the part of the axis of rotation that lies in the interior of the dust. On the other hand, the mass density grows, against intuition, perpendicular to the axis of rotation. We show in Section 4.2 that this is a generic behavior: For any axially symmetric, stationary and rigidly rotating dust configurations the mass density increases perpendicular to the axis independently of the mass density prescribed along the axis. We end Section 4.2 by posing some open problems.

[1] Paper IV consists partly of results obtained during the work on my diploma thesis [36]. In Prague, additional results were found and the theorems in Paper IV were formulated in their final form. The version presented in the following differs slightly from the published article [37] because we corrected some typing errors.

The interior solution of axially symmetric, stationary and rigidly rotating dust configurations

Norman Gürlebeck

Abstract It is shown that the interior solution of axially symmetric, stationary and rigidly rotating dust configurations is completely determined by the mass density along the axis of rotation. The particularly interesting case of a mass density, which is cylindrical symmetric in the interior of the dust configuration, is presented. Among other things, this proves the non-existence of homogeneous dust configurations.

Keywords general relativity · exact solution · dust · non-existence

PACS 02.30.Em · 04.20.Jb

1 Introduction

Dust configurations played an important role in the search for global and physically meaningful solutions of Einstein's field equations. Already in the 1920s, Lanczos obtained solutions describing rigidly rotating, cylindrically symmetric and stationary dust configurations, see [7, 8]. A larger class of solutions including the one given by Lanczos was obtained by van Stockum in [12]. These solutions describe the interior of all rigidly rotating, axially symmetric and stationary dust configurations in terms of an arbitrary solution of a certain second order partial differential equation. A closed form of these solutions involving one arbitrary function is given up to integrations in [6]. Unfortunately, this arbitrary function lacks a direct physical interpretation. One intention of this paper is to describe the degrees of freedom in the solutions by a physically interpretable function, more precisely, the mass density given on the axis of rotation.

Norman Gürlebeck
Institute of Theoretical Physics, Charles University, V Holešovickách 2,
180 00 Praha 8 - Holešovice, Czech Republic
E-mail: norman.guerlebeck@gmail.com

A further generalization was made by Winicour in [14], where differential rotation was considered as well. In this case two functions can be chosen. One is completely arbitrary and the other must be an element of the kernel of the Laplacian in the flat three dimensional Euclidean space $\mathbb{R}^3$. However, in the present paper the attention is turned to rigidly rotating dust, i.e., the van Stockum class.

In Newton's theory of gravity it was shown that *isolated*[1], axially symmetric, rotating dust configuration unavoidably collapse to a disk lying in a plane perpendicular to the axis of rotation and hence they cannot be stationary, see [10] and references therein. However, this scenario can be prevented by distant, stabilizing matter distributions [10]. Therefore, no assumptions about the exterior of the dust configuration are made in the approach presented here.

In general relativity a similar non-existence theorem is still lacking. But some partial results are already known. For instance, in [3] it is shown that axially symmetric and stationary dust configurations do not yield an asymptotically flat spacetime provided that the mass density is strictly positive in the entire spacetime. This is also the reason, why the singularity in the mass density of Bonnor's dust cloud [2], which is a special member of the van Stockum class, is inevitable. In this paper this result is generalized to dust configurations with a boundary seperating it from an arbitrary exterior, but the mass density is required to vanish on the boundary, see [15] as well. Furthermore, in [4] the non-existence of dust configuration in a spatially compact manifold was proven. But note that in both theories, i.e., Newton's theory of gravity and general relativity, axially symmetric, stationary and rotating disks of dust perpendicular to the axis of rotation exist. An important example is given by the Neugebauer-Meinel disk of rigidly rotating dust and its Newtonian limit (Maclaurin disks) [9].

Bonnor's dust cloud serves as an example providing another interesting property of dust configurations in general relativity. The mass density of this solution admits a non vanishing gradient along the axis of rotation. This is not possible in Newton's theory of gravity, because there the angular velocity profile determines the mass density completely. In the case of rigid rotation this yields constant mass density. However, we will show that in general relativity there is no restriction on the mass density along the axis of rotation. In order to do so the Einstein equations for axially symmetric, stationary and rigidly rotating dust are solved for an arbitrary real analytic mass density given along the axis of rotation. This mass density already yields the interior solution up to constants. Hence, the radial profile of the mass density is obtained, too. This can be interesting for astrophysical observations. Moreover, it is even shown that dust configurations with the Newtonian mass density, i.e., homogeneous, do not exist in general relativity. The sole mass density constant along the axis of rotation turns out to be the one given by Lanczos in the cylindrical symmetric case [7].

[1] The support of the mass density is assumed to be compact.

The paper is organized as follows. Section 2 is devoted to the Newtonian case. In particular, attention is paid to the interior solution and its implications. It is shown that given the angular velocity curve the mass density is uniquely determined and the gravitational potential up to an additive constant. After the formulation of the problem of rigidly rotating, axially symmetric and stationary dust configurations in general relativity in Sect. 3 some non-existence results for dust configurations with a boundary are proven in this framework. Afterwards, in Sect. 4, the solution of the interior field equations is obtained in terms of the mass density on the axis of rotation. These results are used in Sect. 5 for a discussion of mass densities, which are constant along the axis of rotation.

Throughout the text geometrical units, in which $c = G = 1$ holds, are chosen.

2 Dust configurations in Newton's theory of gravity

To compare dust configurations in general relativity with the corresponding configurations in Newton's theory of gravity some results regarding stationary, axially symmetric rotating dust in the latter theory are recapitulated in this section. The matter is characterized by a velocity field $\mathbf{v}$, which vanishes on the axis of symmetry, and a mass density μ, such that

$$\mathbf{v}(\mathbf{x}, t) = \omega(\rho, \zeta)\rho\mathbf{e}_\varphi, \quad \mu(\mathbf{x}, t) = \mu(\rho, \zeta) \tag{1}$$

holds, where $\omega = \omega(\rho, \zeta)$ denotes the angular velocity and $\{\rho, \zeta, \varphi\}$ are the cylindrical coordinates with the corresponding unit vectors $\{\mathbf{e}_\rho, \mathbf{e}_\zeta, \mathbf{e}_\varphi\}$. The gravitational potential U has to satisfy the Poisson equation and the Euler equation

$$\nabla^2 U = 4\pi\mu, \quad \mu\frac{\mathrm{d}}{\mathrm{d}t}\mathbf{v} = -\mu\nabla U. \tag{2}$$

The field equations and their consequences are investigated in an arbitrary open subset Ω of the support of the mass density. Hence, it is not necessary to exclude other matter distributions in the exterior of Ω. Furthermore, the behavior at infinity is not restricted and cylindrically symmetric dust configurations are included in our considerations as well as distant objects stabilizing the dust configuration like in [10].

In this section we impose the following smoothness conditions for Ω and the functions U and μ:

Assumptions 1
1. *The boundary of Ω denoted by $\partial\Omega$ is continuously differentiable,*
2. *the mass density $\mu \neq 0$ in Ω,*
3. *$U \in C^2(\Omega)$.*

Note that the first condition is only for concreteness. Others, not necessarily equivalent, like a Ljapunov surface [5] can be considered, too. The third condition leads with the Poisson equation (2) to $\mu \in C^0(\Omega)$ and thus with the Euler equation to $\omega \in C^1(\Omega)$. Weaker differentiability conditions are possible, if weak solutions for the gravitational potential are considered as well.

From the Euler equation (2) and the particular form of the velocity field (1) it follows that

$$U_{,\varphi} = U_{,\zeta} = 0, \quad U_{,\rho} = \rho\omega(\rho,\zeta)^2, \tag{3}$$

where a comma denotes a partial derivative. Therefore, the gravitational potential U is cylindrically symmetric in Ω and consequently the angular velocity. Hence, U is given up to an additive constant in Ω by

$$U(\rho) = U_0 + \int \rho\omega(\rho)^2 \mathrm{d}\rho. \tag{4}$$

The constant U_0 can be fixed using the solution in the exterior of Ω and a smoothness condition for U across $\partial\Omega$. If (3) is inserted in the Poisson equation (2) all possible mass densities can be obtained given an angular velocity profile by

$$(\omega(\rho)^2\rho)_{,\rho} + \omega(\rho)^2 = 4\pi\mu(\rho). \tag{5}$$

Therefore, for every angular velocity curve exists one and only one mass density. In the case of $\omega = \omega_0$ in Ω, i.e., rigidly rotating dust, the constant mass density

$$\mu = \frac{\omega_0^2}{2\pi} \tag{6}$$

is obtained. It is worth noting that this proves the non-existence of static dust configurations under the assumptions 1 in Newton's theory of gravity. With (4) the solution is completely determined by the constant ω_0 in Ω.

Conversely, the angular velocity is determined for a given mass density as a solution of the ordinary differential equation (5), which is given by

$$\omega(\rho) = \pm\frac{1}{\rho}\sqrt{4\pi\int \mu(\rho')\rho'\mathrm{d}\rho' + \alpha}. \tag{7}$$

If the rotational axis intersects Ω, the constant α must be chosen to preserve the differentiability of the angular velocity in Ω. If it does not, additional information about the solution in the exterior of Ω is necessary in order to determine α.

The non-existence of isolated, axially symmetric and stationary dust configurations in vacuum can be shown provided that $U \in C^1(\mathbb{R}^3)$ and U vanishes in infinity, see [2, 10].

3 Rigidly rotating dust configurations in general relativity

In the case of general relativity we restrict ourselves to axially symmetric and stationary spacetimes. Hence, it is convenient to use the Lewis-Papapetrou line element in quasi cylindrical coordinates

$$\mathrm{d}s^2 = \mathrm{e}^{-2U}[\mathrm{e}^{2k}(\mathrm{d}\rho^2 + \mathrm{d}\zeta^2) + W^2\mathrm{d}\varphi^2] - \mathrm{e}^{2U}(\mathrm{d}t + a\mathrm{d}\varphi)^2, \tag{8}$$

where the functions U, k, a, W depend only one the coordinates $\rho,\ \zeta$. Since the field equations are discussed in a spacetime region $\mathcal{G}$, where the matter can be interpreted as dust, the function W can be chosen to be the radial coordinate ρ by means of a conformal mapping. Furthermore, for rigidly rotating dust a transformation in a co-moving coordinate system is possible without changing the form of the metric. Let us for simplicity of notation assume the metric (8) is already given in these co-moving, canonical Weyl-coordinates and let us denote with Ω an open subset of $\mathbb{R}^3$, such that the closure of Ω is a subset of the restricted coordinate map of $\mathcal{G}$ with respect to $\{\rho, \varphi, \zeta\}$.

The only non-vanishing component of the stress-energy tensor in $\mathcal{G}$ reads

$$T^{tt} = \mu\mathrm{e}^{-2U} \tag{9}$$

in this coordinate system, where μ denotes the non-negative mass density.

In analogy to the last section we assume the following:

Assumptions 2
1. *The boundary $\partial\Omega$ of Ω is continuously differentiable,*
2. *the mass density $\mu \neq 0$ in Ω,*
3. $U,\ a,\ k \in C^2(\Omega)$.

Note that again the first condition could be substituted by others like the Ljapunov conditions. Furthermore, it is not assumed that the dust configuration is an isolated object, i.e., that the spacetime is asymptotically flat. Other matter distributions can be present in the exterior of $\mathcal{G}$. In particular, if several non-connected components of the dust configuration exist, they can be treated independently in the approach to be described.

If we denote the part of the axis of rotation, which intersects Ω, by $\mathcal{A}$, then it is convenient for the Theorem 2 to formulate a second set of assumptions:

Assumptions 3
1. *The set $\mathcal{A}$ is not empty,*
2. *the origin $(\rho, \zeta) = (0, 0)$ lies in $\mathcal{A}$,*
3. *the spacetime is elementarily flat.*

If the first condition holds, the second can always be realized by a coordinate shift in the ζ-direction. If the Assumption 2.3 and the elementary flatness condition are satisfied, then

$$a_{,\rho},\ k_{,\rho}\ U_{,\rho} \in O(\rho) \quad \text{and} \quad a_{,\zeta},\ k_{,\zeta} \in O(\rho^2) \tag{10}$$

holds.

Now we turn our attention to the field equations. The contracted Bianchi identity $T^{ab}{}_{;a} = 0$ and the Assumptions 2 imply that the function U must be a finite constant U_0 in Ω. Therefore, the non-redundant field equations simplify in Ω, see, e.g., [11], to

$$\frac{\mathrm{e}^{6U_0}}{\rho^2}\left(\nabla a\right)^2 = 8\pi\mu\mathrm{e}^{2k}, \qquad \Delta a - \frac{a_{,\rho}}{\rho} = 0, \tag{11}$$

where Δ is the Laplace operator in cylindrical coordinates in the three dimensional Euclidean space for axially symmetric functions. The function k is given by the line integration

$$k = \frac{\mathrm{e}^{4U_0}}{4}\int\left[\frac{1}{\rho}((a_{,\zeta})^2 - (a_{,\rho})^2)\mathrm{d}\rho - \frac{2}{\rho}a_{,\rho}a_{,\zeta}\mathrm{d}\zeta\right]. \tag{12}$$

Equations (11) and (12) are well defined in a neighborhood of the rotation axis because of (10).

It is a well known fact that the field equations in the vacuum can be simplified to the Ernst equations with the transformation

$$b_{,\rho} = -\frac{a_{,\zeta}}{\rho}\mathrm{e}^{4U}, \quad b_{,\zeta} = \frac{a_{,\rho}}{\rho}\mathrm{e}^{4U}. \tag{13}$$

The integrability condition of this transformation holds because of the field equations (11) in Ω, too, and the function b is twice continuously differentiable in Ω because of Assumptions 2. The transformed field equations read

$$\Delta b = 0, \tag{14a}$$

$$\left(\nabla b\right)^2 = 8\pi\mu\mathrm{e}^{2k+2U_0}, \tag{14b}$$

$$k = \frac{\mathrm{e}^{-4U_0}}{4}\int\rho\left[((b_{,\rho})^2 - (b_{,\zeta})^2)\mathrm{d}\rho + 2b_{,\rho}b_{,\zeta}\mathrm{d}\zeta\right], \tag{14c}$$

where the first equation is the integrability condition of the inverse transformation. The behavior of the functions a, k close to the axis (10) ensures that the transformation (13) and the field equations (14) are also valid on the axis. Note that since b is harmonic it is real analytic in Ω, as well. With (14c) and (14b) k and μ are real analytic, too. Therefore, singularities in the mass density are excluded by the assumptions and the field equations. Conversely, only real analytic mass densities can be given in order to obtain a solution b in $C^2(\Omega)$, which is more restrictive than in Newtonian physics, where only a continuous mass density is required.

4 The solution of the field equations

Before the general solution is obtained, we prove some non-existence statements in the formalism presented in the last section.

Theorem 1 *Let us suppose the Assumptions 2.1 and 2.2 are satisfied. Then the field equations* (14) *do not admit solutions* $b, k, U_0 \in C^2(\Omega) \cap C(\Omega \cup \partial\Omega)$ *in* Ω*, if one of the following properties is satisfied:*

1. *The mass density* $\mu \in C^0(\Omega \cup \partial\Omega)$ *vanishes on* $\partial\Omega$*,*
2. b *is constant on* $\partial\Omega$*,*
3. *the normal derivative of* b *on* $\partial\Omega$ *vanishes.*

Proof The first case can be reduced to the third using (14b). The cases 2 and 3 follow directly from the uniqueness of the solution of the Laplace equation for b under the given assumptions. In both cases the unique solution is given by $b = \text{const.}$ which in return leads to $\mu = 0$ in Ω with the field equation (14b) and the fact that e^{2k+2U} is finite and positive, which can be seen from the differentiability assumptions. However, this is in contradiction with the definition of Ω and the Assumption 2.2. □

The first part was also shown in [15]. The theorem includes also the fact that solutions in the van Stockum class, which describe a spacetime filled completely with dust and a mass density vanishing at infinity,[2] necessarily have to violate some of the assumptions of Theorem 1, see, e.g,. for other proofs [3] or for a recent approach [1]. In particular the differentiability conditions of b are not satisfied by the solution given in [2], because there is a singularity at the origin.

As we will show in the remainder of this section the conditions which are implied by the assumption of rigid rotation are not as restrictive as in the case of Newton's theory of gravity. More precisely, to *every* real analytic mass density chosen arbitrarily at $\mathcal{A}$ two solutions of the inner field equations in Ω can be assigned at least locally. Let us denote by B_ϵ the open ball with the radius ϵ and the origin of $\mathbb{R}^3$ as center.

Theorem 2 *Let us suppose that Assumptions 2 and 3 hold. Furthermore, let us assume that the mass density* μ *is real analytic in* ζ *in a neighborhood of the origin with the radius of convergence* ϵ *of the series expansion in* ζ*. Then the solution* $b \in C^2(\Omega)$ *of the field equations* (14) *is completely determined in a non-empty set* $B_\sigma \subset B_\epsilon \cap \Omega$ *by the mass density and its derivatives at the origin, an arbitrary constant* $b_\pm(0)$ *and a choice of a sign:*

$$b_\pm = b_\pm(0) \pm \sqrt{8\pi \mathrm{e}^{2U_0+2k_0}} \sum_{l=1}^{\infty} \frac{1}{l!} (\sqrt{\mu})^{(l-1)} r^l P_l(\cos\theta), \tag{15}$$

where $(\sqrt{\mu})^{(n)}$ *denotes the nth derivative of* $\sqrt{\mu}$ *with respect to* ζ *at the point* $(\rho, \zeta) = (0, 0)$ *and* k_0 *is the value of* k *at the axis, see Assumption 3.3. The* P_l *denote the Legendre polynomials of the first kind. Furthermore, polar coordinates* $\rho = r \sin\theta$ *and* $\zeta = r\cos\theta$ *are used.*

[2] In order to interpret the last theorem physically the assumptions, which were necessary to ensure the validity of the transformation (13) and which were summarized in the last section, have to hold.

Proof With (10) and (13) it follows that $b_{,\rho}$ vanishes along $\mathcal{A}$. Hence, the second field equation (14b) simplifies along $\mathcal{A}$ to

$$b_{,\zeta} = \pm\sqrt{8\pi\mu \mathrm{e}^{2U_0+2k_0}}. \tag{16}$$

Therefore, the mass density given along $\mathcal{A}$ determines the function b up to a sign and a constant. Since Ω is an open set and $(\rho, \zeta) = (0, 0)$ is assumed to be an inner point a radius $\sigma > 0$ exists, such that $B_\sigma \subset B_\epsilon \cap \Omega$. In B_σ the square root of the mass density at the axis admits the convergent series expansion

$$\sqrt{\mu(0,\zeta)} = \sum_{l=0} \frac{1}{l!}(\sqrt{\mu})^{(l-1)}\zeta^l. \tag{17}$$

Because b is an axially symmetric harmonic function in B_σ, it can be written in the form

$$b(r,\theta) = \sum_{l=0}^{\infty} A_l r^l P_l(\cos\theta). \tag{18}$$

The coefficients A_l can be derived using the identity theorem of power series, (16), (17) and (18). This yields the coefficients A_l given in (15). □

Some remarks are expedient here. The introduction of the set B_σ is for purely technical reasons, i.e., to avoid different assumptions, e.g about the topology of Ω. If the convergence radius ϵ is such that $B_\epsilon \supset \Omega$ and Ω is a region, then the result (15) can be extended to the entire set Ω. The assumptions about the analyticity of μ is necessary and sufficient in order to obtain a solution b of the field equations in accordance with the differentiability assumptions.

To obtain also solutions admitting a non-constant mass density along the axis seems surprising in the light of the results in Newtonian gravity in Sect. 2, where a constant mass density is implied by rigid rotation (6). One possible explanation is that gravitomagnetic effects due to the motion of the dust will act like a force in ζ-direction. Thus, other solutions of a generalized Euler equation (2), at least in a slow motion limit, are possible. These results and how to assign to such solutions a proper Newtonian limit using Ehlers frame theory will be discussed elsewhere.

The constants in (15) cannot be determined any further. If b is a solution of the field equations (14) in Ω so are $b + \text{const.}$ and $-b$ and the same mass density is obtained from them. The constant $b_\pm(0)$ is the usual freedom due to the transformation formulas (13).

Theorem 2 provides us together with the field equation (14c) with an algorithm to determine the general solution of the field equation if an analytic mass density is given along the axis. By (15) b is obtained from the mass density up to a constant and a sign. With (14) the function k as well as the mass density can be determined independently of the chosen constant and sign. The sign in (15) and the constants U_0 and k_0 can be fixed, provided that a solution of the field equations in the exterior of Ω is known.

In order to obtain an exterior solution of the Einstein equations several approaches are possible. In some cases the mass density along the axis can be extended in ζ, e.g., if the radius of convergence of the Taylor expansion in ζ is infinite such that a globally valid cosmological solution can be obtained and no exterior solution arises. Such spacetimes describe a universe filled with axially symmetric, stationary, rigidly rotating dust.

If the interior solution described in (15) should be joined to an asymptotically flat vacuum exterior one has to solve a "Dirichlet problem" with a free boundary for the Ernst equation. Whether such a solution exists, especially in the light of the non-existence of such dust configurations in the Newtonian gravity, is still an open and difficult question. Perhaps our form of the interior solution will prove useful to answer it. However, if the vacuum exterior is *not* supposed to be asymptotic flat, then global solutions exist, e.g., van Stockums cylindrically symmetric dust [12] or [13] joining the dust to a vacuum exterior.

Another possibility would be to consider an exterior, where matter can be present. A first approach to such an "stabilizing" matter configuration could be to consider a shell enclosing the dust configuration. However, one has to solve a "Dirichlet problem" for the Ernst equation in the region between the dust and the shell and a "Dirichlet problem" for the asymptotic flat vacuum region outside the shell. Even though this problem is not trivial the limiting case of a shell situated on the surface of the dust seems feasible. These "dust stars with a crust" will be investigated in future work.

5 The non-existence of homogeneous dust configurations

The algorithm described above is now applied to the important example of constant mass density along the rotation axis. It was shown in Sect. 2 that this was the sole possible case for rotating Newtonian dust configurations (3) and that in the case of rigid rotation the mass density must be homogeneous (6) in Ω. As is proven in the following corollary this does not hold in general relativity. The solutions of the field equations in Ω for mass densities independent of the ζ coordinate do *not* yield a homogeneous mass density.

Corollary 1 *If a dust configuration satisfies Assumptions 2 and 3 and the mass density μ is constant $\mu = \mu_0 \neq 0$ along the axis of symmetry, then there exists a $\sigma > 0$ such that the mass density is given in $B_\sigma \subset \Omega$ by*

$$\mu(\rho, \zeta) = \mu_0 \exp(2\pi\mu_0 \mathrm{e}^{-2U_0+2k_0}\rho^2). \tag{19}$$

Proof Because the mass density is constant in $\mathcal{A}$ all derivatives with respect to ζ vanish at the origin and the convergence radius ϵ of the series representation at this point is infinite. Using the Theorem 2 and the transformation between cylindrical and polar coordinates the solution of the field equations (14a) and (14b) can be written as

$$b(\rho, \zeta) = b_\pm(0) \pm \sqrt{8\pi \mathrm{e}^{2U_0+2k_0}\mu_0}\zeta \tag{20}$$

in a $B_\sigma \subset \Omega$ with $\sigma > 0$. The function k is obtained by means of the line integration (14c) and (10)

$$k = k_0 - \pi\mu_0 \mathrm{e}^{-2U_0+2k_0}\rho^2. \tag{21}$$

Inserting (20) and (21) in (14a) yields the mass density given in (19) in B_σ. □

This corollary does not only prove the non-existence of homogeneous dust configurations, it also gives the only possible mass density in the cylindrically symmetric case as obtained by Lanczos, see [7]. But here Ω need not be cylindrically symmetric. Only μ must be independent of ζ on the axis of rotation.

Acknowledgements I thank R. Meinel for turning my attention to this interesting topic. Fertile discussions with R. Meinel and D. Petroff are also gratefully acknowledged.

References

1. Bratek, Ł., Jałocha, J., Kutschera, M.: Phys. Rev. D **75**, 107502 (2007)
2. Bonnor, W.B.: J. Phys. A: Math. Gen. **10**, 1673-1677 (1977)
3. Caporali, A.: Phys. Lett. A **66**, 5-7 (1978)
4. Frauendiener, J.: Phys. Lett. A **120**, 119-123 (1987)
5. Günter, N.M.: Die Potentialtheorie und ihre Anwendung auf Grundaufgaben der mathematische Physik, B.G. Teubner Verlagsgesellschaft, Leipzig (1957)
6. Islam, J.N.: Phys. Lett. A **94**, 421-423 (1983)
7. Lanczos, K.: Zeitschr. f. Phys. **21**, 73-110 (1924)
8. Lanczos, K.: Gen. Relativ. Gravit. **29**, 363-399 (1997)
9. Neugebauer, G., Meinel, R.: Phys. Rev. Lett. **75**, 3046-3047 (1995)
10. Schaudt, U.M., Pfister, H.: Gen. Relativ. Gravit. 33, 719-737 (2001)
11. Stephani, H., Kramer, D., MacCallum, M., Hoenselaers, C., Herlt, E.: Exact solutions to Einstein's field equations, Cambridge University Press, New York (2003)
12. van Stockum, W.J.: Proc. Roy. Soc. Edinburgh A **57**, 135 (1937)
13. Vishveshwara, C.V., Winicour, J.: J. Math. Phys. **18**, 1280-1284 (1977)
14. Winicour, J.: J. Math. Phys. **16**, 1806-1808 (1975)
15. Zingg, T., Aste, A., Trautmann, D.: Adv. Stud. Theor. Phys. **1**, 409-432 (2007)

4.1 Addendum to Paper IV: The metric in the interior

In Paper IV we determined the solution in the interior of a general axially symmetric, stationary and rigidly rotating dust configuration.[2] The solution was written down explicitly only for b in Eq. (IV.15). In this section, we give the series expansion of the metric functions a and k in the comoving coordinate system under the same assumptions as in Theorem IV.2. In order to do so we write their definitions (IV.13) and (IV.14c) in the polar coordinates used in Theorem IV.2:

$$\begin{aligned} a_{,r} &= -\mathrm{e}^{-4U_0}\sin\theta b_{,\theta}, \quad a_{,\theta} = r^2\mathrm{e}^{-4U_0}\sin\theta b_{,r}, \\ k_{,r} &= \frac{1}{4}\mathrm{e}^{-4U_0}\left(r\sin^2\theta b_{,r}^2 - \frac{1}{r}\sin^2\theta b_{,\theta}^2 + 2\sin\theta\cos\theta b_{,r}b_{,\theta}\right), \\ k_{,\theta} &= \frac{1}{4}\mathrm{e}^{-4U_0}\left(\sin\theta\cos\theta\left(b_{,\theta}^2 - r^2 b_{,r}^2\right) + 2r\sin^2\theta b_{,r}b_{,\theta}\right). \end{aligned} \tag{4.1}$$

We integrate these equations using the form of b given in Eq. (IV.15). The calculation is lengthy but straightforward, so we give here only the result. It reads

$$\begin{aligned} a(r,\theta) =& a_0 - \mathrm{e}^{-4U_0'}\left(\sum_{l=0}^{\infty} r^{l+2}A_{l+1}\frac{l+1}{l+2}\left(P_{l+1}(\cos\theta)\cos\theta - P_l(\cos\theta)\right)\right), \\ k(r,\theta) =& k_0 + \frac{1}{4}\mathrm{e}^{-4U_0'}\sum_{l=0}^{\infty}\frac{r^{l+2}}{l+2}\sum_{k=0}^{l}(l-k+1)(k+1)A_{l-k+1}A_{k+1}\big(P_{l+k+1}(\cos\theta)P_{k+1}(\cos\theta) - \\ & \cos\theta P_{l-k+1}(\cos\theta)P_k(\cos\theta) - \cos\theta P_{l-k}(\cos\theta)P_{k+1}(\cos\theta) + P_{l-k}(\cos\theta)P_k(\cos\theta)\big), \end{aligned} \tag{4.2}$$

with the integration constant a_0 and k_0. The A_l are the expansion coefficients of b and can be read off Eq. (IV.15):

$$A_l = \pm\sqrt{8\pi\mathrm{e}^{2U_0+2k_0}}\frac{1}{l!}(\sqrt{\mu})_{,\zeta}\Big|_{\rho=\zeta=0}. \tag{4.3}$$

Since U is constant in the co-moving frame, all metric functions are determined in terms of the mass density along the axis.

4.2 The mass density close to the axis of rotation

The mass density along the axis defines the metric completely. On the other hand, we can use the metric functions to determine the mass density everywhere, cf. Eq. (IV.14b). We employ this to show that all axially symmetric, stationary and rigidly rotating dust configurations satisfying the assumptions of Theorem IV.2 exhibit a mass density increasing perpendicular to the axis of rotation.

We take an arbitrary point at the axis of rotation in the interior of the dust. Without loss of generality, we assume that it coincides with the origin of the Weyl coordinate system. Close to this point, the metric can be expanded in r which yields

$$\begin{aligned} (\nabla b)^2 =& A_1^2 + 4A_1A_2r^2\cos\theta + O(r^4), \\ \mathrm{e}^{-2k} =& \mathrm{e}^{-2k_0}\left(1 + \frac{r^2}{4}\mathrm{e}^{-4U_0}A_1^2\sin^2\theta\right) + O(r^4). \end{aligned} \tag{4.4}$$

[2] We use the same notation as in Paper IV in the remainder of this chapter.

Inserting these expansions in Eq. (IV.14b) and using the definition of the A_l in (4.3), determines the mass density close to the axis:

$$\mu = \left((\sqrt{\mu})^{(0)2} + 4(\sqrt{\mu})^{(0)} \mu^{(1)} r^2 \cos\theta + 8\pi r^2 \mathrm{e}^{-2k_0 - 2U_0} (\sqrt{\mu})^{(0)2} \sin^2\theta \right) + O(r^4). \tag{4.5}$$

The $\mu^{(l)}$ are defined as in Theorem IV.2. In ρ-direction, i.e., for $\theta = \frac{\pi}{2}$ and increasing r, the mass density increases, as we wanted to show. Because the origin along the axis of rotation was chosen arbitrarily, our result applies for all points at the axis of rotation in the interior of the dust. We additionally find that the mass density grows perpendicular to the axis exactly in the same manner as for van Stockum dust with the mass density $\mu = (\sqrt{\mu})^{(0)2}$ along the axis, cf. with an expansion for small ρ in Eq. (IV.19). For a sufficiently small neighborhood of a point, the mass density along the axis can essentially be seen as constant along the axis. For a linear and local problem, this would imply that the solution looks locally like in the case where the mass density is constant. However, Eqs. (IV.14b) and (IV.14c) are not linear and that it still holds true is non-trivial.

In future work Eq. (IV.15) and (4.2) might prove useful in the analysis of dust configurations. Can other properties of van Stockum dust, which is investigated thoroughly, be generalized to axially symmetric, stationary and rigidly rotating dust configurations? For instance, in van Stockum dust cylinders and in Bonnor's dust cloud, see [10], causality-violating curves exist, for recent accounts see, e.g., [26, 61]. Is this due to the peculiar solutions admitting cylindrical symmetry or a singularity? Or, is this a generic feature of dust?

CHAPTER

5

THE NEWTONIAN DEDEKIND ELLIPSOIDS

Hitherto, we considered stationary solutions with additional symmetries like spherical symmetry or axial symmetry. In the remainder of this thesis, we concentrate on solutions that are non-axially symmetric and rotating but still stationary. We accomplish this using a PN approximation of Newtonian solutions, which are stationary but non-axially symmetric, namely the Dedekind ellipsoids. The present chapter is devoted to a description of the classical Newtonian ellipsoidal figures of equilibrium. Among the classical ellipsoidal solutions in Newtonian gravity, we regard here the Maclaurin spheroids, the Jacobi ellipsoids, the Dedekind ellipsoids and the Riemann ellipsoids. These solutions are thoroughly discussed in [21]. Hence, we recall the properties of these figures of equilibrium just briefly and insofar it serves the following two purposes. Firstly, we introduce the necessary quantities for a PN approximation and fix the notation. Secondly, we want to list the properties satisfied by the Newtonian Dedekind ellipsoids in order to find an expedient definition of Dedekind ellipsoids in general relativity. These properties are also intended to clarify why we choose the Dedekind ellipsoid as a starting point for the subsequent PN approximation. We describe also in detail how to obtain the solution exterior to the perfect fluid in a closed form and a limit where the Dedekind ellipsoids degenerate to a rod. As far as we are aware, this was not done before. In fact, the interior solution suffices to investigate the normal modes and the stability of the Dedekind ellipsoids. Nonetheless, in PN approximations the exterior solution becomes relevant. Generally speaking, the interior solution in higher PN orders depends on the exterior solution in lower orders. In general, the Dedekind sequence has received much less attention in the development of the theory of ellipsoidal figures of equilibrium than, say, the Maclaurin or Jacobi ellipsoids. As Chandrasekhar states in [13], this sequence of solutions is not mentioned at all in the original works of Poincaré, Darwin and Jeans. This might be due to Dedekind's theorem stating that the Dedekind sequence is geometrically equivalent to the Jacobi one. However, this does not imply physical equivalence, see [13].

Non-axially symmetric ellipsoidal figures of equilibrium play a role in astrophysics, for example, in modeling elliptical galaxies using homoeoidally striated density profiles, see, e.g., [12]. There a sequence of homoeoids of Jacobi ellipsoids with different mass densities is considered to obtain theoretical bounds on the flattening of elliptical galaxies.

5.1 The field equations

The ellipsoidal figures of equilibrium discussed here are self-gravitating perfect fluid solutions with a homogeneous mass density μ. The support of μ is an ellipsoid with the semiaxes $a_1 \geq a_2 \geq a_3$. The surface of this ellipsoid is defined in Cartesian coordinates $\{x^1, x^2, x^3\}$ by

$$S(x^a) = -1 + \sum_{i=1}^{3} \left(\frac{x^i}{a_i}\right)^2 = 0, \tag{5.1}$$

whereas the interior is characterized by $S(x^a) < 0$. The Poisson equation defining the gravitational potential U reads

$$\Delta U = -4\pi G\mu, \tag{5.2a}$$

where G denotes Newton's constant of gravity. The pressure p and the velocity $\mathbf{v}$ of the perfect fluid have to satisfy the continuity equation and the Navier-Stokes equation:

$$\frac{\partial \mu}{\partial t} + \nabla \cdot (\mu \mathbf{v}) = 0, \quad \mu \frac{\mathrm{d}\mathbf{v}}{\mathrm{d}t} = \mu \nabla U - \nabla p. \tag{5.2b}$$

For stationary solutions, e.g., the Dedekind ellipsoids it is additionally required that the pressure vanishes at the surface of the configuration.

To compare different solutions with each other it is sometimes more useful to introduce the total mass of a system rather than the mass density. Both are related by

$$\mu = \frac{3M}{4\pi a_1 a_2 a_3}. \tag{5.3}$$

However, in certain limits like $a_1 \to \infty$ the configuration can extents to infinity and the total mass M is not defined anymore. Moreover, we show in Section 5.3.1 that the total Newtonian mass has to vanish in the limit $\frac{a_2}{a_1} \to 0$ to allow a PN approximation. Thus, it cannot be used to compare solutions in this limit.

All families of solutions studied below are characterized by several parameters of which some are "trivial" and not counted further. For instance, a preferred length does not exist in Newtonian gravity and hydrostatics of perfect fluids. Thus, one parameter related to the size of the ellipsoid – usually the largest semiaxis a_1 is chosen – is not determined by Eq. (5.2). Therefore, we introduce the dimensionless parameters

$$\bar{a}_2 = \frac{a_2}{a_1}, \quad \bar{a}_3 = \frac{a_3}{a_1}. \tag{5.4}$$

Furthermore, the mass density μ is arbitrary in the solutions described below.

5.2 Ellipsoidal figures of equilibrium

We recall some of the classical ellipsoidal figures of equilibrium – the Maclaurin, Jacobi and Riemann sequences – and the main properties that are of interest for later analysis. We also give a short account of previous results on the PN approximation for these figures of equilibrium. The Dedekind ellipsoids are discussed in more detail in Section 5.3.

5.2.1 Maclaurin ellipsoids

The Maclaurin spheroids constitute a 1-parameter family, not counting the aforementioned parameters μ and a_1, of stationary, axially symmetric and rigidly rotating oblate spheroids, i.e., $a_1 = a_2$. The sequence of Maclaurin spheroids is parameterized by a_3 or the eccentricity. The parameter a_3 varies from $a_3 = 0$, where the Maclaurin ellipsoid degenerates to the Maclaurin disk, to $a_3 = a_1$, where the ellipsoid becomes a non-rotating sphere. In Cartesian coordinates the velocity profile is given by

$$\mathbf{v} = (-\Omega x^2, \Omega x^1, 0), \tag{5.5}$$

where the angular velocity Ω can be obtained from the condition of equilibrium[1]. This yields

$$\Omega^2 = 4\pi G\mu \frac{a_3}{(a_1^2 - a_3^2)^{3/2}} \left(\left(a_1^2 + 2a_3^2\right) \arccos \frac{a_3}{a_1} - 3a_3 \sqrt{a_1^2 - a_3^2} \right). \tag{5.6}$$

For later convenience, we define the dimensionless angular velocity $\bar{\Omega} = \frac{\Omega}{\sqrt{2\pi G\mu}}$, which is depicted in Fig. 5.1 for different kinds of ellipsoids.

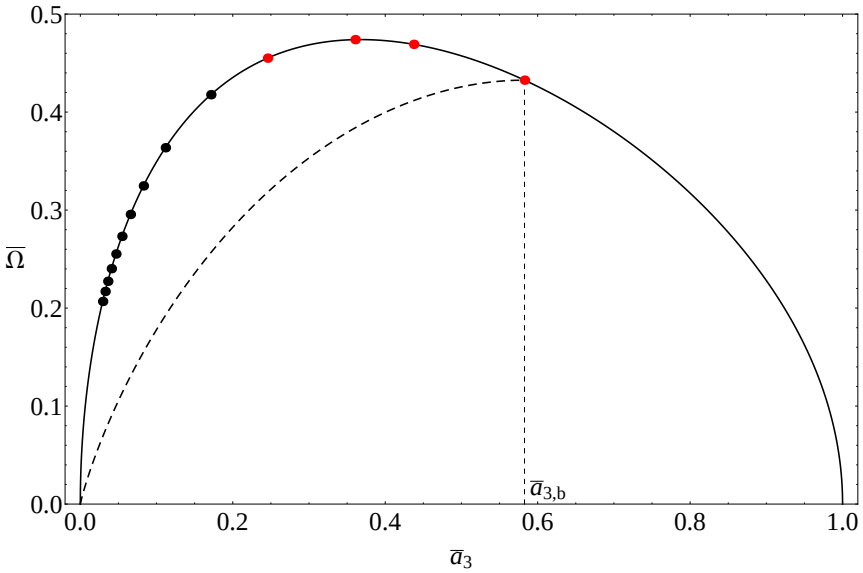

Figure 5.1: The constant $\bar{\Omega}$ is depicted along the Maclaurin sequence (solid line) and along the Dedekind/Jacobi sequence (dashed line). Some bifurcation points where non-axially symmetric configurations branch off (red) are indicated. Additionally, the first bifurcation points, i.e., those with smallest eccentricity where axially symmetric, rigidly rotating, and homogeneous configurations branch off (black) are shown.

Going along the sequence of Maclaurin ellipsoids starting at $\bar{a}_2 = 1$ several bifurcation points are encountered, cf. Fig. 5.1. The Jacobi and the Dedekind sequence described below branch off at the first bifurcation point $\bar{a}_3 = 0.582724\ldots = \bar{a}_{3,\mathrm{b}}$. This point coincides with the onset of a secular instability with respect to a toroidal mode, see [21]. For the present considerations, this

[1] For Newton's telling canal gedankenexperiment, see [21].

point is important as one of the end points of the Dedekind sequence. The Dedekind ellipsoids become axially symmetric and rigidly rotating at $\bar{a}_{3,b}$. For higher eccentricities other bifurcation points of non-axially symmetric sequences, the "triangle", "square" and "ammonite" sequence, were found, see [27]. For eccentricities close to 1 an infinite number of sequences of homogeneous, rigidly rotating, axially symmetric stationary perfect fluid solution branches off, see [2, 16, 28] and for a detailed description [1]. Obviously, the space of homogeneous, rigidly rotating, axially symmetric and stationary perfect fluid solutions is not restricted to the Maclaurin sequence. However, the assumption of an ellipsoidal shape singles out the Maclaurin solutions, i.e., an ansatz for the shape is crucial. In addition, it is the only sequence continuously connected to a static sphere. If this ambiguity is fixed for the Newtonian solution, the family of PN Maclaurin ellipsoids can be determined, cf. [2, 20, 56]. It turns out that the bifurcation points for axially symmetric configurations show themselves in the PN approximation as singularities, see [56].

5.2.2 Jacobi ellipsoids

The sequence of the Jacobi ellipsoids, which branches off at the first bifurcation point $\bar{a}_{3,\mathrm{b}}$, consists of rigidly rotating, homogeneous triaxial ellipsoids; they are not axially symmetric. The sequence is parameterized by $\bar{a}_2$. The velocity field for them is the same as (5.5) with a different angular velocity Ω. The entire Jacobi ellipsoid rotates rigidly. Equilibrium requires Ω and a_3 to satisfy

$$\begin{aligned} \Omega &= (2\pi G\mu B_{12})^{\frac{1}{2}}\,, \\ a_1^2 a_2^2 A_{12} &= a_3^2 A_3. \end{aligned} \tag{5.7}$$

The index symbols $A_{i_1 i_2 \ldots}$ and $B_{i_1 i_2 \ldots}$ are used throughout the publications on non-axially symmetric, ellipsoidal equilibrium figures, especially in [21]. We list their definitions and properties necessary in this thesis in Appendix A. There we also introduce dimensionless versions, which are denoted by a bar, e.g., $\bar{A}_{i_1 i_2 \ldots}$. In the definition of the dimensionless index symbols the semiaxis a_1 is eliminated and the equations (5.7) become manifestly independent of a_1:

$$\begin{aligned} \bar{\Omega} &= \bar{B}_{12}^{\frac{1}{2}}, \\ \bar{a}_2^2 \bar{A}_{12} &= \bar{a}_3^2 \bar{A}_3. \end{aligned} \tag{5.8}$$

The angular velocity $\bar{\Omega}$ for the Jacobi ellipsoids is depicted in Fig. 5.1. The second equation in (5.8) defines the $\bar{a}_2$ in terms of $\bar{a}_3$ or vice versa. Thus, only two of the semiaxes, say, a_1 and $\bar{a}_2$ can be chosen arbitrarily in $\mathbb{R}$ and $[0, 1]$, respectively. The third semiaxis follows from (5.8).

The parameter $\bar{a}_2$ runs from 1 to 0. In the former case the solution coincides with a Maclaurin spheroid and in the latter case Eq. (5.8) implies $\bar{a}_3 \to 0$ as well, i.e., the ellipsoid degenerates to a rod. Because the Jacobi ellipsoids rotate in an inertial frame, they are not stationary; the mass quadrupole moment is time dependent. This can be used to approximate the energy loss due to gravitational waves, see [24], which was done in [18]. It turned out that under the assumptions in [18] the Jacobi ellipsoids evolve towards the bifurcation point, and become eventually a Maclaurin spheroid. These spheroids do not emit gravitational radiation anymore. Nevertheless, this evolution does not manifest itself in the 1-PN approximation. It only appears in the 2.5-PN order. An investigation without accounting for the energy loss to 1-PN order can be found in [17].

5.2.3 Riemann ellipsoids

The Riemann ellipsoids are a "combination" of the Jacobi and Dedekind ellipsoids described below. The ellipsoids rotate with a constant angular velocity with respect to an inertial frame. Additionally, there is an internal motion in a co-rotating frame with a uniform vorticity. However, such

ellipsoids are in general not stationary similar to the case of Jacobi ellipsoids.[2] Therefore, if these solutions are used as a starting point for a PN approximation scheme the energy carried away by gravitational radiation is not vanishing. This effect can again be estimated by the Newtonian mass quadrupole moment and its time derivatives.

A special sequence of the Riemann ellipsoids is the irrotational one. The vorticity of the internal motion vanishes for these ellipsoids in an inertial frame. A 1-PN approximation for this sequence was discussed in [64]. Note that these ellipsoids are prolate.

5.3 Dedekind ellipsoids

In this section, we discuss the sequence of Dedekind ellipsoids in detail. It is congruent (adjoint) to the Jacobi sequence in the sense of Dedekind's theorem, see, e.g., [21]. Thus, Eq. (5.8) holds here as well and $\bar{a}_2 \in [0,1]$ is a parameter for the sequence. For $\bar{a}_2 = 1$ the Dedekind ellipsoids become axially symmetric and rigidly rotating. They then coincide with a Maclaurin spheroid at the point $\bar{a}_{3,\mathrm{b}}$, cf. Section 5.2.1. We discuss the limit, $\bar{a}_2 \to 0$, in detail in Section 5.3.1. The solution in the interior is given by

$$\begin{aligned} U &= 2\pi G\mu \left(A_\emptyset - \sum_{i=1}^{3} A_i \left(x^i\right)^2 \right), \\ \mathbf{v} &= \left(-\frac{a_1}{a_2}\Omega x^2, \frac{a_2}{a_1}\Omega x^1, 0 \right), \\ p &= \pi G\mu^2 a_3^2 A_3 \left(1 - \sum_{i=1}^{3} \left(\frac{x^i}{a_i}\right)^2 \right), \end{aligned} \tag{5.9}$$

with the same Ω as in the Jacobi case (5.7) and as depicted in Fig. 5.1. The vorticity of the internal motion is constant and points in x^3-direction. The angular momentum points in this direction as well and reads

$$L_1 = L_2 = 0, \quad L_3 = \frac{8\pi}{15}\mu\Omega a_1^2 a_2^2 a_3. \tag{5.10}$$

The Dedekind ellipsoids are stationary, i.e., they preserve their shape in an inertial frame due to internal motion. This implies that the time derivative of the Newtonian mass quadrupole moment vanishes and no gravitational radiation is emitted to 2.5-PN order. Therefore, the Dedekind ellipsoids are a promising starting point to answer the question whether stationary, non-axially symmetric and rotating solutions exist in general relativity (at least in a PN approximation scheme). The Dedekind ellipsoids were previously investigated to 1-PN order in [22, 23] the results of which are corrected and improved in Chapter 6.

5.3.1 The rod-limit of the Dedekind ellipsoids

Since we did not find an account of this limit in the literature, we describe it here thoroughly with the PN approximation already in mind. The limit $\bar{a}_2 \to 0$ of the Dedekind sequence, which implies $\bar{a}_3 \to 0$ by virtue of Eq. (5.8), depends on the behavior of the free constants μ and a_1. We pose several conditions in the Newtonian case that eventually allow a PN approximation in the limit $\bar{a}_2 \to 0$. In particular, Eq. (6.4a) suggests that the kinetic energy δE_{kin} and the gravitational

[2] The Dedekind and Maclaurin sequences are limiting cases of the Riemann ellipsoids. In these limits, the Riemann ellipsoids are, of course, stationary.

potential energy δE_{pot} contained in a small volume around the axis have to be finite so that the inhomogeneity might form a distributional line density, i.e., a Dirac sequence[3]. It is not required that the total mass or the total kinetic energy is finite, primarily because we permit $a_1 \to \infty$ in this limit as well.

For an analytical treatment of the limit, we introduce a series expansion of $\bar{a}_2$, $\bar{A}_1$ and $\bar{A}_2$ in terms of $\bar{a}_3$. Let us define some notation used in these expansions. A function $f(x) \in \tilde{O}(g(x))$ if

$$\lim_{x\to 0} x^\beta \frac{f(x)}{g(x)} = 0, \ \forall\, \beta > 0. \tag{5.11}$$

For example, $x \log x \in \tilde{O}(x)$, but not $x \log x \in O(x)$.

As one can easily check, $\bar{a}_2(\bar{a}_3) - \bar{a}_3 \in \tilde{O}(\bar{a}_3^3)$. This allows us to expand first the index symbols using (A.6) in $\bar{a}_2$ at the point $\bar{a}_3$. The result is inserted in Eq. (5.8). This yields a polynomial in $\bar{a}_2$. The positive root of this polynomial[4] defines the axis ratio $\bar{a}_2$ of the ellipsoid in terms of $\bar{a}_3$. Subsequently, this root is plugged in the aforementioned expansion of the index symbols. This algorithm gives the following expansions:

$$\begin{aligned}
\bar{a}_2 =& \bar{a}_3 + \bar{a}_3^3 (\log 4 - 3 - 2\log \bar{a}_3) + 2\bar{a}_3^5 (\log \bar{a}_3 (7 \log \bar{a}_3 + 19 - 14 \log 2) + 14 + \\
& \log 2(\log 128 - 19)) + \tilde{O}(\bar{a}_3^7), \\
\bar{A}_1 =& -2\bar{a}_3^2 \left(\log \frac{\bar{a}_3}{2} + 1\right) + \bar{a}_3^4 \left(\log \bar{a}_3 (4 \log \bar{a}_3 + 9 - 8 \log 2) + \frac{13}{2} + \log 2(\log 16 - 9)\right) + \\
& \bar{a}_3^6 \left(-\frac{1}{4} \log \bar{a}_3 (4 \log \bar{a}_3 (28 \log \bar{a}_3 + 109 - 84 \log 2) + 607 + 4(42 \log 2 - 109) \log 4) - \right. \\
& \left. \frac{1187}{16} + 28(\log 2)^3 - 109(\log 2)^2 + \frac{607 \log 2}{4}\right) + \tilde{O}(\bar{a}_3^8), \\
\bar{A}_2 =& 1 + \bar{a}_3^2 \left(2 \log \bar{a}_3 + \frac{5}{2} - \log 4\right) + \bar{a}_3^4 \left((-8 \log \bar{a}_3 - 21 + 16 \log 2) \log \bar{a}_3 - \frac{63}{4} + \right. \\
& \left. (21 - 8 \log 2) \log 2\right) + \tilde{O}(\bar{a}_3^6).
\end{aligned} \tag{5.12}$$

The remaining index symbols can be inferred from the properties (A.4). Note that these results are independent of μ and a_1.

In order to obtain an inhomogeneity in the 1-PN Eq. (6.4a) that is a Dirac sequence, we ensure that the kinetic energy contained in a slice $\mathcal{S}\left(\delta x^1, x_0^1\right)$ of the Dedekind ellipsoid of height δx^1 at x_0^1 is finite for $\bar{a}_2 \to 0$. In addition, we determine the mass δM in such a slice to interpret the solution. The gravitational potential energy and the inner energy, which contribute to the source in (6.4a), are considered in the end of this section. δM and δE_{kin} calculate to

$$\delta M = \int\limits_{\mathcal{S}\left(\delta x^1, x_0^1\right)} \mu \mathrm{d}^3 x = -\frac{\mu}{3} \bar{a}_2 \bar{a}_3 \delta x^1 \pi \left(-3a_1^2 + \left(\delta x^1\right)^2 + 3\delta x^1 x_0^1 + 3\left(x_0^1\right)^2\right), \tag{5.13}$$

[3] More precisely, it is a Dirac net.

[4] To be able to obtain the zeros analytically the expansion should not go further then to fifth order. In fact, it is sufficient to expand Eq. (5.8) only to leading order and find the solution $\bar{a}_2(\bar{a}_3)$ up to this order. After the expansions of $\bar{a}_2$, $\bar{A}_1$ and $\bar{A}_2$ are found with this approximation, a recursion scheme can be adopted to go to arbitrary orders.

$$\delta E_{\text{kin}} = \int\limits_{\mathcal{S}\left(\delta x^1, x_0^1\right)} \frac{\mu}{2}\mathbf{v}^2 \mathrm{d}^3x = \frac{\pi^2}{60}\bar{a}_2\bar{a}_3\delta x^1 \left(15a_1^4 + 10a_1^2\left(-1+2\bar{a}_2^2\right)\left(\left(\delta x^1\right)^2 + 3\delta x^1 x_0^1 + 3\left(x_0^1\right)^2\right) - 3\left(-1+4\bar{a}_2^2\right)\left(\left(\delta x^1\right)^4 + 5\left(\delta x^1\right)^3 x_0^1 + 10\left(\delta x^1\right)^2\left(x_0^1\right)^2 + 10\delta x^1\left(x_0^1\right)^3 + 5\left(x_0^1\right)^4\right)\right)\mu^2 B_{12}.$$

If $\frac{\delta M}{\mu}$ is expanded in $\bar{a}_2$ close to 0, then it is quadratic in $\bar{a}_3$. Hence, we obtain a finite mass in the limit if the mass density reads to leading order

$$\mu = \frac{\eta}{\pi a_1^2 \bar{a}_3^2} \tag{5.14}$$

with an arbitrary constant η. This results in the following line mass density $\hat{\mu}$ for $\bar{a}_2 \to 0$:

$$\hat{\mu} = \eta\left(1 - \left(\frac{x_0^1}{a_1^2}\right)^2\right), \text{ for } x^1 \in [-a_1, a_1]. \tag{5.15}$$

Inserting the mass density (5.14) and the expansion of the index symbol B_{12}, cf. (A.4) and (5.12), into the kinetic energy, yields a logarithmic singularity in $\bar{a}_3$. In order to achieve a finite δE_{kin} for $\bar{a}_2 \to 0$, the leading order of the mass density has to be

$$\mu = \frac{\eta}{\pi G a_1^2 \bar{a}_3^2 (-\log \bar{a}_3)^{\frac{1}{2}}}. \tag{5.16}$$

The kinetic energy volume density reduces to the density e_{kin} along the x^1-axis for $\bar{a}_2 \to 0$:

$$e_{\text{kin}} = \frac{1}{2}\eta^2\left(1 - \frac{\left(x^1\right)^2}{a_1^2}\right)^2, \text{ for } x^1 \in [-a_1, a_1]. \tag{5.17}$$

The above considerations must be altered if $a_1 \to 0$ together with $\bar{a}_2 \to 0$, which implies that the Dedekind ellipsoid degenerates to a point.[5] In this case, the integrals in Eqs. (5.13) have to be taken over the entire ellipsoid, i.e., $\delta x^1 = 2a_1$ and $x_0^1 = -a_1$. The behavior of the mass density and the total kinetic energy is then given by

$$\begin{aligned} \mu &= \frac{\tilde{\eta}}{\pi G a_1^{\frac{5}{2}} \bar{a}_3^2 (-\log \bar{a}_3)^{\frac{1}{2}}}, \\ E_{\text{kin}} &= \frac{8}{15}\tilde{\eta}^2. \end{aligned} \tag{5.18}$$

We treat both cases, (5.16) and (5.18), simultaneously and write

$$\mu = \frac{\eta_s}{a_1^s \bar{a}_3^2 (-\log \bar{a}_3)^{\frac{1}{2}}}, \tag{5.19}$$

where $s = \frac{5}{2}$ and $\eta_{\frac{5}{2}} = \tilde{\eta}$ in case the Dedekind ellipsoids degenerate to a point, and $s = 2$, $\eta_2 = \eta$ if a line distribution is obtained. The meaning of η_s depends, of course, on s. The constant η_2 is a kinetic energy per unit length and $\eta_{\frac{5}{2}}$ is proportional to the square root of the total kinetic energy. Note that the limit $a_1 \to 0$ is independent of the behavior of $\bar{a}_2$ and $\bar{a}_3$ in the above considerations. Thus, the case $a_1 \to 0$ and $\bar{a}_2 > 0$ is included.

[5] Actually, it is not necessary that $\bar{a}_2 \to 0$. The Dedekind ellipsoids always contract to a point for $a_1 \to 0$.

Additionally, the Newtonian gravitational potential energy density μU of a fluid element serves as a source for the gravitational field in a 1-PN approximation. With the mass density (5.19), this yields for $s = 2$ and $s = \frac{5}{2}$:

$$e_{\text{pot}} = 4e_{\text{kin}} \quad \text{and} \quad E_{\text{pot}} = 4e_{\text{pot}}. \tag{5.20}$$

The inner energy contained in a slice, the term $\frac{3}{2}p^{(0)}$ in the inhomogeneity of Eq. (6.4a), vanishes logarithmically. Hence, it does not form a line density[6] and does not contribute to Φ in the limit.

Note that the mass δM and consequently the total mass vanish for μ as in Eq. (5.19). Therefore, $U \to 0$ in the exterior for $\bar{a}_2 \to 0$. Nonetheless, the PN approximation is not trivial, since the kinetic and the potential energy are sources of the gravitational field, see (6.4a). The velocity in x^1-direction is still diverging for $\bar{a}_2 \to 0$ independently of a_1.[7] More precisely, two non-interacting streams in the x^1-direction with infinite and opposite velocities emerge. Thus, the velocity of fluid elements exceeds the velocity of light for $\bar{a}_2 \to 0$. In fact, this happens already for $\bar{a}_2 > 0$. Hence, a PN approximation breaks down in the interior. This is not surprising, since mass distributions with a support of the dimension 0 or 1 generally lack a well-defined description by limits in general relativity as long as one confines oneself to the ordinary theory of distributions, cf. [33, 62]. A solution to this dilemma is to discard the interior for $\bar{a}_2 \to 0$ and to take into account only its effects that can be seen from the exterior like the energy and the angular momentum. In lieu of using the perfect fluid interpretation of the interior solution, we consider a singularity at the x^1-axis in the limit $\bar{a}_2 \to 0$ in the 1-PN approach. We elaborate this in Section 6.8. Nonetheless, it is not clear if the choice (5.19) suffices to have a similar limit in higher PN-orders.

If the velocity field is required to be finite the stronger requirement $\mu \sim \frac{\eta}{a_1^2 \bar{a}_3^2 \log \bar{a}_3}$ must be met. With this choice, the kinetic and the gravitational potential energy are vanishing and no energy is contained in the limiting space-time to first PN order. Therefore, the only choice for the behavior of μ for $\bar{a}_2 \to 0$ that leads to a reasonable and non-trivial space-time in a 1-PN approximation is (5.19).

In case $a_1 \to \infty$, then $\bar{a}_2 \to 0$ does not imply necessarily that $a_2 \to 0$. If $a_2 > 0$ in the limit, an infinite cylinder aligned with the x^1-axis is obtained with a finite or infinite radius. However, the velocity still diverges in the interior. But we cannot easily interpret this region as a singularity in the 1-PN solution. Thus, we assume for $a_1 \to \infty$ additionally $a_2 \to 0$, which yields a constant line density along the x^1-axis. This is the Newtonian limit of a general relativistic string and is included in the discussion above, in particular in Eq. (5.19).

5.3.2 The exterior solution

We describe how to obtain the exterior solution of the Newtonian Dedekind ellipsoids in detail as an instance of the formalism used to determine the 1-PN metric functions in Chapter 6. As far as we are aware, this solution was not given explicitly before.

[6] All multipole moments of this term vanish in the limit.

[7] However, the momentum contained in a slice $\mathcal{S}\left(\delta x^1, x_0^1\right)$ vanishes.

The exterior solution is best studied in ellipsoidal coordinates λ^i, see, e.g., [11]:

$$\begin{aligned}
\left(x^1\right)^2 &= \frac{\left(\lambda^1\right)^2\left(\lambda^2\right)^2\left(\lambda^3\right)^2}{h^2k^2},\\
\left(x^2\right)^2 &= \frac{\left(\left(\lambda^1\right)^2-h^2\right)\left(\left(\lambda^2\right)^2-h^2\right)\left(h^2-\left(\lambda^3\right)^2\right)}{h^2\left(k^2-h^2\right)},\\
\left(x^3\right)^2 &= \frac{\left(\left(\lambda^1\right)^2-k^2\right)\left(k^2-\left(\lambda^2\right)^2\right)\left(k^2-\left(\lambda^3\right)^2\right)}{h^2\left(k^2-h^2\right)},\\
h^2 &= a_1^2-a_2^2, \quad k^2 = a_1^2-a_3^2,\\
\lambda^1 &> k > \lambda^2 > h > \lambda^3 > 0.
\end{aligned} \tag{5.21}$$

These coordinates cover the octant $x^i > 0$, which is sufficient, because the Newtonian problem is reflection-symmetric with respect to the coordinate surfaces $x^i = 0$. In fact, we assume that the PN configuration has this symmetry as well. The surfaces of constant λ^1, λ^2 and λ^3 form concentric ellipsoids, one-sheeted hyperboloids and two-sheeted hyperboloids, respectively. The surface of the Dedekind ellipsoid is characterized in these coordinates by $\lambda^1 = a_1$.

Using the ellipsoidal coordinates, a separation of variables for the Poisson equation with a density the support of which is an ellipsoid is possible. The solution of $\Delta f = -4\pi\hat{\mu}$ is of the form

$$f(\lambda^i) = \sum_{n=0}^{\infty}\sum_{m=1}^{2n+1} f_m^n\left(\lambda^1\right) E_m^n\left(\lambda^2\right) E_m^n\left(\lambda^3\right), \tag{5.22}$$

where the functions E_m^n are the Lamé functions of the first kind. The first few members of this complete set of functions can be found in Appendix B. The functions f_m^n are obtained by solving the inhomogeneous Lamé equation $L_m^n(\lambda^1)[f_m^n] = \tilde{\mu}_m^n\left(\lambda^1\right)$. The Lamé operator $L_m^n(\lambda^1)$ is given in (B.1). The inhomogeneities $\tilde{\mu}_m^n\left(\lambda^1\right)$ are the expansion coefficients of the density $\hat{\mu}$ with respect to the ellipsoidal surface harmonics $E_m^n(\lambda^2)E_m^n(\lambda^3)$, i.e.,

$$\left(\left(\lambda^1\right)^2-\left(\lambda^2\right)^2\right)\left(\left(\lambda^1\right)^2-\left(\lambda^3\right)^2\right)\hat{\mu}\left(\lambda^i\right) = \sum_{n=0}^{\infty}\sum_{m=1}^{2n+1}\tilde{\mu}_m^n\left(\lambda^1\right) E_m^n\left(\lambda^2\right) E_m^n\left(\lambda^3\right). \tag{5.23}$$

Since the density $\hat{\mu}$ vanishes outside the ellipsoid, the Poisson equation becomes homogeneous and the sole solution with the correct asymptotics is given by

$$f_m^n\left(\lambda^1\right) = C_m^n F_m^n\left(\lambda^1\right), \tag{5.24}$$

where F_m^n denotes the Lamé functions of the second kind where the first few members are also given in Appendix B. In general, the task is to find a solution to the inhomogeneous Lamé equation. In our case, however, we can rely on a result given in [29]. In this article, Ferrers gives the interior solution of a Poisson equation where the inhomogeneity is a polynomial in Cartesian coordinates and has its support in an ellipsoid. The solution in the interior is a polynomial in Cartesian coordinates, too. Furthermore, he established the fact that this interior solution can be connected to an exterior solution vanishing at infinity.[8] The Newtonian density and the densities in the PN approximation are polynomials. The support of these polynomials is an ellipsoid. Thus, we obtain $f_m^n\left(\lambda^1\right)$ for $\lambda^1 \le a_1$ by a coordinate transformation of the interior solution from Cartesian to ellipsoidal coordinates. Because the interior solution is polynomial in Cartesian coordinates,

[8] The resulting function is continuously differentiable everywhere.

its expansion in ellipsoidal surface harmonics $E_m^n\left(\lambda^2\right) E_m^n\left(\lambda^3\right)$ terminates at finite order and we can simply read off $f_m^n(\lambda^1)$. Hence, C_m^n can afterwards be obtained by

$$C_m^n = f_m^n\left(a_1\right) F_m^n\left(a_1\right)^{-1}, \tag{5.25}$$

which determines the exterior solution completely.

We illustrate the method described above with the help of Dedekind ellipsoids. The interior solution (5.9) can be written after a transformation to ellipsoidal coordinates as

$$\begin{aligned} U =& f_1^0\left(\lambda^1\right) E_1^0\left(\lambda^2\right) E_1^0\left(\lambda^3\right) + \sum_{i=1}^{2} f_i^2\left(\lambda^1\right) E_i^2\left(\lambda^2\right) E_i^2\left(\lambda^3\right), \\ f_1^0\left(\lambda^1\right) =& -\frac{4}{3}\pi G\mu\left(3\left(\lambda^1\right)^4 - 2\left(\lambda^1\right)^2\left(h^2+k^2\right) + h^2k^2\right), \\ f_{1/2}^2\left(\lambda^1\right) =& -2\pi G\mu\left(1 \pm \frac{3\left(\lambda^1\right)^2 - h^2 - k^2}{\sqrt{h^4 - h^2k^2 + k^4}}\right). \end{aligned} \tag{5.26}$$

Therefore, we deduce that the exterior solution is of the form

$$U = C_1^0 F_1^0\left(\lambda^1\right) E_1^0\left(\lambda^2\right) E_1^0\left(\lambda^3\right) + \sum_{i=1}^{2} C_i^2 F_i^2\left(\lambda^1\right) E_i^2\left(\lambda^2\right) E_i^2\left(\lambda^3\right), \tag{5.27}$$

where the constants C_m^n are obtained from Eqs. (5.25), (5.26) and (B.5).

The potentials of the mass densities $\hat{\mu}_{i_1 i_2 \ldots i_k} = \mu x^{i_1} x^{i_2} \cdots x^{i_k}$ – the higher moments – are important in the next chapter. They are discussed in Appendix C including their explicit form in the exterior. The same method as in this section is applied there.

CHAPTER

6

THE 1-PN CORRECTIONS TO THE NEWTONIAN DEDEKIND ELLIPSOIDS

> One would make a grave mistake if one supposed that the spheroids are the only admissible figures of equilibrium even under the restrictive assumption of second degree surfaces[1].
>
> Carl Gustav Jacob Jacobi, [44][2]

In Newtonian physics it was believed long time that ellipsoidal figures of equilibrium have to be axially symmetric. Naturally, it came as a surprise when Jacobi presented his non-axially symmetric ellipsoidal figures of equilibrium, the Jacobi ellipsoids, in [44]. Is the situation similar in general relativity? There, a PN approximation of the axially symmetric Maclaurin ellipsoids to arbitrary order was established, see [56]. Even though convergence was not proven analytically, the numerical evidence of the existence of fully relativistic generalizations of the Maclaurin ellipsoids is very compelling, see, e.g., [52]. However, the existence of a similar generalization of non-axially symmetric solutions is controversial. The main argument against their existence is an energy loss due to gravitational radiation. This can be estimated to 2.5-PN order by the quadrupole formula using the Newtonian solution. As discussed in the last chapter the Newtonian Dedekind ellipsoids have a constant mass quadrupole moment. Thus, no gravitational radiation is present to 2.5-PN order. If Einstein's field equation for a stationary space-time filled with a self-gravitating fluid is used for a PN approximation, the effect of an energy loss due to gravitational radiation is ruled out completely. Furthermore, we consider an isolated source, which implies an asymptotically flat space-time. Consequently, we exclude incoming radiation, which could in principle counterbalance outgoing radiation. Bearing this in mind, Jacobi's statement becomes relevant in broader context again. Are we making a mistake if we suppose that axially symmetric, rotating and stationary configurations are the only admissible figures of equilibrium in general relativity?

In [49], Lindblom raised the additional question assuming the existence of non-axially symmetric, stationary perfect fluid solutions: Do they have necessarily additional discrete symmetries like reflection symmetries? The Newtonian Dedekind ellipsoids are eigenfunctions of reflections with respect to the coordinate planes $x^a = 0$. This is preserved by construction in our 1-PN approximation. Is such a symmetry necessary or sufficient?

[1] In the scope of astrophysical objects, only closed surfaces are of interest and closed surfaces of second degree are ellipsoids.

[2] The translation into English originates from [21].

Chandrasekhar and Elbert discussed already a 1-PN approximation to the Dedekind ellipsoids in [22]. However, there was a mistake in the ansatz for the velocity field that was canceled by an erroneous subsequent analysis. Both problems where in [23]. Still, the numerical results presented in [23] are false, though the analytical treatment is correct up to typing errors.[3] Besides the problem with the numerical values, the solution obtained in [23] lacks some properties known from the Newtonian solutions. For example, we show in Paper V that the sequence of 1-PN solutions in [23] cannot be continuously connected to the 1-PN Maclaurin spheroids. Therefore, we suggest a generalization of the ansatz in [23] with which those properties can be satisfied and discuss the resulting solution in detail afterwards. In particular, a limit where the Newtonian Dedekind ellipsoids degenerate to a rod is studied.

6.1 What do we expect of 1-PN Dedekind ellipsoids?

The 1-PN Dedekind ellipsoids[4] should constitute a family of stationary self-gravitating perfect fluid solutions. Since the source is isolated, the space-time is supposed to be asymptotically flat. Furthermore, we assume that the solutions have a discrete "ellipsoidal symmetry", i.e., the metric, velocity field, the surface and the pressure are eigenfunctions to the transformation $x^a \to -x^a$ in suitable coordinates[5]. This ensures that it is sufficient to study the solution in just one octant in the asymptotic Cartesian coordinates system. Moreover, it simplifies the use of ellipsoidal coordinates and the analysis for the exterior solution. In addition, the sequence of the 1-PN Dedekind ellipsoids is expected to be continuously connected to the sequence of the 1-PN Maclaurin spheroids. This means that at one end of the sequence the solutions describe rigidly rotating and axially symmetric configurations. If possible, the family of solutions should be singularity-free.

The above requirements are physical in nature. If the results in [29] regarding polynomial inhomogeneities are used, it is technically advantageous to make the following assumption: Inside the Newtonian ellipsoid all metric and matter functions are polynomials of minimal degree in asymptotic Cartesian coordinates. We show that all the above requirements (physical and technical) are met with our ansatz for the velocity field in Eq. (6.5b).

6.2 The 1-PN field equations

In [15], a set of 1-PN field equations was discussed whose solution describes a perfect fluid dynamically to first order in c^{-2} (c denotes the velocity of light). In a series of papers [14, 16, 17, 19, 20] solutions to these equations were found using the Newtonian Maclaurin and Jacobi ellipsoids as starting points. In [22, 23], the 1-PN Newtonian Dedekind ellipsoids were investigated.

The equations used in all those papers have the obvious advantage that they are more general than those arising in the elegant projection formalism for stationary space-times described in [32]. In contrast to this formalism, they are applicable also in non-stationary settings. The method used for determining these equations suffers from a disadvantage, too. In case of stationary problems like the PN Dedekind ellipsoids, we also have to determine the equations belonging to the dynamical aspects of the fluid. However, they must be satisfied identically. Obtaining and solving these dynamical equations is a redundant task. Therefore, it is for higher orders easier to

[3] For a detailed discussion, we refer the reader to Appendix A in Paper V.

[4] Of course, the shape of the 1-PN configuration does not need to be an ellipsoid in the considered coordinate system. However, in the light that the corrections are small we still call the solution "ellipsoid" in the following.

[5] Covariantly formulated, we require that there exist three discrete isometries whose fixed points form distinct timelike 3-hypersurfaces. Additionally, we assume that the intersection of all three fixed point sets is a timelike curve, and the intersections of any two of them form timelike 2-surfsaces.

expand the equations given in the projection formalism [32] in $\frac{1}{c}$. Nonetheless, the 1-PN equations given in [15] reduce in the case of stationarity exactly to the 1-PN equations obtained from [32]. So, we follow the notation of [15].

We use the same PN expansion of the metric, i.e., the same parameterization of the 1-PN metric, as in [15]:

$$\begin{aligned} g_{ab} &= -\left(1+\frac{2U^{(0)}}{c^2}\right)\delta_{ab}, \quad g_{a0} = 4U_a^{(3)}c^{-3}, \\ g_{00} &= 1-2U^{(0)}c^{-2}+2\left(U^{(0)2}-\delta U-2\Phi\right)c^{-4}, \end{aligned} \tag{6.1}$$

where Greek indices run from 0 to 3 and Latin from 1 to 3. δ_{ab} denotes the Kronecker delta, $x^0 = ct$ is the Killing time, and $U^{(0)}$ is the Newtonian gravitational potential for the Dedekind ellipsoids as given in Eq. (5.9) and (5.27). Latin indices are raised and lowered with the Euclidean metric δ_{ab}. The signature of the metric is $(1,-1,-1,-1)$.

The pressure, velocity and the surface are also corrected in 1-PN order as follows:

$$p = p^{(0)} + p^{(2)}c^{-2}, \quad v^a = v^{(0)a} + v^{(2)a}c^{-2}, \quad S(x^a) = S^{(0)}\left(x^a\right) + c^{-2}S^{(2)}\left(x^a\right) \tag{6.2}$$

where $v^{(0)a}$, $p^{(0)}$ and $S^{(0)}$ are the velocity[6], pressure and surface of the Newtonian Dedekind ellipsoids, see Eqs. (5.1) and (5.9). As a convention, the PN corrections to the mass density μ are assumed to vanish.[7]

An explanation of the different terms in Eq. (6.1) is expedient. In Eq. (6.2), we introduce the 1-PN correction $S^{(2)}$, which can be interpreted as a perturbation of the Newtonian surface. This means a new Newtonian gravitational potential U' has to be determined for a homogeneous mass density with a support in the perturbed ellipsoid $S(x^b) \leq 0$. The difference $U' - U^{(0)}$, i.e., the perturbation of the Newtonian potential, is denoted by $\frac{\delta U}{c^2}$. Moreover, in the c^{-4}-order of g_{00} a potential Φ is introduced rather than $\Psi = 2\Phi - U^{(0)2}$ in order to ensures that the inhomogeneity in the 1-PN field equations (6.4) is vanishing outside the Newtonian ellipsoid. We refer to the highest order terms in $\frac{1}{c}$ in Eq. (6.1) as 1-PN corrections of the metric. The c^{-2}-term in g_{00} defines the Newtonian limit.

We show that the ansatz for the spatial part of the metric in (6.1) is indeed justified. Of course, the spatial metric[8] is conformally flat because the Cotton tensor always vanishes to 1-PN order. Nonetheless, let us assume a general spatial metric $g_{ab} = -\delta_{ab} + c^{-2}g_{ab}^{(2)}$. Then the 1-PN equations for the spatial components of the metric read

$$\begin{aligned} 0 &= -2g_{12,12}^{(2)} + \left(g_{11}^{(2)} + 2U^{(0)}\right)_{,22} + \left(g_{22}^{(2)} + 2U^{(0)}\right)_{,11}, \\ 0 &= -g_{12,13}^{(2)} - g_{13,12}^{(2)} + g_{23,11}^{(2)} + \left(g_{11}^{(2)} + 2U^{(0)}\right)_{,23}, \end{aligned} \tag{6.3}$$

where the remaining equations are obtained by cyclic permutations of $\{1,2,3\}$. It is obvious that the ansatz in Eq. (6.1) satisfies these equations. This special ansatz can be seen as a choice of a coordinate system where the spatial metric is proportional to δ_{ab} and the conformal factor is

[6] The 3-velocity v^a is defined as in [22, 23]. It does not refer to the spatial components of the 4-velocity $u^\mu = \frac{\mathrm{d}x^\mu}{\mathrm{d}\tau}$ where τ is the proper time of the fluid element. Instead, it is defined as $v^a = \frac{\mathrm{d}x^a}{\mathrm{d}t} = c\frac{u^a}{u^0}$.

[7] Possible 1-PN corrections to the mass density are equivalent to considering a Newtonian Dedekind ellipsoid with a mass density $\mu + c^{-2}\mu^{(2)}$ as starting point for a 1-PN approximation. This is analog to the discussion of the coordinate volume in Section 6.9.

[8] In the projection formalism, the contravariant components of the spatial metric form the inverse metric of the manifold of the trajectories of the Killing vector.

defined by $-1-c^{-2}2U^{(0)}$. In fact, this determines the spatial coordinates uniquely if we take two additional requirements into account. Firstly, the Newtonian potential should be given as in Eq. (5.9) which allows only "1-PN coordinate transformations", i.e., coordinate transformations of the form $y^\mu = x^\mu + c^{-2}f^\mu(x^\nu)$. Secondly, the three 2-surfaces of fixed points of the discrete transformations described in Section 6.1 should be characterized by $y^a = 0$ in admissible coordinate systems. The time coordinate is not defined uniquely.

Note that we use as expansion parameter $\frac{1}{c}$ to retain the compatibility with previous works, e.g., [14–17, 19, 20, 22–25]. However, one could transform the results easily to a dimensionless expansion parameter, for instance, $\varepsilon^2 = \frac{2MG}{c^2 a_1}$ in order to compare the results to [56].

The 1-PN equations of a self-gravitating perfect fluid in general relativity were given in [15] and read

$$\Delta\Phi = -4\pi G\mu\left(v^2 + \frac{3p^{(0)}}{2\mu} + U^{(0)}\right), \tag{6.4a}$$

$$\Delta U_a^{(3)} = -4\pi G\mu v_a^{(0)}, \tag{6.4b}$$

$$v^{(2)a}{}_{,a} = -\left(\left(v^{(0)}\right)^2 + \frac{p^{(0)}}{\mu} + 2U^{(0)}\right)_{,a} v^{(0)a}, \tag{6.4c}$$

$$\begin{aligned}\frac{p^{(2)}_{,a}}{\mu} = &\left(\delta U + 2\Phi + \frac{1}{2}\left(\frac{p^{(0)}}{\mu}\right)^2\right)_{,a} - 2\left(v^{(0)}\right)^2 U^{(0)}_{,a} + 4v^{(0)b}\left(U^{(3)}_{a,b} - U^{(3)}_{b,a}\right) - \\ &v^{(0)b}\left(\left(\left(v^{(0)}\right)^2 + 4U^{(0)}\right)v^{(0)}_{a,b} + 4v^{(0)}_a U^{(0)}_{,b}\right) - v^{(0)b}v^{(2)}_{a,b} - v^{(2)b}v^{(0)}_{a,b},\end{aligned} \tag{6.4d}$$

where $\left(v^{(0)}\right)^2$ is the square of the Newtonian velocity field. The sole equations that remain to be solved in order to determine the metric to 1-PN order are the first two and the one which determines δU given below, see (6.9). It is important that the inhomogeneities in the first two equations have their support in the Newtonian ellipsoid. This is ensured by the parameterization of the expansion of the metric component g_{00} in (6.1), cf. the remarks after Eq. (6.1). This enables us to use – also to this order – the results of [29] because the inhomogeneities in the Poisson equations for Φ and $U_a^{(3)}$ are polynomials in the asymptotic Cartesian coordinates, cf. Eq. (5.9). It is doubtful if a similar parameterization of the metric exists in higher PN orders, see for the 2-PN equations [15]. If it does not, we cannot use the results of [29] anymore and the entire problem has to be tackled in ellipsoidal coordinates. We were able to obtain a 1-PN solution also in this approach. But the solution to higher orders still has to be investigated.

6.3 The ansatz for the 1-PN velocity field and the surface

Eqs. (6.4c) and (6.4d) are coupled equations for $v^{(2)a}$ and $p^{(2)}$, which are hard to solve directly. However, the symmetry assumptions and the technical requirement of polynomial 1-PN corrections, cf. Section 6.1, simplifies this task considerably. Thus, we make the following ansatz for the 1-PN contributions to the surface S and to the velocity v^a:

$$\begin{aligned}S^{(2)}\left(x^b\right) = -2\pi G\mu\Bigg(&a_1^2\sum_{i=1}^{2} S_i\left(\left(\frac{x^i}{a_i}\right)^2 - \left(\frac{x^3}{a_3}\right)^2\right) + S_3\left(x^1\right)^2\left(\frac{\left(x^1\right)^2}{3\left(a_1\right)^2} - \left(\frac{x^2}{a_2}\right)^2\right) + \\ &S_4\left(x^2\right)^2\left(\frac{\left(x^2\right)^2}{3\left(a_2\right)^2} - \left(\frac{x^3}{a_3}\right)^2\right) + S_5\left(x^3\right)^2\left(\frac{\left(x^3\right)^2}{3\left(a_3\right)^2} - \left(\frac{x^1}{a_1}\right)^2\right)\Bigg),\end{aligned} \tag{6.5a}$$

$$\begin{aligned}
\frac{v_1^{(2)}}{(\pi G\mu)^{\frac{3}{2}}} &= x^2\left(a_1^2 w_1 + \hat{q}_1\left(x^1\right)^2 + r_1\left(x^2\right)^2 + t_1\left(x^3\right)^2\right),\\
\frac{v_2^{(2)}}{(\pi G\mu)^{\frac{3}{2}}} &= x^1\left(a_2^2 w_2 + \hat{q}_2\left(x^2\right)^2 + r_2\left(x^1\right)^2 + t_2\left(x^3\right)^2\right),\\
\frac{v_3^{(2)}}{(\pi G\mu)^{\frac{3}{2}}} &= q_3 x^1 x^2 x^3.
\end{aligned} \tag{6.5b}$$

In [23] neither w_1 nor w_2 are considered. In Paper V, we show that these linear contributions are crucial to allow a rigidly rotating and axially symmetric limit of the 1-PN Dedekind ellipsoid coinciding with the 1-PN Maclaurin spheroids! Moreover, it seems natural to introduce a 1-PN correction to the linear terms in the Newtonian velocity. In fact, the sole 1-PN correction to the velocity field of the Jacobi and Maclaurin ellipsoids was to the angular velocity Ω, see [16, 17]. This was sufficient, because of the rigid rotation of these ellipsoids. Additionally, we introduce the constants $\hat{q}_1 = q_1 + q$ and $\hat{q}_2 = q_2 - q$ in contrast to [23].[9]

The ansatz for the 1-PN corrections to the surface $S^{(2)}$ is the same as in [23], i.e., it originates from a Lagrangian displacement of all fluid elements. The Lagrangian displacement, which preserves the coordinate volume, reads

$$\begin{aligned}
\xi_a =& \frac{\pi G\mu a_1^2}{c^2}\sum_{A=1}^{5} S_A \xi_a^A,\\
\left(\xi_a^1\right) =& \left(x^1, 0, -x^3\right), \qquad \left(\xi_a^2\right) = \left(0, x^2, -x^3\right), \qquad \left(\xi_a^3\right) = \frac{1}{3a_1^2}\left(\left(x^1\right)^3, -3\left(x^1\right)^2 x^2, 0\right),\\
\left(\xi_a^4\right) =& \frac{1}{3a_1^2}\left(0, \left(x^2\right)^3, -3\left(x^2\right)^2 x^3\right), \qquad \left(\xi_a^5\right) = \frac{1}{3a_1^2}\left(-3\left(x^3\right)^2 x^1, 0, \left(x^3\right)^3\right),
\end{aligned} \tag{6.6}$$

cf. Eq. (41) in [23]. As was pointed out in [2], it is more physical not to fix the coordinate volume but to rather to fix some physical parameters like the baryonic mass. However, this constraint is technically useful in the subsequent analysis. The coordinate volume can later be chosen arbitrarily, which can be interpreted as a change of the underlying Newtonian configuration of order c^{-2}, cf. Section 6.9. Note that higher order polynomials could also be allowed in this ansatz, which leads eventually to a homogeneous system of equations for the coefficients of the higher order monomials. The ansatz we use here is the minimal one with which the inhomogeneous equations can be satisfied and with which Dedekind-like solutions with the properties discussed in Section 6.1 can be obtained. In particular, the ansatz is reflection-symmetric with respect to the coordinate planes $x^a = 0$.

Even though the additional parameters w_i in the ansatz do not change the analysis in [22, 23] fundamentally, we describe the calculations in more detail and give intermediate results and analytic expressions. The main reason for doing so is that we were unable to reproduce the numerical data given in [23] for the case $w_1 = w_2 = 0$ in which both solutions agree (see the discussion in Paper V for further details). The analytic expressions could prove helpful for identifying the problems in [23] or, at the very least, they make our calculations repeatable.

[9] There the constant q was superfluous and was only used for technical reasons. However, it is used in Paper V as well.

6.4 The 1-PN metric

In this section, we recall the interior[10] solution found in [22]. We obtain the exterior solution, which was not included in [22, 23], as well. Even though we have a different ansatz for the 1-PN velocity, this does not affect the first two equations of (6.4). The inhomogeneities of these two Poisson equations are polynomial. Hence, the results of [29] apply. Knowing the higher moments in the interior as defined in Appendix C is sufficient to construct them in the exterior explicitly using the method described in Section 5.3.2. This is done in Appendix C, too. In terms of these higher moments $D_{i_1 i_2 \ldots}$, the metric functions read

$$\begin{aligned}\Phi = \pi G\mu \Bigg[U^{(0)} \left(\frac{3}{2} a_3^2 A_3 + A_\emptyset \right) - \frac{5}{2} A_3 D_{33} - \left(A_1 + \frac{3}{2} \frac{a_3^2}{a_1^2} A_3 - \frac{a_2^2}{a_1^2} \bar{\Omega}^2 \right) D_{11} - \\ \left(A_2 + \frac{3a_3^2}{2a_2^2} A_3 - \frac{a_1^2}{a_2^2} \bar{\Omega}^2 \right) D_{22} \Bigg], \\ U_1^{(3)} = -\frac{a_1}{a_2} \Omega D_2, \quad U_2^{(3)} = \frac{a_2}{a_1} \Omega D_1, \quad U_3^{(3)} = 0.\end{aligned} \tag{6.7}$$

Only D_1, D_2 and the diagonal terms of the higher moments of the second order (two coinciding indices) are required.

For δU a similar approach can be taken. It results from the perturbation of the surface of the Newtonian configuration. It can be written as sum of derivatives of Poisson integrals:

$$\frac{\delta U}{c^2} = -G \frac{\partial}{\partial x^a} \int \frac{\mu \xi^a}{|\mathbf{x} - \mathbf{x}'|} \mathrm{d}^3 x', \tag{6.8}$$

cf. Eq. (58) in [16]. As such, δU is not continuously differentiable across the Newtonian surface, which is a problem inherent to this coordinate system and the approximation. After a coordinate transformation $y^a = x^a - \xi^a$ to surface adapted Cartesian coordinates, the metric components are continuously differentiable. In these coordinates, the surface does not change because its PN corrections translate into corrections to the inhomogeneity of the Poisson equation of Φ. This also implies that no term δU has to be considered. We are not using these surface adapted coordinates here, but they prove useful in higher PN orders.

With the Lagrangian displacement ξ^a defined in Eq. (6.6), it is clear that the densities in the Newtonian (volume) potentials in Eq. (6.8) are polynomials in the asymptotic Cartesian coordinates. Thus, the algorithm described in Section 5.3.2 can be employed. The derivatives have to be applied, afterwards. The result of this yields

$$\begin{aligned}\delta U = -\mu^2 G^2 \pi a_1^2 \Bigg((D_{1,1} - D_{3,3}) S_1 + (D_{2,2} - D_{3,3}) S_2 + (D_{111,1} - 3D_{112,2}) \frac{S_3}{3a_1^2} + \\ (D_{222,2} - 3D_{223,3}) \frac{S_4}{3a_1^2} + (D_{333,3} - 3D_{331,1}) \frac{S_5}{3a_1^2} \Bigg).\end{aligned} \tag{6.9}$$

The higher moments with three indices are polynomials of fifth order in the interior of the ellipsoid. But the coefficients in front of the S_i are only polynomials of fourth order. The coefficients satisfy a Poisson equation with a density distributed at the surface of the Newtonian ellipsoid. Therefore, they are continuous everywhere. Thus, we can construct the exterior solution for those coefficients analogously to the method presented in Section 5.3.2. First, we have to transform the coefficients of the S_i to ellipsoidal coordinates. Secondly, we have to expand the result in ellipsoidal harmonics. The expansion coefficients (at the surface) together with Eq. (5.25) are sufficient to write down the solution in the exterior. This is done explicitly in Appendix C.

[10] The interior and exterior refer here to the Newtonian ellipsoid because the inhomogeneities in Eqs. (6.4a) and (6.4b) have their support in the interior of $S^{(0)}$.

6.5 The Bianchi identity

The pressure, the velocity field and the surface follow from the equations resulting from the Bianchi identity, i.e., the Eqs. (6.4c) and (6.4d). Inserting our ansatz (6.5) in the integrability condition for the gradient of the pressure (6.4d) yields a polynomial that has to vanish everywhere. This implies the following values of the parameters in the ansatz:

$$\begin{aligned}
t_2 &= \bar{a}_2^2 t_1, \\
r_2 &= 4\left(\bar{a}_2^3 - \bar{a}_2\right)\bar{\Omega}\left(\bar{B}_{112} + \bar{B}_{122}\right) + \left(\frac{1}{\bar{a}_2} - \bar{a}_2^3\right)\bar{\Omega}^3 + \frac{1}{3}\left(\hat{q}_1\left(\bar{a}_2^2 + 2\right) + \hat{q}_2\left(2\bar{a}_2^2 + 1\right) - 3r_1\bar{a}_2^2\right), \\
q_3 &= -4\left(\bar{a}_2 - \frac{1}{\bar{a}_2}\right)\bar{\Omega}\left(\bar{B}_{123} + \bar{B}_{13}\right).
\end{aligned} \tag{6.10}$$

Note that the constant q_3 is already determined completely and is independent of the parameters w_i. It also coincides with the solution given in [23] including the numerical values. Using the results (6.10) in Eq. (6.4d), the pressure can be defined easily by an integration of the right hand side of Eq. (6.4d). This leaves one free constant, say, the central pressure p_c.

Inserting the ansatz (6.5) and the Eq. (6.10) in the continuity equation (6.4c) leads to another constraint on the constants:

$$\hat{q}_2 = 2\left(\bar{a}_2 - \frac{1}{\bar{a}_2}\right)\bar{\Omega}\left(\bar{a}_2^2\bar{B}_{123} + \bar{B}_{23}\right) + 2\left(\bar{a}_2 - \frac{1}{\bar{a}_2}\right)\bar{\Omega}^3 - \hat{q}_1. \tag{6.11}$$

A further simplification is achieved by requiring that the velocity normal to the surface vanishes to 1-PN order. This gives

$$\begin{aligned}
t_1 =& \frac{1}{2\bar{a}_2\bar{a}_3^2}\left[2\bar{\Omega}\left(S_2 - S_1 - \bar{a}_2^2 S_4 + \bar{a}_3^2 S_5 + 2\left(\bar{a}_2^2 - 1\right)\left(\bar{B}_{123} + \bar{B}_{13}\right)\right) - \bar{a}_2\left(w_1 + w_2\right)\right], \\
r_1 =& \frac{1}{\bar{a}_2^3}\left[\bar{\Omega}\left(\frac{1}{3\left(\bar{a}_2^2 - 1\right)}\left[3(5\bar{a}_2^2 + 1)(S_2 - S_1) - 3(3\bar{a}_2^2 - 1)S_3 + 2\bar{a}_2^2(2\bar{a}_2^2 + 1)S_4\right]\right.\right. \\
& \left. -6\bar{a}_2^2\left(\bar{B}_{112} + \bar{B}_{122}\right) - 2\left(2\bar{a}_2^2 + 1\right)\left(\bar{a}_2^2\bar{B}_{123} + \bar{B}_{23}\right)\right) - \frac{\left(w_1 + w_2\right)\bar{a}_2\left(5\bar{a}_2^2 + 1\right)}{2\left(\bar{a}_2^2 - 1\right)} - \\
& \left.\frac{\left(5\bar{a}_2^2 + 1\right)\bar{\Omega}^3}{2}\right], \\
\hat{q}_1 =& \bar{\Omega}\left(\frac{1}{3\bar{a}_2\left(\bar{a}_2^2 - 1\right)}\left[3(\bar{a}_2^2 + 1)(S_2 - S_1) - (5\bar{a}_2^2 + 3)S_3 + 2\bar{a}_2^2 S_4\right] - 6\bar{a}_2\left(\bar{B}_{112} + \bar{B}_{122}\right)\right. \\
& \left. -2\frac{\left(\bar{a}_2^2 + 2\right)}{\bar{a}_2}\left(\bar{a}_2^2\bar{B}_{123} + \bar{B}_{23}\right)\right) - \frac{3\left(w_1 + w_2\right)\left(\bar{a}_2^2 + 1\right)}{2\left(\bar{a}_2^2 - 1\right)} - \frac{\left(\bar{a}_2^2 + 5\right)\bar{\Omega}^3}{2\bar{a}_2}.
\end{aligned} \tag{6.12}$$

Hitherto, we gave all parameters entering the 1-PN corrections in terms of w_i and S_i. To determine the surface coefficients S_i, we have to impose the condition that the pressure vanishes at the surface up to 1-PN. This leads to a linear system of equations:

$$\sum_{j=0}^{5} M_{ij} S_j = b_i^{(0)} + b_i^{(1)} w_1 + b_i^{(2)} w_2 = b_i. \tag{6.13}$$

The equations for $i = 1, \ldots, 5$ ensure that the pressure at the surface is constant. Having solved these, the 1-PN contribution to the central pressure $p_c^{(2)} = S_0 a_1^4 \mu(\mu G)^2$ is obtained using the

equation for $i = 0$ such that the pressure vanishes at the surface. We give the analytic expressions for the coefficient matrix and the inhomogeneity in Appendix D.

A solution S_i of this equation depends linearly on w_i, as do the constants entering our ansatz (6.5). The free parameters w_i must be chosen such that the resulting surface (6.5) is still closed. This is just a reformulation of the fact that the 1-PN correction must be small compared to the Newtonian quantities, but it also offers here an explicit and necessary criterion. Note that, although we refer to the w_i as parameters, they can, in fact, be chosen arbitrarily for every $\bar{a}_2$. They are functions of $\bar{a}_2$ along the sequence. If we want to obtain a continuous sequence of 1-PN Dedekind ellipsoids, these functions are required to be continuous as well. Stronger conditions have to be posed in the subsequent discussion of the properties of the 1-PN Dedekind ellipsoids at certain points. So, we assume that $w_i(\bar{a}_2)$ are smooth functions.

The singularity, which was discovered in [23], has its origin in a vanishing determinant of the coefficient matrix (M_{ij}). It can be removed with a special choice of the w_i as discussed in Section 6.6.2.

6.6 Properties of the solution

The solution of the surface condition is too lengthy to be given here explicitly. Thus, we present the solution along the sequence of 1-PN Dedekind ellipsoids in Figs. 6.1 and 6.2. Afterwards, the 1-PN Dedekind ellipsoids and their properties are discussed in detail.

Let us denote an arbitrary parameter in the ansatz (6.5) C. It can always be written as

$$C = C^0 + C^1 w_1 + C^2 w_2. \tag{6.14}$$

The part C^0 coincides with the solution obtained in [23]. However, as discussed at length in Paper V the numerical values do not agree. There are three special points in these graphs. First, there is the obvious singularity at[11] $\bar{a}_2^s = 0.33700003168\ldots$, which can be removed with a special choice of w_i as proved in Section 6.6.2. Note that this is a singularity in the parameter space of the solution. The entire solution is not well-defined at this point of the sequence. For example, the central pressure and the angular momentum are singular at $\bar{a}_2^s$, cf. Figs. 6.2(h) and 6.3(b). In addition, the surface of the configuration is not closed at this point anymore. In fact, the PN approximation breaks down in the neighborhood of $\bar{a}_2^s$, and the solutions along the 1-PN Dedekind sequence are not anymore continuously connected through this point unless the singularity is removed. We have to distinguish this kind of singularity from the singularities in an otherwise well-defined space-time. Such occur in the limit $\bar{a}_2 \to 0$. The limit $\bar{a}_2 \to 1$ is also of interest, since the 1-PN Dedekind ellipsoids are required to coincide with the 1-PN Maclaurin spheroids. This can also be achieved by a choice of w_i, as shown in Paper V in Section 6.7. The limit $\bar{a}_2 \to 0$, where the Newtonian Dedekind ellipsoid degenerates to a rod, is investigated in detail in Section 6.8. To get a physically meaningful solution there, a special choice of w_i in the neighborhood of $\bar{a}_2 = 0$ is necessary, too.

We also investigate the trajectories of fluid elements, the shape of the body and corrections to the mass and the angular momentum.

[11] Hereafter, if not indicated otherwise, numerical values are truncated after six digits; we do not write this explicitly using dots.

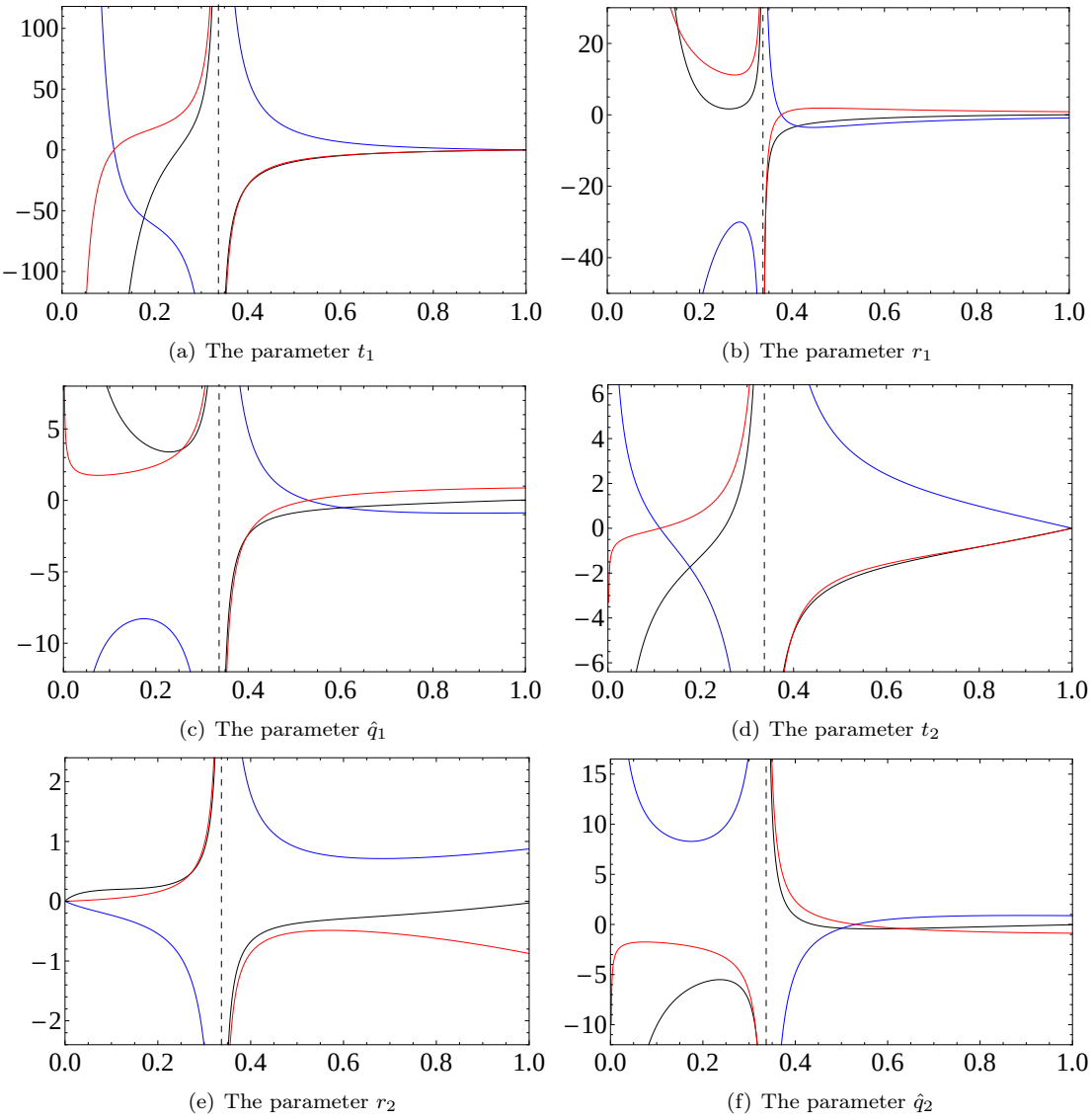

(a) The parameter t_1

(b) The parameter r_1

(c) The parameter $\hat{q}_1$

(d) The parameter t_2

(e) The parameter r_2

(f) The parameter $\hat{q}_2$

Figure 6.1: The values of the parameters t_1, t_2, etc. in the 1-PN correction to the velocity (see Eq. (6.5b)) are depicted as functions of $\bar{a}_2$. Theses constants are split according to Eq. (6.14) into C^0 (black), C^1 (blue) and C^2 (red) where $C = t_1,\ t_2,\ r_1,\ r_2,\ \hat{q}_1,\ \hat{q}_2$. The dashed line marks the axis ratio $\bar{a}_2^s$.

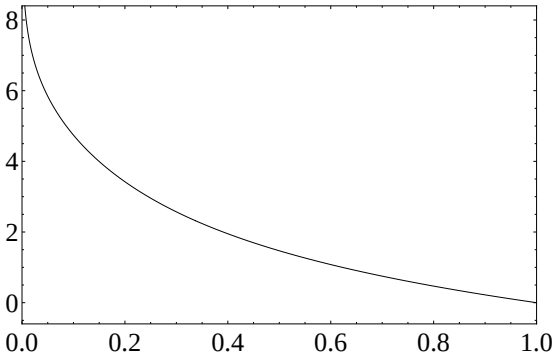

(g) The parameter q_3 is independent of w_1 and w_2.

Figure 6.1: *continued*

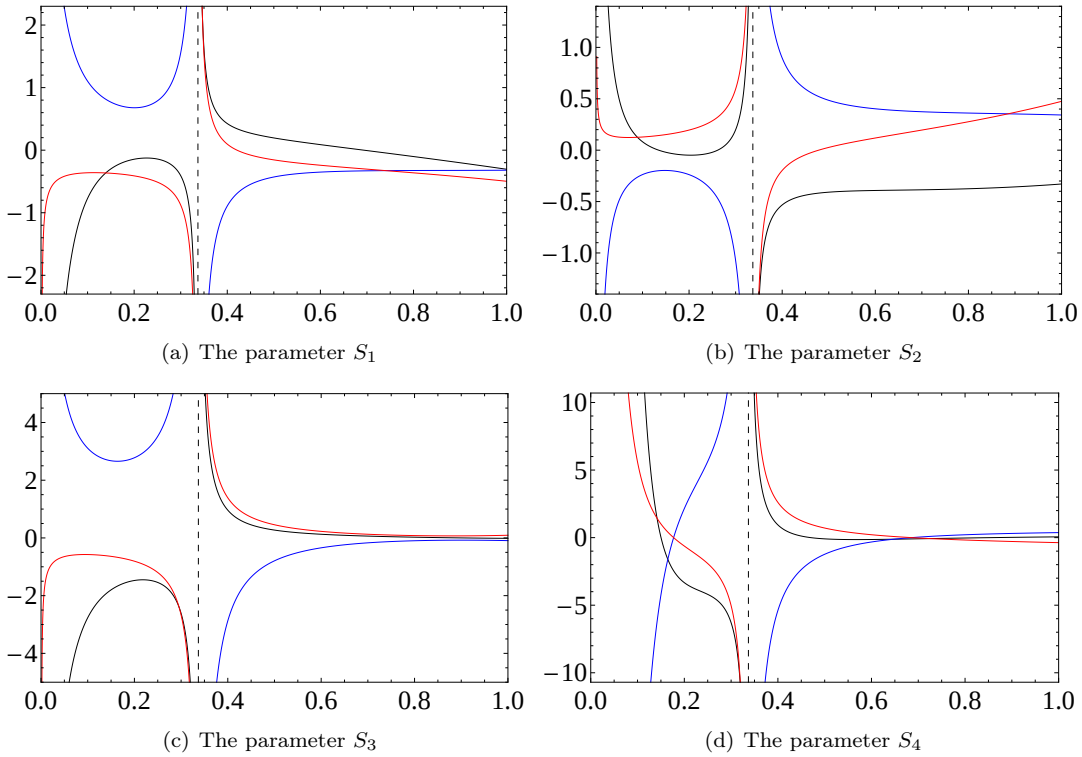

(a) The parameter S_1

(b) The parameter S_2

(c) The parameter S_3

(d) The parameter S_4

Figure 6.2: The values of the parameters S_i in the 1-PN correction to the surface (see (6.5a)) are depicted as well as the 1-PN correction to the central pressure p_c as functions of $\bar{a}_2$. These constants are split according to Eq. (6.14) into C^0 (black), C^1 (blue) and C^2 (red) where $C = S_i,\ p_c$. The dashed line marks the axis ratio $\bar{a}_2^s$.

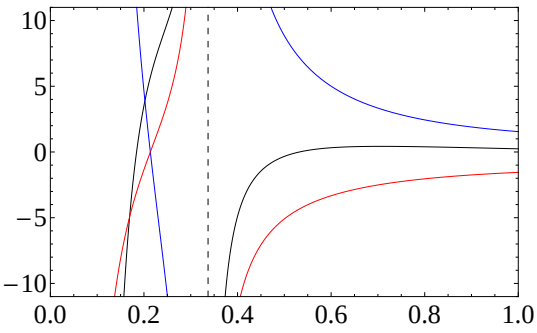

(g) The parameter S_5

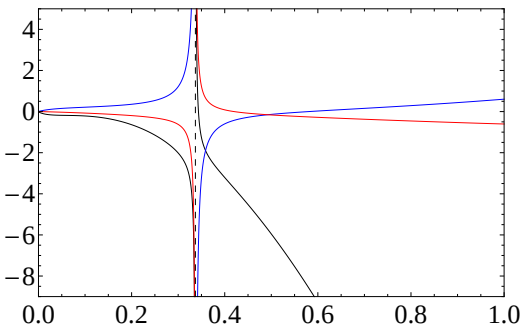

(h) The central pressure $\frac{p_c}{\mu^3 G^2}$

Figure 6.2: *continued*

6.6.1 The 1-PN corrections to the mass and the angular momentum

A definition of the total mass to 1-PN order denoted by $M = M^{(0)} + c^{-2}M^{(2)}$ can be found in [15]. $M^{(0)}$ is the mass of the Newtonian configuration. The 1-PN correction to the total mass is given by

$$M^{(2)} = \int\limits_{S^{(0)}(x^a)\leq 0} \left(\frac{1}{2}v^{(0)2} + U^{(0)}\right) \mathrm{d}x^1\,\mathrm{d}x^2\,\mathrm{d}x^3 = M^{(0)}\frac{\pi G\mu}{5}(12A_\emptyset + (a_1^2 + a_2^2)B_{12}). \tag{6.15}$$

The integral has to be taken over the Newtonian ellipsoid, because of the ansatz of the surface (6.5a), which preserves the coordinate volume. Of course, the total mass is increased to 1-PN. It does not depend on the free parameters w_i.

The 1-PN contribution to the angular momentum is defined in terms of the linear momentum density

$$\pi_a = \mu\left(v_a^{(0)} + \epsilon^2\left(v_a^{(0)}\left(v^{(0)2} + 6U^{(0)} + \frac{p^{(0)}}{\mu}\right) - 4U_a^{(3)}\right)\right). \tag{6.16}$$

Whereas the components in x^1 and x^2-direction are vanishing to 1-PN order, the angular momentum in x^3-direction L_3 is given correctly up to 1-PN by

$$L_3 = L_3^{(0)} + c^{-2}L_3^{(2)} = \int\limits_{S(x^a)\leq 0} \left(x^1\pi^2 - x^2\pi^1\right) \mathrm{d}x^1\,\mathrm{d}x^2\,\mathrm{d}x^3. \tag{6.17}$$

The integral is taken over the 1-PN surface. Higher orders than c^{-2} have to be discarded in the result. The angular momentum of the Newtonian configuration is denoted by $L_3^{(0)}$, cf. (5.10) for its value. This integral can be solved using the surface adapted coordinates introduced after Eq. (6.9). The determinant of the Jacobian matrix of this coordinate transformation is 1 to 1-PN order since the coordinate volume is preserved, i.e., the divergence of ξ^i vanishes. This yields the

angular momentum

$$L_3^{(2)} = L_3^{(0)} \frac{\pi G}{7} \mu \Bigg(-26 a_1^2 A_1 - \frac{1}{(a_1^2 - a_2^2)} \left(\left(5a_1^2 + 19a_2^2\right) a_1^2 S_1 + \left(19a_1^2 + 5a_2^2\right) a_1^2 S_2 + 4\left(a_1^2 - 3a_2^2\right) \times \right.$$
$$a_1^2 S_3 + a_2^2 \left(7a_1^2 + a_2^2\right) S_4 \Big) - a_3^2 S_5 + 2 \Big(3a_1^4 A_{11} + 2a_1^2 \Big(a_2^2 \left(6\left(B_{112} + B_{122}\right) + A_{12} + 3B_{123}\right) +$$
$$4B_{12} + 3B_{23}\Big) + a_2^2 \left(8B_{12} + 3a_2^2 \left(2B_{123} + A_{22}\right) + 6B_{23}\right) + a_3^2 \left(a_1^2 A_{13} + a_2^2 A_{23} - 2A_3\right) +$$
$$\left. 21 A_\emptyset \Big) - 26 a_2^2 A_2 \right) - \frac{4\pi^{5/2} a_3 a_1^3 a_2^3 \mu (G\mu)^{3/2}}{105\left(a_1^2 - a_2^2\right)} \left(\left(19a_1^2 + 5a_2^2\right) w_1 - \left(5a_1^2 + 19a_2^2\right) w_2 \right). \tag{6.18}$$

The plots for the 1-PN contributions to the total mass and the angular momentum are shown in Fig. 6.3. The function $\frac{a_1 M^{(2)}}{G M^{(0)}}$ has a singularity for $\bar{a}_2 \to 0$. In order that $M^{(2)}$ stays finite, the

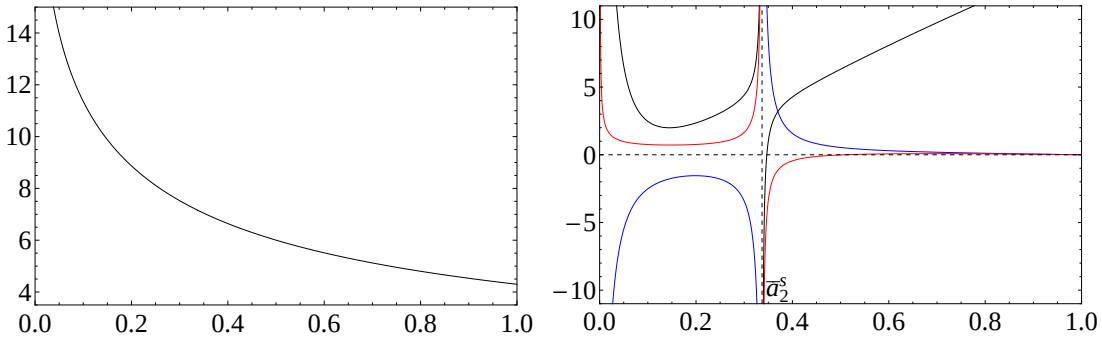

(a) $\frac{a_1 M^{(2)}}{G M^{(0)}}$ (b) $\frac{L^i}{a_1^2 \mu G L_3^{(0)}}$

Figure 6.3: The 1-PN corrections to the total mass and the angular momentum along the 1-PN Dedekind sequence, i.e., depending on $\bar{a}_2$, are shown. The angular momentum can be split analogously to Eq. (6.14) as $L_3^{(2)} = L^0 + L^1 w_1 + L^2 w_2$ where L^0, L^1 and L^2 are illustrated in black, blue and red, respectively.

mass of the Newtonian configuration $M^{(0)}$ has to vanish in this limit, cf. Fig. 6.3(a). This is discussed in detail – giving also the convergence behavior – in Section 5.3.1. There the behavior of the mass density was derived such that Φ is well-defined in a 1-PN approximation. This behavior implied $M^{(0)} \to 0$ for $\bar{a}_2 \to 0$. In fact, it also leads to $L_3^{(0)} \to 0$, which accounts for the singularity in Fig. 6.3(b) at $\bar{a}_2 = 0$. As we show in Section 6.8, a special choice of the w_i in this limit yields a static space-time, i.e., the 1-PN angular momentum vanishes in this limit.

The angular momentum has another singularity at $\bar{a}_2^s$. This shows that this singularity, which we encountered before, is not just a coordinate singularity. It originates from the dependence of $L_3^{(2)}$ on the S_i in Eq. (6.18) and the vanishing determinant of (M_{ij}) at $\bar{a}_2^s$, see Eq. (6.13). The singularity can be removed, if the S_i (which depend also on w_i) can be made finite with a special choice of the w_i. We prove that this is possible in the next section. The points $\bar{a}_2 = 0$, $\bar{a}_2 = \bar{a}_2^s$ and $\bar{a}_2 = 1$ are the only points in whose neighborhood some requirements for w_i have to be met. Otherwise, they can be chosen arbitrarily.

$\bar{a}_2$	0.35	0.32	0.31	0.29	0.28	0.25
$S_1^J + \frac{1}{3}S_3^J$	0.36377	0.74872	1.26287	−1.96593	−0.758267	−0.20061

Table 6.1: The values of the 1-PN correction to the coordinate distance of the two poles for $x^2 = x^3 = 0$ of the 1-PN Jacobi ellipsoids calculated using the values of Table 1 in [19].

6.6.2 Removing the singularity

The question where the singularities in the 1-PN Dedekind sequence are situated is interesting because of results obtained in the 1-PN Maclaurin case. In [16], it was shown that the singularity in the 1-PN Maclaurin sequence at $\bar{a}_3^1 = 0.171236$ coincides with the first bifurcation point of an axially symmetric, stationary, rigidly rotating and homogeneous sequence, cf. Fig. 5.1 and the discussion thereafter. A conjecture due to Bardeen, see [2], stating that all the bifurcation points of such sequences are reflected by a singularity in the PN approximation was proven in [56]. There it was pointed out that, if we order the bifurcation points by decreasing axis length a_3, i.e., $\bar{a}_3^{b_1} > \bar{a}_3^{b_2} > \ldots$, then the bifurcation points at $\bar{a}_3^{b_n}$ lead to a singularity in the n-PN order and higher orders. However, the bifurcation points of non-axially symmetric sequences are not associated with a singularity in the PN approximation. Naturally, the question arises if a similar result can be found for the 1-PN Dedekind ellipsoids as well. Since the result for the PN-Maclaurin sequence includes only bifurcation points where axially symmetric sequences branch off, a generalization to the non-axially symmetric case is not straightforward.

Therefore, let us discuss the singularities in the parameter space of the 1-PN Jacobi ellipsoids, which are non-axially symmetric. It was shown in [17] that the singularity at $\bar{a}_2^J = 0.29179$ in the 1-PN Jacobi sequence is related to the occurrence of a fourth-harmonic neutral mode of deformation of the Newtonian Jacobi ellipsoids. In [19], the condition of a fixed coordinate volume for the ansatz of the 1-PN surface was relaxed and an additional parameter introduced such that the 1-PN correction to the baryonic mass vanishes. In this choice, the singularity disappeared at least in the binding energy and in the angular momentum. Nevertheless, the constants, say S_i^J, describing the surface ansatz[12] still diverge. No comments were made whether the entire solution or just the two aforementioned physical quantities are singularity free. In particular, it is questionable if the surface remains closed. For a brief investigation, we look at the coordinate distance Δx^1 between two "poles" on the x^1-axis which reads to 1-PN:

$$(\Delta x^1)^2 = 2a_1^2 + \frac{2\pi a_1^4 G\mu}{c^2}\mu\left(S_1^J + \frac{1}{3}S_3^J\right). \tag{6.19}$$

The values close to the singularity, inferred from Table 1 in [19], can be found in Table 6.1 where it is indicated that a singularity still occurs[13] in this quantity. In particular, provided that μa_1^2 is not going to vanish then for $\bar{a}_2 > \bar{a}_2^J$ (case 1) it holds that $(\Delta x^1)^2 \to \infty$ and for $\bar{a}_2 < \bar{a}_2^J$ (case 2) it holds that $(\Delta x^1)^2 \to -\infty$. Case 2 implies that the coordinate distance becomes imaginary[14] which is related to a transition from a closed to an open surface like a perturbed hyperboloid. On the other hand, in case 1 the ellipsoid extends to infinity. Therefore, the solution is still singular and needs additional investigation. But this is beyond the scope of this thesis. We can draw two

[12]The ansatz for the surface of the 1-PN Jacobi ellipsoids coincides with the ansatz for the 1-PN Dedekind ellipsoids (6.5). This can be seen as relativistic generalization of a part of Dedekind's theorem.

[13]The same singular behavior as for the other parameters in [19] is encountered. For a more detailed discussion, however, more values are necessary.

[14]It is sufficient that the values in Table 6.1 are negative.

conclusions: The singularity cannot be removed and it coincides with a fourth-harmonic neutral mode of the Newtonian sequence.

For the 1-PN Dedekind ellipsoids, more degrees of freedom are involved as in the Maclaurin or Jacobi case. The Dedekind ellipsoids are neither axially symmetric except for the endpoints of the sequence nor rigidly rotating. Furthermore, no axially symmetric bifurcation points apart from the one where Maclaurin "branches off" nor non-trivial fourth-harmonic neutral modes of deformation exist[15], cf. [23]. This leads us to the conclusion that we should not expect any singularities. On the other hand, we are able to introduce, via w_i, artificially new singularities anywhere. These singularities are obviously not connected to special points along the Newtonian sequence. We show in this section that the singularity at $\bar{a}_2^s$, say in $L_3^{(2)}$, is due to a "bad" parameterization and can be removed completely, i.e., all parameters in (6.5) and all metric functions can be made singularity free. In this way, we can show that there is no contradiction to the aforementioned relation between the Newtonian Maclaurin or Jacobi ellipsoids and parameter singularities of their 1-PN approximation.

First, we identify the origin of the singularity. Evaluating the determinant of the coefficient matrix (M_{ij}) numerically, cf. Eqs. (6.13) and (D.1), shows that it changes sign at $\bar{a}_2^s = 0.33700003168\ldots$. One of the eigenvalues, say Λ, of the coefficient matrix (M_{ji}) vanishes and

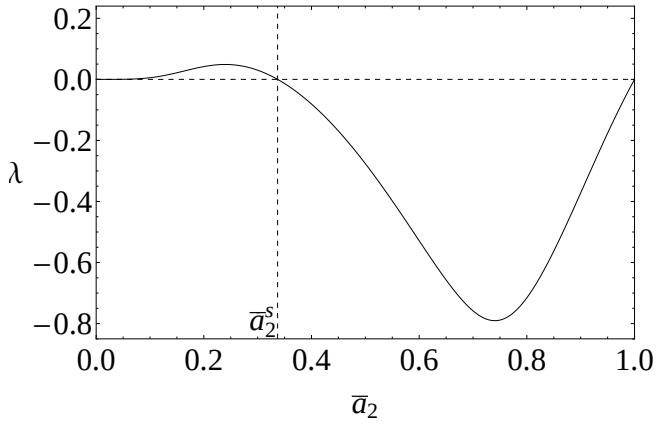

Figure 6.4: The eigenvalue Λ, which vanishes at the singularity $\bar{a}_2^s$, is depicted. The other zeros of Λ at $\bar{a}_2 = 0$ and $\bar{a}_2 = 1$ lead to an indeterminacy of Eq. (6.13) *at* those points, cf. Paper V.

the eigenspace has the dimension 1. The behavior of Λ along the sequence is depicted in Fig. 6.4. Multiplying equation (6.13) with the eigenvector (β_i) of the transposed matrix to the eigenvalue Λ yields the condition

$$\sum_{i=1}^{3} \beta_i b_i = 0.083600 - 0.235534 w_1 + 0.099994 w_2 = 0. \tag{6.20}$$

With the ansatz taken in [23], i.e., $w_1 = w_2 = 0$, Eq. (6.20) is not satisfied. Hence, a singularity is inevitable. In lieu of [23], we have a more general inhomogeneity[16], cf. $b_i^{(1/2)}$ in (6.13) and (D.2).

[15] However, as shown in [23] an onset for a dynamical instability does exist at $\bar{a}_2 = 0.3121\ldots \neq \bar{a}_2^s$.

[16] In Footnote 2 in [23], Chandrasekhar and Elbert state that an introduction of parameters analogous to our w_i does not affect the singularity, since the determinant of (M_{ij}) is independent of these parameters. The deter-

For the choice

$$w_1^s = 0.354937 + 0.424544 w_2, \tag{6.21}$$

Eq. (6.20) is identically satisfied at the point $\bar{a}_2 = \bar{a}_2^s$ and no singularity is present. To ensure that this holds true in the limit $\bar{a}_2 \to \bar{a}_2^s$, higher orders have to be taken into account. As one can readily check numerically and support analytically by eigenvalue approximations, the equation

$$\sum_{i,j=1}^{5} \beta_i M_{ij} S_j = \Lambda^{-1} \sum_{i=1}^{5} \beta_i b_i \tag{6.22}$$

is a well-defined and non-trivial equation for the S_i in the limit $\bar{a}_2 \to \bar{a}_2^s$ if $w_1 - w_1^s \in O(\Lambda)$. It can be used instead of, for instance, the equation $\sum_{j=1}^{5} M_{1j} S_j = b_1$. The resulting coefficient matrix is now regular and the solution finite. We use a new variable $\hat{w}_1$ defined by $w_1 = w_1^s(w_2) + \Lambda \hat{w}_1$ where now the parameters $\hat{w}_1$ and w_2 are arbitrary but finite. Near the singularity, the solution for the surface coefficients at the singularity reads

$$\begin{aligned}
S_1^s &= 0.136453 - 0.243073 w_2 + 0.054186 \hat{w}_1, \\
S_2^s &= -0.195876 + 0.154884 w_2 - 0.044769 \hat{w}_1, \\
S_3^s &= -0.119902 + 0.212999 w_2 + 0.221751 \hat{w}_1, \\
S_4^s &= -1.393285 + 0.412379 w_2 + 0.429324 \hat{w}_1, \\
S_5^s &= 4.761466 - 1.470110 w_2 - 1.530518 \hat{w}_1.
\end{aligned} \tag{6.23}$$

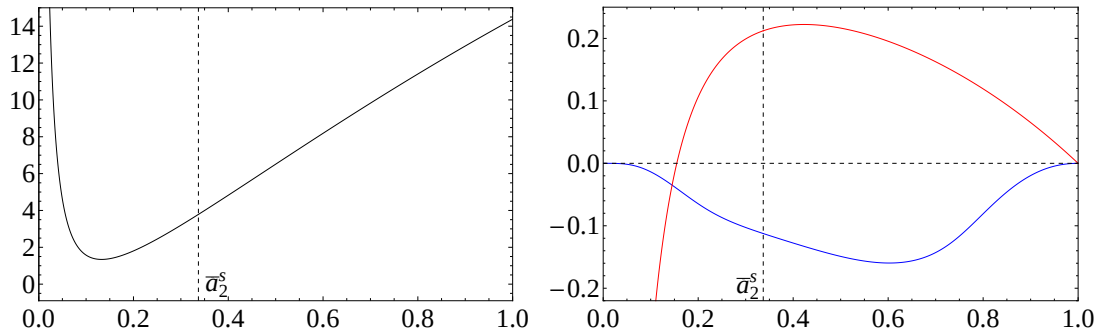

(a) $L_3^{(2)0}$ (b) $L_3^{(2)1}$ and $L_3^{(2)2}$

Figure 6.5: The 1-PN corrections to the angular momentum $L_3^{(2)} = L_3^{(2)0} + L_3^{(2)1}\hat{w}_1 + L_3^{(2)2} w_2$ depending on $\bar{a}_2$ are depicted after the singularity is removed ($L_3^{(2)0}$ in black, $L_3^{(2)1}$ in blue and $L_3^{(2)2}$ in red).

The metric functions Φ and $U_a^{(3)}$ are not singular for $\bar{a}_2 \to \bar{a}_2^s$, because they do not depend on S_i. Since the coefficients S_i^s given in Eq. (6.23) are finite, δU stays finite. Finally, the parameters S_i enter the velocity field only linearly and their coefficients in Eqs. (6.10)-(6.12) are well defined.

minant is indubitably independent of the w_i. Nonetheless, the removal of the singularity is possible provided the inhomogeneity satisfies (6.20). As a simple example, consider the equation $\epsilon x = \epsilon^\gamma$ in x. The determinant vanishes in the limit $\epsilon \to 0$ independently of γ, but the solution $x = \epsilon^{\gamma-1}$ is singular for $\epsilon \to 0$ only for $\gamma < 1$.

Hence, the entire solution is regular. For instance, the singularity in Fig. 6.3(b) is removed as shown in Fig. 6.5. Only Eq. (6.21) is obtained as an extra condition for the behavior of the w_i in the limit $\bar{a}_2 \to \bar{a}_2^s$. The remaining singularity at $\bar{a}_2 = 0$ is investigated in Section 6.8.

6.6.3 The surface and the gravitomagnetic effect

The shape of the 1-PN Dedekind ellipsoids follows directly and analytically from the solution of Eq. (6.13). Since the solution is very lengthy, we discuss here the shape of the body qualitatively and give some examples in Fig. 6.6. We focus in our explanation on the gravitomagnetic effect, which describes in general relativity the repulsion between two parallel matter streams and the attraction between two antiparallel matter streams. Other aspects of the self-gravitating fluid are neglected.

What shape of the 1-PN body can we expect, if no additional constraints are given and if we bear only the gravitomagnetic effect in mind? Two neighboring fluid elements with different heights in the Newtonian Dedekind ellipsoids move along concentric ellipses in two parallel planes, cf. Eq. (5.9) and Section 6.6.4. Hence, these matter streams are parallel and the 1-PN Dedekind ellipsoids should be elongated in x^3-direction. This is corroborated by the 1-PN Maclaurin ellipsoids which are also elongated in this direction close to the bifurcation point, see, e.g., Table 3 in [55]. The matter streams in the x^2-direction for $x^1 > 0$ are all parallel to each other and antiparallel to those in $x^1 < 0$. The latter are on average at a larger distance and the repulsive effect should prevail. In x^2-direction, we have an elongation as well but generally smaller than in x^3-direction. A similar argument holds for the x^1-direction. Whether the repulsion is stronger in x^2-direction or in x^1-direction depends on the choice of w_i. They contribute to the velocity in those directions. The surface for some values of the parameters is depicted in Fig. 6.6.

Why do we see some contraction in the x^2-direction in Figs. 6.6(a) and 6.6(b) or in the x^1-direction in Figs. 6.6(b) and 6.6(c)? Usually, additional constraints are in place in PN approaches to ellipsoidal figures of equilibrium. For instance, in [16] the Maclaurin ellipsoids are restricted (at least for a numerical elucidation of the results) by the choice $S_1^{\text{Maclaurin}} = 0$ in the ansatz for the surface, which results in a fixed position of the "north pole" at $x^1 = x^2 = 0$, $x^3 = a_3$. As we discussed above, an elongation along the x^3-axis is the strongest effect. However, it is not possible for this constraint. Other requirements in use are that there are no PN contributions to the rest mass or/and angular momentum, cf. [2]. The constraint in place here – a fixed coordinate volume – restricts the shape of the 1-PN body as well: An elongation in all three directions is not possible. The strongest effect – the elongation in the x^3-direction – can always be observed. The changes in the other directions depend on the mutual strength of the repulsion in all three directions. This is affected by the choice of w_1 and w_2. Since a positive w_1 reduces the velocity in the x^1-direction, the gravitomagnetic repulsion is also reduced. A positive w_2 increases the repulsion in x^2-direction. In fact, w_i can be adjusted so that all three cases are possible – a contraction in x^1- and x^2-direction, an elongation in x^1-direction and a contraction in x^2-direction or vice versa, see Fig. 6.6.

Even though we considered here only coordinate distances instead of proper distances the overall picture is the same. Only the regions of w_i in the parameter space associated with the three classes characterized above change slightly.

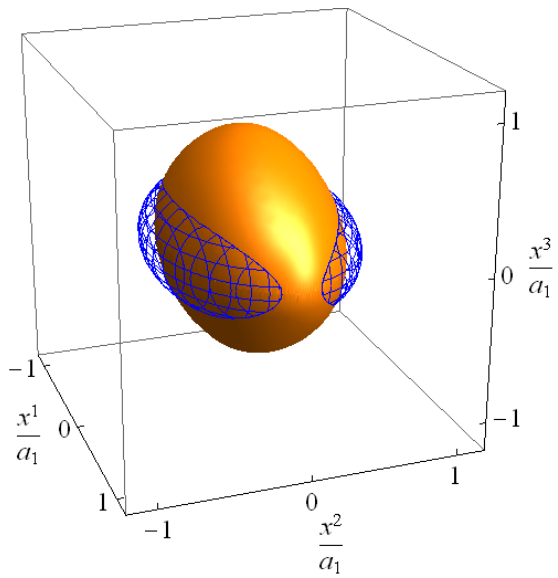

(a) $w_1 = w_2 = 0,\ \frac{G\mu}{c^2}a_1^2 = 0.45$

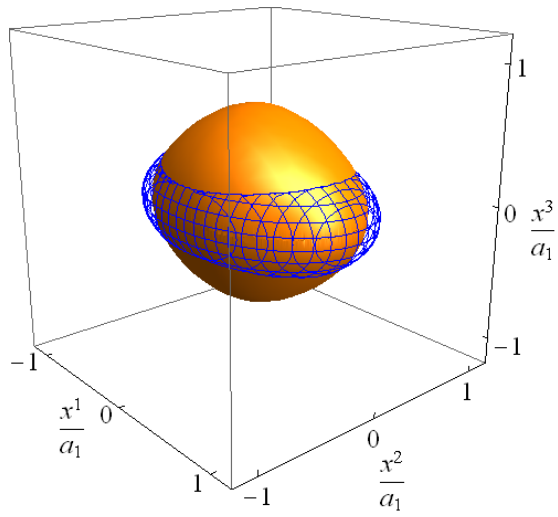

(b) $w_1 = w_2 = 0.4,\ \frac{G\mu}{c^2}a_1^2 = 0.4$

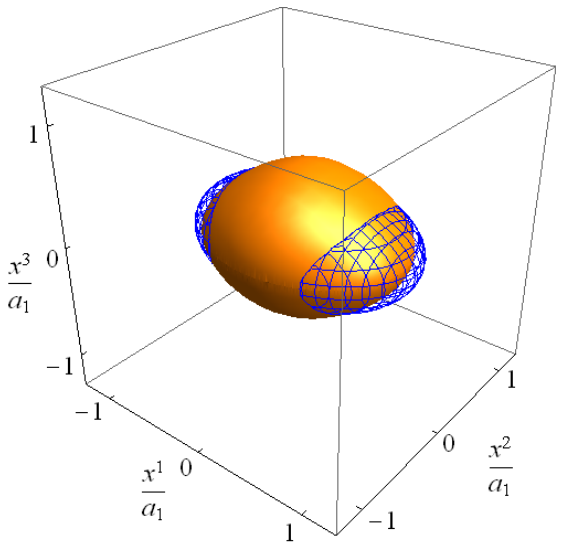

(c) $w_1 = 0.5,\ w_2 = 1,\ \frac{G\mu}{c^2}a_1^2 = 0.3$

Figure 6.6: Several 1-PN surfaces (solid, orange) are depicted for an axis ratio $\bar{a}_2 = 0.7$ and different w_i. They are compared to the Newtonian Dedekind ellipsoid (wireframe, blue) with $\bar{a}_2 = 0.7$; it is the same Newtonian surface in all three figures. The Newtonian ellipsoid is shown only if it lies outside the 1-PN surface in order to highlight in which direction an elongation or contraction takes place. The parameter $\frac{G\mu}{c^2}a_1^2$ is not chosen on physical grounds but rather to elucidate the 1-PN corrections.

6.6.4 The motion of the fluid

An ansatz for the 1-PN velocity field of 1-PN Maclaurin and Jacobi ellipsoids is straightforward, since the Newtonian configurations are rigidly rotating. A property easily generalized to 1-PN. Unfortunately, this not possible for the 1-PN Dedekind ellipsoids and the more complicated ansatz (6.5) was employed instead. To explicate the inner motion of the 1-PN Dedekind ellipsoids, we integrate the 4-velocity field u^μ, see Eq. (6.5) and Footnote 6 in this chapter, and show the trajectories of a generic fluid element. The most notable feature of the motion is that a component in x^3-direction is required for a consistent solution of Eq. (6.4).[17] For an illustration of the other

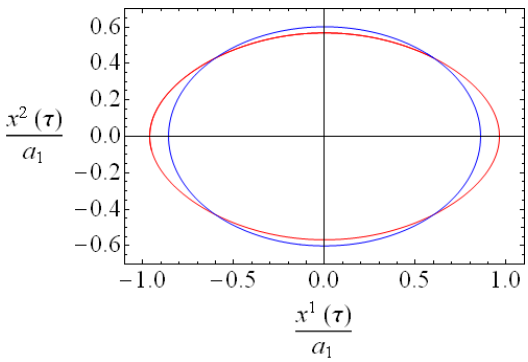

(a) The motion of a fluid element in the x^1, x^2-plane

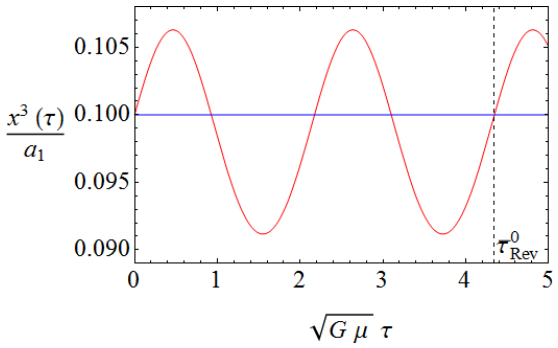

(b) The altitude $x^3(\tau)$ of a fluid element

Figure 6.7: The motion of a fluid element in a 1-PN approximation (red) for $\bar{a}_2 = 0.7$, $\frac{\mu G}{a_1^2 c^2} = 0.45$ and $w_1 = w_2 = 0$, compared to the Newtonian trajectory (blue). The starting point is $x_0^1 = 0.6a_1$, $x_0^2 = 0.43a_1$ and $x_0^3 = 0.1a_1$.

features of the motion of a fluid element (with the proper time τ), we use the curves $(x^1(\tau), x^2(\tau))$. The equations are integrated starting at $x^1(0) = 0.6a_1$, $x^2(0) = 0.43a_1$, $x^3(0) = 0.1a_1$ for $w_1 = w_2 = 0$ and $\frac{G\mu}{c^2}a_1^2 = 0.45$. The latter parameters are the same as in Fig. 6.6(a). Hence, the motion depicted in Fig. 6.7(a) can be explained on similar grounds, cf. Section 6.6.3. Fig. 6.7(b) shows the changes of the coordinate height $x^3(\tau)$ of the fluid element during the motion. A periodic motion is obtained and u^3 changes the sign when the fluid element passes from one octant to another. If the starting point $x^3(0) \to 0$, this velocity component vanishes because of the reflection symmetry. The curve $(x^1(\tau), x^2(\tau), x^3(\tau))$ of the fluid element with the above initial conditions is closed and the time of one revolution is $\hat{\tau}^0_{Rev} = \sqrt{G\mu}\tau^0_{Rev} = 4.34691$ – compared with the Newtonian value $\hat{\tau}^{Newt}_{Rev} = 5.94395$. This is commensurate with two periods in Fig. 6.7(b).

Contrary to the Newtonian case, the proper time for one revolution depends on the initial point as shown in Fig. 6.8. A similar picture is obtained if the coordinate time is used instead.

[17] In fact, this component was omitted in the original paper on 1-PN Dedekind [22]. The equations were only solvable, because the surface condition (6.13) was applied incorrectly. Both problems were remedied in [23].

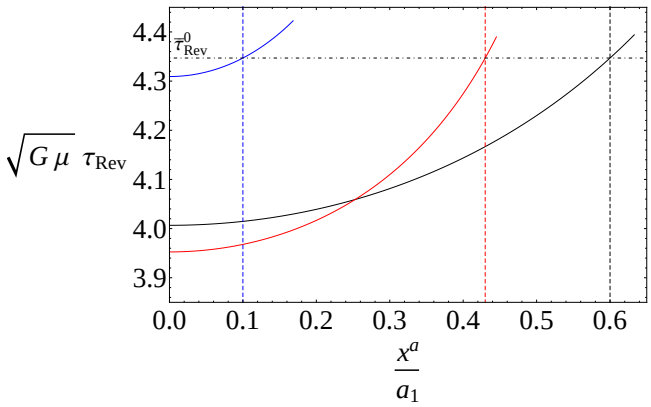

Figure 6.8: The proper time τ_{Rev} of a full revolution of a fluid element is shown depending on its starting point for $w_1 = w_2 = 0$. The black, red and blue lines show $\sqrt{G\mu}\tau_{Rev}$ depending on either $\frac{x^1}{a_1}$ or $\frac{x^2}{a_1}$ or $\frac{x^3}{a_1}$ whereas the other coordinates are fixed such that these curves pass through the point $(x^a_0) = (x^1 = 0.6a_1, x^2 = 0.43a_1, x^3 = 0.1a_1)$. The dash-dotted line shows $\bar{\tau}^0_{Rev}$, which intersects the black, red and blue curves at the point (x^a_0).

6.7 The axially symmetric limit of the 1-PN Dedekind ellipsoids

Our expectations of a 1-PN Dedekind ellipsoid, cf. Section 6.1, include among others that a continuous transition of the 1-PN Dedekind ellipsoids to the 1-PN Maclaurin spheroids at the bifurcation point $\bar{a}_{2,\mathrm{b}}$ should exist. As we prove below in Paper V, this yields another restriction on the two remaining parameters w_i besides the one resulting from the removal of the singularity. The restrictions amount to $w_1 = -w_2 = 0.01646051799\ldots$.

THE ASTROPHYSICAL JOURNAL, 722:1207–1215, 2010 October 20 doi:10.1088/0004-637X/722/2/1207

THE AXISYMMETRIC CASE FOR THE POST-NEWTONIAN DEDEKIND ELLIPSOIDS

NORMAN GÜRLEBECK[1] AND DAVID PETROFF[2]
[1] Institute of Theoretical Physics, Charles University, Prague, Czech Republic; norman.guerlebeck@gmail.com
[2] Institute of Theoretical Physics, Friedrich-Schiller University, Jena, Germany; D.Petroff@tpi.uni-jena.de
Received 2010 June 16; accepted 2010 August 19; published 2010 September 28

ABSTRACT

We consider the post-Newtonian approximation for the Dedekind ellipsoids in the case of axisymmetry. The approach taken by Chandrasekhar & Elbert excludes the possibility of finding a uniformly rotating (deformed) spheroid in the axially symmetric limit, though the solution exists at the point of axisymmetry. We consider an extension to their work that permits the possibility of such a limit.

Key words: gravitation – hydrodynamics – methods: analytical – stars: general

1. INTRODUCTION

The Dedekind tri-axial ellipsoids are an example of non-axisymmetric, but stationary solutions within Newtonian gravity. Due to internal motions, they are, in fact, stationary in an inertial frame. When addressing the question of whether or not stationary, but non-axisymmetric solutions are possible within general relativity, this property makes the Dedekind ellipsoids a natural choice upon which to base one's considerations. It was, in part, with this question in mind that Chandrasekhar & Elbert (1974, 1978) turned their attentions to the post-Newtonian (PN) approximation of the Dedekind ellipsoids. In a paper from the same series, Chandrasekhar (1967b) had already considered the axisymmetric limit of the PN Jacobi ellipsoids at length and was able to show that it coincides with a certain PN Maclaurin spheroid (just as their Newtonian counterparts coincide at the point of bifurcation). This is related to the fact that the PN figures were chosen to rotate uniformly. On the other hand, the PN velocity field chosen in Chandrasekhar & Elbert (1978) excludes the possibility of uniform rotation in the axisymmetric *limit* although it is possible in the axisymmetric *case*. This restriction seems neither natural nor advisable in the context of trying to settle the question as to the existence of relativistic, non-axisymmetric, stationary solutions. The naïve expectation is that the axisymmetric PN Dedekind ellipsoids contain the PN Maclaurin spheroids in the axisymmetric limit (up to arbitrary order).

In this article, we begin in Section 2 by examining the axisymmetric case of a generalization to the solution presented in Chandrasekhar & Elbert (1978). We proceed in Section 3 to consider a (continuous) limit to axisymmetry. In Section 4, the connection to the PN Maclaurin spheroids is examined.

2. THE AXISYMMETRIC SOLUTION OF A GENERALIZATION TO CHANDRASEKHAR AND ELBERT'S PAPER

We consider a generalization of the PN Dedekind ellipsoids presented in Chandrasekhar & Elbert (1978) (referred to from here on in as CE78) in which we add PN terms to the velocity. We comply with the notation used in CE78 and refer the reader to the definitions there for the various quantities. The PN contributions to the velocity, which we introduce here are

$$\begin{aligned}\delta v_1 &= a_1^2 w_1 x_2 + (q_1+q)x_1^2 x_2 + r_1 x_2^3 + t_1 x_2 x_3^2\\ \delta v_2 &= a_2^2 w_2 x_1 + (q_2-q)x_1 x_2^2 + r_2 x_1^3 + t_2 x_1 x_3^2\\ \delta v_3 &= q_3 x_1 x_2 x_3,\end{aligned} \tag{1}$$

where the terms with w_1 and w_2 have been added for reasons that will be made clear when we discuss the solution. Note that we could eliminate one constant by introducing variables to denote q_1+q and q_2-q, but choose instead to retain the notation in CE78.[3]

The Newtonian ellipsoid is characterized by the semi-major axes $a_1 \geqslant a_2 \geqslant a_3$. Let us assume for the moment that, as in the Newtonian setting, the axisymmetric case is obtained by considering $a_2 = a_1$, an assumption that will be verified shortly. In this case, the index "2" in the index symbols $A_{ijk\ldots}$ and $B_{ijk\ldots}$ used in CE78 and discussed at length in Section 21 of Chandrasekhar (1987) can be replaced by "1" as is evident from the definitions. Using the relations given in that book, it is possible to reduce all the index symbols to A_1 and A_2. At the point $a_2 = a_1$, the value for A_1 (and thus A_2) is given by Equation (36) in Section 17 of Chandrasekhar (1987). Furthermore, Equation (2) from Chandrasekhar & Elbert (1974) shows us that

$$Q_2 \overset{a}{=} -Q_1, \tag{2}$$

where we define the symbol $\overset{a}{=}$ to mean that the expression is evaluated at the point $a_2 = a_1$, i.e.,

$$C|_{a_2=a_1} = D|_{a_2=a_1} \text{ is denoted by } C \overset{a}{=} D. \tag{3}$$

The value for a_3 can be found from the equation

$$a_1^2 a_2^2 A_{12} = a_3^2 A_3, \tag{4}$$

which holds for the Dedekind (and Jacobi) ellipsoids and gives the value

$$\frac{a_3}{a_1} \overset{a}{=} 0.5827241661\ldots. \tag{5}$$

Throughout this paper, a_3 is to be understood as a function of a_1 and a_2, given by Equation (4).

We can now consider the integrability conditions for the pressure and the continuity equation. We again follow CE78 and shall refer to the equation numbers there by adding a prime. It turns out that Equation (38′) (of CE78) remains unchanged despite the modification to the velocity, so that we find

$$q_3 \overset{a}{=} 0 \tag{6}$$

[3] The three-velocity v^i in CE78 does not refer to the spatial components of the four- velocity $u^\alpha = dx^\alpha/d\tau$, but is instead defined as $v^i = dx^i/dt = u^i/u^0$.

and then from Equation (24′) that

$$q_2 \overset{a}{=} -q_1. \tag{7}$$

Equation (28′) is identically fulfilled for $a_2 = a_1$, meaning that q_1 is left undetermined, in contrast to the general case.

With the changes to the velocity, Equations (30′) and (31′) gain the additional terms $(a_1^2 Q_2 w_1 + a_2^2 Q_1 w_2)x_1$ and $(a_1^2 Q_2 w_1 + a_2^2 Q_1 w_2)x_2$, respectively. Equations (32′)–(38′) remain unchanged. Equation (32′) yields

$$r_2 \overset{a}{=} -r_1 \tag{8}$$

and Equation (37′) gives

$$t_2 \overset{a}{=} t_1 \tag{9}$$

(we shall see shortly that each t_i becomes zero). There are additional terms in Equation (39′) corresponding to adding $-(a_1^2 Q_2 w_1 + a_2^2 Q_1 w_2)/2 = a_2^2 Q_1 (w_1 - w_2)/2$ both to[4] α_1^{78} and α_2^{78}.

Requiring for the new velocity that its normal component vanishes on the surface leads to a change in Equation (50′) and thus the resulting equations (52′)–(56′) by which the terms with $S_1 - S_2$ are modified. They now become

$$S_1 - S_2 - \frac{w_1 + w_2}{2Q_1}. \tag{10}$$

Using Equations (2), (7), and (8), we can subtract Equation (54′) from (55′) in CE78 to arrive at

$$q + q_1 - r_1 \overset{a}{=} \frac{4}{3} Q_1 (4S_3 + S_4). \tag{11}$$

Next, we turn our attention to the system of Equations (58′) from CE78.[5] In the case being considered here, the first of these equations becomes

$$\begin{aligned} 0 &= Q_{11}^{78} + \frac{a_2^4}{a_1^4} Q_{22}^{78} - \frac{a_2^2}{a_1^2} Q_{12}^{78} \\ &\overset{a}{=} P_{11}^{78} + P_{22}^{78} - P_{12}^{78} - \frac{2a_3^2}{3a_1^2} A_3 (4S_3 + S_4) \\ &= \alpha_{11}^{78} + \alpha_{22}^{78} - \alpha_{12}^{78} + Q_1 (q - r_1) \\ &\quad - \frac{2a_3^2}{3a_1^2} A_3 (4S_3 + S_4) + \sum_{i=3}^{5} S_i \left(u_{11}^{(i)} + u_{22}^{(i)} - u_{12}^{(i)} \right) \\ &= \frac{2}{3} Q_1^2 (4S_3 + S_4) - \frac{2a_3^2}{3a_1^2} A_3 (4S_3 + S_4) + \frac{2}{3} a_1^6 A_{1111} (4S_3 + S_4), \end{aligned} \tag{12}$$

where the values for the α's and their axisymmetric limits can be found in Appendix A, and the u's are given in Chandrasekhar (1967b) (hereafter C67b)[6] equations (72) and (73) and where we made use of Equation (11) from the current paper. The unique solution to this equation is

$$S_4 \overset{a}{=} -4S_3 \tag{13}$$

as it is for the analog equation (100) of C67b despite the fact that the term with $q - r_1$ is absent there. With the result Equation (13), Equation (11) becomes

$$q + q_1 - r_1 \overset{a}{=} 0 \tag{14}$$

and for Equation (53′) from CE78,[7] or equivalently the sum of Equations (54′) and (55′), we find

$$S_1 - S_2 \overset{a}{=} -\frac{5}{3} S_3. \tag{15}$$

The third minus the second of equations (58′) is the analog of Equation (101) in C67b and is in fact precisely the same equation despite the different definitions for P_{ij}:

$$\begin{aligned} 0 &= Q_{11}^{78} - \frac{a_2^4}{a_1^4} Q_{22}^{78} - \frac{a_3^2}{a_1^2} Q_{31}^{78} - \frac{a_2^2 a_3^2}{a_1^4} Q_{23}^{78} \\ &\overset{a}{=} P_{11}^{78} - P_{22}^{78} - \frac{a_3^2}{a_1^2} \left(P_{31}^{78} - P_{23}^{78} \right) - 2\frac{a_3^2}{a_1^4} A_3 \left(\frac{17}{3} a_1^2 S_3 + a_3^2 S_5 \right) \\ &= \alpha_{11}^{78} - \alpha_{22}^{78} - \frac{a_3^2}{a_1^2} \left(\alpha_{31}^{78} - \alpha_{23}^{78} \right) - 2\frac{a_3^2}{a_1^4} A_3 \left(\frac{17}{3} a_1^2 S_3 + a_3^2 S_5 \right) \\ &\quad + \sum_{i=3}^{5} S_i \left[\left(u_{11}^{(i)} - u_{22}^{(i)} \right) - \frac{a_3^2}{a_1^2} \left(u_{31}^{(i)} - u_{23}^{(i)} \right) \right] \\ &= -2\frac{a_3^2}{a_1^4} A_3 \left(\frac{17}{3} a_1^2 S_3 + a_3^2 S_5 \right) \\ &\quad + \left(a_1^2 A_{111} + 6a_3^2 A_{113} - 7a_3^2 A_{1113} \right) \left(\frac{17}{3} a_1^2 S_3 + a_3^2 S_5 \right). \end{aligned} \tag{16}$$

The unique solution to this equation is

$$S_5 \overset{a}{=} -\frac{17a_1^2}{3a_3^2} S_3. \tag{17}$$

We can use Equation (56′) together with Equations (9), (13), (15), and (17) to conclude that

$$t_1 \overset{a}{=} t_2 \overset{a}{=} 0. \tag{18}$$

Equation (47′) of CE78 tells us that the bounding surface is axisymmetric to the first PN order if and only if Equations (13), (15), and (17) hold. The PN velocity field of CE78 can then be seen to be axisymmetric in the limit we are discussing, when we additionally require

$$w_2 \overset{a}{=} -w_1. \tag{19}$$

Using what has been shown above, the third equation of (58′) in CE78 can be used to find the value of S_3 (where the

[4] We use the superscripts "67" and "78" to distinguish the quantities defined in Chandrasekhar (1967b) from those in Chandrasekhar & Elbert (1978).

[5] Please note that we have been unable to reproduce the values from Table 1′ in CE78 that result from solving Equation (58′). A detailed discussion can be found in Appendix A.

[6] As mentioned in C67b, the u's belonging to the displacements $\boldsymbol{\xi}^{(4)}$ and $\boldsymbol{\xi}^{(5)}$ are generated by cyclically permuting the indices. The precise meaning is best understood via the example that $u_1^{(4)}$ can be generated from $u_3^{(3)} = -\frac{1}{2} a_1^2 (a_2^2 B_{123} - a_1^2 B_{113})$ and becomes $u_1^{(4)} = -\frac{1}{2} a_2^2 (a_3^2 B_{231} - a_2^2 B_{221})$.

[7] In Equation (53′) of CE78, the factor Q_1 is missing from the term with $(S_1 - S_2)$.

relationship between the α^{78}'s and the α^{67}'s can be found in Appendix A.1)

$$\begin{aligned}
0 &= a_1^4 Q_{11}^{78} + a_3^4 Q_{33}^{78} - a_1^2 a_3^2 Q_{31}^{78} \\
&\overset{a}{=} a_1^4 P_{11}^{78} + a_3^4 P_{33}^{78} - a_1^2 a_3^2 P_{31}^{78} + \frac{130}{9} a_1^2 a_3^2 A_3 S_3 \\
&= a_1^4 \alpha_{11}^{78} + a_3^4 \alpha_{33}^{78} - a_1^2 a_3^2 \alpha_{31}^{78} + \frac{a_1^4 Q_1}{4}(q + r_1) + \frac{130}{9} a_1^2 a_3^2 A_3 S_3 \\
&\quad + \sum_{i=3}^{5} S_i \left(a_1^4 u_{11}^{(i)} + a_3^4 u_{33}^{(i)} - a_1^2 a_3^2 u_{31}^{(i)} \right) \\
&= a_1^4 \alpha_{11}^{67} + a_3^4 \alpha_{33}^{67} - a_1^2 a_3^2 \alpha_{31}^{67} + \frac{a_1^4 Q_1}{2} r_1 + \frac{130}{9} a_1^2 a_3^2 A_3 S_3 \\
&\quad + \sum_{i=3}^{5} S_i \left(a_1^4 u_{11}^{(i)} + a_3^4 u_{33}^{(i)} - a_1^2 a_3^2 u_{31}^{(i)} \right). \qquad (20)
\end{aligned}$$

The solution for S_3 is then

$$S_3 \overset{a}{\approx} -0.01742648312 + 0.1061462885\, r_1, \qquad (21)$$

the analytic expression of which can be found in Appendix (B).

We now turn to the fifth of the equations (58′) to solve for S_1. The equation is

$$\begin{aligned}
0 &= a_3^4 Q_{33}^{78} - a_1^4 Q_{11}^{78} + a_3^2 \bar{Q}_3^{78} - a_1^2 \bar{Q}_1^{78} \\
&\overset{a}{=} a_3^4 P_{33}^{78} - a_1^4 P_{11}^{78} + a_3^2 P_3^{78} - a_1^2 P_1^{78} + 2 a_1^2 a_3^2 \left(3 S_1 + \frac{35}{9} S_3 \right) \\
&= a_3^4 \alpha_{33}^{67} - a_1^4 \alpha_{11}^{67} + a_3^2 \alpha_3^{67} - a_1^2 \alpha_1^{67} - \frac{a_1^4 Q_1}{2} r_1 \\
&\quad + 2 a_1^2 a_3^2 \left(3 S_1 + \frac{35}{9} S_3 \right) - a_1^4 Q_1 w_1 + \sum_{i=1}^{2} a_1^2 S_i \left(a_3^2 u_3^{(i)} - a_1^2 u_1^{(i)} \right) \\
&\quad + \sum_{i=3}^{5} S_i \left(a_3^4 u_{33}^{(i)} - a_1^4 u_{11}^{(i)} + a_3^2 u_3^{(i)} - a_1^2 u_1^{(i)} \right) \qquad (22)
\end{aligned}$$

and the solution is

$$\begin{aligned}
S_1 \overset{a}{\approx} -(&0.2836731908 + 0.7419729757\, r_1 \\
&+ 1.121542227\, w_1), \qquad (23)
\end{aligned}$$

cf. Appendix (B) for the analytic expression. The fourth equation is then identically fulfilled. We have obtained a solution to all the equations at the point $a_2 = a_1$ and have two remaining constants, w_1 and r_1 (although q and q_1 are not determined, they always appear in the combination $q + q_1$, which is equal to r_1, cf. Equation (14)).

3. THE AXISYMMETRIC LIMIT OF A GENERALIZATION TO CHANDRASEKHAR AND ELBERT'S PAPER

Before discussing the solution obtained above, we consider the solution to the PN equations not at the point $a_2 = a_1$, but in the *limit* $a_2 \to a_1$. The equations listed above are also obtained as limiting relations. However, in the limit, we also obtain two new equations, one of which allows us to determine $\lim_{a_2 \to a_1} q_1$ and the other, say $\lim_{a_2 \to a_1} r_1$.

Equations (24′), (28′), and (38′) of CE78 provide a system of three linear equations for the quantities q_1, q_2, and q_3. After solving this linear system, the limit $a_2 \to a_1$ can be taken to give

$$\begin{aligned}
q_1 &\to -6\sqrt{2 B_{11}} \left(4 a_1^2 B_{111} + \frac{a_1^4}{a_3^2} B_{113} \right) \\
&= \frac{-\left(2e^2 + 1\right)^2 Q_1^3}{e^4} \\
&\approx 2.827158725, \qquad (24)
\end{aligned}$$

where we have defined the eccentricity

$$e := \sqrt{1 - a_3^2/a_1^2} \qquad (25)$$

and where the explicit expression for Q_1 is

$$\lim_{a_2 \to a_1} Q_1 = \lim_{a_2 \to a_1} -\sqrt{\frac{8e^2(1 - e^2)}{3 + 8e^2 - 8e^4}} \qquad (26)$$

(we remind the reader that a_3 depends on a_1 and a_2 via Equation (4)).

The fourth of equations (58′) is identically fulfilled for $a_2 = a_1$. Therefore, we introduce

$$\varepsilon := 1 - a_2^2/a_1^2 \qquad (27)$$

and expand the quantities involved and solve to first order in ε to give

$$\lim_{a_2 \to a_1} r_1 \approx 0.02880590648 - 1.75 \lim_{a_2 \to a_1} w_1. \qquad (28)$$

We provide the analytic expression in Appendix B.

Strictly speaking, we have to show that the fourth of the equations (58′) is fulfilled to all orders in ε to be certain that Equation (28) is continuously connected to the PN Dedekind solutions. We were able to solve the whole system of equations along the PN Dedekind sequence for arbitrary w_1 and w_2, meaning that the limit presented here can be tacked on continuously.

4. DISCUSSION

The axially symmetric PN solutions we have generated depend on two parameters or one if we require that the solution be continuously connected to the PN Dedekind "ellipsoids" with the velocity field (1). The solutions are not uniformly rotating in general. If we add this constraint, then requiring that the four-velocity be shear free tells us that

$$r_1 \to 0 \quad \text{(shear free)} \qquad (29)$$

must hold.

We now show that with this additional constraint, the solution is indeed the PN Maclaurin solution (thereby demonstrating that the shear free condition is not only necessary, but also sufficient for uniform rotation in our case). Let us first note that upon taking into account the results above and in particular $Q_2 \to -Q_1$, the components of the velocity become

$$\begin{aligned}
v_1 &= \sqrt{\pi G \rho} \left(Q_1 + \frac{\pi G \rho}{c^2} a_1^2 w_1 \right) x_2 \\
v_2 &= -\sqrt{\pi G \rho} \left(Q_1 + \frac{\pi G \rho}{c^2} a_1^2 w_1 \right) x_1 \\
v_3 &= 0. \qquad (30)
\end{aligned}$$

Table 1
The Numerical Values We Find for the Quantities Listed in Table 1 of Chandrasekhar & Elbert (1978)

a_2/a_1	q_1	q_2	q_3	S_1	S_2	S_3	S_4	S_5	q	r_1	r_2	t_1	t_2
1.00	2.8272	−2.8272	0.0000	−0.3050	−0.3290	−0.0144	0.0574	0.2398	−2.7984	0.0288	−0.0288	0.0000	0.0000
0.99	2.8173	−2.8370	0.0211	−0.2944	−0.3323	−0.0132	0.0542	0.2481	−2.7984	0.0196	−0.0378	−0.0454	−0.0445
0.98	2.8073	−2.8470	0.0424	−0.2838	−0.3355	−0.0120	0.0508	0.2565	−2.7984	0.0101	−0.0466	−0.0923	−0.0887
0.97	2.7972	−2.8570	0.0639	−0.2733	−0.3387	−0.0107	0.0474	0.2648	−2.7984	0.0002	−0.0553	−0.1407	−0.1324
0.96	2.7869	−2.8671	0.0857	−0.2628	−0.3416	−0.0093	0.0438	0.2732	−2.7984	−0.0101	−0.0638	−0.1906	−0.1757
0.95	2.7766	−2.8774	0.1077	−0.2524	−0.3445	−0.0078	0.0401	0.2815	−2.7985	−0.0207	−0.0722	−0.2422	−0.2186
0.90	2.7231	−2.9297	0.2213	−0.2010	−0.3573	0.0010	0.0200	0.3223	−2.7989	−0.0804	−0.1121	−0.5287	−0.4282
0.85	2.6665	−2.9843	0.3414	−0.1509	−0.3675	0.0121	−0.0030	0.3610	−2.7999	−0.1528	−0.1486	−0.8741	−0.6316
0.80	2.6067	−3.0412	0.4691	−0.1019	−0.3754	0.0258	−0.0288	0.3949	−2.8020	−0.2413	−0.1818	−1.2996	−0.8317
0.75	2.5439	−3.1006	0.6052	−0.0538	−0.3813	0.0426	−0.0572	0.4198	−2.8064	−0.3506	−0.2120	−1.8363	−1.0329
0.70	2.4781	−3.1627	0.7511	−0.0064	−0.3856	0.0636	−0.0871	0.4280	−2.8152	−0.4872	−0.2398	−2.5324	−1.2409
0.66	2.4236	−3.2146	0.8758	0.0313	−0.3882	0.0845	−0.1106	0.4131	−2.8280	−0.6222	−0.2610	−3.2547	−1.4177
0.65	2.4098	−3.2279	0.9082	0.0408	−0.3888	0.0905	−0.1161	0.4049	−2.8324	−0.6603	−0.2662	−3.4656	−1.4642
0.64	2.3958	−3.2414	0.9412	0.0503	−0.3895	0.0968	−0.1215	0.3944	−2.8374	−0.7005	−0.2715	−3.6910	−1.5118
0.63	2.3818	−3.2550	0.9747	0.0598	−0.3901	0.1037	−0.1265	0.3814	−2.8432	−0.7427	−0.2768	−3.9323	−1.5607
0.62	2.3677	−3.2687	1.0087	0.0693	−0.3907	0.1109	−0.1311	0.3653	−2.8497	−0.7873	−0.2821	−4.1913	−1.6111
0.61	2.3536	−3.2826	1.0434	0.0789	−0.3914	0.1187	−0.1352	0.3459	−2.8573	−0.8343	−0.2876	−4.4697	−1.6632
0.60	2.3394	−3.2967	1.0786	0.0886	−0.3921	0.1271	−0.1388	0.3225	−2.8659	−0.8840	−0.2931	−4.7697	−1.7171
0.59	2.3252	−3.3109	1.1145	0.0983	−0.3929	0.1362	−0.1416	0.2947	−2.8758	−0.9367	−0.2989	−5.0939	−1.7732
0.58	2.3109	−3.3254	1.1510	0.1082	−0.3938	0.1460	−0.1436	0.2616	−2.8872	−0.9924	−0.3048	−5.4449	−1.8317
0.57	2.2967	−3.3400	1.1881	0.1182	−0.3948	0.1567	−0.1444	0.2224	−2.9004	−1.0516	−0.3110	−5.8262	−1.8929
0.56	2.2824	−3.3548	1.2260	0.1284	−0.3960	0.1685	−0.1439	0.1763	−2.9155	−1.1146	−0.3175	−6.2416	−1.9574
0.55	2.2681	−3.3699	1.2646	0.1387	−0.3973	0.1814	−0.1418	0.1219	−2.9330	−1.1818	−0.3244	−6.6957	−2.0254
0.50	2.1975	−3.4487	1.4690	0.1956	−0.4087	0.2720	−0.0912	−0.3361	−3.0751	−1.5988	−0.3691	−9.7775	−2.4444
0.45	2.1301	−3.5353	1.6959	0.2722	−0.4377	0.4537	0.1171	−1.4497	−3.4139	−2.2489	−0.4521	−15.4156	−3.1217
0.40	2.0694	−3.6327	1.9502	0.4253	−0.5330	0.9625	0.9405	−4.8952	−4.4794	−3.5956	−0.6789	−29.1295	−4.6607
0.35	2.0208	−3.7456	2.2386	1.6155	−1.4902	5.7347	10.0089	−37.9506	−15.1294	−13.4666	−2.7757	−137.5070	−16.8446
0.34	2.0132	−3.7707	2.3012	6.5850	−5.5917	26.0552	49.3174	−178.2659	−60.8513	−54.2058	−11.6728	−582.0542	−67.2855
0.33	2.0065	−3.7968	2.3655	−2.6453	2.0383	−11.7342	−23.8765	82.4680	24.2357	21.4267	4.8654	241.2314	26.2701
0.32	2.0007	−3.8240	2.4317	−1.0183	0.6975	−5.0896	−11.0416	36.4961	9.3003	8.0964	1.9536	94.8022	9.7077
0.30	1.9925	−3.8819	2.5703	−0.4078	0.1986	−2.6145	−6.2981	19.0909	3.7752	3.1511	0.8615	37.3393	3.3605
0.28	1.9892	−3.9456	2.7179	−0.2340	0.0578	−1.9180	−4.9749	13.7746	2.2579	1.8969	0.5449	17.7005	1.3877
0.25	1.9960	−4.0540	2.9584	−0.1417	−0.0205	−1.5433	−4.1994	9.8393	1.4994	1.8182	0.3549	0.1194	0.0075

This is precisely the form of the velocity for the PN Maclaurin spheroids, as can be found in Chandrasekhar (1967a) (hereafter C67a) equation (3), where Ω is a constant containing a Newtonian and PN contribution, cf. (Equation (28)) of that paper.

Next we note that for a given equation of state, an axially symmetric, stationary, and uniformly rotating fluid is described by two parameters. For our purposes, we can take them to be a_3/a_1, which we prescribe using Equation (4), and the value for a_1, which we leave undetermined.

One has two additional degrees of freedom, which amount to the mapping between a Newtonian and PN solution and is a matter of convention (cf. Bardeen 1971). For example, one can write the coordinate volume of the star to be

$$V = V_0 + V_1\delta + \cdots, \tag{31}$$

where δ is some relativistic parameter, and then *choose* to have the PN contribution vanish, $V_1 = 0$. This is the choice that was made in CE78 and C67b and also in Chandrasekhar's original paper on the PN Maclaurin spheroids, C67a. We have followed this convention in the current paper, making it easy to compare our results to those of C67a. The second degree of freedom one has was left unspecified in much of C67a, though Table 1 lists values with the choice $S_1^{\rm M} = S_3^{\rm M} = 0$.[8]

[8] Where necessary, we distinguish the constants of C67a from those used here by adding the superscript "M".

If we introduce the new coordinate

$$\varpi^2 := x_1^2 + x_2^2, \tag{32}$$

and make use of Equations (13), (15), and (17), then the bounding surface (cf. Equation (47) in CE78) is given by

$$\begin{aligned} 0 = \frac{\varpi^2}{a_1^2} + \frac{x_3^2}{a_3^2} - 1 - \frac{2\pi G\rho}{c^2}\Bigg\{ & S_1\left(\varpi^2 - \frac{2a_1^2x_3^2}{a_3^2}\right) \\ & + S_3\Bigg[\frac{5}{3}\left(\varpi^2 - \frac{a_1^2x_3^2}{a_3^2}\right) - \frac{4}{3}\frac{\varpi^4}{a_1^2} + 4\varpi^2\frac{x_3^2}{a_3^2} \\ & - \frac{17}{9}\frac{a_1^2x_3^4}{a_3^4} + \frac{5}{3}x_1^2\left(\frac{\varpi^2}{a_1^2} + \frac{x_3^2}{a_3^2} - 1\right)\Bigg]\Bigg\}. \end{aligned} \tag{33}$$

Using the equation for the surface $\varpi^2/a_1^2 = 1 - x_3^2/a_3^2$, which holds at the Newtonian level and can thus be inserted into the PN term above, one sees that the term with x_1^2 vanishes and one finds that the equation is identical to Equation (42) of C67a if

$$S_3 = -\frac{9}{13}S_2^{\rm M} + \frac{3a_3^2}{13a_1^2}S_3^{\rm M} \qquad \text{and} \tag{34}$$

$$S_1 = S_1^{\rm M} + \frac{16}{13}S_2^{\rm M} - \frac{a_3^2}{13a_1^2}S_3^{\rm M} \tag{35}$$

hold. As mentioned in that paper, $S_3^{\rm M} = 0$ may be chosen without loss of generality[9] which then leads to a unique relationship between S_3 and $S_2^{\rm M}$, which is shown to be correct in Equation B3. The constant $S_1^{\rm M}$ can be chosen arbitrarily just as with S_1 (which depends on w_1).

If one considers the *limit* $a_2 \to a_1$ and simultaneously requires that the star rotates uniformly, then Equation (28) provides the unique value for w_1,

$$w_1 \approx 0.01646051799, \tag{36}$$

which is equivalent to making a choice for $S_1^{\rm M}$ different from the one made in C67a, but no more and no less physically meaningful.

The most significant result of the analysis of the axisymmetric limit is that Equation (28) shows us that the rigidly rotating limit ($r_1 = 0$) and the original choice of velocity field in CE78 ($w_1 = w_2 = 0$) are incompatible. While it is possible with that velocity field to find the PN Maclaurin solution *at* the bifurcation point, this solution is not continuously connected to any other solution. When considering the question of the existence or non-existence of non-axially symmetric but stationary solutions, it seems important to retain the possibility of studying a neighborhood of the axially symmetric and uniformly rotating limit, especially since such solutions are known to exist.[10] This possibility was excluded by the approach taken in CE78.

In a follow-up paper, we intend to tackle the problem with a more general approach that lends itself better to proceeding to higher PN orders, is not as restrictive in the solutions it permits, and allows one to show that the singularity discussed in CE78 is an artifact of the specific method chosen and not an inherent property of the PN Dedekind solutions (cf. Gürlebeck & Petroff 2010).

We gratefully acknowledge helpful discussions with M. Ansorg, J. Bičák, J. Friedman, and R. Meinel. The first author was financially supported by the grants GAUK 116-10/258025 and GACR 205/09/H033 and the second by the Deutsche Forschungsgemeinschaft as part of the project "Gravitational Wave Astronomy" (SFB/TR7–B1).

APPENDIX A

A DETAILED DISCUSSION OF CHANDRASEKHAR AND ELBERT'S WORK

We mentioned in footnote 5 that we have been unable to reproduce the values from Table 1′ in CE78 that result from solving (58′) nor have we succeeded in finding the source of the discrepancy. It is important to rule out an error in our understanding of that paper or an error in our own solutions to the equations presented there, and we therefore provide a detailed discussion here (in this section we use the velocity field in that paper, i.e., $w_1 = w_2 = 0$).

The calculations we performed were done with the aid of computer algebra. As a test, we did all the calculations using both Maple and Mathematica. To be absolutely certain that we solved the equations correctly, we wrote down the line element and energy–momentum tensor as given in Chandrasekhar (1965), had Mathematica (TTC package) determine Einstein's equations to first PN order, and then verified that they are indeed fulfilled. When the values from Table 1′ of CE78 are inserted, one then finds that the condition that pressure vanishes on the surface is violated at a level 3 orders of magnitude higher than with the values from our Table 1. We also verified that the violation vanishes in our case as more significant figures are added.

The solutions we found for q_1, q_2, and q_3 agree with those given in Table 1′ of CE78. This provides strong evidence suggesting that our numerical evaluation of a_3/a_1 for a given a_2/a_1 and of the index symbols is correct. Moreover, the dependence of q, r_1, r_2, t_1, and t_2 on S_i as given in Equations (37′) and (53′)–(56′) can be seen to hold both in Table 1′ and Table 1. This indicates strongly that the typo in Equation (53′) of CE78 mentioned in footnote 7 is truly only that and that the quantities in the integrability condition of Equation (11′) are treated correctly in both papers, leaving only δU and Φ to be verified.

The system of linear equations providing the values for S_i, i.e., Equation (58′), can of course be written as follows:

$$\begin{pmatrix} M_{11} & \cdots & M_{15} \\ \vdots & \ddots & \vdots \\ M_{51} & \cdots & M_{55} \end{pmatrix} \begin{pmatrix} S_1 \\ \vdots \\ S_5 \end{pmatrix} = \begin{pmatrix} N_1 \\ \vdots \\ N_5 \end{pmatrix}. \tag{A1}$$

For a given value of a_2/a_1, the matrix (M_{ij}) depends on the u's from C67b and via their S_i dependence, indirectly on q, r_1, r_2, t_1, and t_2. The vector (N_i) depends on the α's and again on the (non-S_i dependent part of) q, r_1, r_2, t_1, and t_2. We return to a discussion of this equation after mentioning a few incongruities in CE78.

In Equation (44′) a factor $1/(\pi G\rho)$ is missing in δU because the equation is copied directly from Equation (74) of C67b, whereas the relationship between p/ρ and δU is not the same in Equation (39′) of CE78 and Equation (75) of C67b. This mistake is corrected in Equations (45′) and (46′) however. In Equation (39′) there is also a factor $1/(\pi G\rho)^2$ missing in the term $2\Phi + 2v^2U + \frac{1}{2}(\frac{p}{\rho})^2$ as can be seen by checking dimensions[11] and comparing to Equation (11) in Chandrasekhar & Elbert (1974). Finally, we note that Equation (A1) from above only ensures that the pressure is constant on the surface of the PN ellipsoid as discussed in C67b, cf. Equation (75) in loc. cit., but not that it vanishes. The constant that would have to be determined to ensure vanishing pressure was not

[9] Note that Equations (34) and (35) together with Equation (15) are equivalent to the three equations (123) of C67b as can be seen either by taking $S_3^{\rm M} = 0$ or identifying α of that equation with $S_1^{\rm M} + \frac{a_3^2}{3a_1^2} S_3^{\rm M}$ and β with $S_2^{\rm M} - \frac{a_3^2}{3a_1^2} S_3^{\rm M}$.

[10] As far as we know, there exists no formal proof demonstrating the existence of such solutions. Steps in that direction were taken by Heilig (1995) and the existence has been demonstrated by many groups that are able to solve Einstein's equations numerically to extremely high accuracy (see, e.g., Ansorg et al. 2003).

[11] We advise the reader that, as mentioned after Equation (14) in Chandrasekhar & Elbert (1974), the units in which Q_1 and Q_2 are measured change as of this point by a factor $\sqrt{\pi G\rho}$.

written in Equation (39′) or (40′)[12] and the constant that is a part of δU in Equation (44′) was dropped when proceeding to Equation (45′). Since the determination of this constant plays no role in the paper however, we need not discuss it further and have not done so in our own paper.

We find that the determinant of (M_{ij}) vanishes at $a_2/a_1 = 0.33700003168\ldots$ just as in CE78, where it is given to four significant figures. This provides evidence suggesting that the matrices agree (and thus the δU) and that the vectors (N_i) disagree. If we multiply δU by a factor π, as suggested in the last paragraph, then the determinant becomes zero for $a_2/a_1 = 0.30874\ldots$. Nonetheless, we tested that neither an arbitrary factor in front of this term, nor one in front of the term $2\Phi+2v^2U+\frac{1}{2}(\frac{p}{\rho})^2$ can explain the results in CE78.

A natural explanation for a disagreement between the vectors (N_i) in our case and in CE78 would be that one of the α's contains a mistake. We checked, however, to see that an arbitrary change in a single α cannot account for the differences in the results. Since an explicit expression for these α's is not provided in CE78, we cannot test directly to see whether or not each agrees. However, in the implicit expressions from (39′) and (40′), only the contributions from $2\Phi + 2v^2U + \frac{1}{2}(\frac{p}{\rho})^2$ are not written out. These can easily be compared to those written out explicitly for the α's of C67b, where the appropriate modifications for the different Newtonian velocity have to be taken into account and show perfect agreement with our expressions. In particular, the relationship to the α's of C67b for $a_2 = a_1$, which is discussed in Appendix A.1, provides additional evidence for the correctness of our expressions. We also generated the α's with computer algebra by typing out the expressions for (11′), solving the integrability condition and integrating it and showed that these agree with the expressions provided below:[13]

$$\begin{aligned}
\alpha_1^{78} &= -\frac{a_3^4}{a_1^2}A_3^2 - 4a_2^2B_{12}(A_1+A_2) - 2IQ_1Q_2 - \big(2I+3a_3^2A_3\big)A_1 \\
&\quad + \left(a_1^2A_{11} - \frac{1}{2}B_{11}\right)\big(2a_1^2Q_2^2 - 2a_1^2A_1 - 3a_3^2A_3\big) - \frac{1}{2}B_{12}\big(2a_2^2Q_1^2 - 2a_2^2A_2 - 3a_3^2A_3\big) + \frac{5}{2}a_3^2A_3B_{13} \qquad \text{(A2)}\\
\alpha_2^{78} &= -\frac{a_3^4}{a_2^2}A_3^2 - 4a_1^2B_{12}(A_1+A_2) - 2IQ_1Q_2 - \big(2I+3a_3^2A_3\big)A_2 \\
&\quad + \left(a_2^2A_{22} - \frac{1}{2}B_{22}\right)\big(2a_2^2Q_1^2 - 2a_2^2A_2 - 3a_3^2A_3\big) - \frac{1}{2}B_{12}\big(2a_1^2Q_2^2 - 2a_1^2A_1 - 3a_3^2A_3\big) + \frac{5}{2}a_3^2A_3B_{23} \qquad \text{(A3)}\\
\alpha_3^{78} &= -a_3^2A_3^2 - \big(2I+3a_3^2A_3\big)A_3 - \frac{1}{2}B_{23}\big(2a_2^2Q_1^2 - 2a_2^2A_2 - 3a_3^2A_3\big) \\
&\quad - \frac{1}{2}B_{13}\big(2a_1^2Q_2^2 - 2a_1^2A_1 - 3a_3^2A_3\big) + \frac{5}{2}a_3^2A_3\big(B_{33} - 2a_3^2A_{33}\big) \qquad \text{(A4)}\\
\alpha_{12}^{78} &= \frac{a_3^4}{a_1^2a_2^2}A_3^2 - 2Q_1^2\left(A_1 + \frac{a_2^4}{a_1^4}A_2\right) + \big(2a_1^2Q_2^2 - 2a_1^2A_1 - 3a_3^2A_3\big)\left(-a_1^2A_{112} + \frac{1}{2}B_{112}\right) \\
&\quad + \big(2a_2^2Q_1^2 - 2a_2^2A_2 - 3a_3^2A_3\big)\left(-a_2^2A_{122} + \frac{1}{2}B_{122}\right) - \frac{5}{2}a_3^2A_3B_{123} + 2Q_1Q_2\left(1 - \frac{a_2^2}{a_1^2}\right)A_2 \\
&\quad - \frac{1}{2}Q_1^3Q_2 - 2a_2^2Q_1Q_2(3A_{22}+A_{12}) + 4Q_1^2\left(A_1 - \frac{a_2^2}{a_1^2}A_2\right) - Q_1\left(q_1 + \frac{1}{2}q_2\right) \qquad \text{(A5)}\\
\alpha_{23}^{78} &= \frac{a_3^2}{a_2^2}A_3^2 - 2Q_1^2A_3 + 2Q_1^2\left(1 - \frac{a_2^2}{a_1^2}\right)A_3 - 2a_1^2Q_1Q_2(A_{13}+A_{23}) + \big(2a_1^2Q_2^2 - 2a_1^2A_1 - 3a_3^2A_3\big)\left(\frac{1}{2}B_{123}\right) \\
&\quad + \big(2a_2^2Q_1^2 - 2a_2^2A_2 - 3a_3^2A_3\big)\left(-a_2^2A_{223} + \frac{1}{2}B_{223}\right) - \frac{5}{2}a_3^2A_3\big(-2a_3^2A_{233} + B_{233}\big) \qquad \text{(A6)}\\
\alpha_{31}^{78} &= \frac{a_3^2}{a_1^2}A_3^2 - 2Q_2^2A_3 + 2Q_1Q_2\left(1 - \frac{a_2^2}{a_1^2}\right)A_3 - 2a_2^2Q_1Q_2(A_{13}+A_{23}) - \frac{5}{2}a_3^2A_3\big(-2a_3^2A_{133} + B_{133}\big) \\
&\quad + \big(2a_1^2Q_2^2 - 2a_1^2A_1 - 3a_3^2A_3\big)\left(-a_1^2A_{113} + \frac{1}{2}B_{113}\right) + \big(2a_2^2Q_1^2 - 2a_2^2A_2 - 3a_3^2A_3\big)\left(\frac{1}{2}B_{123}\right) \qquad \text{(A7)}\\
\alpha_{11}^{78} &= \frac{1}{2}\frac{a_3^4}{a_1^4}A_3^2 - 2Q_2^2A_1 + \big(2a_1^2Q_2^2 - 2a_1^2A_1 - 3a_3^2A_3\big)\left(-a_1^2A_{111} + \frac{1}{4}B_{111}\right) \\
&\quad + \big(2a_2^2Q_1^2 - 2a_2^2A_2 - 3a_3^2A_3\big)\left(\frac{1}{4}B_{112}\right) - \frac{5}{4}a_3^2A_3B_{113} + Q_1Q_2\left(1 - \frac{a_2^2}{a_1^2}\right)A_1 \\
&\quad - \frac{1}{4}Q_1Q_2^3 - a_2^2Q_1Q_2(3A_{11}+A_{12}) - \frac{1}{4}Q_2q_1 \qquad \text{(A8)}
\end{aligned}$$

[12] The constant contained in δU is completely determined by Equation (44′) and is thus not available as a variable to ensure that the pressure vanishes on the surface.

[13] For the terms in Equation (11′), we checked our expressions by ensuring that $\nabla^2U = -4\pi G\rho$, Equation (8′) and the Newtonian equations hold. Furthermore, we tested the u's by first ensuring that the moments $\mathfrak{D}_i$, $\mathfrak{D}_{ijk}$ fulfill the appropriate Poisson equation and that the $\delta U^{(i)}$ of Equation (69) from C67b agree with Equations (70) and (71) from the same paper.

$$\alpha_{22}^{78} = \frac{1}{2}\frac{a_3^4}{a_2^4}A_3^2 - 2Q_1^2A_2 + \left(2a_1^2Q_2^2 - 2a_1^2A_1 - 3a_3^2A_3\right)\left(\frac{1}{4}B_{122}\right)$$
$$+ \left(2a_2^2Q_1^2 - 2a_2^2A_2 - 3a_3^2A_3\right)\left(-a_2^2A_{222} + \frac{1}{4}B_{222}\right) - \frac{5}{4}a_3^2A_3B_{223} + Q_1^2\left(1 - \frac{a_2^2}{a_1^2}\right)A_2$$
$$- \frac{1}{4}Q_1^3Q_2 - Q_1Q_2a_1^2(3A_{22} + A_{12}) - \frac{1}{4}Q_1q_2 \tag{A9}$$

$$\alpha_{33}^{78} = \frac{1}{2}A_3^2 + \frac{1}{4}\left(2a_1^2Q_2^2 - 2a_1^2A_1 - 3a_3^2A_3\right)B_{133} + \frac{1}{4}\left(2a_2^2Q_1^2 - 2a_2^2A_2 - 3a_3^2A_3\right)B_{233}$$
$$- \frac{5}{2}a_3^2A_3\left(-2a_3^2A_{333} + \frac{1}{2}B_{333}\right). \tag{A10}$$

Let us summarize the arguments from above. We have checked all the equations in Part I of CE78 and find the analytic expressions to be free of error, except for the few minor points mentioned above. We have good reason to believe that both in that paper and here, Einstein's PN equations are solved correctly including the PN-Bianchi identity. We obtain different numerical values for S_i which we suspect is related to a problem with the numerical evaluation of the α's in CE78, though we cannot be certain that our matrices (M_{ij}) agree simply because their determinants vanish at the same point. The various tests of our α's and the fact that we find the PN Maclaurin spheroids in the axisymmetric case convince us that our values are correct.

A.1. The Solution at the Bifurcation Point

At the point $a_2 = a_1$, i.e., at the bifurcation point along the Maclaurin sequence, the following relations can be used to simplify the expressions for the α's, where Ω refers to the angular velocity of the uniformly rotating Newtonian solution and has the same meaning as in C67b:

$$a_3^2A_3 = a_1^4A_{11} = a_1^2(A_1 - B_{11}) = I - 2a_1^2A_1 = a_1^2\left(A_1 - \frac{1}{2}Q_1^2\right), \qquad \Omega^2 = 2B_{11} = Q_1^2. \tag{A11}$$

Note that at this point, the α's of C67b and C67a agree and we find

$$\alpha_1^{78} = -\frac{a_3^4}{a_1^2}A_3^2 - 8a_1^2B_{11}A_1 + 2IQ_1^2 - \left(2I + 3a_3^2A_3\right)A_1 + \left(a_1^2A_{11} - B_{11}\right)\left(2a_1^2Q_1^2 - 2a_1^2A_1 - 3a_3^2A_3\right) + \frac{5}{2}a_3^2A_3B_{13}$$
$$= -15a_1^2A_1^2 - \frac{19}{4}a_1^2Q_1^4 + 14a_1^2A_1Q_1^2 + \frac{5}{2}a_3^2A_3B_{13}$$
$$= \alpha_1^{67} = \alpha_2^{78} = \alpha_2^{67} \tag{A12}$$

$$\alpha_3^{78} = -a_3^2A_3^2 - \left(2I + 3a_3^2A_3\right)A_3 - B_{13}\left(2a_1^2Q_1^2 - 2a_1^2A_1 - 3a_3^2A_3\right) + \frac{5}{2}a_3^2A_3\left(B_{33} - 2a_3^2A_{33}\right)$$
$$= a_1^2\left(2Q_1^2 - 10A_1\right)A_3 + a_1^4Q_1^2A_{13}$$
$$= \alpha_3^{67} \tag{A13}$$

$$\alpha_{12}^{78} = \frac{a_3^4}{a_1^4}A_3^2 - 4Q_1^2A_1 + a_1^2\left(\frac{7}{2}Q_1^2 - 5A_1\right)\left(-2a_1^2A_{111} + B_{111}\right) - \frac{5}{2}a_3^2A_3B_{113} + \frac{1}{2}Q_1^4 + 8a_1^2Q_1^2A_{11} - \frac{1}{2}q_1Q_1$$
$$= \alpha_{12}^{67} - \frac{1}{2}q_1Q_1 \tag{A14}$$

$$\alpha_{23}^{78} = \frac{a_3^2}{a_1^2}A_3^2 - 2Q_1^2A_3 + 4a_1^2Q_1^2A_{13} + a_1^2\left(\frac{7}{2}Q_1^2 - 5A_1\right)\left(B_{113} - a_1^2A_{113}\right) - \frac{5}{2}a_3^2A_3\left(-2a_3^2A_{133} + B_{133}\right)$$
$$= \alpha_{23}^{67} = \alpha_{31}^{78} = \alpha_{31}^{67} \tag{A15}$$

$$\alpha_{11}^{78} = \alpha_{22}^{78} = \frac{1}{2}\alpha_{12}^{78} + \frac{1}{2}Q_1q_1 = \alpha_{11}^{67} + \frac{1}{4}Q_1q_1 \tag{A16}$$

$$\alpha_{33}^{78} = \frac{1}{2}A_3^2 + \frac{1}{2}a_1^2\left(\frac{7}{2}Q_1^2 - 5A_1\right)B_{133} - \frac{5}{2}a_3^2A_3\left(-2a_3^2A_{333} + \frac{1}{2}B_{333}\right)$$
$$= \alpha_{33}^{67}. \tag{A17}$$

APPENDIX B

EXPLICIT EXPRESSIONS FOR S_1, S_3, AND R_1

At the point $a_2 = a_1$, the u's from C67b and C67a are related by

$$u_{ij}^{(2)\mathrm{M}} = -\frac{9}{13}\left(u_{ij}^{(3)} - 4u_{ij}^{(4)} - \frac{17a_1^2}{3a_3^2}u_{ij}^{(5)}\right)\Bigg|_{a_2=a_1}, \tag{B1}$$

which follows from Equation (119) of C67b.

Using these relations, those between the α's and Equations (11), (13), and (17), one finds that the third of the equations (58′) of CE78 becomes

$$\begin{aligned} 0 &= a_1^4 Q_{11}^{78} - a_1^2 a_3^2 Q_{13}^{78} + a_3^4 Q_{33}^{78} \\ &\stackrel{a}{=} a_1^4\alpha_{11}^{67} - a_1^2 a_3^2\alpha_{13}^{67} + a_3^4\alpha_{33}^{67} + \frac{a_1^4 Q_1}{2}r_1 + \frac{130}{9}a_1^2 a_3^2 A_3 S_3 - \frac{13}{9}\left(a_1^4 u_{11}^{(2)\mathrm{M}} - a_1^2 a_3^2 u_{13}^{(2)\mathrm{M}} + a_3^4 u_{33}^{(2)\mathrm{M}}\right) S_3. \end{aligned} \tag{B2}$$

We thus have the solution

$$S_3 = \frac{9}{13}\frac{a_1^4\alpha_{11}^{67} - a_1^2 a_3^2\alpha_{13}^{67} + a_3^4\alpha_{33}^{67} + a_1^4 Q_1 r_1/2}{a_1^4 u_{11}^{(2)\mathrm{M}} - a_1^2 a_3^2 u_{13}^{(2)\mathrm{M}} + a_3^4 u_{33}^{(2)\mathrm{M}} - 10a_1^2 a_3^2 A_3}, \tag{B3}$$

which agrees with Equation (99) of C67a if we take Equation (34) of this paper into account. In order to provide concise explicit formulae, we again make use of the eccentricity

$$e = \sqrt{1 - a_3^2/a_1^2},$$

the quantity

$$C := 104e^6 - 444e^4 + 630e^2 - 245 \tag{B4}$$

and recall that Q_1 is

$$Q_1 \stackrel{a}{=} -\sqrt{\frac{8e^2(1-e^2)}{3 + 8e^2 - 8e^4}}.$$

We now provide explicit expressions for S_1, S_3, and r_1. Note that the expressions for S_1 and S_3 can be obtained either as limiting values or by placing oneself directly on the point $a_2 = a_1$. On the other hand, r_1 can only be obtained by a limiting process. The formulae read

$$\begin{aligned} S_1 \stackrel{a}{=} \frac{e}{2e^2-1}\Bigg[&\frac{-1}{26eC}(2864e^8 - 10128e^6 + 14712e^4 - 8120e^2 + 1365)Q_1^2 \\ &+ \frac{e}{3Q_1}w_1 + \frac{4e}{39CQ_1}(224e^6 - 840e^4 + 1170e^2 - 455)r_1\Bigg], \end{aligned} \tag{B5}$$

$$S_3 \stackrel{a}{=} \frac{36e^4}{65C}\left[\frac{(272e^4 - 244e^2 + 35)Q_1^2}{8e^2} - \frac{3e^2}{Q_1}r_1\right], \tag{B6}$$

$$r_1 \to \frac{-Q_1^3}{8e^2(2e^2+1)}(24e^4 - 12e^2 - 1) - \frac{7}{4}w_1. \tag{B7}$$

In deriving these expressions, we have made use of the identities

$$a_3^2\left(4A_{11} - \frac{2}{a_1^2}\right) - 4a_1^2 A_{11} + 3A_1\Big|_{a_2=a_1} = 0, \tag{B8}$$

$$3A_1^2 - 3A_1 - 4a_1^2 A_1 A_{11} + 5a_1^2 A_{11} - 2a_1^4 A_{11}^2\big|_{a_2=a_1} = 0. \tag{B9}$$

REFERENCES

Ansorg, M., Kleinwächter, A., & Meinel, R. 2003, A&A, 405, 711
Bardeen, J. M. 1971, ApJ, 167, 425
Chandrasekhar, S. 1965, ApJ, 142, 1488
Chandrasekhar, S. 1967a, ApJ, 147, 334 (C67a)
Chandrasekhar, S. 1967b, ApJ, 148, 621 (C67b)
Chandrasekhar, S. 1987, Ellipsoidal Figures of Equilibrium (New York: Dover)
Chandrasekhar, S., & Elbert, D. D. 1974, ApJ, 192, 731
Chandrasekhar, S., & Elbert, D. D. 1978, ApJ, 220, 303 (erratum) (CE78)
Gürlebeck, N., & Petroff, D. 2010, arXiv:1003.2061
Heilig, U. 1995, Commun. Math. Phys., 166, 457

6.8 The rod-limit of the 1-PN Dedekind ellipsoids

In this section, we investigate the limit at the other end of the sequence, i.e., for $\bar{a}_2 \to 0$ or equivalently $\bar{a}_3 \to 0$. The behavior of μ for $\bar{a}_3 \to 0$ was chosen in the Newtonian case such that the inhomogeneity in Eq. (6.4a) approaches a line or a point density of the form given in Eqs. (5.17)-(5.20). The Newtonian kinetic and gravitational potential energy serve as a source of the gravitational field in the PN approximation. The solution Φ of the Eq. (6.4a) approaches the potential of either of the densities[18]

$$3\eta_2^2 G\left(1-\frac{\left(x^1\right)^2}{a_1^2}\right)^2\delta(x^2)\delta(x^3) \quad \text{or} \quad \frac{16}{5}\eta_{\frac{5}{2}}^2 G\delta(x^1)\delta(x^2)\delta(x^3), \tag{6.24}$$

where $\delta(x)$ denotes the Dirac delta distribution. Both are axially symmetric. In the first case, the potential[19] Φ_s in cylindrical coordinates ($x^2=\rho\cos\varphi$ and $x^3=\rho\sin\varphi$) reads

$$\begin{aligned}\Phi_2 =&\frac{\eta_2^2 G}{8a_1^4}\left(\sqrt{\left(a_1+x^1\right)^2+\rho^2}\left(-9a_1\rho^2+58a_1^2x^1+26a_1\left(x^1\right)^2-18a_1^3+55\rho^2x^1-50\left(x^1\right)^3\right)+\right.\\ &\sqrt{\left(a_1-x^1\right)^2+\rho^2}\left(-9a_1\rho^2-58a_1^2x^1+26a_1\left(x^1\right)^2-18a_1^3-55\rho^2x^1+50\left(x^1\right)^3\right)+\\ &\left.3\left(8\rho^2\left(a_1^2-3\left(x^1\right)^2\right)+8\left(a_1^2-\left(x^1\right)^2\right)^2+3\rho^4\right)\log\left(\frac{\sqrt{\left(a_1-x^1\right)^2+\rho^2}+a_1-x^1}{\sqrt{\left(a_1+x^1\right)^2+\rho^2}-a_1-x^1}\right)\right),\end{aligned} \tag{6.25a}$$

and in the second case, it is given by

$$\Phi_{\frac{5}{2}}=\frac{16\eta_{\frac{5}{2}}^2 G}{5\sqrt{\rho^2+\left(x^1\right)^2}}. \tag{6.25b}$$

Hence, Φ_s is axially symmetric in the limit. If $a_1 \to \infty$ subsequently, the arguments in Footnote 18 in this chapter do not apply directly because the boundary conditions change. A constant – diverging in the limit – has to be subtracted in this limit.

The Newtonian gravitational potential $U^{(0)}$ vanishes in the exterior for $\bar{a}_3 \to 0$ and for μ as in Eq. (5.19). Therefore, the spatial metric $g_{ab} \to -\delta_{ab}$. The metric function $U_a^{(3)}$ is still undetermined for $\bar{a}_3 \to 0$. We show that the metric is static in the limit, i.e., $U_a^{(3)} \to 0$. In order to do so, one can take the limit of the solution described in (6.7) and (C.3) employing the transition of ellipsoidal harmonics to spheroidal harmonics as described in [41]. In this limit, one finds, after lengthy calculations, that the $U_a^{(3)}$ vanish. But the more physical argument used in Section 5.3.1 leads us faster to that goal. The inhomogeneity in Eq. (6.4b) for $U_1^{(3)}$ is proportional to the Newtonian linear momentum density in x^1-direction. The integral of this density over a slice $\mathcal{S}(x_0^1,\delta x^1)$, i.e., the linear momentum contained in $\mathcal{S}(x_0^1,\delta x^1)$ vanishes because of the anti-symmetry in x^2.[20] The momentum $P_\pm^1$ contained in the halves of $\mathcal{S}(x_0^1,\delta x^1)$ with $x^2 \geq 0$ and

[18] Since our sequence of inhomogeneities converges in the appropriate Sobolev space (with negative index), standard theorems of functional analysis ensure that the solution converges as well. This allows us to solve the Eq. (6.4a) for the limiting inhomogeneity knowing that it coincides with the limit of the solutions along the 1-PN Dedekind sequence, cf. [42, 51].

[19] The index s has the same meaning as in the end of Section 5.3.1.

[20] This corroborates the interpretation that two anti-parallel streams emerge in the limit.

$x^2 \leq 0$, respectively, can be calculated using Eqs. (5.8), (A.4) and (5.12). The momentum density does not change sign in these halves of $\mathcal{S}(x_0^1, \delta x^1)$. Close to $\bar{a}_2 = 0$, this yields[21]

$$P_\pm^1 = \pm \frac{\eta_s^{\frac{3}{2}} a_1^{3-\frac{3s}{2}}}{3\pi} \delta x^1 \sqrt{-4\log\bar{a}_3 - 6 + \log 16} \left(\frac{\left(\delta x^1\right)^2}{a_1^2} + \frac{3\delta x^1 x_0^1}{a_1^2} + \frac{3\left(x_0^1\right)^2}{a_1^2} - 3 \right) \times \left(-\frac{G}{\log\bar{a}_3} \right)^{3/4} + \tilde{O}\left(\bar{a}_3^2\right). \tag{6.26}$$

Hence, the $P_\pm^1$ vanish logarithmically in $\bar{a}_3$ and the resulting inhomogeneity does not form a dipole line density. We have $|x^2| \leq a_2$ and $|x^3| \leq a_3$ in the interior of the ellipsoid. Thus, higher multipole moments of this inhomogeneity vanish in the limit as well. Therefore, the resulting potential $U_1^{(3)} \to 0$ in the exterior for $\bar{a}_3 \to 0$. With an analogous argument one can show that $U_2^{(3)} \to 0$ for $\bar{a}_3 \to 0$, too. These conclusions are independent of s, so that the resulting metric is always *static*.

It remains to see, if δU and the 1-PN surface are well-defined. Since the S_i diverge in the limit $\bar{a}_3 \to 0$, it is not clear if the surface is still closed. The function δU can be written as $\delta U = U' - U^{(0)}$. The potential U' satisfies

$$\Delta U' = -4\pi G\mu\, \mathbf{1}\left(\left\{ (x^a) \in \mathbb{R}^3 \,\middle|\, S^{(0)} + c^{-2} S^{(2)} \leq 0 \right\} \right), \tag{6.27}$$

where we wrote the support of the mass density explicitly with the indicator function $\mathbf{1}(A)$ of a subset $A \subset \mathbb{R}^3$. The 1-PN correction to the total mass for this inhomogeneity vanishes because of ansatz (6.5). The following reasoning is done for $s = 2$. The choice $s = \frac{5}{2}$ is discussed afterwards.

The surface of the 1-PN Dedekind ellipsoid in cylindrical coordinates ($x^2 = \rho\cos\varphi$, $x^3 = \rho\sin\varphi$) reads

$$\hat{\rho}(x^1, \varphi) = \rho^{(0)}(x^1, \varphi) + c^{-2}\rho^{(2)}(x^1, \varphi), \tag{6.28}$$

with a Newtonian contribution $\rho^{(0)}(x^1, \varphi) \in O(\bar{a}_3)$. This implies that the Newtonian potential $U^{(0)}$ vanishes in the exterior in the limit $\bar{a}_3 \to 0$. More precisely, the mass δM in a slice $\mathcal{S}\left(\delta x^1, x_0^1\right)$ vanishes for a mass density μ as in Eq. (5.19):

$$\delta M = \int_{x_0^1}^{x_0^1 + \delta x^1} \int_0^{2\pi} \int_0^{\rho^{(0)}} \mu\rho \,\mathrm{d}\rho \,\mathrm{d}\varphi \,\mathrm{d}x^1 \to 0 \quad \text{for} \quad \bar{a}_3 \to 0. \tag{6.29}$$

The vanishing of higher multipole moments can be inferred from Eq. (6.29) as well, because μ is positive in the entire interior of the ellipsoid. Thus, no line density is formed. Analogously, we have to show that $\delta M \to 0$ also for slices of the 1-PN ellipsoid to see that $U' \to 0$. We see below that in general $\rho^{(0)}\rho^{(2)} \notin O(\bar{a}_3^2)$ but rather $\rho^{(0)}\rho^{(2)} \in \tilde{O}(\bar{a}_3^2)$. Hence, a careful analysis is required to show that there exists a choice of parameters w_i for which $\delta M \to 0$ in the limit.

To determine $\rho^{(0)}\rho^{(2)}$, we first have to obtain the surface to second order in $\bar{a}_3$. Even though the interior is discarded in the limit, the surface is still determined by the condition of a vanishing pressure, see Eq. (6.13) and Appendix D. The leading orders of the solutions S_i are given as follows:

$$S_i = \begin{cases} S_{i0}(w_1, w_2, \bar{a}_3) + S_{i2}(w_1, w_2, \bar{a}_3)\bar{a}_3^2 + \tilde{O}(\bar{a}_3^4), & i \in \{1, 2, 3\} \\ S_{i0}(w_1, w_2, \bar{a}_3)\bar{a}_3^{-2} + S_{i2}(w_1, w_2, \bar{a}_3) + \tilde{O}(\bar{a}_3^2), & i \in \{4, 5\}, \end{cases} \tag{6.30}$$

[21] For $s = \frac{5}{2}$ one has to set $x_0^1 = -a_1$ and $\delta x^1 = 2a_1$ to integrate over the entire half of the ellipsoid and not just a slice.

where the functions[22] $S_{i0/2}(w_i,\bar{a}_3) \in \tilde{O}_{\bar{a}_3}(1)$ are linear in w_i. The different orders in $\bar{a}_3$ have their origin in ansatz (6.5) where the S_4 and S_5 have an additional factor $\left(x^2\right)^2$ or $\left(x^3\right)^2$ in their coefficients. These factors vanish in the limit as well.

The leading order in $\bar{a}_3$ of the 1-PN correction to $\hat{\rho}(x^1,\varphi)^2$ close to $\bar{a}_3 = 0$ is

$$\begin{aligned}2\rho^{(0)}\rho^{(2)} =&\frac{\pi G\eta_2}{12a_1^2\sqrt{-\log\bar{a}_3}}\left(\left(a_1^2-\left(x^1\right)^2\right)\left((4S_{40}+S_{50})\cos(4\varphi)\left(a_1^2-\left(x^1\right)^2\right)+4\cos(2\varphi)\times\right.\right.\\ &\left.\left(a_1^2\left(3S_{10}+6S_{20}+S_{40}-S_{50}\right)-\left(3S_{30}+S_{40}-4S_{50}\right)\left(x^1\right)^2\right)\right)+6a_1^2\left(6S_{10}-\\ &\left.2S_{30}-3S_{50}\right)\left(x^1\right)^2+3a_1^4\left(S_{50}-4S_{10}\right)+5\left(4S_{30}+3S_{50}\right)\left(x^1\right)^4\right)+\tilde{O}(\bar{a}_3^2).\end{aligned} \tag{6.31}$$

Hence, $\rho^{(0)}\rho^{(2)}$ vanishes for $\bar{a}_3 \to 0$ but not sufficiently fast. It does not ensure $\delta M \to 0$. To have $\delta M \to 0$ for $\bar{a}_3 \to 0$, we have to find w_i for which the S_{i0} vanish. Therefore, we must calculate the parameters S_i to leading order in $\bar{a}_3$. With an ansatz for the w_i analogous to Eq. (6.30),

$$w_{i0}(\bar{a}_3) + w_{i2}(\bar{a}_3)\bar{a}_3^2 + \tilde{O}(\bar{a}_3^4), \quad i \in \{1,2\}, \tag{6.32}$$

the leading order of Eq. (6.13) reads

$$\begin{aligned}0 =& -6S_{10}-12S_{20}+10S_{40}+5S_{50},\\ 0 =& -4S_{40}-S_{50},\\ 0 =& S_{10}\left(-25+\log 4096-12\log\bar{a}_3\right)-2S_{20}+S_{30}\left(\frac{31}{3}-4\log 2+4\log\bar{a}_3\right)+\frac{1}{3}S_{40}+\\ &S_{50}\left(\frac{197}{12}-6\log 2+6\log\bar{a}_3\right)-w_{10}\left(-6+\log 16-4\log\bar{a}_3\right)^{\frac{1}{2}}+w_{20}\left(-6+\log 16-4\log\bar{a}_3\right)^{\frac{1}{2}},\\ 0 =& 4S_{30}-\frac{20}{3}S_{40}-\frac{22}{3}S_{50},\\ 0 =& 96(S_{20}-S_{10})(-3+2\log 2-2\log\bar{a}_3)+\frac{8}{3}S_{30}(-109+54\log 2-54\log\bar{a}_3)+\\ &S_{40}(-146+96\log 2-96\log\bar{a}_3)+\frac{15}{2}S_{50}(-23+8\log 2-8\log\bar{a}_3)+\\ &24(-\sqrt{2}(w_{10}+w_{20})\left(-3+2\log 2-2\log\bar{a}_3\right)^{\frac{1}{2}}+2(-3+2\log 2-2\log\bar{a}_3)).\end{aligned} \tag{6.33}$$

The solution S_{i0} of this system of equations can be obtained easily, but we do not write it down explicitly. It is sufficient to remark that the coefficient matrix of this system of equations is regular and that the inhomogeneity vanishes for the choice

$$w_{10} = w_{20} = \left(-\frac{3}{2}+\log 2-\log\bar{a}_3\right)^{\frac{1}{2}}. \tag{6.34}$$

Hence, for these w_{i0} the S_{i0} vanish as required. This implies that $S_1,\ S_2,\ S_3 \to 0$ for $\bar{a}_3 \to 0$.

[22] The index $\bar{a}_3$ in $\tilde{O}_{\bar{a}_3}(1)$ indicates with respect to which variable the limit in the definition (5.11) has to be taken.

The next-to-leading order[23] in $\bar{a}_3$ of the 1-PN correction of $\hat{\rho}^{(2)}(x^1,\varphi)$ is

$$\begin{aligned}2\rho^{(0)}\rho^{(2)} =&\frac{\pi G\eta_2\bar{a}_3^2}{12a1^2\sqrt{-\log\bar{a}_3}}\left(\left(a_1^2-\left(x^1\right)^2\right)\left((4S_{42}+S_{52})\cos(4\phi)\left(a_1^2-\left(x^1\right)^2\right)+4\cos(2\phi)\times\right.\right.\\&\left.\left(a_1^2\left(3S_{12}+6S_{22}+S_{42}-S_{52}\right)-\left(3S_{32}+S_{42}-4S_{52}\right)\left(x^1\right)^2\right)\right)+6a_1^2\left(6S_{12}-\\&\left.2S_{32}-3S_{52}\right)\left(x^1\right)^2+3a_1^4\left(S_{52}-4S_{12}\right)+5\left(4S_{32}+3S_{52}\right)\left(x^1\right)^4\right)+\tilde{O}(\bar{a}_3^4).\end{aligned} \tag{6.35}$$

Even though this is not yet sufficient for $\delta M\to 0$, it shows that the 1-PN surface degenerates to a rod. We determine the length of the rod in Eq. (6.39). The exact dependence of the S_{i2} on $\bar{a}_3$ is necessary, to see if $\delta M\to 0$ is possible. Therefore, we solve Eq. (6.13) to the next-to-leading order in $\bar{a}_3$. Using Eq. (6.34), the surface condition reads to this order as follows:

$$\begin{aligned}0=&-2S_{12}-4S_{22}+\frac{10}{3}S_{42}+\frac{5}{3}S_{52}-\frac{8}{3}2w_{10}^2,\\0=&-4S_{42}-S_{52}-4w_{10}^2,\\0=&\left(-12\log\bar{a}_3-25+12\log 2\right)S_{12}-2S_{22}+\left(\frac{31}{3}-4\log 24+\log\bar{a}_3\right)S_{32}+\frac{1}{3}S_{42}+\\&\left(6\log\bar{a}_3+\frac{197}{12}-6\log 2\right)S_{52}+2w_{10}(w_{22}-w_{12})+\frac{8}{3}\left(-6\log\bar{a}_3-19+12\log 2\right)\log\bar{a}_3-\\&35+\frac{8}{3}(19-6\log 2)\log 2,\\0=&\frac{40}{3}w_{10}^2+2S_{32}-\frac{10}{3}S_{42}-\frac{11}{3}S_{52},\\0=&-192w_{10}^2S_{12}+192w_{10}^2S_{22}+\frac{8}{3}\left(-109+54\log 2-54\log\bar{a}_3\right)S_{32}+\left(-146+96\log 2-\right.\\&\left.96\log\bar{a}_3\right)S_{42}+\frac{15}{2}\left(-23+8\log 2-8\log\bar{a}_3\right)S_{52}-48w_{10}(w_{12}+w_{22})+8\log\bar{a}_3\left(36\log\bar{a}_3+\right.\\&\left.83-72\log 2\right)+338+8\log 2(36\log 2-83).\end{aligned} \tag{6.36}$$

The solution of these equations is given by

$$\begin{aligned}S_{12}=&\frac{1}{\log\frac{\bar{a}_3}{2}+8}\left(-\frac{w_{10}}{78}\left((1207-504\log 2+504\log\bar{a}_3)w_{14}+113w_{24}\right)+\frac{1}{312}\left(-148314+\right.\right.\\&\log 2(240213+2\log 2(10584\log 2-62665))-\log\bar{a}_3\left(2\log\bar{a}_3\left(10584\log\bar{a}_3+62665-\right.\right.\\&\left.\left.\left.31752\log 2\right)+240213+4\log 2(15876\log 2-62665)\right)\right),\\S_{22}=&\frac{1}{\log\frac{\bar{a}_3}{2}+8}\left(\frac{1}{156}w_{10}\left(w_{14}\left(288\log\bar{a}_3+829-288\log 2\right)+59w_{24}\right)+\frac{1}{312}\left(4\log\bar{a}_3\left(\log\bar{a}_3\times\right.\right.\right.\\&\left.\left.(1512\log\bar{a}_3+9799-4536\log 2)+20838+2\log 2(2268\log 2-9799)\right)+56499-\\&\left.\left.4\log 2(20838+\log 2(1512\log 2-9799))\right)\right),\end{aligned} \tag{6.37}$$

[23] With the choice of w_i as in Eq. (6.34), this is actually the leading order.

$$
\begin{aligned}
S_{32} =& \frac{1}{\log\frac{\bar{a}_3}{2}+8}\left(\frac{153}{65}w_{10}\left(w_{14}-w_{24}\left(-4\log\bar{a}_3-7+4\log 2\right)\right)+\frac{3}{520}\left(-\log\bar{a}_3\left(2\log\bar{a}_3\times\right.\right.\right.\\
&\left(8568\log\bar{a}_3+44885-25704\log 2\right)+149389+4\log 2(12852\log 2-44885))-\\
&\left.\left.\left.80020+\log 2(149389+\log 2(8568\log 2-44885))\right)\right),\\
S_{42} =& \frac{1}{\log\frac{\bar{a}_3}{2}+8}\left(\frac{27}{65}w_{10}\left(w_{14}\left(4\log\bar{a}_3+7-4\log 2\right)+w_{24}\right)+\frac{3}{520}\left(\log\bar{a}_3\left(2\log\bar{a}_3\left(1512\log\bar{a}_3+\right.\right.\right.\right.\\
&\left.8135-4536\log 2\right)+30431+4\log 2(2268\log 2-8135))+19260+\log 2(2(8135-\\
&\left.\left.\left.\left.1512\log 2)\log 2-30431))\right)\right),\\
S_{52} =& \frac{1}{\log\frac{\bar{a}_3}{2}+8}\left(\frac{108}{65}w_{10}\left(w_{14}\left(-4\log\bar{a}_3-7+4\log 2\right)-w_{24}\right)+\frac{1}{130}\left(-\log\bar{a}_3\left(2\log\bar{a}_3\times\right.\right.\right.\\
&\left(4536\log\bar{a}_3+24145-13608\log 2\right)+86353+4\log 2(6804\log 2-24145))-51540+\\
&\left.\left.\left.\log 2(86353+2\log 2(4536\log 2-24145))\right)\right).
\end{aligned}
$$

We insert Eqs. (6.35) and (6.37) in Eq. (6.29). Assuming that $\delta M \to 0$ for $\bar{a}_3 \to 0$ puts the following constraints on w_{i2}:

$$
\begin{aligned}
w_{12} =& -\frac{21}{2}(-\log\bar{a}_3)^{\frac{3}{2}}-\frac{7}{16}(-\log\bar{a}_3)^{\frac{1}{2}}(-65+36\log 2)+c_1+o(1),\\
w_{14} =& -\frac{5}{2}(-\log\bar{a}_3)^{\frac{3}{2}}-c_2\log\bar{a}_3+O((-\log\bar{a}_3)^{\frac{1}{2}}).
\end{aligned}
\tag{6.38}
$$

The constants c_i determine the 1-PN contribution to the length of the rod as we show below. Since $\delta M \to 0$, all other multipole moments vanish for $\bar{a}_3 \to 0$, ergo $U' \to 0$ and $\delta U \to 0$ in the exterior. The length of the rod Δx^1 ensues from the surface (6.5) for $x^2 = x^3 = 0$. It is given by

$$
\Delta x^1 = 2a_1^2 - \frac{2}{15c^2}\pi a_1^2 G\eta_2(288c_1 - 67c_2). \tag{6.39}
$$

Of course, c_1 and c_2 must be chosen such that this is still a positive quantity. Therefore, the 1-PN surface is well-defined and degenerates to a rod of the length given in Eq. (6.39). Moreover, all metric functions are determined in the exterior for $\bar{a}_3 \to 0$, namely $U_a^{(3)} \to 0$, $\delta U \to 0$ and for Φ_2 see Eq. (6.25a). Thus, the metric is *static* and *axially symmetric* – it is in the Weyl class.

The above considerations can be repeated for $s = \frac{5}{2}$. In this case, fewer restrictions need to be satisfied depending on how fast $\bar{a}_3 \to 0$ compared to $a_1 \to 0$. In case it converges sufficiently slow compared to a_1, the w_i are not constrained any further. Otherwise, the S_{i0} have to vanish. Since the derivation of Eq. (6.34) does not depend on a_1, the same choice yields $S_{i0} = 0$. So, Eq. (6.34) is sufficient and no condition similar to Eq. (6.38) arises. The 1-PN Dedekind ellipsoids contract to a point and are a member of the Weyl class for $a_1 \to 0$.

Finally, we show that the singularity, which forms at the axis, is a physical one and not just a coordinate singularity. The metric is static in the limit and the spatial metric is Euclidean. Therefore, we need only to insert Φ_s from Eq. (6.25a) into the Kretschmann scalar and find for $x^1 \in (-a_1, a_1)$ and $s = 2$

$$
R^{\alpha\beta\gamma\delta}R_{\alpha\beta\gamma\delta} \sim \rho^{-4}(\log\rho)^{-2}. \tag{6.40}
$$

For $x^1 \notin [-a_1, a_1]$ the Kretschmann scalar is finite.[24] For $s = \frac{5}{2}$ the Kretschmann scalar reads in spherical coordinates $r = \rho^2 + x_1^2$

$$R^{\alpha\beta\gamma\delta} R_{\alpha\beta\gamma\delta} = \frac{17}{4r^2}. \tag{6.41}$$

Thus, a singularity lies in both cases at the x^1-axis. However, to 1-PN order the x^1-axis is still elementary flat, because the spatial metric is Euclidean.

We can distinguish three different types of Weyl metrics in the limit $\bar{a}_3 \to 0$. Firstly, the 1-PN Dedekind ellipsoids approach at least formally a 1-PN approximation of the Curzon-Chazy particle for $s = \frac{5}{2}$, see [45]. The Curzon-Chazy metric depends on a "mass" parameter m. In a PN expansion of this parameter the "Newtonian" order has to vanish in order match the above solution. If this transition can be found also in higher orders remains to be seen. For this, the 2-PN order approximation is indispensable, since several qualitatively new properties emerge. For example, the x^1-axis in the Churzon-Chazy space-time is not elementary flat anymore in 2-PN order, see for a recent review [34]. Despite it form, the solution is not spherically symmetric.

In the second case, $a_1 \to \infty$ and $\bar{a}_3 \to 0$. This implies that the 1-PN Dedekind ellipsoids approach formally the 1-PN approximation of the cylindrically symmetric Levi-Civita metric. The Newtonian order of the "line mass density" σ, which parameterizes the Levi-Civita metric, has to vanish. An interpretation of this limit as the field of a constant line mass along the x^1 axis is possible (depending on η_2), because σ can be chosen to be "small" (for a detailed discussion and a definition of small in this context, see [34]). In [34], the authors give also a list of other perfect fluid sources for which the metric in the exterior coincides with the Levi-Civita metric. This means, in the limit a physical interpretation of the solution is possible.

In the last case, the sole non-trivial metric function Φ_2 describes a Newtonian potential for a non-constant line mass density, see Eqs. (6.24) and (6.25a). Of course, this is a special solution in the Weyl class.

6.9 An arbitrary coordinate volume

Hitherto, we kept the coordinate volume fixed to provide compatibility with the most part of [22, 23]. In this section, we discuss how to relax this condition. As in [20] and at the end of [22] one can introduce another Lagrangian displacement vector

$$\left(\xi^0_\mu\right) = \tilde{S}_6\left(x^1, x^2, x^3\right) \tag{6.42}$$

and sum in Eq. (6.6) over A from 1 to 6. Then it is clear that $\tilde{S}_6$ can be chosen independently of the rest of the parameters. It can be used to fix the proper volume of the configuration rather than the coordinate volume as was done at the end of [22].

This free parameter can be understood by using as "starting" Newtonian Dedekind ellipsoid not one with the major axis a_1 but with $a_1 - \epsilon^2 \pi \mu G a_1^3 \tilde{S}_6$. These two Newtonian solutions differ only by terms of the order c^{-2}. If we plug this new value in our 1-PN solution, which is depicted in Figs. 6.1 and 6.2, and expand it to the c^{-2} order, we obtain a solution where the 1-PN correction to the coordinate volume is arbitrary. The surface ansatz $S(x^i)$, the perturbation of the Newtonian

[24] For the points $x^1 = \pm a_1$, where the line density in Eq. (6.24) vanishes, a more detailed analysis is necessary. Probably other curvature scalars involving derivatives of the Riemann tensor are diverging at this point.

potential δU, and the pressure acquire additional terms denoted by a tilde:

$$\begin{aligned} \tilde{S}(x^i) &= -2\tilde{S}_6 a_1^2 \pi\mu G c^{-2}, \\ \widetilde{\delta U} &= 2(a_1\pi\mu G)^2 \tilde{S}_6 c^{-2} A_\emptyset, \\ \tilde{p} &= -2\tilde{S}_6 (a_1 a_3 \pi\mu)^2 \mu c^{-2} A_3. \end{aligned} \tag{6.43}$$

The last two alterations affect only the central pressure in the 1-PN Dedekind ellipsoid. The other parameters remain unchanged. In particular, the Newtonian velocity is independent of a_1. This is apparent if the velocity is written in dimensionless quantities. Thus, a 1-PN correction to a_1 does not contribute to the 1-PN velocity.

6.10 Concluding remarks

For higher PN orders, the analysis becomes exceedingly difficult. For an algorithmic approach, it is useful to introduce surface adapted ellipsoidal coordinates for solving the occurring Poisson equations. The ellipsoidal coordinates become necessary because the inhomogeneities of the Poisson equations do not have their support anymore in the Newtonian ellipsoid. The advantage of the surface adapted coordinates is that the perturbation of the surface is translated into an inhomogeneity in the field equations. This implies, once we determined a function to a certain PN order, say $U^{(0)}$, we do not need to calculate perturbations to these solutions in higher orders. Thus, terms like the δU do not appear.

In the presented limits, the 1-PN Dedekind ellipsoids approach either the 1-PN Maclaurin spheroids or a metric in the Weyl class. For the PN Maclaurin ellipsoids an algorithm exists that allows determining arbitrary PN order, see [56]. The solutions in the Weyl class are given explicitly, see [45]. Thus, these limits could provide the possibility to attach a sequence of new solutions – the PN Dedekind ellipsoids – at the two end points to known solutions. This provides a test for the presumably very complicated sequence. The rod-limit is interesting on its own, since transitions to well-known metrics occur, namely to the Curzon-Chazy and to the Levi-Civita metric.

SUMMARY AND CONCLUSIONS

We investigated several matter models with different degrees of symmetry in general relativity. These were massive and massless shells endowed with electromagnetic sources, axially symmetric, stationary and rigidly rotating dust configurations with a non-vanishing proper volume as well as non-axially symmetric, rotating and stationary perfect fluid solutions.

In Chapter 2, we studied relativistic spherical condensers in detail. These are spherical symmetric systems of two concentric charged massive shells with an electric field only between the shells. We employed the Israel formalism to construct the shells and interpreted them as charged perfect fluids. Afterwards, we imposed energy conditions (null, weak, dominant and strong), which set constraints on the total charges, the masses and the radii of the shells. The implications for the matter were investigated thoroughly. For instance, we showed that at least one energy condition is violated if horizons are present in the space-time. Thus, the inner shell or the entire condenser cannot be hidden below a horizon. Furthermore, we found that the interior shell can be made of dust with a positive mass density. In this case, the piece of Reissner-Nordström space-time between the shells becomes extreme. Newton-Maxwell spherical condensers corroborate this result. Additionally, an exterior shell can be found so that both shells satisfy all energy conditions. However, the exterior shell is supported by a positive pressure, i.e., it cannot be made of dust (independently of the interior shell). We also studied the behavior of the mass parameter of the respective piece of Reissner-Nordström space-times. Even in case all energy conditions are met, the mass parameter can decrease, if the exterior shell is crossed (going radially outwards). This is due to the electromagnetic field, which decreases the quasi local mass.

It is not possible to construct a dipole shell in a limiting process from a condenser even without taking the energy conditions into account. Since the charge has to diverge in such a limit, the piece of Reissner-Nordström space-time between the shells becomes singular. This is expected because the energy momentum tensor of a dipole shell is not anymore well-defined in the ordinary theory of distributions. We circumvented this problem by neglecting the back-reaction of the electromagnetic field on the geometry. In this test field approach, we generalized the Israel formalism to include shells endowed with electric or magnetic dipoles in Chapter 3. Firstly, we constructed the 4-current for a general test dipole density distributed on a shell in a general curved background. With this general source, we derived the jump conditions of the electromagnetic field and the 4-potential across such a dipole shell. These jump conditions implied the equivalence of the field outside of the shell of a magnetic dipole 4-current to a 4-current of electric charges. More precisely, we can construct to each surface current of magnetic dipoles a surface current of electric charges, which produces exactly the same field outside of the shell. The difference between these two fields manifests itself in the trajectories of charged particles crossing the shell. In Maxwell theory, this equivalence is well-known. In curved backgrounds, such general result was not yet

available, but it was proved in special instances, e.g., for point dipoles and charge current loops in the Kerr space-time, see [6]. These results are now extended to arbitrary backgrounds and arbitrary dipole shells.

We used the generalized Israel formalism to construct an axially symmetric, stationary space-time containing a massive disk (Schwarzschild disk) carrying a test charge or test electric/magnetic dipole distribution. We did this indirectly using two different test fields – the asymptotic homogeneous electric/magnetic field and the field produced by a test charge at an arbitrary position. The resulting charge and dipole distribution were corroborated by the membrane paradigm. Our general formalism can be used to study other backgrounds and test dipole distributions therein as well. We also verified the jump conditions in a direct approach: The Maxwell equations for spherical shells endowed with an arbitrary charge and dipole density were solved directly in a Schwarzschild background. The electromagnetic field and 4-potential were determined and their discontinuities across the shells calculated. The jumps were expressed in terms of the charge or dipole distribution.

In a fully relativistic approach, the Einstein-Maxwell equations have to be solved. This necessarily involves generalized distributions and Colombeau algebras. Even though the astrophysical importance of such solutions would be limited, it is, nonetheless, interesting to see, if the intuition from Maxwell theory predicts the correct results. Is the induced metric on the shell, say, continuously differentiable, and is the distributional character only reflected in the normal components of the metric? And how singular is the distributional metric, can it still be interpreted physically and in terms of ordinary functions?

In the chapters that followed, we abandoned the idealization of shells and studied matter distributions with a non-vanishing proper volume. In Chapter 4, we considered axially symmetric, stationary and rigidly rotating dust. Einstein's equation is integrable in the interior of such a matter distribution. The metric was given explicitly as a function of the largely arbitrary mass density along the axis of rotation. This was possible without any knowledge of the exterior solution. With the explicit solution in the interior and the special form of the field equations, several non-existence results were established. Firstly, there are no dust distributions for which the mass density vanishes at the surface. Secondly, there are no dust configurations with a homogeneous mass density, even though this is the sole solution in Newtonian gravity. Both can be seen as an instance of a more general result on the mass density of such dust configurations. The explicit solution of the metric in the interior allowed a series expansion of the mass density close to the axis. This was used to prove that the mass density grows always perpendicular to the axis of rotation like for the van Stockum dust cylinder, which is astrophysically questionable. The explicit solution might prove useful for further analyses. For instance, it might help answering the following questions: Do causality violating curves or geodesics exist in all dust clouds? What are the requirements in terms of the mass density at the axis and the diameter of the configuration for their existence?

Subsequently, we dropped the assumption of axially symmetry, and used a PN approximation to investigate non-axially symmetric, stationary and rotating perfect fluids. As a starting point for the PN approximation, we chose the Newtonian Dedekind ellipsoids. They are stationary in an inertial frame, but admit internal motion. We introduced them in Chapter 5 where we gave also the explicit solution of the gravitational potential in the exterior. We investigated in detail a limit in which the Newtonian Dedekind ellipsoids degenerate to a line distribution. This limit was of particular interest in the 1-PN approximation. In Chapter 6, the 1-PN field equations were solved using an ansatz for the 1-PN velocity field and the 1-PN surface. Whereas the ansatz for the surface was the same as in previous works, see [22], we used a different ansatz for the velocity field. The differences amount to allowing 1-PN corrections to the constants in the Newtonian velocity field. These two constants turned out to be free parameters of the 1-PN sequence and we used

them to generalize properties of the Newtonian Dedekind ellipsoids. For example, we showed that these two parameters can be chosen such that the 1-PN Dedekind ellipsoids approach the 1-PN Maclaurin spheroids. The absence of this bifurcation point in the previously proposed sequence in [23] raises the question if their solutions should indeed be called 1-PN Dedekind ellipsoids. Another puzzling property of the 1-PN sequence in [23] is that a singularity occurs in the parameter space, i.e., the PN approximation breaks down at a point that was not expected. The investigation of the 1-PN Maclaurin and Jacobi sequences suggested that such singularities occur at points of onsets of secular instabilities or at certain bifurcation points. The observed singularity, however, was placed on no such point. In fact, there is no such point along the Dedekind sequence. The additional degrees of freedom in our solution allowed us to remove the singularity by posing one additional constraint on the free parameters. Consequently, a PN approximation can be found along the entire sequence.

Furthermore, we studied a 1-PN approximation to the Newtonian Dedekind ellipsoids in the rod-like limit. The limiting 1-PN space-time is a member of Weyl's family of solutions, i.e., it is static and axially symmetric. A singularity emerges along the greatest principle axis of the Newtonian ellipsoid. In two special cases, transitions to 1-PN approximations of the Curzon-Chazy particle and the Levi-Civita metric are possible. The existence of this rod-like limit was ensured by further constraints on our free parameters. Taking all conditions together, our free parameters are only determined in the neighborhood of three points, namely the (removed) singularity, the 1-PN Maclaurin limit and the rod-like limit. Otherwise, they are arbitrary along the 1-PN Dedekind sequence. They can be used to adjust the surface and the velocity field, which were described in detail, too. We discussed the former qualitatively on grounds of the gravitomagnetic effect. The most notable feature of the latter is that a motion parallel to the axis of rotation is required for a consistent solution.

Both limits – the PN Maclaurin limit or the rod-like limit – can be determined to arbitrary PN order. This provides tests of higher PN orders of the Dedekind ellipsoids, because it allows to attach the new sequence of PN Dedekind ellipsoids to already known solutions. Since the solutions become exceedingly difficult in higher PN orders, this will certainly prove useful. Hitherto, we obtained the 1-PN Dedekind ellipsoids. However, whether non-axially symmetric, stationary and rotating perfect fluid solutions exist in general relativity is not shown yet. The existence of the 1-PN solution is not sufficient and higher PN orders have to be taken into account. Although in principle all orders have to be calculated and convergence has to be shown, a solution to 2-PN or 3-PN would already be a strong hint. This would allow to test the convergence at least numerically. Nevertheless, this does not ensure that higher orders indeed exist. To see this, an algorithmic approach like in [56] is necessary. The equations resulting from the Bianchi identity are the main obstacle for an analogous algorithm for the PN Dedekind ellipsoids. In the Maclaurin case, they could be integrated due to the assumption of rigid rotation. A similar definition, which would define the velocity to arbitrary PN order, is still lacking for the PN Dedekind ellipsoids. Certainly, the properties of the 1-PN Dedekind sequence that we presented in this thesis contribute to such a definition.

APPENDIX

A

INDEX SYMBOLS

The index symbols are certain integrals that appear frequently in the analysis of ellipsoidal figures of equilibrium, see, e.g., [21]. We use them in this thesis as well, and we define them in this appendix. A list of properties is given without the proofs, which are mostly straightforward. Most of these properties of the index symbols can be found in [21], or as direct consequences of the formulas given there.

A.1 Definitions

Using the abbreviations

$$z_i = u + a_i^2, \quad G(u) = \frac{\sqrt{z_1 z_2 z_3}}{a_1 a_2 a_3}, \tag{A.1}$$

the general definitions of the index symbols read as follows ($i_1, \ldots, i_k \in \{1, 2, 3\}$):

$$\begin{aligned} A_{i_1 i_2 \ldots i_k} &= \int_0^\infty [G(u) z_{i_1} z_{i_2} \cdots z_{i_k}]^{-1} \, \mathrm{d}u, \\ B_{i_1 i_2 \ldots i_k} &= \int_0^\infty \frac{u}{G(u) z_{i_1} z_{i_2} \cdots z_{i_k}} \, \mathrm{d}u, \\ C_{i_1 i_2 \ldots i_k} &= \int_0^\infty \frac{u^2}{G(u) z_{i_1} z_{i_2} \cdots z_{i_k}} \, \mathrm{d}u. \end{aligned} \tag{A.2}$$

The "index symbol without an index" is denoted by $A_\emptyset$. It is defined analogously to (A.2) by[1]:

$$A_\emptyset = \int_0^\infty [G(u)]^{-1} \, \mathrm{d}u. \tag{A.3}$$

[1] The integrals $B_\emptyset$ and $C_\emptyset$ do not converge.

A.2 Properties

In this section, we list some identities satisfied by the index symbols:

$$C_{i_1 i_2 \ldots i_k} = B_{i_2 \ldots i_k} - a_{i_1}^2 B_{i_1 i_2 \ldots i_k}, \tag{A.4a}$$

$$B_{i_1 i_2 \ldots i_k} = A_{i_2 \ldots i_k} - a_{i_1}^2 A_{i_1 i_2 \ldots i_k}, \tag{A.4b}$$

$$A_{i_1 \ldots i_k} = A_{\sigma(i_1 \ldots i_k)}, \text{ where } \sigma \text{ denotes a permutation of } k \text{ numbers}, \tag{A.4c}$$

$$A_{i_1 i_2 i_3 \ldots i_k} = -(a_{i_1}^2 - a_{i_2}^2)^{-1}(A_{i_1 i_3 \ldots i_k} - A_{i_2 i_3 \ldots i_k}), \text{ if } i_1 \neq i_2, \tag{A.4d}$$

$$A_{\emptyset} = a_1^2 A_1 + a_2^2 A_2 + a_3^2 A_3, \tag{A.4e}$$

$$A_3 = 2 - A_1 - A_2, \tag{A.4f}$$

$$A_{\underbrace{i \ldots i}_{k \text{ times}}} = \frac{1}{2k-1}\left[a_i^{2-2k} - \sum_{l=1,\, l\neq i}^{3} A_{\underbrace{i \ldots i}_{k-1 \text{ times}}\, l}\right], \tag{A.4g}$$

$$A_{i_1 i_2 \ldots i_k} = A_{j_1 i_2 \ldots i_k}, \text{ if } a_{i_1} = a_{j_1}. \tag{A.4h}$$

For $B_{i_1 \ldots i_k}$ and $C_{i_1 \ldots i_k}$, properties analogous to (A.4d)-(A.4h) hold. With the first two identities, all C's and all B's can be expressed by A's. Using (A.4c) and (A.4d), all index symbols $A_{i_1 i_2 \ldots i_k}$ with $k \geq 2$ indices of which at least two differ can be expressed by index symbols with $k-1$ indices. Index symbols for which all indices coincide can be expressed by index symbols with different indices via (A.4g). By repeated use of these identities and together with (A.4e), all index symbols are written in terms of A_1, A_2. Property (A.4h) is important for the axially symmetric limits of the Dedekind ellipsoids, which we investigate in Section 6.7.

A.3 Dimensionless index symbols

The notation is considerably shortened if we introduce the dimensionless versions of the index symbols. Since the index symbols are homogeneous in a_1, we can write

$$\begin{aligned} A_{i_1 \ldots i_k}(a_1, a_2, a_3) &= a_1^{2-2k} A_{i_1 \ldots i_k}(1, \bar{a}_2, \bar{a}_3), \\ B_{i_1 \ldots i_k}(a_1, a_2, a_3) &= a_1^{4-2k} B_{i_1 \ldots i_k}(1, \bar{a}_2, \bar{a}_3), \\ C_{i_1 \ldots i_k}(a_1, a_2, a_3) &= a_1^{6-2k} C_{i_1 \ldots i_k}(1, \bar{a}_2, \bar{a}_3). \end{aligned} \tag{A.5}$$

The axis ratios $\bar{a}_i$ are defined in (5.4). We denote the dimensionless index symbols $A_{i_1 \ldots i_k}(1, \bar{a}_2, \bar{a}_3)$, $B_{i_1 \ldots i_k}(1, \bar{a}_2, \bar{a}_3)$ and $C_{i_1 \ldots i_k}(1, \bar{a}_2, \bar{a}_3)$ by $\bar{A}_{i_1 \ldots i_k}$, $\bar{B}_{i_1 \ldots i_k}$ and $\overline{C}_{i_1 \ldots i_k}$, respectively.

A.4 Explicit formulas of the index symbols

Since all index symbols can be expressed in terms of A_1 and A_2, it is sufficient to give explicit formulas for these two only. Furthermore, $A_1 = \bar{A}_1$ and $A_2 = \bar{A}_2$ so that the index symbols read

$$\begin{aligned} \alpha &= \sqrt{1 - \bar{a}_3^2}, \quad \beta = \sqrt{\frac{\bar{a}_2^2 - 1}{\bar{a}_3^2 - 1}}, \\ \bar{A}_1 &= \frac{2\bar{a}_2\bar{a}_3}{(1-\bar{a}_2^2)\,\alpha}\left(\mathrm{F}\left(\alpha;\beta\right) - \mathrm{E}\left(\alpha;\beta\right)\right), \\ \bar{A}_2 &= \frac{2\bar{a}_3\bar{a}_2}{(1-\bar{a}_2^2)\,(\bar{a}_2^2 - \bar{a}_3^2)\,\alpha}\left(\alpha^2 \mathrm{E}\left(\alpha;\beta\right) + \left(\bar{a}_3^2 - \bar{a}_2^2\right)\mathrm{F}\left(\alpha;\beta\right) - \alpha\left(1-\bar{a}_2^2\right)\bar{a}_3\right). \end{aligned} \tag{A.6}$$

The functions $\mathrm{F}(x;m)$ and $\mathrm{E}(x;m)$ are the incomplete elliptic integrals of the first and second kind, respectively. For later convenience, we introduce here the incomplete elliptic integrals of the third kind $\Pi(n;x;m)$ as well. In order to fix the notation of these functions, which varies in the literature and in the computer algebra programs, we repeat here their definition:

$$\begin{aligned}
\mathrm{F}(x;m) &= \int_0^x \left(\left(1-t^2\right)\left(1-m^2t^2\right)\right)^{-\frac{1}{2}}\mathrm{d}t,\\
\mathrm{E}(x;m) &= \int_0^x \left(1-t^2\right)^{-\frac{1}{2}}\left(1-m^2t^2\right)^{\frac{1}{2}}\mathrm{d}t,\\
\Pi(n;x;m) &= \int_0^x \left(1-nt^2\right)^{-1}\left(\left(1-t^2\right)\left(1-m^2t^2\right)\right)^{-\frac{1}{2}}\mathrm{d}t.
\end{aligned} \tag{A.7}$$

APPENDIX

B

THE LAMÉ FUNCTIONS OF THE FIRST AND SECOND KIND

The Lamé functions of the first kind $E_m^n(x)$ and of the second kind $F_m^n(x)$ are solutions of the Lamé equation $L_m^n(x)[f] = 0$. The linear differential operator L_m^n is defined by

$$L_m^n(x) = \left(x^2 - h^2\right)\left(x^2 - k^2\right)\frac{\mathrm{d}^2}{\mathrm{d}x^2} + x\left(2x^2 - h^2 - k^2\right)\frac{\mathrm{d}}{\mathrm{d}x} + \left(K_m^n - n\left(n+1\right)x^2\right), \tag{B.1}$$

where K_m^n are the characteristic values of the Lamé functions. They are listed in Table B.2. The first few Lamé functions of the first and second kind can be found in the Table B.1 and Eq. (B.5). The Lamé functions of the first kind are always of the form[1]

$$E_m^n(x) = \left(|x^2 - h^2|\right)^{\frac{u}{2}}\left(|x^2 - k^2|\right)^{\frac{v}{2}} x^w \left(x^{n-u-w-v} + \sum_{k=0}^{\frac{n-u-w-v-2}{2}} a_{2k}x^{2k}\right), \tag{B.2}$$

$$\tilde{n} = \left\lfloor \frac{n}{2} \right\rfloor, \quad w = \begin{cases} 0: & n \text{ is even} \\ 1: & n \text{ is odd.} \end{cases}$$

The Lamé functions are divided into four species according to the values of (u, v):

$$(u,v) = \begin{cases} (0,0): & 1 \le m \le \tilde{n}+1, & \text{(first species)} \\ (1,0): & \tilde{n}+2 \le m \le n+1, & \text{(second species)} \\ (0,1): & n+2 \le m \le 2n-\tilde{n}, & \text{(third species)} \\ (1,1): & 2n+1-\tilde{n} \le m \le 2n+1. & \text{(fourth species)} \end{cases} \tag{B.3}$$

Note that in the normalization used here the coefficient in front of the highest power is always 1.

The Lamé functions of the second kind are constructed from the Lamé functions of the first kind via

$$F_m^n(x) = E_m^n(x)\int_x^\infty \left(E_m^n(u)\right)^{-2}\left(\left(u^2 - h^2\right)\left(u^2 - k^2\right)\right)^{-\frac{1}{2}}\mathrm{d}u. \tag{B.4}$$

[1]The floor function $\lfloor\cdot\rfloor$ maps a real number x to the greatest integer not greater than x.

Note that sometimes this definition includes an additional factor $2n+1$. These rational integrals can – at least theoretically – always be reduced to incomplete elliptic integrals, which are given in Eq. (A.7). In the 1-PN approximation of the Dedekind ellipsoids we need the Lamé functions of the second kind only to orders where this can be done explicitly. The first few members are given in the list (B.5).

Because of the dependence of the Lamé operator (B.1) on h and k and the ansatz of the Lamé functions (B.2) the following symmetry is apparent: If $K_m^n(h,k)$ is the characteristic value of a Lamé function of the second species E_m^n, then $K_m^n(k,h)$ is the characteristic value of the Lamé function of the third species $E_{\widetilde{m}}^n$ with $\widetilde{m} = m + \left\lfloor \frac{n+1}{2} \right\rfloor$. The latter Lamé function is obtained from the former also by an exchange of h and k. Thus, we do not give the third species quantities explicitly.

As is obvious from the coordinate transformation (5.21), functions that are even in x^2 and x^3 exhibit in their series expansions in ellipsoidal surface harmonics $E_m^n(\lambda^2)E_m^n(\lambda^3)$ only Lamé functions of the first species. In the expansion of functions that are odd in x^2 and even in x^3 occur only Lamé functions of the second species, etc.

n	$E_m^n(x)$
The first species	
0	1
1	x
2	$x^2 + \frac{1}{6}\left(K_m^2 - 4h^2 - 4k^2\right)$
3	$x^3 + \frac{1}{10}\left(K_m^3 - 9h^2 - 9k^2\right)x$
4	$x^4 + \frac{1}{14}\left(K_m^4 - 16\left(h^2+k^2\right)\right)x^2 + \frac{1}{280}\left(\left(K_m^4\right)^2 - 20K_m^4\left(h^2+k^2\right) + 8\left(8h^4 + 37h^2k^2 + 8k^4\right)\right)$
The second species	
1	$\sqrt{\lvert x^2-h^2\rvert}$
2	$\sqrt{\lvert x^2-h^2\rvert}x$
3	$\sqrt{\lvert x^2-h^2\rvert}\left(x^2 + \frac{1}{10}\left(K_m^3 - 4h^2 - 9k^2\right)\right)$
4	$\sqrt{\lvert x^2-h^2\rvert}\left(x^3 + \frac{1}{14}\left(K_m^4 - 9h^2 - 16k^2\right)x\right)$
The fourth species	
2	$\sqrt{\lvert x^2-h^2\rvert}\sqrt{\lvert x^2-k^2\rvert}$
3	$\sqrt{\lvert x^2-h^2\rvert}\sqrt{\lvert x^2-k^2\rvert}x$
4	$\sqrt{\lvert x^2-h^2\rvert}\sqrt{\lvert x^2-k^2\rvert}\left(\frac{1}{14}\left(K_m^4 - 9\left(h^2+k^2\right)\right) + x^2\right)$

Table B.1: The Lamé functions of the first kind

n	m	K_m^n
0	1	0
1	1	h^2+k^2
1	2	k^2
2	1	$2\left(h^2+k^2-\sqrt{h^4-h^2k^2+k^4}\right)$
2	2	$2\left(h^2+k^2+\sqrt{h^4-h^2k^2+k^4}\right)$
2	3	h^2+4k^2
2	5	h^2+k^2
3	1	$5h^2+5k^2-2\sqrt{4h^4-7h^2k^2+4k^4}$
3	2	$5h^2+5k^2+2\sqrt{4h^4-7h^2k^2+4k^4}$
3	3	$2h^2+5k^2-2\sqrt{h^4-h^2k^2+4k^4}$
3	4	$2h^2+5k^2+2\sqrt{h^4-h^2k^2+4k^4}$
3	7	$4\left(h^2+k^2\right)$
4	1	$-\frac{2}{3}2^{2/3}D_1+\frac{20}{3}\left(h^2+k^2\right)+\frac{-208h^4+208h^2k^2-208k^4}{6\,2^{2/3}D_1}$
4	2	$\frac{1}{3}2^{2/3}\left(1-\mathrm{i}\sqrt{3}\right)D_1+\frac{20}{3}\left(h^2+k^2\right)-\frac{\left(1+\mathrm{i}\sqrt{3}\right)\left(-208h^4+208h^2k^2-208k^4\right)}{12\,2^{2/3}D_1}$
4	3	$\frac{1}{3}2^{2/3}\left(1+\mathrm{i}\sqrt{3}\right)D_1+\frac{20}{3}\left(h^2+k^2\right)-\frac{\left(1-\mathrm{i}\sqrt{3}\right)\left(-208h^4+208h^2k^2-208k^4\right)}{12\,2^{2/3}D_1}$
4	4	$5h^2+10k^2-2\sqrt{4h^4-9h^2k^2+9k^4}$
4	5	$5h^2+10k^2+2\sqrt{4h^4-9h^2k^2+9k^4}$
4	8	$5h^2+5k^2-2\sqrt{4h^4+h^2k^2+4k^4}$
4	9	$5h^2+5k^2+2\sqrt{4h^4+h^2k^2+4k^4}$

$$D_1=\left(-35\left(2h^6-3h^4k^2-3h^2k^4+2k^6\right)+\sqrt{27}\sqrt{D_2}\right)^{\frac{1}{3}}$$
$$D_2=-144h^{12}+432h^{10}k^2-2089h^8k^4+3458h^6k^6-2089h^4k^8+432h^2k^{10}-144k^{12}$$

Table B.2: The characteristic values

For brevity, we use λ rather than λ^1 in the remainder of this appendix. The Lamé functions of the second kind and the first species are

$$\begin{aligned}
F_m^0(\lambda)&=\tfrac{1}{k}\mathrm{F}\left(\tfrac{k}{\lambda};\tfrac{h}{k}\right),\\
F_m^1(\lambda)&=\tfrac{\lambda}{h^2k}\left(\mathrm{F}\left(\tfrac{k}{\lambda};\tfrac{h}{k}\right)-\mathrm{E}\left(\tfrac{k}{\lambda};\tfrac{h}{k}\right)\right),\\
F_m^2(\lambda)&=\frac{\sqrt{\left(\lambda^2-h^2\right)\left(\lambda^2-k^2\right)}}{2\lambda\left(\Lambda_{m,0}^2+h^2\right)\left(\Lambda_{m,0}^2+k^2\right)}+\frac{k\mathrm{E}\left(\frac{k}{\lambda};\frac{h}{k}\right)E_m^2(\lambda)}{2\Lambda_{m,0}^2\left(\Lambda_{m,0}^2+h^2\right)\left(\Lambda_{m,0}^2+k^2\right)}-\\
&\quad\frac{E_m^2(\lambda)\left(2\left(h^2+k^2\right)\Lambda_{m,0}^2+3\left(\Lambda_{m,0}^2\right)^2+h^2k^2\right)\Pi\left(-\frac{\Lambda_{m,0}^2}{k^2};\frac{k}{\lambda};\frac{h}{k}\right)}{2k\left(\Lambda_{m,0}^2\right)^2\left(\Lambda_{m,0}^2+h^2\right)\left(\Lambda_{m,0}^2+k^2\right)}+\\
&\quad\frac{\mathrm{F}\left(\frac{k}{\lambda};\frac{h}{k}\right)\left(2\Lambda_{m,0}^2+k^2\right)E_m^2(\lambda)}{2k\left(\Lambda_{m,0}^2\right)^2\left(\Lambda_{m,0}^2+k^2\right)},
\end{aligned}\tag{B.5a}$$

$$
\begin{aligned}
F_m^3(\lambda) = {} & \frac{\mathrm{F}\left(\frac{k}{\lambda};\frac{h}{k}\right) E_m^3(\lambda)\left(2\Lambda_{m,1}^3\left(\Lambda_{m,1}^3 - 2h^2 + k^2\right) - 3h^2k^2\right)}{2h^2k\left(\Lambda_{m,1}^3\right)^3\left(\Lambda_{m,1}^3 + k^2\right)} - \\
& \frac{\mathrm{E}\left(\frac{k}{\lambda};\frac{h}{k}\right) E_m^3(\lambda)\left(2\Lambda_{m,1}^3\left(\Lambda_{m,1}^3 + h^2 + k^2\right) + 3h^2k^2\right)}{2h^2k\left(\Lambda_{m,1}^3\right)^2\left(\Lambda_{m,1}^3 + h^2\right)\left(\Lambda_{m,1}^3 + k^2\right)} - \frac{\sqrt{\left(h^2-\lambda^2\right)\left(k^2-\lambda^2\right)}}{2\Lambda_{m,1}^3\left(\Lambda_{m,1}^3 + h^2\right)\left(\Lambda_{m,1}^3 + k^2\right)} + \\
& \frac{E_m^3(\lambda)\left(4\left(h^2+k^2\right)\Lambda_{m,1}^3 + 5\left(\Lambda_{m,1}^3\right)^2 + 3h^2k^2\right)\Pi\left(-\frac{\Lambda_{m,1}^3}{k^2};\frac{k}{\lambda};\frac{h}{k}\right)}{2k\left(\Lambda_{m,1}^3\right)^3\left(\Lambda_{m,1}^3 + h^2\right)\left(\Lambda_{m,1}^3 + k^2\right)}, \\
F_m^4(\lambda) = {} & \left(2\lambda k\left(R_{m,-}^4\right)^2\left(R_{m,+}^4\right)^2\left(h^2 - R_{m,-}^4\right)\left(k^2 - R_{m,-}^4\right)\left(h^2 - R_{m,+}^4\right)\left(k^2 - R_{m,+}^4\right)\times\right. \\
& \left.\left(R_{m,-}^4 - R_{m,+}^4\right)^3\right)^{-1}\left(k^2\lambda E_m^4(\lambda)R_{m,-}^4R_{m,+}^4\mathrm{E}\left(\frac{k}{\lambda};\frac{h}{k}\right)\left(R_{m,-}^4 - R_{m,+}^4\right)\left(\left(h^2+k^2\right)\times\right.\right. \\
& \left.\left(R_{m,-}^4\right)^2 - h^2k^2R_{m,-}^4 - \left(R_{m,-}^4\right)^3 + R_{m,+}^4\left(h^2 - R_{m,+}^4\right)\left(R_{m,+}^4 - k^2\right)\right) - \lambda E_m^4(\lambda)\times \\
& \left(R_{m,+}^4\right)^2\left(h^2 - R_{m,+}^4\right)\left(k^2 - R_{m,+}^4\right)\left(-3\left(R_{m,-}^4\right)^2\left(R_{m,+}^4 + 2\left(h^2+k^2\right)\right) + R_{m,-}^4\times\right. \\
& \left.\left(2\left(h^2+k^2\right)R_{m,+}^4 + 5h^2k^2\right) + 7\left(R_{m,-}^4\right)^3 - h^2k^2R_{m,+}^4\right)\Pi\left(\frac{R_{m,-}^4}{k^2};\frac{k}{\lambda};\frac{h}{k}\right) + \lambda E_m^4(\lambda)\times \\
& \left(R_{m,-}^4\right)^2\left(h^2 - R_{m,-}^4\right)\left(R_{m,-}^4 - k^2\right)\left(R_{m,-}^4\left(-2\left(h^2+k^2\right)R_{m,+}^4 + 3\left(R_{m,+}^4\right)^2 + h^2k^2\right) + \right. \\
& \left.R_{m,+}^4\left(6\left(h^2+k^2\right)R_{m,+}^4 - 7\left(R_{m,+}^4\right)^2 - 5h^2k^2\right)\right)\Pi\left(\frac{R_{m,+}^4}{k^2};\frac{k}{\lambda};\frac{h}{k}\right) + \lambda E_m^4(\lambda)\mathrm{F}\left(\frac{k}{\lambda};\frac{h}{k}\right)\times \\
& \left(h^2 - R_{m,-}^4\right)\left(h^2 - R_{m,+}^4\right)\left(R_{m,-}^4 - R_{m,+}^4\right)\left(\left(R_{m,-}^4\right)^3\left(-\left(k^2 - 2R_{m,+}^4\right)\right) + \left(R_{m,-}^4\right)^2\times\right. \\
& \left.\left(2k^2R_{m,+}^4 - 4\left(R_{m,+}^4\right)^2 + k^4\right) + 2R_{m,-}^4R_{m,+}^4\left(k^2R_{m,+}^4 + \left(R_{m,+}^4\right)^2 - 2k^4\right) + k^2\left(R_{m,+}^4\right)^2\times\right. \\
& \left.\left(k^2 - R_{m,+}^4\right)\right) + k\sqrt{\left(h^2-\lambda^2\right)\left(k^2-\lambda^2\right)}\left(R_{m,-}^4\right)^2\left(R_{m,+}^4\right)^2\left(R_{m,-}^4 - R_{m,+}^4\right)\times \\
& \left(\left(h^2+k^2+\lambda^2\right)\left(R_{m,-}^4\right)^2 - \left(h^2\left(k^2+\lambda^2\right) + k^2\lambda^2\right)R_{m,-}^4 - \left(R_{m,-}^4\right)^3 + \left(h^2+k^2+\lambda^2\right)\times\right. \\
& \left.\left(R_{m,+}^4\right)^2 - \left(h^2\left(k^2+\lambda^2\right) + k^2\lambda^2\right)R_{m,+}^4 - \left(R_{m,+}^4\right)^3 + 2h^2k^2\lambda^2\right).
\end{aligned}
$$

The constants $\Lambda_{m,i}^n$ are the coefficients of the powers of λ in the Lamé polynomial $E_m^n(\lambda)$. The reader finds them in Tab. B.1. The roots of the Lamé polynomial $E_m^4(\lambda)$ of the first species are denoted by $R_{m;\pm}^4 = \frac{1}{2}\left(-\Lambda_{m,2}^4 \pm \sqrt{\left(\Lambda_{m,2}^4\right)^2 - 4\Lambda_{m,0}^4}\right)$. The Lamé functions of the second kind and of the second species are given by

$$
\begin{aligned}
F_m^1(\lambda) = {} & \frac{\sqrt{\lambda^2-k^2}}{\left(h^2-k^2\right)\lambda} + \frac{kE_m^1(\lambda)\mathrm{E}\left(\frac{k}{\lambda};\frac{h}{k}\right)}{h^2\left(k^2-h^2\right)} - \frac{E_m^1(\lambda)\mathrm{F}\left(\frac{k}{\lambda};\frac{h}{k}\right)}{h^2k}, \\
F_m^2(\lambda) = {} & \frac{\sqrt{\lambda^2-k^2}}{h^4-h^2k^2} + \frac{\left(h^2-2k^2\right)E_m^2(\lambda)\mathrm{E}\left(\frac{k}{\lambda};\frac{h}{k}\right)}{h^4k\left(h^2-k^2\right)} - \frac{2E_m^2(\lambda)\mathrm{F}\left(\frac{k}{\lambda};\frac{h}{k}\right)}{h^4k}, \\
F_m^3(\lambda) = {} & -\frac{E_m^3(\lambda)F\left(\frac{k}{\lambda};\frac{h}{k}\right)\left(2\left(h^2+k^2\right)\Lambda_{m,1}^3 + 2\left(\Lambda_{m,1}^3\right)^2 + h^2k^2\right)}{2h^2k\left(\Lambda_{m,1}^3\right)^2\left(\Lambda_{m,1}^3 + h^2\right)\left(\Lambda_{m,1}^3 + k^2\right)} + \\
& \frac{E_m^3(\lambda)\left(2\left(h^2+2k^2\right)\Lambda_{m,1}^3 + 5\left(\Lambda_{m,1}^3\right)^2 + h^2k^2\right)\Pi\left(-\frac{\Lambda_{m,1}^3}{k^2};\frac{k}{\lambda};\frac{h}{k}\right)}{2k\left(\Lambda_{m,1}^3\right)^2\left(\Lambda_{m,1}^3 + h^2\right)^2\left(\Lambda_{m,1}^3 + k^2\right)} - \\
& \frac{kE_m^3(\lambda)\mathrm{E}\left(\frac{k}{\lambda};\frac{h}{k}\right)\left(2k^2\Lambda_{m,1}^3 + 2\left(\Lambda_{m,1}^3\right)^2 + h^4 - h^2k^2\right)}{2h^2\left(h^2-k^2\right)\Lambda_{m,1}^3\left(\Lambda_{m,1}^3 + h^2\right)^2\left(\Lambda_{m,1}^3 + k^2\right)} +
\end{aligned}
\tag{B.5b}
$$

$$\frac{\sqrt{\lambda^2-k^2}\left(2\left(k^2+\lambda^2\right)\Lambda_{m,1}^3+2\left(\Lambda_{m,1}^3\right)^2+h^4-h^2\left(k^2+\lambda^2\right)+3k^2\lambda^2\right)}{2\lambda\left(h^2-k^2\right)\left(\Lambda_{m,1}^3+h^2\right)^2\left(\Lambda_{m,1}^3+k^2\right)},$$

$$F_m^4(\lambda)=-\frac{E_m^4(\lambda)\left(\left(4h^2+6k^2\right)\Lambda_{m,1}^4+7\left(\Lambda_{m,1}^4\right)^2+3h^2k^2\right)\Pi\left(-\frac{\Lambda_{m,1}^4}{k^2};\frac{k}{\lambda};\frac{h}{k}\right)}{2k\left(\Lambda_{m,1}^4\right)^3\left(\Lambda_{m,1}^4+h^2\right)^2\left(\Lambda_{m,1}^4+k^2\right)}+$$

$$\frac{E_m^4(\lambda)\mathrm{F}\left(\frac{k}{\lambda};\frac{h}{k}\right)\left(4h^4\Lambda_{m,1}^4-4k^2\left(\Lambda_{m,1}^4\right)^2-4\left(\Lambda_{m,1}^4\right)^3+3h^4k^2\right)}{2h^4k\left(\Lambda_{m,1}^4\right)^3\left(\Lambda_{m,1}^4+h^2\right)\left(\Lambda_{m,1}^4+k^2\right)}+$$

$$\frac{E_m^4(\lambda)\mathrm{E}\left(\frac{k}{\lambda};\frac{h}{k}\right)}{2h^4k\left(h^2-k^2\right)\left(\Lambda_{m,1}^4\right)^2\left(\Lambda_{m,1}^4+h^2\right)^2\left(\Lambda_{m,1}^4+k^2\right)}\left(\left(2\left(h^2-2k^2\right)\left(\Lambda_{m,1}^4\right)^3+\right.\right.$$

$$\left.\left(4h^4-2h^2k^2-4k^4\right)\left(\Lambda_{m,1}^4\right)^2+2\left(h^6+h^4k^2-2h^2k^4\right)\Lambda_{m,1}^4+3h^4k^2\left(h^2-k^2\right)\right))+$$

$$\frac{\sqrt{\lambda^2-k^2}\left(2\left(k^2+\lambda^2\right)\left(\Lambda_{m,1}^4\right)^2+2k^2\lambda^2\Lambda_{m,1}^4+2\left(\Lambda_{m,1}^4\right)^3-h^2\left(h^2-k^2\right)\left(h^2-\lambda^2\right)\right)}{2h^2\left(h^2-k^2\right)\Lambda_{m,1}^4\left(\Lambda_{m,1}^4+h^2\right)^2\left(\Lambda_{m,1}^4+k^2\right)}.$$

The first members of the fourth species read

$$F_m^2(\lambda)=-\frac{h^2+k^2-2\lambda^2}{\lambda\left(h^2-k^2\right)^2}-\frac{E_1^2(\lambda)\mathrm{F}\left(\frac{k}{\lambda};\frac{h}{k}\right)}{h^2k(h^2-k^2)}-\frac{\left(h^2+k^2\right)E_m^2(\lambda)\mathrm{E}\left(\frac{k}{\lambda};\frac{h}{k}\right)}{kh\left(h^2-k^2\right)^2},$$

$$F_m^3(\lambda)=\frac{E_m^3(\lambda)\left(h^2-2k^2\right)\mathrm{F}\left(\frac{k}{\lambda};\frac{h}{k}\right)}{h^4k^3\left(h^2-k^2\right)}-\frac{2E_m^3(\lambda)\left(h^4-h^2k^2+k^4\right)\mathrm{E}\left(\frac{k}{\lambda};\frac{h}{k}\right)}{h^4k^3\left(h^2-k^2\right)^2}+$$

$$\frac{-h^4+h^2\lambda^2-k^4+k^2\lambda^2}{h^2k^2\left(h^2-k^2\right)^2},$$

$$F_m^4(\lambda)=-\frac{E_m^4(\lambda)\left(4\left(h^2+k^2\right)\Lambda_{m,0}^4+7\left(\Lambda_{m,0}^4\right)^2+h^2k^2\right)\Pi\left(-\frac{\Lambda_{m,0}^4}{k^2};\frac{k}{\lambda};\frac{h}{k}\right)}{2k\left(\Lambda_{m,0}^4\right)^2\left(\Lambda_{m,0}^4+h^2\right)^2\left(\Lambda_{m,0}^4+k^2\right)^2}+$$

$$\frac{E_m^4(\lambda)\mathrm{F}\left(\frac{k}{\lambda};\frac{h}{k}\right)}{2h^2k\left(h^2-k^2\right)\left(\Lambda_{m,0}^4\right)^2\left(\Lambda_{m,0}^4+h^2\right)\left(\Lambda_{m,0}^4+k^2\right)^2}\left(2\left(h^2-2k^2\right)\left(\Lambda_{m,0}^4\right)^2+\right.$$

$$\left(4h^4-2h^2k^2-2k^4\right)\Lambda_{m,0}^4-2\left(\Lambda_{m,0}^4\right)^3+h^2k^2\left(h^2-k^2\right))+$$

$$\frac{E_m^4(\lambda)\mathrm{E}\left(\frac{k}{\lambda};\frac{h}{k}\right)}{2h^2k\left(h^2-k^2\right)^2\Lambda_{m,0}^4\left(\Lambda_{m,0}^4+h^2\right)^2\left(\Lambda_{m,0}^4+k^2\right)^2}\left(-2\left(h^6+k^6\right)\Lambda_{m,0}^4-\right.$$

$$4\left(h^4+k^4\right)\left(\Lambda_{m,0}^4\right)^2-2\left(h^2+k^2\right)\left(\Lambda_{m,0}^4\right)^3+h^2k^2\left(h^2-k^2\right)^2\Big)+$$

$$\frac{-2}{2\lambda\left(h^2-k^2\right)^2\left(\Lambda_{m,0}^4+h^2\right)^2\left(\Lambda_{m,0}^4+k^2\right)^2}\left(\left(h^2+k^2-2\lambda^2\right)\left(\Lambda_{m,0}^4\right)^3+\left(-4h^4+\right.\right.$$

$$2h^2\lambda^2-4k^4+4\lambda^4+2k^2\lambda^2\left)\left(\Lambda_{4,0}^m\right)^2-2\left(h^6+h^4\lambda^2-2h^2\lambda^4+k^6+k^4\lambda^2-\right.\right.$$

$$\left.2k^2\lambda^4\right)\Lambda_{m,0}^4+h^6\left(k^2-3\lambda^2\right)+h^4\left(-2k^4+3\lambda^4+\lambda^2k^2\right)+h^2\left(k^6+\lambda^2k^4-\right.$$

$$\left.\left.2\lambda^4k^2\right)-3k^6\lambda^2+3k^4\lambda^4\right). \tag{B.5c}$$

Note that the coefficients in front of the elliptic functions are proportional to Lamé functions.

APPENDIX

C

HIGHER ORDER MOMENTS

The higher order moments $D_{i_1 i_2 \ldots i_k}$ are defined as solutions, which vanish at infinity, to the following Poisson equation:

$$\Delta D_{i_1 i_2 \ldots i_k} = -4\pi G \mu x^{i_1} x^{i_2} \cdots x^{i_k}. \tag{C.1}$$

The support of the homogeneous mass density μ is an ellipsoid. The interior solutions for the higher order moments were obtained in [29] and used in [21]. These solutions are continuously differentiable across the surface of the ellipsoid. We need only the higher order moments $D_{i_1 i_2 \ldots i_k}$ with $k \leq 3$. The interior solution to these higher order moments are repeated here, cf. [21]:

$$\begin{aligned}
D_i =& \pi G \mu a_i^2 x^i \left(A_i - \sum_{l=1}^{3} A_{il} \left(x^l\right)^2 \right), \\
D_{ij} =& \pi G \mu a_i^2 \left(a_j^2 \left(A_{ij} - \sum_{l=1}^{3} A_{ijl} \left(x^l\right)^2 \right) x^i x^j + \frac{1}{4} \delta_{ij} \left(B_i - 2 \sum_{l=1}^{3} B_{il} \left(x^l\right)^2 + \right. \right. \\
& \left. \left. \sum_{l=1}^{3} \sum_{k=1}^{3} B_{ilk} \left(x^l\right)^2 \left(x^k\right)^2 \right) \right), \\
D_{ijk} =& \pi G \mu a_i^2 a_j^2 a_k^2 \left(A_{ijk} - \sum_{l=1}^{3} A_{ijkl} \left(x^l\right)^2 \right) x^i x^j x^k + \frac{1}{4} \left(V_{ijk} + V_{jki} + V_{kij} \right), \\
V_{ijk} =& a_i^2 a_j^2 \delta_{jk} \left(B_{ij} - \sum_{l=1}^{3} \left(2B_{ijl} - \sum_{m=1}^{3} B_{ijlm} \left(x^m\right)^2 \right) \left(x^l\right)^2 \right) x^i.
\end{aligned} \tag{C.2}$$

To find the exterior solution in a closed form for these potentials, they have to be transformed to ellipsoidal coordinates. Afterwards, the higher order moments have to be expanded in ellipsoidal surface harmonics $E_m^n(\lambda^2) E_m^n(\lambda^3)$, cf. Section 5.3.2. Since the calculations are straightforward but tedious, we give here only the expansion coefficients $f_{ij\ldots,m}^n(a_1)$ for the moments $D_{ij\ldots}$. The constants for $f_{3,m}^n$ follow from $f_{2,\widetilde{m}}^n$ with $\widetilde{m} = m + \left\lfloor \frac{n+1}{2} \right\rfloor$ by exchanging[1] h with k or, analogously,

[1] This includes the index symbols where the index 2 will be replaced by 3, and the characteristic values, cf. the remark after Eq. (B.4).

$a_2 \leftrightarrow a_3$; for instance,[2] $f^3_{3,5}(h,k) = -f^3_{2,3}(k,h)$. The non-vanishing constants for the first order moments are:

$$\begin{aligned}
f^1_{1,1}(a_1) =& \frac{\pi G\mu a_1^3}{100h^3k^3\left(h^2-k^2\right)}\left(100h^2k^2A_1\left(h^2-k^2\right)-a_1^2A_{11}\left(h^2-k^2\right)\left(9h^2+9k^2-K_1^3\right)\times\right.\\
&\left(9h^2+9k^2-K_2^3\right)-k^2A_{12}\left(a_1^2-h^2\right)\left(h^2-9k^2+K_1^3\right)\left(h^2-9k^2+K_2^3\right)+\\
&\left.h^2A_{13}\left(a_1^2-k^2\right)\left(-9h^2+k^2+K_1^3\right)\left(-9h^2+k^2+K_2^3\right)\right),\\
f^3_{1,1}(a_1) =& \frac{\pi G\mu a_1^3}{h^3k^3\left(K_1^3-K_2^3\right)\left(h^2-k^2\right)}\left(-a_1^2A_{11}\left(h^2-k^2\right)\left(9h^2+9k^2-K_2^3\right)+k^2A_{12}\left(a_1^2-h^2\right)\times\right.\\
&\left.\left(h^2-9k^2+K_2^3\right)+h^2A_{13}\left(a_1^2-k^2\right)\left(9h^2-k^2-K_2^3\right)\right)=f^3_{1,1}(a_1)[K_1^3,K_2^3],\\
f^3_{1,2}(a_1) =& f^3_{1,1}(a_1)[K_2^3,K_1^3],\\
f^1_{2,2}(a_1) =& \frac{\pi G\mu\left(a_1^2-h^2\right)^{\frac{3}{2}}}{100h^3k^2\left(\left|k^2-h^2\right|\right)^{\frac{3}{2}}}\left(a_1^2A_{12}\left(h^2-k^2\right)\left(4h^2+9k^2-K_3^3\right)\left(4h^2+9k^2-K_4^3\right)\right.\\
&-100h^2k^2A_2\left(h^2-k^2\right)+k^2A_{22}\left(a_1^2-h^2\right)\left(6h^2-9k^2+K_3^3\right)\left(6h^2-9k^2+K_4^3\right)\\
&\left.-h^2A_{23}\left(a_1^2-k^2\right)\left(4h^2-k^2-K_3^3\right)\left(4h^2-k^2-K_4^3\right)\right),\\
f^3_{2,3}(a_1) =& \frac{\pi G\mu\left(a_1^2-h^2\right)^{\frac{3}{2}}}{h^3k^2\left(K_3^3-K_4^3\right)\left(\left|k^2-h^2\right|\right)^{\frac{3}{2}}}\left(a_1^2A_{12}\left(h^2-k^2\right)\left(4h^2+9k^2-K_4^3\right)-k^2A_{22}\left(a_1^2-h^2\right)\times\right.\\
&\left.\left(6h^2-9k^2+K_4^3\right)-h^2A_{23}\left(a_1^2-k^2\right)\left(4h^2-k^2-K_4^3\right)\right)=f^3_{2,3}(a_1)[K_3^3,K_4^3],\\
f^3_{2,4}(a_1) =& f^3_{2,3}(a_1)[K_4^3,K_3^3].
\end{aligned} \tag{C.3a}$$

We need only the exterior solution of the "diagonal" moments of the second order, i.e., D_{11}, D_{22} and D_{33}. The characteristic values of a Lamé function of fixed degree n and of a fixed species are the roots of the same characteristic polynomials. Hence, they satisfy the following identities, which simplify the results greatly:

$$\begin{aligned}
K_1^2+K_2^2=4(h^2+k^2),\quad K_1^2K_2^2=12h^2k^2,\quad K_1^4+K_2^4+K_3^4=20(h^2+k^2),\\
\left(K_1^4\right)^2+\left(K_2^4\right)^2+\left(K_3^4\right)^2=272h^4+128h^2k^2+272k^4,\\
K_1^4K_2^4+K_1^4K_3^4+K_2^4K_3^4=64h^4+336h^2k^2+64k^4.
\end{aligned} \tag{C.3b}$$

The constants for D_{11} read:

$$\begin{aligned}
f^0_{11,1}(a_1) =& \frac{2}{15}\pi G\mu a_1^2\left(k^2A_1-A_2\left(h^2-k^2\right)+2\left(a_1^2-k^2\right)\right),\\
f^2_{11,1}(a_1) =& \frac{\pi a_1^2G\mu}{14h^4k^4\left(h^2-k^2\right)\sqrt{h^4-h^2k^2+k^4}}\left(A_1\left(a_1^4\left(-4h^6+3h^4k^2+2k^6\right)+\right.\right.\\
&\sqrt{h^4-h^2k^2+k^4}\left(a_1^4\left(4h^4-h^2k^2-2k^4\right)+a_1^2\left(3h^2k^4-6h^4k^2\right)+2h^4k^4\right)+\\
&a_1^2\left(6h^6k^2-6h^4k^4-3h^2k^6\right)-2h^6k^4+4h^4k^6\Big)+A_2\left(3a_1^2h^2k^2\left(h^4-4h^2k^2+k^4\right)+\right.\\
&\sqrt{h^4-h^2k^2+k^4}\left(-3a_1^2h^2k^2\left(h^2+k^2\right)+2a_1^4\left(h^4-h^2k^2+k^4\right)+4h^4k^4\right)+\\
&a_1^4\left(-2h^6+3h^4k^2+3h^2k^4-2k^6\right)+2h^4k^4\left(h^2+k^2\right)\Big)-2h^2\left(k^2-a_1^2\right)\times\\
&\left.\sqrt{h^4-h^2k^2+k^4}\left(a_1^2\left(k^2-2h^2\right)+2h^2k^2\right)+2h^2\left(a_1^2-k^2\right)\left(a_1^2\left(2h^4-2h^2k^2-k^4\right)\right.\right.
\end{aligned} \tag{C.3c}$$

[2]The minus sign is a result of the absolute value taken in Eq. (C.3a).

$$
\begin{aligned}
&-2h^4k^2+4h^2k^4\big)\big)\,,\\
f^4_{11,1}(a_1)=&\frac{\pi a_1^2G\mu}{4h^4k^4\left(K_1^4-K_2^4\right)\left(K_1^4-K_3^4\right)\left(k^2-h^2\right)^2}\left(4a_1^6A_{111}(h-k)^2(h+k)^2\left(64h^4-8h^2\times\right.\right.\\
&\left(3k^2+2K_1^4\right)-\left(16k^2-K_2^4\right)\left(16k^2-K_3^4\right)\big)-a_1^4B_{111}(h-k)^2(h+k)^2\left(64h^4-8h^2\times\right.\\
&\left(3k^2+2K_1^4\right)-\left(16k^2-K_2^4\right)\left(16k^2-K_3^4\right)\big)+4a_1^4k^2A_{112}\left(a_1^2-h^2\right)\left(h^2-k^2\right)\left(64h^4-\right.\\
&2h^2\left(12k^2+K_1^4\right)-\left(16k^2-K_2^4\right)\left(16k^2-K_3^4\right)\big)+2a_1^2k^2B_{112}\left(h^2-a_1^2\right)\left(h^2-k^2\right)\times\\
&\left(64h^4-2h^2\left(12k^2+K_1^4\right)-\left(16k^2-K_2^4\right)\left(16k^2-K_3^4\right)\right)+4a_1^4h^2A_{113}\left(a_1^2-k^2\right)\times\\
&\left(h^2-k^2\right)\left(h^2\left(40k^2-4K_1^4\right)+K_1^4\left(K_1^4-18k^2\right)\right)+2a_1^2h^2B_{113}\left(k^2-a_1^2\right)\times\\
&\left(h^2-k^2\right)\left(h^2\left(40k^2-4K_1^4\right)+K_1^4\left(K_1^4-18k^2\right)\right)+k^4B_{122}\left(a_1-h\right)^2\left(a_1+h\right)^2\times\\
&\left(216h^4+12h^2\left(2k^2-K_1^4\right)+\left(16k^2-K_2^4\right)\left(16k^2-K_3^4\right)\right)+2h^2k^2B_{123}\left(h^2-a_1^2\right)\times\\
&\left(a_1^2-k^2\right)\left(2h^2\left(160k^2-9K_1^4\right)+K_1^4\left(K_1^4-18k^2\right)\right)+h^4B_{133}\left(a_1-k\right)^2\left(a_1+k\right)^2\times\\
&\left.\left(h^2\left(40k^2-4K_1^4\right)+280k^4-32k^2K_1^4+\left(K_1^4\right)^2\right)\right)=f^4_{11,1}(a_1)[K_1^4,K_2^4,K_3^4],\\
f^4_{11,2}(a_1)=&f^4_{11,1}(a_1)[K_2^4,K_1^4,K_3^4],\\
f^4_{11,3}(a_1)=&f^4_{11,1}(a_1)[K_3^4,K_2^4,K_1^4].
\end{aligned}
$$

The components $f^2_{ii,2}(a_1)$ follow from $f^2_{ii,1}(a_1)$ by a substitution of the square root $\sqrt{h^4-h^2k^2+k^4}$ in Eq. (C.3c) with its negative $-\sqrt{h^4-h^2k^2+k^4}$. The expansion for the moment D_{22} is given by

$$
\begin{aligned}
f^0_{22,1}(a_1)=&\frac{2}{15}\pi G\mu\left(a_1^2-h^2\right)\left(k^2A_1-A_2\left(h^2-k^2\right)+2\left(a_1^2-k^2\right)\right),\\
f^2_{22,1}(a_1)=&\frac{\pi G\mu\left(h^2-a_1^2\right)}{14h^4k^2\left(h^2-k^2\right)^2\sqrt{h^4-h^2k^2+k^4}}\big(A_1\big(\sqrt{h^4-h^2k^2+k^4}\left(2a_1^4\left(h^4-h^2k^2+k^4\right)+\right.\right.\\
&a_1^2\left(2h^6-5h^4k^2-h^2k^4\right)-h^6k^2+3h^4k^4\big)+a_1^4\left(-2h^6+3h^4k^2+3h^2k^4-2k^6\right)+\\
&a_1^2\left(-2h^8+6h^6k^2-9h^4k^4+h^2k^6\right)+h^4k^2\left(h^4-2h^2k^2+3k^4\right)\big)+A_2\left(-a_1^2h^2\times\right.\\
&\left(h^2+k^2\right)^3+\sqrt{h^4-h^2k^2+k^4}\left(a_1^2h^2\left(h^4-10h^2k^2+k^4\right)+a_1^4\left(h^4+5h^2k^2-2k^4\right)+\right.\\
&\left.h^4k^2\left(h^2+3k^2\right)\right)-a_1^4\left(h^6-9h^4k^2+6h^2k^4-2k^6\right)+2h^8k^2-h^6k^4+3h^4k^6\big)-2h^2\times\\
&\left(a_1^2-k^2\right)\sqrt{h^4-h^2k^2+k^4}\left(a_1^2\left(h^2+k^2\right)+h^4-3h^2k^2\right)+2h^2\left(a_1^2-k^2\right)\left(a_1^2\times\right.\\
&\left.\left.\left(h^4-4h^2k^2+k^4\right)+h^6-2h^4k^2+3h^2k^4\right)\right),\\
f^4_{22,1}(a_1)=&\frac{\pi G\mu\left(h^2-a_1^2\right)}{4h^4k^4\left(K_1^4-K_2^4\right)\left(K_1^4-K_3^4\right)\left(h^2-k^2\right)^2}\left(-a_1^4B_{112}\left(h^2-k^2\right)^2\left(h^2\left(40k^2-4K_1^4\right)+\right.\right.\\
&K_1^4\left(K_1^4-4k^2\right)\big)+4a_1^2k^2A_{122}\left(a_1^2-h^2\right)^2\left(h^2-k^2\right)\left(2h^2\left(20k^2-9K_1^4\right)+K_1^4\left(K_1^4-\right.\right.\\
&\left.4k^2\right)\big)-2a_1^2k^2B_{122}\left(a_1^2-h^2\right)\left(h^2-k^2\right)\left(2h^2\left(20k^2-9K_1^4\right)+K_1^4\left(K_1^4-4k^2\right)\right)+\\
&2a_1^2h^2B_{123}\left(a_1^2-k^2\right)\left(h^2-k^2\right)\left(h^2\left(40k^2-4K_1^4\right)+K_1^4\left(K_1^4-18k^2\right)\right)+4k^4A_{222}\times\\
&\left(a_1^2-h^2\right)^3\left(280h^4+8h^2\left(5k^2-4K_1^4\right)+K_1^4\left(K_1^4-4k^2\right)\right)-k^4B_{222}\left(a_1^2-h^2\right)^2\times\\
&\left(280h^4+8h^2\left(5k^2-4K_1^4\right)+K_1^4\left(K_1^4-4k^2\right)\right)-4h^2k^2A_{223}\left(a_1^2-h^2\right)^2\left(a_1^2-k^2\right)\times\\
&\left(2h^2\left(160k^2-9K_1^4\right)+K_1^4\left(K_1^4-18k^2\right)\right)+2h^2k^2B_{223}\left(a_1^2-h^2\right)\left(a_1^2-k^2\right)\left(2h^2\times\right.
\end{aligned}
\tag{C.3d}
$$

$$
\begin{aligned}
&\left(160k^2-9K_1^4\right)+K_1^4\left(K_1^4-18k^2\right)\big)+h^4B_{233}\left(-\left(a_1^2-k^2\right)^2\right)\big(h^2\left(40k^2-4K_1^4\right)+\\
&280k^4-32k^2K_1^4+\left(K_1^4\right)^2\big)\big)=f^4_{22,1}(a_1)[K_1^4,K_2^4,K_3^4],\\
f^4_{22,2}(a_1)=&f^4_{22,1}(a_1)[K_2^4,K_1^4,K_3^4],\\
f^4_{22,3}(a_1)=&f^4_{22,1}(a_1)[K_3^4,K_2^4,K_1^4].
\end{aligned}
$$

For the second order moments only D_{33} remains to be determined in the exterior. The expansion coefficients read

$$
\begin{aligned}
f^0_{33,1}(a_1)=&\frac{2}{15}\pi G\mu\left(a_1^2-k^2\right)\left(k^2A_1+A_2\left(k^2-h^2\right)+2\left(a_1^2-k^2\right)\right),\\
f^2_{33,1}(a_1)=&\frac{\pi G\mu\left(k^2-a_1^2\right)}{14h^2k^4\left(h^2-k^2\right)^2\sqrt{h^4-h^2k^2+k^4}}\left(A_1\left(\sqrt{h^4-h^2k^2+k^4}\left(a_1^4\left(4h^4-7h^2k^2+k^4\right)+\right.\right.\right.\\
&a_1^2\left(-2h^4k^2+5h^2k^4+k^6\right)-2h^2k^6\big)-a_1^4\left(4h^6-9h^4k^2+6h^2k^4+k^6\right)+a_1^2\left(2h^6k^2-\right.\\
&\left.6h^4k^4+9h^2k^6-k^8\right)-h^2k^6\left(h^2+k^2\right)\big)+A_2\left(a_1^2k^2\left(h^2+k^2\right)^3+\sqrt{h^4-h^2k^2+k^4}\times\right.\\
&\left(-a_1^2k^2\left(h^4-10h^2k^2+k^4\right)+a_1^4\left(2h^4-5h^2k^2-k^4\right)-h^2k^4\left(3h^2+k^2\right)\right)+a_1^4\times\\
&\left(-2h^6+6h^4k^2-9h^2k^4+k^6\right)-3h^6k^4+h^4k^6-2h^2k^8\ \big)-4h^2\left(a_1^2-k^2\right)\times\\
&\sqrt{h^4-h^2k^2+k^4}\left(a_1^2\left(h^2-2k^2\right)+k^4\right)+2h^2\left(a_1^2-k^2\right)\left(a_1^2\left(2h^4-5h^2k^2+5k^4\right)-\right.\\
&\left.\left.k^4\left(h^2+k^2\right)\right)\right),\\
f^4_{33,1}(a_1)=&\frac{\pi G\mu\left(a_1^2-k^2\right)}{4h^4k^4\left(K_1^4-K_2^4\right)\left(K_1^4-K_3^4\right)\left(h^2-k^2\right)^2}\left(a_1^4B_{113}\left(h^2-k^2\right)^2\left(h^2\left(40k^2-4K_1^4\right)+K_1^4\times\right.\right.\\
&\left.\left(K_1^4-4k^2\right)\right)+2a_1^2k^2B_{123}\left(a_1^2-h^2\right)\left(h^2-k^2\right)\left(2h^2\left(20k^2-9K_1^4\right)+K_1^4\left(K_1^4-\right.\right.\\
&\left.4k^2\right)\big)+4a_1^2h^2A_{133}\left(a_1^2-k^2\right)^2\left(h^2-k^2\right)\left(h^2\left(40k^2-4K_1^4\right)+K_1^4\left(K_1^4-18k^2\right)\right)+\\
&2a_1^2h^2B_{133}\left(a_1^2-k^2\right)\left(k^2-h^2\right)\left(h^2\left(40k^2-4K_1^4\right)+K_1^4\left(K_1^4-18k^2\right)\right)+k^4B_{223}\\
&\left(a_1^2-h^2\right)^2\left(280h^4+8h^2\left(5k^2-4K_1^4\right)+K_1^4\left(K_1^4-4k^2\right)\right)+4h^2k^2A_{233}\left(a_1^2-h^2\right)\\
&\left(a_1^2-k^2\right)^2\left(2h^2\left(160k^2-9K_1^4\right)+K_1^4\left(K_1^4-18k^2\right)\right)+2h^2k^2B_{233}\left(h^2-a_1^2\right)\left(a_1^2-k^2\right)\\
&\left(2h^2\left(160k^2-9K_1^4\right)+K_1^4\left(K_1^4-18k^2\right)\right)-4h^4A_{333}\left(a_1^2-k^2\right)^3\left(h^2\left(40k^2-4K_1^4\right)+\right.\\
&280k^4-32k^2K_1^4+\left(K_1^4\right)^2\big)+h^4B_{333}\left(a_1^2-k^2\right)^2\left(h^2\left(40k^2-4K_1^4\right)+280k^4-\\
&\left.32k^2K_1^4+\left(K_1^4\right)^2\right)\big)=f^4_{33,1}(a_1)[K_1^4,K_2^4,K_3^4],\\
f^4_{33,2}(a_1)=&f^4_{33,1}(a_1)[K_2^4,K_1^4,K_3^4],\\
f^4_{33,3}(a_1)=&f^4_{33,1}(a_1)[K_3^4,K_2^4,K_1^4].
\end{aligned}
\tag{C.3e}
$$

With these expansion coefficients, the constants C_m^n in equation (5.22) and (5.25) can be obtained easily. Thus, together with (6.7) the metric functions Φ and $U_a^{(3)}$ are determined also in the exterior in a closed form. For δU – as indicated after Eq. (6.9) – we do not have to find the exterior of the moments to third order but rather the exterior to the combinations

$$
\begin{aligned}
&\hat{D}_1=D_{1,1}-D_{3,3},\quad \hat{D}_2=D_{2,2}-D_{3,3},\quad \hat{D}_3=D_{111,1}-3D_{112,2},\\
&\hat{D}_4=D_{222,2}-3D_{223,3},\qquad\qquad\qquad\quad \hat{D}_5=D_{333,3}-3D_{331,1}.
\end{aligned}
\tag{C.4}
$$

These functions are even in the x^a. Hence, only ellipsoidal surface harmonics of the first species occur in the expansion. Furthermore, the form of the ξ_i^a in Eq. (6.6) (which preserves the

coordinate volume) and Eq. (6.8) imply that the potentials $\hat{D}_i$ do not have a monopole term in their expansion. We give here only the non-vanishing expansion coefficients[3], which are denoted by $\hat{f}^n_{i,m}$:

$$\begin{aligned}
\hat{f}^2_{1,1} = {} & \frac{\pi G\mu}{2h^4k^4\left(h^2-k^2\right)^2\sqrt{h^4-h^2k^2+k^4}}\left(A_1\left(2\sqrt{h^4-h^2k^2+k^4}\left(a_1^2\left(-2h^4+2h^2k^2+k^4\right)+\right.\right.\right.\\
& \left.h^2k^2\left(h^2-2k^2\right)\right)\left(k^2\left(a_1^2+h^2\right)-2a_1^2h^2\right)+2a_1^2h^2k^2\left(4h^6-9h^4k^2+6h^2k^4+k^6\right)+a_1^4\times\\
& \left(-8h^8+16h^6k^2-9h^4k^4+h^2k^6-2k^8\right)-2h^8k^4+5h^6k^6-5h^4k^8\Big)+A_2\left(-4a_1^4h^8+2k^8\times\right.\\
& \left(a_1^2-2h^2\right)\left(a_1^2+h^2\right)+a_1^2h^6k^2\left(11a_1^2+4h^2\right)+h^2k^6\left(18a_1^2h^2-4a_1^4+h^4\right)-h^4k^4\left(12a_1^2h^2+\right.\\
& \left.9a_1^4+h^4\right)+\sqrt{h^4-h^2k^2+k^4}\left(2a_1^2h^2k^2\left(-2h^4+5h^2k^2+k^4\right)+a_1^4\left(h^2-2k^2\right)\left(4h^4-h^2k^2+\right.\right.\\
& \left.\left.k^4\right)+h^4k^4\left(h^2-5k^2\right)\right)\Big)+2h^2\left(k^2-a_1^2\right)\sqrt{h^4-h^2k^2+k^4}\left(a_1^2\left(4h^4-7h^2k^2+k^4\right)-\right.\\
& \left.\left.2h^4k^2+4h^2k^4\right)+2h^2\left(a_1^2-k^2\right)\left(a_1^2\left(4h^6-9h^4k^2+6h^2k^4+k^6\right)-2h^6k^2+5h^4k^4-5h^2k^6\right)\Big)\Big)\,,\\
\hat{f}^2_{2,1} = {} & \frac{\pi G\mu}{2h^4k^4\left(h^2-k^2\right)^2\sqrt{h^4-h^2k^2+k^4}}\left(A_1\left(-4a_1^4h^8+2k^8\left(a_1^2-2h^2\right)\left(a_1^2+h^2\right)+a_1^2h^6k^2\times\right.\right.\\
& \left(11a_1^2+4h^2\right)+h^2k^6\left(18a_1^2h^2-4a_1^4+h^4\right)-h^4k^4\left(12a_1^2h^2+9a_1^4+h^4\right)+\sqrt{h^4-h^2k^2+k^4}\times\\
& \left(2a_1^2h^2k^2\left(-2h^4+5h^2k^2+k^4\right)+a_1^4\left(h^2-2k^2\right)\left(4h^4-h^2k^2+k^4\right)+h^4k^4\left(h^2-5k^2\right)\right)\Big)+\\
& A_2\Big(2a_1^2h^2k^2\left(h^2+k^2\right)^3+2\sqrt{h^4-h^2k^2+k^4}\left(a_1^2\left(h^2+k^2\right)-2h^2k^2\right)\left(a_1^2\left(h^4-4h^2k^2+k^4\right)+\\
& h^2k^2\left(h^2+k^2\right)\right)+a_1^4\left(-2h^8+7h^6k^2-18h^4k^4+7h^2k^6-2k^8\right)-5h^8k^4+2h^6k^6-5h^4k^8\Big)+\\
& 2h^2\left(k^2-a_1^2\right)\sqrt{h^4-h^2k^2+k^4}\left(a_1^2\left(2h^4-5h^2k^2-k^4\right)+h^4\left(-k^2\right)+5h^2k^4\right)+\\
& \left.2h^2\left(k^2-a_1^2\right)\left(a_1^2\left(-2h^6+6h^4k^2-9h^2k^4+k^6\right)+h^2k^2\left(h^4-h^2k^2+4k^4\right)\right)\right)\,,\\
\hat{f}^2_{3,1} = {} & \frac{\pi G\mu}{14h^4k^4\left(h^2-k^2\right)^2\sqrt{h^4-h^2k^2+k^4}}\left(A_1\left(-4a_1^4h^8-k^8\left(h^2-2a_1^2\right)^2-h^6k^4\left(6a_1^2+h^2\right)+\right.\right.\\
& a_1^2h^6k^2\left(5a_1^2+4h^2\right)+h^2k^6\left(-6a_1^2h^2+5a_1^4+4h^4\right)+\sqrt{h^4-h^2k^2+k^4}\left(4a_1^4h^6+k^6\left(h^2-\right.\right.\\
& \left.\left.2a_1^2\right)^2+h^2k^4\left(4a_1^2h^2-3a_1^4+h^4\right)-a_1^2h^4k^2\left(3a_1^2+4h^2\right)\right)\Big)+A_2\left(-2a_1^4h^8+k^8\left(h^2-2a_1^2\right)^2+\right.\\
& 2a_1^2h^6k^2\left(2a_1^2+h^2\right)-h^2k^6\left(-12a_1^2h^2+11a_1^4+h^4\right)+h^4k^4\left(-18a_1^2h^2+9a_1^4+4h^4\right)+\\
& \sqrt{h^4-h^2k^2+k^4}\left(2a_1^4h^6-k^6\left(h^2-2a_1^2\right)^2+h^2k^4\left(-10a_1^2h^2+9a_1^4+5h^4\right)-a_1^2h^4k^2\left(3a_1^2+\right.\right.\\
& \left.\left.2h^2\right)\right)\Big)+2h^2\left(k^2-a_1^2\right)\sqrt{h^4-h^2k^2+k^4}\left(2a_1^2\left(h^4-h^2k^2+k^4\right)-h^2k^2\left(h^2+k^2\right)\right)+\\
& \left.2h^2\left(k^2-a_1^2\right)\left(a_1^2\left(-2h^6+3h^4k^2+3h^2k^4-2k^6\right)+h^2k^2\left(h^4-4h^2k^2+k^4\right)\right)\right)\,,\\
\hat{f}^4_{3,1} = {} & \frac{\pi G\mu}{12h^4k^4\left(K_1^4-K_2^4\right)\left(K_1^4-K_3^4\right)\left(h^2-k^2\right)^2}\left(20\left(h^2-k^2\right)^2A_{1111}\left(\left(40k^2-4K_1^4\right)h^2+K_1^4\times\right.\right.\\
& \left.\left(K_1^4-4k^2\right)\right)a_1^8+12h^2\left(h^2-k^2\right)\left(k^2-a_1^2\right)A_{1113}\left(\left(40k^2-4K_1^4\right)h^2+K_1^4\left(K_1^4-18k^2\right)\right)a_1^6-\\
& 15\left(h^2-k^2\right)^2B_{1111}\left(\left(40k^2-4K_1^4\right)h^2+K_1^4\left(K_1^4-4k^2\right)\right)a_1^6+12\left(h^2-k^2\right)\left(h^2-a_1^2\right)A_{1112}\times\\
& \left(\left(40k^2-4K_1^4\right)h^4+\left(-80k^4+18K_1^4k^2+\left(K_1^4\right)^2\right)h^2+2k^2\left(4k^2-K_1^4\right)K_1^4\right)a_1^6+12h^2\times\\
& \left(h^2-k^2\right)\left(a_1^2-h^2\right)\left(a_1^2-k^2\right)A_{1123}\left(\left(40k^2-4K_1^4\right)h^2+K_1^4\left(K_1^4-18k^2\right)\right)a_1^4+18h^2\times\\
& \left.\left(h^2-k^2\right)\left(a_1^2-k^2\right)B_{1113}\left(\left(40k^2-4K_1^4\right)h^2+K_1^4\left(K_1^4-18k^2\right)\right)a_1^4-36k^2\left(h^2-k^2\right)\times\right.
\end{aligned} \tag{C.5a}$$

[3]The expansion coefficients $f^2_{i,2}(a_1)$ follow from $f^2_{i,1}(a_1)$ by a substitution of the square root $\sqrt{h^4-h^2k^2+k^4}$ in Eq. (C.5) with its negative.

$$\left(a_1^2-h^2\right)^2 A_{1122}\left(2\left(20k^2-9K_1^4\right)h^2+K_1^4\left(K_1^4-4k^2\right)\right)a_1^4+3\left(h^2-k^2\right)\left(a_1^2-h^2\right)\times$$
$$B_{1112}\left(\left(40k^2-4K_1^4\right)h^4+\left(-280k^4+108K_1^4k^2+\left(K_1^4\right)^2\right)h^2+7k^2\left(4k^2-K_1^4\right)K_1^4\right)a_1^4-$$
$$3k^2\left(a_1^2-h^2\right)^2 B_{1122}\left(4\left(10k^2+27K_1^4\right)h^4+2\left(140k^4-58K_1^4k^2-3\left(K_1^4\right)^2\right)h^2+7k^2\times\right.$$
$$\left.K_1^4\left(K_1^4-4k^2\right)\right)a_1^2-6h^2\left(a_1^2-h^2\right)\left(a_1^2-k^2\right)B_{1123}\left(\left(40k^2-4K_1^4\right)h^4+\left(-360k^4+\right.\right.$$
$$\left.\left.4K_1^4k^2+\left(K_1^4\right)^2\right)h^2+2k^2\left(18k^2-K_1^4\right)K_1^4\right)a_1^2-3h^4\left(a_1^3-k^2a_1\right)^2 B_{1133}\left(280k^4-\right.$$
$$\left.32K_1^4k^2+\left(K_1^4\right)^2+h^2\left(40k^2-4K_1^4\right)\right)-3h^4\left(h^2-a_1^2\right)\left(a_1^2-k^2\right)^2 B_{1233}\left(280k^4-\right.$$
$$\left.32K_1^4k^2+\left(K_1^4\right)^2+h^2\left(40k^2-4K_1^4\right)\right)+18h^2k^2\left(k^2-a_1^2\right)\left(a_1^2-h^2\right)^2 B_{1223}\left(2\left(160k^2-\right.\right.$$
$$\left.\left.9K_1^4\right)h^2+K_1^4\left(K_1^4-18k^2\right)\right)+15k^4\left(a_1^2-h^2\right)^3 B_{1222}\left(280h^4+8\left(5k^2-4K_1^4\right)h^2+\right.$$
$$\left.K_1^4\left(K_1^4-4k^2\right)\right)\Big)=\hat{f}_{3,1}^4(a_1)[K_1^4,K_2^4,K_3^4],$$

$$\hat{f}_{3,2}^4(a_1)=\hat{f}_{3,1}^4(a_1)[K_2^4,K_1^4,K_3^4],$$

$$\hat{f}_{3,3}^4(a_1)=\hat{f}_{3,1}^4(a_1)[K_3^4,K_2^4,K_1^4],$$

$$\hat{f}_{4,1}^2=\frac{\pi G\mu\left(a_1^2-h^2\right)}{14a_1^2h^4k^4\left(h^2-k^2\right)^2\sqrt{h^4-h^2k^2+k^4}}\Big(A_1\Big(-4a_1^4h^8+2k^8\left(a_1^2-2h^2\right)\left(a_1^2+h^2\right)+$$
$$a_1^2h^6k^2\left(11a_1^2+4h^2\right)+h^2k^6\left(18a_1^2h^2-4a_1^4+h^4\right)-h^4k^4\left(12a_1^2h^2+9a_1^4+h^4\right)+$$
$$\sqrt{h^4-h^2k^2+k^4}\left(2a_1^2h^2k^2\left(-2h^4+5h^2k^2+k^4\right)+a_1^4\left(h^2-2k^2\right)\left(4h^4-h^2k^2+k^4\right)+\right.$$
$$\left.h^4k^4\left(h^2-5k^2\right)\right)\Big)+A_2\Big(2a_1^2h^2k^2\left(h^2+k^2\right)^3+2\sqrt{h^4-h^2k^2+k^4}\left(a_1^2\left(h^2+k^2\right)-\right.$$
$$\left.2h^2k^2\right)\left(a_1^2\left(h^4-4h^2k^2+k^4\right)+h^2k^2\left(h^2+k^2\right)\right)+a_1^4\left(-2h^8+7h^6k^2-18h^4k^4+\right.$$
$$\left.7h^2k^6-2k^8\right)-5h^8k^4+2h^6k^6-5h^4k^8\Big)+2h^2\left(a_1^2-k^2\right)\sqrt{h^4-h^2k^2+k^4}\left(a_1^2\left(-2h^4+\right.\right.$$
$$\left.\left.5h^2k^2+k^4\right)+h^2k^2\left(h^2-5k^2\right)\right)+2h^2\left(a_1^2-k^2\right)\left(2a_1^2h^6-k^6\left(a_1^2+4h^2\right)+h^2k^4\left(9a_1^2+\right.\right.$$
$$\left.\left.h^2\right)-h^4k^2\left(6a_1^2+h^2\right)\right)\Big),$$

$$\hat{f}_{4,1}^4=\frac{\pi G\mu\left(h^2-a_1^2\right)}{12a_1^2h^4k^4\left(K_1^4-K_2^4\right)\left(K_1^4-K_3^4\right)\left(h^2-k^2\right)^2}\Big(-15\left(a_1^2-k^2\right)^3 B_{2333}\left(280k^4-\right.$$
$$\left.32K_1^4k^2+\left(K_1^4\right)^2+h^2\left(40k^2-4K_1^4\right)\right)h^4-36k^2\left(a_1^2-h^2\right)^2\left(a_1^2-k^2\right)^2 A_{2233}\left(2\times\right.$$
$$\left.\left(160k^2-9K_1^4\right)h^2+K_1^4\left(K_1^4-18k^2\right)\right)h^2+18\left(h^2-k^2\right)a_1^2\left(a_1^2-k^2\right)^2 B_{1233}\left(\left(40k^2-\right.\right.$$
$$\left.\left.4K_1^4\right)h^2+K_1^4\left(K_1^4-18k^2\right)\right)h^2+3\left(a_1^2-h^2\right)\left(a_1^2-k^2\right)^2 B_{2233}\left(\left(40k^2-4K_1^4\right)h^4+\right.$$
$$\left.\left(2200k^4-140K_1^4k^2+\left(K_1^4\right)^2\right)h^2+6k^2K_1^4\left(K_1^4-18k^2\right)\right)h^2-12k^2\left(h^2-k^2\right)a_1^2\times$$
$$\left(a_1^2-h^2\right)^3 A_{1222}\left(2\left(20k^2-9K_1^4\right)h^2+K_1^4\left(K_1^4-4k^2\right)\right)+12(h^2-k^2)k^2a_1^2\left(a_1^2-h^2\right)^2\times$$
$$\left(a_1^2-k^2\right)A_{1223}\left(2\left(20k^2-9K_1^4\right)h^2+K_1^4\left(K_1^4-4k^2\right)\right)+18k^2\left(h^2-k^2\right)a_1^2\left(a_1^2-h^2\right)^2\times$$
$$B_{1222}\left(2\left(20k^2-9K_1^4\right)h^2+K_1^4\left(K_1^4-4k^2\right)\right)-20k^4\left(a_1^2-h^2\right)^4 A_{2222}\left(280h^4+8\left(5k^2-\right.\right.$$
$$\left.\left.4K_1^4\right)h^2+K_1^4\left(K_1^4-4k^2\right)\right)+15k^4\left(a_1^2-h^2\right)^3 B_{2222}\left(280h^4+8\left(5k^2-4K_1^4\right)h^2+K_1^4\times\right.$$
$$\left.\left(K_1^4-4k^2\right)\right)+3\left(h^2-k^2\right)^2 a_1^4\left(a_1^2-h^2\right)B_{1122}\left(\left(40k^2-4K_1^4\right)h^2+K_1^4\left(K_1^4-4k^2\right)\right)-$$
$$3\left(h^2-k^2\right)^2 a_1^4\left(a_1^2-k^2\right)B_{1123}\left(\left(40k^2-4K_1^4\right)h^2+K_1^4\left(K_1^4-4k^2\right)\right)+12k^2\left(a_1^2-h^2\right)^3\times$$
$$\left(a_1^2-k^2\right)A_{2223}\left(6\left(100k^2-3K_1^4\right)h^4+\left(40k^4-50K_1^4k^2+\left(K_1^4\right)^2\right)h^2+k^2K_1^4\left(K_1^4-\right.\right.$$
$$\left.\left.4k^2\right)\right)-6(h-k)(h+k)a_1^2\left(a_1^2-h^2\right)\left(a_1^2-k^2\right)B_{1223}\left(\left(40k^2-4K_1^4\right)h^4+\left(40k^4-\right.\right.$$
$$\left.\left.36K_1^4k^2+\left(K_1^4\right)^2\right)h^2+k^2K_1^4\left(K_1^4-4k^2\right)\right)-3k^2\left(a_1^2-h^2\right)^2\left(a_1^2-k^2\right)\times$$

$$B_{2223}\left(4\left(550k^2-27K_1^4\right)h^4+2\left(20k^4-70K_1^4k^2+3\left(K_1^4\right)^2\right)h^2+k^2K_1^4\left(K_1^4-4k^2\right)\right)=\hat{f}_{4,1}^4(a_1)[K_1^4,K_2^4,K_3^4],$$

$$\hat{f}_{4,2}^4(a_1)=\hat{f}_{4,1}^4(a_1)[K_2^4,K_1^4,K_3^4],$$

$$\hat{f}_{4,3}^4(a_1)=\hat{f}_{4,1}^4(a_1)[K_3^4,K_2^4,K_1^4],$$

$$\hat{f}_{5,1}^2(a_1)=\frac{\pi G\mu\left(a_1^2-k^2\right)}{14a_1^2h^4k^4\left(h^2-k^2\right)^2\sqrt{h^4-h^2k^2+k^4}}\Big(A_1\Big(-2\sqrt{h^4-h^2k^2+k^4}\left(a_1^2\left(-2h^4+2h^2k^2+k^4\right)+h^2k^2\left(h^2-2k^2\right)\right)\left(k^2\left(a_1^2+h^2\right)-2a_1^2h^2\right)-2a_1^2h^2k^2\left(4h^6-9h^4k^2+6h^2k^4+k^6\right)+a_1^4\left(8h^8-16h^6k^2+9h^4k^4-h^2k^6+2k^8\right)+2h^8k^4-5h^6k^6+5h^4k^8\Big)+A_2\Big(2a_1^2h^2k^2\left(-2h^6+6h^4k^2-9h^2k^4+k^6\right)+\sqrt{h^4-h^2k^2+k^4}\left(-4a_1^4h^6+k^6\left(2a_1^4+5h^4-2a_1^2h^2\right)-h^2k^4\left(10a_1^2h^2+3a_1^4+h^4\right)+a_1^2h^4k^2\left(9a_1^2+4h^2\right)\right)+a_1^4\left(4h^8-11h^6k^2+9h^4k^4+4h^2k^6-2k^8\right)+h^4k^4\left(h^4-h^2k^2+4k^4\right)\Big)+2h^2\left(a_1^2-k^2\right)\sqrt{h^4-h^2k^2+k^4}\times\left(a_1^2\left(4h^4-7h^2k^2+k^4\right)-2h^4k^2+4h^2k^4\right)-2h^2\left(a_1^2-k^2\right)\left(a_1^2\left(4h^6-9h^4k^2+6h^2k^4+k^6\right)-2h^6k^2+5h^4k^4-5h^2k^6\right)\Big),$$

$$\hat{f}_{5,1}^4(a_1)=\frac{\pi G\mu\left(a_1^2-k^2\right)}{12a_1^2h^4k^4\left(K_1^4-K_2^4\right)\left(K_1^4-K_3^4\right)\left(h^2-k^2\right)^2}\Big(15\left(h^2-k^2\right)^2B_{1113}\left(\left(40k^2-4K_1^4\right)h^2+K_1^4\left(K_1^4-4k^2\right)\right)a_1^6+36h^2\left(h^2-k^2\right)\left(a_1^2-k^2\right)^2A_{1133}\left(\left(40k^2-4K_1^4\right)h^2+K_1^4\left(K_1^4-18k^2\right)\right)a_1^4+18k^2\left(h^2-k^2\right)\left(a_1^2-h^2\right)B_{1123}\left(2\left(20k^2-9K_1^4\right)h^2+K_1^4\left(K_1^4-4k^2\right)\right)a_1^4-3\left(k^2-h^2\right)\left(a_1^2-k^2\right)B_{1133}\left(28\left(K_1^4-10k^2\right)h^4+\left(40k^4+108K_1^4k^2-7\left(K_1^4\right)^2\right)h^2+k^2K_1^4\left(K_1^4-4k^2\right)\right)a_1^4+12h^2k^2\left(a_1^2-h^2\right)\left(a_1^2-k^2\right)^2A_{1233}\left(2\left(160k^2-9K_1^4\right)h^2+K_1^4\left(K_1^4-18k^2\right)\right)a_1^2+6k^2\left(a_1^2-h^2\right)\left(a_1^2-k^2\right)B_{1233}\left(36\left(K_1^4-10k^2\right)h^4+\left(40k^4+4K_1^4k^2-2\left(K_1^4\right)^2\right)h^2+k^2K_1^4\left(K_1^4-4k^2\right)\right)a_1^2-12h^2\left(a_1^2-k^2\right)^3A_{1333}\left(\left(80k^2-8K_1^4\right)h^4+2\left(120k^4-23K_1^4k^2+\left(K_1^4\right)^2\right)h^2+k^2\left(18k^2-K_1^4\right)K_1^4\right)a_1^2+3h^2B_{1333}\times\left(a_1^2-k^2\right)^2\left(28\left(10k^2-K_1^4\right)h^4+\left(40k^4-116K_1^4k^2+7\left(K_1^4\right)^2\right)h^2+6k^2\left(18k^2-K_1^4\right)\times K_1^4\right)a_1^2+20h^4\left(a_1^2-k^2\right)^4A_{3333}\left(280k^4-32K_1^4k^2+\left(K_1^4\right)^2+h^2\left(40k^2-4K_1^4\right)\right)-15h^4\left(a_1^2-k^2\right)^3B_{3333}\left(280k^4-32K_1^4k^2+\left(K_1^4\right)^2+h^2\left(40k^2-4K_1^4\right)\right)+12h^2k^2\times\left(h^2-a_1^2\right)\left(a_1^2-k^2\right)^3A_{2333}\left(2\left(160k^2-9K_1^4\right)h^2+K_1^4\left(K_1^4-18k^2\right)\right)+18h^2k^2B_{2333}\times\left(a_1^2-h^2\right)\left(a_1^2-k^2\right)^2\left(2\left(160k^2-9K_1^4\right)h^2+K_1^4\left(K_1^4-18k^2\right)\right)+3k^4B_{1223}\times\left(a_1^3-h^2a_1\right)^2\left(280h^4+8\left(5k^2-4K_1^4\right)h^2+K_1^4\left(K_1^4-4k^2\right)\right)-3k^4\left(a_1^2-h^2\right)^2B_{2233}\times\left(a_1^2-k^2\right)\left(280h^4+8\left(5k^2-4K_1^4\right)h^2+K_1^4\left(K_1^4-4k^2\right)\right)\Big)=\hat{f}_{5,1}^4(a_1)[K_1^4,K_2^4,K_3^4],$$

$$\hat{f}_{5,2}^4(a_1)=\hat{f}_{5,1}^4(a_1)[K_2^4,K_1^4,K_3^4],$$

$$\hat{f}_{5,3}^4(a_1)=\hat{f}_{5,1}^4(a_1)[K_3^4,K_2^4,K_1^4].$$

APPENDIX

D

THE SURFACE CONDITION

The reason why our numerical results do not coincide with the numerical results in [23] is discussed in detail in Paper V. As the most likely cause, we identified a problem in the numerical evaluation of the right-hand side of Eq. (6.13) (the α's entering Eq. (58) in [23]). However, this could not be verified, since those expressions were not given explicitly. To avoid similar problems, the lengthy analytical expressions for equation (6.13) are given here. The coefficient matrix reads

$$
\begin{aligned}
M_{00} =& \frac{1}{\pi^2},\\
M_{01} =& 3\bar{a}_3^2\bar{B}_{33} - \bar{B}_{13},\\
M_{02} =& 3\bar{a}_3^2\bar{B}_{33} - \bar{a}_2^2\bar{B}_{23},\\
M_{03} =& \frac{1}{4}\left(\bar{a}_2^2-1\right)\left(\bar{C}_{112} - 2\bar{a}_3^2\bar{C}_{1123} + \bar{a}_3^4\bar{C}_{11233}\right),\\
M_{04} =& -\frac{\bar{a}_2^2}{4}\left(\left(\bar{a}_2^2-\bar{a}_3^2\right)\left(\bar{C}_{223} - 2\bar{a}_3^2\bar{C}_{2233} + \bar{a}_3^4\bar{C}_{22333}\right) + 4\bar{a}_3^4\bar{C}_{2333}\right),\\
M_{05} =& -\frac{\bar{a}_3^2}{12}\left(\bar{a}_3^2\left(11\bar{C}_{133} + \bar{a}_3^2\left(-10\bar{C}_{1333} + 11\left(\bar{a}_3^2-1\right)\bar{C}_{13333} + 24\bar{a}_3^2\bar{B}_{3333}\right) + 14\bar{C}_{1333}\right) - 3\bar{C}_{133}\right),\\
M_{10} =& M_{20} = M_{30} = M_{40} = M_{50} = 0,\\
M_{11} =& \frac{2}{\bar{a}_2^2}\left(\left(\bar{a}_3^2-1\right)\left(\bar{a}_3^2-\bar{a}_2^2\right)\bar{C}_{1233} - 2\bar{a}_3^2\bar{B}_{33}\right),\\
M_{12} =& \frac{2}{\bar{a}_2^2}\left(3\left(\bar{a}_2^2-\bar{a}_3^2\right)^2\bar{C}_{2233} - 4\bar{a}_3^2\bar{B}_{23}\right),\\
M_{13} =& \frac{1}{\bar{a}_2^2}\left(\left(\left(\bar{a}_2^2-1\right)\bar{a}_3^2 + \bar{a}_2^2\right)\bar{C}_{1123} - \left(\bar{a}_2^2-1\right)\bar{a}_3^4\bar{C}_{11233} - 3\bar{a}_2^4\bar{C}_{1223}\right),\\
M_{14} =& 5\bar{a}_2^4\bar{C}_{2223} - 4\bar{a}_3^4\bar{a}_2^4\bar{A}_{2233} - 2\left(\bar{a}_2^4 + \bar{a}_3^2\bar{a}_2^2 + \bar{a}_3^4\right)\bar{C}_{2233} + 5\bar{a}_3^4\bar{C}_{2333} + 4\bar{a}_3^2\bar{A}_3,\\
M_{15} =& \frac{\bar{a}_3^2}{3\bar{a}_2^2}\left(3\bar{a}_3^4\left(-2\bar{C}_{1233} + 3\bar{C}_{1333} + 5\bar{C}_{2333} - 9\bar{C}_{3333}\right) + \bar{a}_3^2\left(3\left(\bar{a}_2^2-1\right)\bar{C}_{1233} + 6\bar{C}_{1333} + 8\bar{A}_3\right) -\right.\\
& \left. 3\bar{a}_2^2\bar{C}_{1233} - 8\bar{a}_3^8\bar{A}_{3333}\right),\\
M_{21} =& -M_{22} = \frac{48\left(2\bar{a}_2^2+1\right)\bar{B}_{12}}{\bar{a}_2^2\left(\bar{a}_2^2-1\right)},
\end{aligned}
\tag{D.1}
$$

$$M_{23} = \left(\left(\frac{12}{\bar{a}_2^2} - 6\right)\bar{a}_3^2 - 6\right)\bar{C}_{11223} + \frac{6\left(\bar{a}_2^2 - 1\right)\bar{a}_3^4\bar{C}_{11233}}{\bar{a}_2^4} + \frac{\left(48 - 96\bar{a}_2^2\right)\bar{B}_{12}}{\bar{a}_2^2 - \bar{a}_2^4} + 30\left(\bar{a}_2^2 - \bar{a}_3^2\right)\bar{C}_{12223},$$

$$M_{24} = -\frac{16\left(\bar{a}_2^2 + 2\right)\bar{B}_{12}}{\bar{a}_2^2 - 1} + 16\bar{a}_2^6\bar{A}_{2222} + 54\left(\bar{a}_3^2 - \bar{a}_2^2\right)\bar{a}_2^2\bar{C}_{22223} + 12\left(2\bar{a}_2^4 - \bar{a}_3^2\bar{a}_2^2 - \bar{a}_3^4\right)\bar{C}_{22233} +$$
$$48\bar{a}_3^4\bar{a}_2^2\bar{A}_{2233} + 30\bar{a}_3^4\left(\frac{\bar{a}_3^2}{\bar{a}_2^2} - 1\right)\bar{C}_{22333} - \frac{64\bar{a}_3^2\bar{A}_3}{\bar{a}_2^2},$$

$$M_{25} = \frac{2}{\bar{a}_2^4}\left(-3\bar{a}_2^4\left(\bar{a}_3^2 - 1\right)\bar{a}_3^2\bar{C}_{12233} + 3\left(4\bar{a}_3^4 + \bar{a}_3^2 - \bar{a}_2^2\left(3\bar{a}_3^2 + 2\right)\right)\bar{a}_3^4\bar{C}_{12333} - 8\bar{a}_3^4\bar{A}_3 + 8\bar{a}_3^{10}\bar{A}_{3333} +$$
$$27\left(\bar{a}_2^2 - \bar{a}_3^2\right)\bar{a}_3^6\bar{C}_{23333}\right),$$

$$M_{31} = -2\left(\left(\bar{a}_3^2 - 1\right)\left(3\bar{B}_{113} + \bar{a}_3^2\bar{B}_{133}\right) + 4\bar{a}_3^2\bar{B}_{33}\right),$$

$$M_{32} = 2\left(\left(\bar{a}_3^2 - 1\right)\left(\bar{a}_3^2 - \bar{a}_2^2\right)\bar{C}_{1233} - 2\bar{a}_3^2\bar{B}_{33}\right),$$

$$M_{33} = -5\left(\bar{a}_2^2 - 1\right)\bar{C}_{1112} + 5\left(\bar{a}_2^2 - 1\right)\bar{a}_3^2\bar{C}_{11123} + \left(\left(\bar{a}_3^2 + 4\right)\bar{a}_2^2 - \bar{a}_3^2 - 2\right)\bar{C}_{1123} - \left(\bar{a}_2^2 - 1\right)\bar{a}_3^4\bar{C}_{11233},$$

$$M_{34} = \left(\bar{a}_2^4 + \left(\bar{a}_2^2 - 1\right)\bar{a}_3^2\bar{a}_2^2\right)\bar{C}_{1223} - 3\bar{a}_2^2\bar{a}_3^4\bar{C}_{1233} + \bar{a}_2^2\left(\bar{a}_3^2 - 2\bar{a}_2^2\right)\bar{a}_3^2\bar{C}_{2233} + 5\bar{a}_2^2\bar{a}_3^4\bar{C}_{2333},$$

$$M_{35} = -3\bar{a}_3^2\bar{B}_{113} + 3\left(-2\bar{a}_3^4 + \bar{a}_3^2 + 1\right)\bar{a}_3^4\bar{C}_{11333} + 2\left(\bar{a}_3^2 + 1\right)\bar{a}_3^4\bar{B}_{133} + \frac{20}{3}\bar{a}_3^4\bar{A}_3 - \frac{20}{3}\bar{a}_3^8\bar{A}_{333} +$$
$$\left(6\bar{a}_3^2 - 7\right)\bar{a}_3^6\bar{B}_{1333} - 5\bar{a}_3^6\bar{B}_{333} + \frac{35}{3}\bar{a}_3^8\bar{B}_{3333},$$

$$M_{41} = -M_{42} = \frac{48\bar{B}_{12}}{\bar{a}_2^2 - 1},$$

$$M_{43} = 10\left(\bar{a}_2^2 - 1\right)\bar{C}_{11122} - 8\bar{a}_2^2\bar{A}_{1122} - \frac{2\left(\bar{a}_2^2 - 1\right)\left(\bar{a}_2^2\left(3\bar{a}_3^2 + 2\right) - 2\bar{a}_3^2\right)\bar{C}_{11223}}{\bar{a}_2^2} +$$
$$\frac{2\left(\bar{a}_2^2 - 1\right)\bar{a}_3^4\bar{C}_{11233}}{\bar{a}_2^2} - \frac{10\left(\bar{a}_2^2 - 1\right)\bar{a}_3^2\bar{C}_{11123}}{\bar{a}_2^2} + \frac{16\bar{B}_{12}}{\bar{a}_2^2 - 1} + \frac{8\bar{a}_3^2\bar{A}_3}{\bar{a}_2^2},$$

$$M_{44} = -\frac{16\bar{a}_2^2\bar{B}_{12}}{\bar{a}_2^2 - 1} + \left(2\left(3\bar{a}_3^2 - 5\right)\bar{a}_2^4 + 4\bar{a}_3^2\bar{a}_2^2\right)\bar{C}_{12223} - 4\left(\bar{a}_3^2 - 1\right)\bar{a}_2^4\bar{C}_{12233} + 6\bar{a}_3^4\left(\bar{a}_3^2 - 1\right)\bar{C}_{12333} +$$
$$4\bar{a}_3^2\left(\bar{a}_2^2 - \bar{a}_3^2\right)\bar{a}_2^2\bar{C}_{22233} + 8\bar{a}_3^4\bar{a}_2^4\bar{A}_{2233} + 4\bar{a}_3^4\left(\bar{a}_3^2 - \bar{a}_2^2\right)\bar{C}_{22333} - 8\bar{a}_3^2\bar{A}_3,$$

$$M_{45} = 6\bar{a}_3^2\bar{B}_{1123} - \frac{12\left(\bar{a}_3^2 - 1\right)\bar{a}_3^4\bar{B}_{1133}}{\bar{a}_2^2} + \frac{18\left(\bar{a}_3^2 - 1\right)\bar{a}_3^4\bar{C}_{11333}}{\bar{a}_2^2} - 4\left(\bar{a}_3^6 + \bar{a}_3^4\right)\bar{B}_{1233} + \frac{8\bar{a}_3^8\bar{A}_{1333}}{\bar{a}_2^2} +$$
$$\frac{2\left(4\bar{a}_3^8 + \bar{a}_3^6\right)\bar{B}_{1333}}{\bar{a}_2^2} + 10\bar{a}_3^6\bar{B}_{2333} - \frac{40\bar{a}_3^4\bar{A}_3}{3\bar{a}_2^2} + \frac{16\bar{a}_3^{10}\bar{A}_{3333}}{3\bar{a}_2^2} - \frac{18\bar{a}_3^8\bar{B}_{3333}}{\bar{a}_2^2},$$

$$M_{51} = -M_{52} = \frac{48\left(\bar{a}_2^2 + 2\right)\bar{B}_{12}}{\bar{a}_2^2 - 1},$$

$$M_{53} = 16\bar{A}_{1111} + 54\left(\bar{a}_2^2 - 1\right)\bar{C}_{11112} - 12\left(\left(\bar{a}_3^2 + 4\right)\bar{a}_2^2 - 3\bar{a}_3^2 - 2\right)\bar{C}_{11123} + 6\left(\bar{a}_2^2 - 1\right)\bar{a}_3^4\bar{C}_{11233} +$$
$$\frac{16\left(5\bar{a}_2^2 - 2\right)\bar{B}_{12}}{\bar{a}_2^2 - 1} - 16\bar{a}_3^2\bar{A}_3,$$

$$M_{54} = \left(6\bar{a}_2^2\bar{a}_3^2 - 6\bar{a}_2^4\right)\bar{C}_{11223} - \frac{48\bar{a}_2^2\bar{B}_{12}}{\bar{a}_2^2 - 1} + 12\bar{a}_2^2\left(\bar{a}_2^2 - \bar{a}_3^2\right)\bar{a}_3^2\bar{C}_{12233} + 24\bar{a}_2^2\left(\bar{a}_3^2 - 1\right)\bar{a}_3^4\bar{C}_{12333} +$$
$$\left(6\bar{a}_2^2\bar{a}_3^6 - 6\bar{a}_2^4\bar{a}_3^4\right)\bar{C}_{22333},$$

$$M_{55} = -30\left(\bar{a}_3^2 - 1\right)\bar{a}_3^2\bar{C}_{11133} + 12\left(6\bar{a}_3^4 - 5\bar{a}_3^2 - 1\right)\bar{a}_3^4\bar{C}_{11333} + 48\bar{a}_3^8\bar{A}_{1333} - 48\left(\bar{a}_3^2 - 1\right)\bar{a}_3^6\bar{B}_{1333} -$$
$$54\left(\bar{a}_3^2 - 1\right)\bar{a}_3^6\bar{C}_{13333} - 64\bar{a}_3^4\bar{A}_3 + 16\bar{a}_3^{10}\bar{A}_{3333}.$$

The components of the inhomogeneity vector are given by

$$
\begin{aligned}
b_0 =& -\frac{1}{4}\left(-2\bar{C}_{13}\left(\bar{A}_1-2\bar{a}_2^2\bar{B}_{12}\right)-\bar{a}_3^2\left(-2\bar{A}_1\left(\bar{C}_{133}+\bar{C}_{233}\right)+\bar{A}_3\left(3\left(\bar{B}_1+\bar{B}_2\right)+\bar{C}_{33}\right)+\right.\right.\\
&\left.\left.2\bar{B}_{12}\left(\bar{a}_2^2\left(2\bar{C}_{133}-\bar{C}_{233}\right)+3\bar{C}_{233}\right)\right)-2\bar{C}_{23}\left(\bar{A}_1+\left(\bar{a}_2^2-3\right)\bar{B}_{12}\right)+\bar{a}_3^6\bar{A}_3\left(3\left(\bar{B}_{133}+\bar{B}_{233}\right)-\right.\\
&\left.16\bar{B}_{333}\right)+\bar{a}_3^4\bar{A}_3\left(6\left(\bar{C}_{133}+\bar{C}_{233}\right)-8\bar{A}_3+9\bar{C}_{333}\right)+8\bar{A}_\emptyset^2\right),\\
b_1 =& -\frac{1}{a_2^2}\left(\bar{A}_1\left(2\bar{a}_2^2\bar{C}_{123}-2\bar{a}_3^2\bar{C}_{133}\right)+\bar{B}_{12}\left(-8\left(\bar{a}_2^2-1\right)\bar{a}_3^2\bar{B}_{123}-4\bar{a}_2^4\bar{C}_{123}-4\left(\bar{a}_2^2-2\right)\bar{a}_3^2\bar{B}_{13}-\right.\right.\\
&4\bar{a}_3^4\bar{a}_2^2\bar{B}_{133}+8\bar{a}_2^4\bar{B}_{223}-4\bar{a}_2^2\bar{C}_{223}+16\bar{a}_3^2\bar{a}_2^2\bar{A}_{23}+4\bar{a}_3^2\bar{C}_{233}+8\left(\bar{a}_2^2-\bar{a}_3^2\right)\bar{A}_3-16\bar{a}_2^2\right)+\\
&\bar{A}_\emptyset\left(8\bar{a}_2^2\bar{B}_{12}+4\left(\bar{a}_3^2-\bar{a}_2^2\right)\bar{B}_{23}\right)+\bar{A}_3\left(3\bar{a}_2^2\bar{a}_3^2\bar{C}_{123}-3\bar{a}_3^4\bar{C}_{133}-6\bar{a}_2^4\bar{a}_3^2\bar{B}_{223}+3\bar{a}_2^2\bar{a}_3^2\bar{C}_{223}+\right.\\
&6\left(\bar{a}_3^2-\bar{a}_2^2\right)\bar{a}_3^2\bar{B}_{23}+\left(5\bar{a}_2^2\bar{a}_3^2-3\bar{a}_3^4\right)\bar{C}_{233}+10\left(\bar{a}_2^2-\bar{a}_3^2\right)\bar{a}_3^6\bar{B}_{2333}+10\bar{a}_3^6\bar{B}_{333}-5\bar{a}_3^4\bar{C}_{333}\Big)+\\
&\bar{A}_2\left(-4\bar{a}_2^6\bar{B}_{223}+2\bar{a}_2^4\bar{C}_{223}-2\bar{a}_3^2\bar{a}_2^2\bar{C}_{233}\right)+\left(w_2-w_1\right)\bar{a}_2^3\bar{\Omega}\Big),\\
b_2 =& -\frac{6}{a_2^4}\left(2\bar{A}_1\left(\bar{a}_2^2\left(4\bar{B}_{12}+\bar{a}_3^2\left(\bar{C}_{1223}+\bar{C}_{1233}\right)\right)+\bar{a}_2^4\left(-\bar{C}_{1223}\right)-\bar{a}_3^4\bar{C}_{1233}\right)+4\bar{B}_{12}\left(\bar{a}_2^4\left(6\bar{B}_{112}+\right.\right.\right.\\
&6\bar{B}_{122}-2\bar{a}_3^2\left(\bar{B}_{123}+2\bar{A}_{223}\right)+2\bar{B}_{123}+7\bar{B}_{222}+4\bar{B}_{23}\Big)+\bar{a}_2^6\left(\bar{B}_{122}+4\bar{B}_{123}+2\bar{A}_{222}\right)+\\
&\bar{a}_2^2\left(2\bar{a}_3^2\left(2\left(\bar{B}_{123}+\bar{B}_{13}\right)-5\bar{B}_{223}\right)+\bar{a}_3^4\bar{B}_{133}+2\bar{B}_{23}\right)+\bar{a}_3^2\left(-4\left(\bar{B}_{123}+\bar{B}_{13}\right)+\bar{a}_3^2\bar{B}_{233}+\right.\\
&\left.4\bar{A}_3\right)\Big)+2\bar{a}_2^2\bar{A}_2\left(\left(\bar{a}_2^2-\bar{a}_3^2\right)\left(4\bar{a}_2^4\bar{B}_{2223}-\bar{a}_2^2\bar{C}_{2223}+\bar{a}_3^2\bar{C}_{2233}\right)-4\left(\bar{a}_2^2+1\right)\bar{B}_{12}\right)+20\bar{a}_2^4\bar{B}_{12}^2+\\
&\bar{a}_3^2\left(\bar{a}_3^2-\bar{a}_2^2\right)\bar{A}_3\left(\bar{a}_2^2\left(3\left(\bar{C}_{1223}+\bar{C}_{2223}\right)+5\bar{C}_{2233}\right)+\bar{a}_3^2\left(-3\left(\bar{C}_{1233}+\bar{C}_{2233}\right)+20\bar{a}_3^2\bar{B}_{2333}-\right.\right.\\
&\left.\left.5\bar{C}_{2333}\right)-12\bar{a}_2^4\bar{B}_{2223}\right)+\frac{2\left(w_1+w_2\right)\left(2\bar{a}_2^2+1\right)\bar{a}_2^3\bar{\Omega}}{\bar{a}_2^2-1}\Bigg),\\
b_3 =& -\left(-2\bar{A}_1\left(2\bar{B}_{113}-\bar{C}_{113}+4\bar{a}_2^2\bar{B}_{12}+\bar{a}_3^2\left(\bar{C}_{133}+3\bar{A}_3\right)\right)+4\bar{A}_\emptyset\left(-\bar{A}_1+2\bar{B}_{12}+\bar{a}_3^2\bar{A}_3\right)+\right.\\
&3\bar{a}_3^2\bar{B}_{11}\bar{A}_3+\bar{B}_{12}\left(\bar{a}_3^2\left(-4\bar{B}_{123}-8\bar{B}_{13}+4\bar{C}_{233}+3\bar{A}_3\right)-4\bar{a}_2^2\left(-2\bar{B}_{113}+\bar{C}_{113}-\bar{a}_3^2\left(2\bar{B}_{123}+\right.\right.\right.\\
&\left.\left.\left.4\bar{A}_{13}+3\bar{B}_{13}-2\bar{A}_3\right)+\bar{a}_3^4\bar{B}_{133}\right)\right)+\bar{a}_3^2\bar{A}_3\left(-3\left(\bar{a}_3^2+2\right)\bar{B}_{113}+\bar{a}_3^2\left(-\left(3\bar{B}_{123}+3\bar{C}_{133}+\right.\right.\right.\\
&\left.\left.\left.5\bar{a}_3^2\left(2\left(\bar{a}_3^2-1\right)\bar{B}_{1333}-\bar{C}_{1333}-2\bar{B}_{333}\right)+5\bar{C}_{1333}+3\bar{C}_{233}+5\bar{B}_{33}\right)\right)+5\bar{B}_{13}\right)-\\
&\left.2\bar{a}_2^2\bar{A}_2\left(3\bar{B}_{12}+\bar{a}_3^2\left(\bar{B}_{123}+\bar{C}_{233}\right)\right)-4\bar{B}_{12}^2+6\bar{a}_3^4\bar{A}_3^2+\left(w_2-w_1\right)\bar{a}_2\bar{\Omega}\right),\\
b_4 =& -\frac{2}{a_2^2}\left(2\left(\bar{a}_2^2-\bar{a}_3^2\right)\bar{A}_1\left(2\bar{B}_{1123}-\bar{C}_{1123}+\bar{a}_3^2\bar{C}_{1233}\right)+4\bar{B}_{12}\left(\bar{a}_2^2\left(6\bar{B}_{112}+\bar{a}_3^2\left(-3\left(\bar{C}_{1123}+\right.\right.\right.\right.\\
&\left.\left.\left.\bar{C}_{1223}\right)+\bar{a}_3^2\bar{C}_{1233}+2\bar{B}_{13}\right)+3\bar{C}_{1223}+6\bar{B}_{23}\right)+\bar{a}_2^4\left(3\bar{C}_{1123}+6\bar{B}_{122}+6\bar{B}_{123}-\bar{a}_3^2\bar{C}_{1233}\right)+\\
&\bar{a}_3^2\left(\left(\bar{a}_3^2-1\right)\bar{C}_{1233}+2\bar{B}_{23}\right)\Big)+\bar{a}_3^2\bar{A}_3\left(\bar{a}_3^2\left(3\left(\bar{C}_{1123}+\bar{C}_{1223}\right)-6\bar{B}_{1123}-\bar{a}_3^2\left(3\left(\bar{C}_{1233}+\right.\right.\right.\right.\\
&\left.\left.\left.\bar{C}_{2233}\right)+10\bar{B}_{1333}+5\bar{C}_{2333}\right)+5\bar{C}_{1233}+10\bar{a}_3^4\left(\bar{B}_{1333}+\bar{B}_{2333}\right)\right)+\bar{a}_2^2\left(-3\left(\bar{C}_{1123}+\bar{C}_{1223}\right)+\right.\\
&6\bar{B}_{1123}+\bar{a}_3^2\left(3\left(\bar{C}_{1233}+\bar{C}_{2233}\right)-10\bar{a}_3^2\bar{B}_{2333}+5\bar{C}_{2333}\right)-5\bar{C}_{1233}\Big)-6\left(\bar{a}_3^2-1\right)\bar{a}_2^4\bar{B}_{1223}\Big)+\\
&\left.12\bar{a}_2^2\bar{B}_{12}^2+2\bar{a}_2^2\bar{A}_2\left(-2\left(\bar{a}_3^2-1\right)\bar{a}_2^4\bar{B}_{1223}+\left(\bar{a}_3^2-\bar{a}_2^2\right)\left(\bar{C}_{1223}-\bar{a}_3^2\bar{C}_{2233}\right)\right)+\frac{6\left(w_1+w_2\right)\bar{a}_2^3\bar{\Omega}}{\bar{a}_2^2-1}\right),
\end{aligned}
\tag{D.2}
$$

$$
\begin{aligned}
b_5 = -6\Bigg(& 2\left(\bar{a}_3^2-1\right)\bar{A}_1\left(-5\bar{B}_{1113}+\bar{B}_{113}+\bar{a}_3^2\left(-\bar{C}_{1133}\right)\right)-24\bar{a}_2^2\bar{C}_{111}\bar{B}_{12}-20\bar{a}_2^2\bar{B}_{111}\bar{B}_{12}+ \\
& 4\bar{B}_{12}\left(\bar{a}_2^2\left(4\left(\bar{a}_3^2-1\right)\bar{B}_{1113}+6\bar{B}_{112}-2\bar{a}_3^2\bar{B}_{113}+6\bar{B}_{122}+4\bar{B}_{123}+4\bar{B}_{13}+\bar{a}_3^4\bar{B}_{133}+2\bar{B}_{23}\right)+\right. \\
& \left.2\bar{B}_{112}+\bar{a}_3^2\left(\bar{B}_{123}+2\bar{C}_{123}\right)+2\bar{a}_2^4\bar{B}_{123}+4\bar{B}_{23}+\bar{a}_3^4\bar{B}_{233}\right)+\bar{a}_3^2\left(\bar{a}_3^2-1\right)\bar{A}_3\left(3\left(\bar{C}_{1113}+\right.\right. \\
& \left.\left.\bar{C}_{1123}\right)-12\bar{B}_{1113}-\bar{a}_3^2\left(3\left(\bar{C}_{1133}+\bar{C}_{1233}\right)+5\bar{C}_{1333}\right)+5\bar{C}_{1133}+20\bar{a}_3^4\bar{B}_{1333}\right)+ \\
& 2\left(\bar{a}_3^2-1\right)\bar{a}_2^2\bar{A}_2\left(\bar{C}_{1123}-\bar{a}_3^2\bar{C}_{1233}\right)+4\left(2\bar{a}_2^2+3\right)\bar{B}_{12}^2+\frac{2\left(w_1+w_2\right)\left(\bar{a}_2^2+2\right)\bar{a}_2\bar{\Omega}}{\bar{a}_2^2-1}\Bigg).
\end{aligned}
$$

BIBLIOGRAPHY

[1] Ansorg, M., Kleinwächter, A., Meinel, R.: Uniformly rotating axisymmetric fluid configurations bifurcating from highly flattened Maclaurin spheroids. Mon. Not. R. Astron. Soc. **339**, 515 (2003)

[2] Bardeen, J.M.: A reexamination of the post-Newtonian Maclaurin spheroids. Astrophys. J. **167**, 425 (1971)

[3] Barrabès, C., Israel, W.: Thin shells in general relativity and cosmology: The lightlike limit. Phys. Rev. D **43**, 1129 (1991)

[4] Bičák, J., Ledvinka, T.: Relativistic disks as sources of the Kerr metric. Phys. Rev. Lett. **71**, 1669 (1993)

[5] Bičák, J., Lynden-Bell, D., Pichon, C.: Relativistic discs and flat galaxy models. Mon. Not. R. Astron. Soc. **265**, 126 (1993)

[6] Bičák, J., Dvořák, L.: Stationary electromagnetic fields around black holes. II. General solutions and the fields of some special sources near a Kerr black hole. Gen. Relat. Gravit. **7**, 959 (1976)

[7] Bičák, J., Dvořák, L.: Stationary electromagnetic fields around black holes. I. General solutions and the fields of some special sources near a Schwarzschild black hole. Czech. J. Phys. **27**, 127 (1977)

[8] Bičák, J., Gürlebeck, N.: Spherical gravitating condensers in general relativity. Phys. Rev. D **81**, 104022 (2010)

[9] Bičák, J., Lynden-Bell, D., Katz, J.: Relativistic disks as sources of static vacuum spacetimes. Phys. Rev. D **47**, 4334 (1993)

[10] Bonnor, W.B.: A rotating dust cloud in general relativity. J. Phys. A: Math. Gen. **10**, 1673 (1977)

[11] Byerly, W.E.: An elementary treatise on Fourier series and spherical, cylindrical and ellipsoidal harmonics with application to problems in mathematical physics. Ginn and Company, Boston (1893)

[12] Caimmi, R., Marmo, C.: Homeoidally striated density profiles: sequences of virial equilibrium configurations with constant anisotropy parameters. Astron. Nachr. **326**, 465 (2005)

[13] Chandrasekhar, S.: The equilibrium and the stability of the Dedekind ellipsoids. Astrophys. J. **141**, 1043 (1965)

[14] Chandrasekhar, S.: The post-Newtonian effects of general relativity on the equilibrium of uniformly rotating bodies. I. The Maclaurin spheroids and the virial theorem. Astrophys. J. **142**, 1513 (1965)

[15] Chandrasekhar, S.: The post-Newtonian equations of hydrodynamics in general relativity. Astrophys. J. **142**, 1488 (1965)

[16] Chandrasekhar, S.: The post-Newtonian effects of general relativity on the equilibrium of uniformly rotating bodies. II. The deformed figures of the Maclaurin spheroids. Astrophys. J. **147**, 334 (1967)

[17] Chandrasekhar, S.: The post-Newtonian effects of general relativity on the equilibrium of uniformly rotating bodies. III. The deformed figures of the Jacobi ellipsoids. Astrophys. J. **148**, 621 (1967)

[18] Chandrasekhar, S.: The evolution of the Jacobi ellipsoid by gravitational radiation. Astrophys. J. **161**, 571 (1970)

[19] Chandrasekhar, S.: The post-Newtonian effects of general relativity on the equilibrium of uniformaly rotating bodies. VI. The deformed figures of the Jacobi ellipsoids (continued). Astrophys. J. **167**, 455 (1971)

[20] Chandrasekhar, S.: The post-Newtonian effects of general relativity on the equilibrium of uniformly rotating bodies. V. The deformed figures of the Maclaurin spheroids (continued). Astrophys. J. **167**, 447 (1971)

[21] Chandrasekhar, S.: Ellipsoidal Figures of Equilibrium. Dover Publications, New York (1987)

[22] Chandrasekhar, S., Elbert, D.D.: The deformed figures of the Dedekind ellipsoids in the post-Newtonian approximation to general relativity. Astrophys. J. **192**, 731 (1974)

[23] Chandrasekhar, S., Elbert, D.D.: The deformed figures of the Dedekind ellipsoids in the post-Newtonian approximation to general relativity - corrections and amplifications. Astrophys. J. **220**, 303 (1978)

[24] Chandrasekhar, S., Esposito, F.P.: The 2 $\frac{1}{2}$-post-Newtonian equations of hydrodynamics and radiation reaction in general relativity. Astrophys. J. **160**, 153 (1970)

[25] Chandrasekhar, S., Nutku, Y.: The second post-Newtonian equations of hydrodynamics in general relativity. Astrophys. J. **158**, 55 (1969)

[26] Collas, P., Klein, D.: Causality violating geodesics in Bonnor's rotating dust metric. Gen. Relat. Gravit. **36**, 2549 (2004)

[27] Eriguchi, Y., Hachisu, I.: New equilibrium sequences bifurcating from Maclaurin sequence. Prog. Theor. Phys. **67**, 844 (1982)

[28] Eriguchi, Y., Sugimoto, D.: Another equilibrium sequence of self-gravitating and rotating incompressible fluid. Prog. Theor. Phys. **65**, 1870 (1981)

[29] Ferrers, N.M.: On the potentials of ellipsoids, ellipsoidal shells, elliptic laminae and elliptic rings of variable densities. Quart. J. Pure and Appl. Math. **14**, 1 (1877)

[30] Fock, V.: The theory of space time and gravitation. Pergamon Press, New York (1959)

[31] Friedman, J.L., Stergioulas, N.: Stability of relativistic stars. Bull. Astr. Soc. India **39**, 21 (2011)

[32] Geroch, R.: A method for generating solutions of Einsten's equations. J. Math. Phys. **12**, 918 (1971)

[33] Geroch, R., Traschen, J.: Strings and other distributional sources in general relativity. Phys. Rev. D **36**, 1017 (1987)

[34] Griffiths, J.B., Podolsky, J.: Exact space-times in Einstein's general relativity. Cambridge University Press, Cambridge (2009)

[35] Guenter, N.: Potential theory and its application to basic problems of mathematical physics. Frederick Ungar Publishing Co. XI (1967)

[36] Gürlebeck, N.: Staubkonfigurationen in der Einsteinschen Gravitationstheorie. Diploma thesis, Friedrich Schiller University, Jena (2007)

[37] Gürlebeck, N.: The interior solution of axially symmetric, stationary and rigidly rotating dust configurations. Gen. Relat. Gravit. **41**, 2687 (2009)

[38] Gürlebeck, N., Bičák, J., Gutiérrez-Piñeres, A.C.: Electromagnetic sources distributed on shells in a Schwarzschild background. accepted for publication in Gen. Relat. Gravit.

[39] Gürlebeck, N., Bičák, J., Gutiérrez-Piñeres, A.C.: Monopole and dipole layers in curved spacetimes: formalism and examples. accepted for publication in Phys. Rev. D

[40] Gürlebeck, N., Petroff, D.: The axisymmetric case for the post-Newtonian Dedekind ellipsoids. Astrophys. J. **722**, 1207 (2010)

[41] Hobson, E.W.: The Theory of Spherical and Ellipsoidal Harmonics. Cambridge University Press, Cambridge (1931)

[42] Hörmander, L.: The analysis of linear partial differential operators. I: Distribution theory and Fourier analysis. Springer Verlag, Berlin (2003)

[43] Israel, W.: Singular hypersurfaces and thin shells in general relativity. Nuovu Cimento B **44**, 1 (1966)

[44] Jacobi, C.G.J.: Ueber die Figur des Gleichgewichts. Ann. Phys. **109**, 229 (1834)

[45] Kramer, D., Stephani, H., Herlt, E., MacCallum, M.: Exact solutions of Einstein's field equations. Cambridge University press, Cambridge (1980)

[46] Kuchař, K.: Charged shells in general relativity and their gravitational collapse. Czech. J. Phys. **18**, 435 (1968)

[47] Lanczos, K.: Über eine stationäre Kosmologie im Sinne der Einsteinschen Gravitationstheorie. Z. Phys. **21**, 73 (1924)

[48] Ledvinka, T., Žofka, M., Bičák, J.: Relativistic disks as sources of Kerr-newman fields. In: T. Piran & R. Ruffini (ed.) Recent Developments in Theoretical and Experimental General Relativity, Gravitation, and Relativistic Field Theories, p. 339 (1999)

[49] Lindblom, L.: On the symmetries of equilibrium stellar models. Phil. Trans. R. Soc. Lond. A **340**, 353 (1992)

[50] Linet, B.: Electrostatics and magnetostatics in the Schwarzschild metric. J. Phys. A: Math. Gen. **9**, 1081 (1976)

[51] Lions, J., Magenes, E.: Non-homogeneous boundary value problems and applications. Vol. I. Springer-Verlag, Berlin (1972)

[52] Meinel, R., Ansorg, M., Kleinwächter, A., Neugebauer, G., Petroff, D.: Relativistic Figures of Equilibrium. Cambridge University Press, Cambridge (2008)

[53] Misner, C.W., Thorne, K.S., Wheeler, J.A.: Gravitation. W.H. Freeman and Co., San Francisco (1973)

[54] Neugebauer, G., Meinel, R.: General relativistic gravitational field of a rigidly rotating disk of dust: Solution in terms of ultraelliptic functions. Phys. Rev. Lett. **75**, 3046 (1995)

[55] Petroff, D.: Die Maclaurin-Ellipsoide in post-Newtonscher Näherung beliebig hoher Ordnung. Ph.D. thesis, Friedrich Schiller University, Jena (2003)

[56] Petroff, D.: Post-Newtonian Maclaurin spheroids to arbitrary order. Phys. Rev. D **68**, 104029 (2003)

[57] Pfister, H.: Do rotating dust stars exist in general relativity? Classical Quant. Grav. **27**, 105016 (2010)

[58] Rezzolla, L., J. Ahmedov, B.: Electromagnetic fields in the exterior of an oscillating relativistic star - I. General expressions and application to a rotating magnetic dipole. Mon. Not. R. Astron. Soc. **352**, 1161 (2004)

[59] Schaudt, U.M., Pfister, H.: Isolated Newtonian dust stars are unstable but can be stabilized by exterior matter. Gen. Relat. Gravit. **33**, 719 (2001)

[60] Schnittman, J.D.: Electromagnetic counterparts to black hole mergers. Classical Quant. Grav. **28**, 094021 (2011)

[61] Steadman, B.R.: Causality violation on van Stockum geodesics. Gen. Relat. Gravit. **35**, 1721 (2003)

[62] Steinbauer, R., Vickers, J.A.: The use of generalized functions and distributions in general relativity. Classical Quant. Grav. **23**, R91 (2006)

[63] van Stockum, W.: The gravitational field of a distribution of particles rotating around an axis of symmetry. Proc. Roy. Soc. Edinburgh A **57**, 135 (1937)

[64] Taniguchi, K., Asada, H., Shibata, M.: Irrotational and incompressible ellipsoids in the first post-Newtonian approximation of general relativity. Prog. Theor. Phys. **100**, 703 (1998)

[65] Will, C.M.: On the unreasonable effectiveness of the post-Newtonian approximation in gravitational physics. PNAS **108**, 5938 (2011)